CANDIDATE.

GORDON LESLIE HILBORNE.

TITLE.

APPLICATION OF FINITE ELEMENT METHOD AND PHOTOELASTICITY TO A LAP WELDED CONNECTION.

SUBMITTED FOR THE DEGREE OF MASTER OF PHILOSOPHY.

DATE. SEPTEMBER 1973

ACKNOWLEDGEMENTS.

The author wishes to acknowledge the invaluable assistance given by Mr. T.H. Richards. His very helpful suggestions and extreme patience have made the completion of this project possible.

SUMMARY

The stress distribution in the plates of lap fillet welded connections is known to be non-uniform. In order to examine the stress distribution in the plates of a double-cover-strap joint with fillet welds, a theoretical model of the joint was analysed using the Finite Element method of analysis. Photo-Elastic model tests were carried out to confirm the assumptions made in the analytical model. An understanding of the Finite Element method of analysis was obtained by applying this method manually to the solution of a single plate under uniform and parabolic tensile loading. A lap weld connection with a very coarse mesh was then examined manually in order to determine the most appropriate method of element and joint numbering. Using a computer programme an analytical model of a side fillet welded connection having equal thickness cover plates and main plate was analysed by the Finite Element method. The effect of varying the relative thickness of the cover and main plate was examined, together with the effect of cutting a hole in the cover plate and welding the cover plate all round. Photo-Elastic models were made for the side fillet welded and the welded all round cover plate cases. The stresses were frozen into the models and after separation of the joint each plate was analysed in a photo-elastic bench. Graphs and pictorial plots were made to compare the Finite Element and Photo-Elastic results. The pictorial plots clearly show that the stress distribution in the plates for the welded all round case is far superior to the side fillet welded case. Results obtained by varying the relative thickness of cover and main plate indicate that the best joint is obtained by using a main plate thickness of half the thickness of each cover plate, and welding the cover plates all round.

To determine the most efficient joint, further work is required to obtain the best weld length for optimum plate and weld stresses.

CONTENTS

I. INTRODUCTION

The solid mechanics section of the Mechanical Engineering Department of the University of Aston was, in 1965, about to move into the Finite Element field and it was thought that a suitable area for development and application of the Finite Element method was in the area of welded connections, where numerous problems occur in which load diffuses from one member to another and the analysis of this type of problem does not normally lead to a simple solution.

Proper joint design is a vital part of a welding procedure and the designer has to work closely with the welding engineer and the metallurgist in order to ensure the quality of workmanship and materials assumed in his design. A major consideration in joint design is the service for which the product is intended. The joint may have to operate under very adverse conditions, such as very high or very low temperatures, or in corrosive atmospheres. The manner in which stress will be applied in service, whether tension, shear, bending or torsion has to be considered. Certain joint designs are suitable only for stress applied in one direction, while others are suitable for use when applications of stress are varied or when stress directions are not predictable. Local discontinuities and abrupt changes in the section of a member cause a concentration of stresses at these points and are usually called 'stress raisers'. The importance of stress concentrations is dependent upon the ductility of the material and the type of loading, that is, whether it is static, impact or dynamic for many cycles. Stress concentrations should be minimised, especially in the case of impact, low temperature or cyclic loading. Brittle materials, unlike ductile materials, will not flow plastically, and therefore no redistribution of stress occurs and the danger of failure occuring at points of stress concentration will result. Stress raisers resulting from sharp corners, fillets, notches, holes etc. might produce stress concentrations equal to many times the average stress and, unless these peak values are held below the endurance limit ultimate failure will occur under fatigue loading. Welded joints, because of their character and shape, are often stress raisers. Basic formulae used in weld design do not take into account local peaks of stress or any residual stresses in the material.

In designing welded connections the designer makes use of welding handbooks and has to comply with the relevant codes of practice.

Palmer(Ref5)had,in the mid 1950's,used the shear lag theory to determine the stress distribution in side fillet welded plates and his results were compared with experimental results obtained by Wade(Ref19)using Strain gauges on welded Aluminium Alloy connections.

The side fillet welded connection was thus chosen for investigation and the purpose of the research was twofold:

(I)to help in the development of the finite element method in the Department of Mechanical Engineering,University of Aston.

(2)to apply the Finite Element method to side fillet welded plates in order to determine the stress distribution in the plates.

An experimental method being used to verify the analytical model used in the Finite Element method of analysis.

In order to fully understand the Finite Element method of operation a series of rectangular plate problems were solved,first manually and then,as the mesh was refined and the relevant matrices became larger a computer programme was used to invert the matrix and determine the element displacements.The lap weld connection was first partly investigated manually,using a very coarse mesh,to determine the best way of numbering the elements and nodes.A Finite Element computer programme devised by Woo(Ref20) was used to solve the lap weld connection,initially with a fairly coarse mesh but finally with a very fine one.Resulting from the initial investigation the mesh was refined in areas of stress concentration.Simultaneous with the Finite Element approach an experimental investigation was undertaken.

Initially it was intended to use Vybak sheet to make a model to be strain gauged and then tested.Vybak was recommended as a suitable model material by Wallace(Ref15) and extensive tests were carried out on a wide variety of models.These preliminary yests showed variations of E of up to 20%.

The initial computer results were showing very high stress concentration in certain areas of the lap welded connection and these could only have been determined from the Vybak model by the use of extremely small and very

expensive strain gauges.For the above reasons the experimental approach using Vybak for the model was discarded in preference to a photo-elastic model analysis.

The Atlas computer at Harwell was used to carry out the computation as the Eliot 803 computer then available at Aston did not have sufficient storage capacity.Computer cards were punched at Aston and then sent to Harwell. This proved to be very time consuming indeed,as although the turn round was very good,liaison was very poor and when errors occured they took a considerable time to sort out. Since this work was undertaken the University of Aston has set up a Computer Centre,installed an ICL 1903 computer and has a special liaison service for users.Had this been in operation earlier much time could have been saved on this project.

2 NOTATION

T_{ij} Stress components

e_{ij} Strain components.

δ_{ij} Kronecker delta.

u_i Component displacements.

$\underline{T}^{n}$ Stress vector.

F_i Body force components.

T_i^{n} Surface force components.

n_j Unit normal.

C_{ij} Constants.

e, ε Strain.

E Modulus of Elasticity.

G Modulus of Rigidity.

λ Lame Constant.

ν Poisson's Ratio.

θ Volumetric strain.

σ_{xx} Direct stress component along x-axis.

σ_{yy} " " " " y-axis.

σ_{xy} Shear stress.

e_{xx} Direct strain along x-axis.

e_{yy} " " " y-axis.

e_{xy} Shear strain.

σ_1 Maximum principal stress.

σ_2 Minimum " "

σ_{12} Maximum shear stress.

u Displacement along x-axis.

v " " y-axis.

F Force.

M Moment.

δ Deflection.

ω Load per unit length.

L Linear dimension.

b Breadth.

t Thickness.

d Diameter.

R Relative retardation.

C Stress optical coefficient.

F' Unit fringe value.

n' Number of whole fringes.

n_o Fringe order, nornal incidence.

n_θ Fringe order, oblique incidence.

λ' Wavelength of light

θ' Angle.

$\sigma_{AV(MP)}$ Average stress in main plate.

V Total potential energy.

U Strain energy.

Ω Potential energy due to external forces.

$\{P\}$ Load

$\{\delta\}$ Nodal displacement.

$\{\alpha\}$ Generalised co-ordinates.

$[k]$ Element stiffness matrix.

$[\bar{k}]$ Generalised co-ordinate stiffness matrix.

$[K]$ Overall stiffness matrix.

$[S]$ Stress matrix

$[I]$ Identity matrix.

$\{q\}$ Boundary load.

$\{\bar{\delta}\}$ - Virtual nodal displacements.

$[D]$ Elasticity matrix.

$\{\bar{f}\}$ Virtual displacements within element.

3. SUMMARY OF ELASTICITY THEORY AND METHODS OF STRESS ANALYSIS

THEORY OF ELASTICITY

3.I Hooke's Law

Hooke's Law states that up to the limit of Proportionality stresses are directly proportional to strains,

$$\tau = E.e$$

where E is a constant of proportionality called the modulus of elasticity.
The above refers to a slender bar under uniaxial tension or compression.

3.2 Generalized Hooke's Law

The question arises as to what is the relation between stresses and strains when the stress system is not a simple tension or compression.
The state of stress in continuous media is completely determined by the stress tensor τ_{ij}, and the state of deformation by the strain tensor e_{ij} $(i,j=1,2,3)$.
It can be shown that $\tau_{12}=\tau_{21}$, $\tau_{13}=\tau_{31}$ and $\tau_{23}=\tau_{32}$ and similarly $e_{12}=e_{21}$, $e_{13}=e_{31}$ and $e_{23}=e_{32}$.
Thus any stress system can be defined by its six components and similarly any strain system can be defined by its six components. A logical generalization of Hooke's Law is to make each stress component a linear function of the strain components. This was done by Cauchy, and the resulting law is called the generalized Hooke's Law,

$$\tau_1 = C_{11}e_1 + C_{12}e_2 + C_{13}e_3 + C_{14}e_4 + C_{15}e_5 + C_{16}e_6$$

- -

$$\tau_6 = C_{61}e_1 + C_{62}e_2 + C_{63}e_3 + C_{64}e_4 + C_{65}e_5 + C_{66}e_6$$

where $\tau_{11}=\tau_1$, $\tau_{22}=\tau_2$, $\tau_{33}=\tau_3$, $\tau_{23}=\tau_4$, $\tau_{31}=\tau_5$, $\tau_{12}=\tau_6$.

$e_{11}=e_1$, $e_{22}=e_2$, $e_{33}=e_3$, $2e_{23}=e_4$, $2e_{31}=e_5$, $2e_{12}=e_6$.

The above equation can be more compactly written in the form,

$$\tau_i = c_{ij}e_j \qquad (i,j=1,2,\text{-----}6)$$

The constants C_{ij} are called the elastic constants, or moduli of the material. These 36 constants have the same dimensions as the stress components due to the fact that that strains e_i are dimensionless.

3.3 ISOTROPY AND HOMOGENEITY

A body is said to be isotropic if its elastic properties are the same in all directions.

Most structural materials are formed of crystalline substances and although very small portions of such materials cannot be regarded as isotropic, the entire body may be regarded as homogeneous and isotropic without any serious discrepancies arising between experimental and the theoretical results. Exceptions to this may occur in cast metals and, rolled and drawn metals. From the definition of the isotropic medium, it follows that its elastic properties are independent of the orientation of co-ordinate axes. Therefore the coefficients C_{ij} must remain invariant. By introducing new co-ordinate axes x_1', x_2', x_3' obtained first by rotation of the x_1, x_2, x_3 system through a right angle about x_1 axis, then by rotation through a right angle about x_3 axis and finally by rotating through an angle of 45° about the x_3 axis and considering the transformed stress components τ_i', the generalized Hooke's Law for a homogeneous isotropic body can be written in the form,

$$\tau_{ij} = \lambda \delta_{ij} \theta + 2G e_{ij} \qquad (i,j = 1,2,3).$$

where λ and G are the Lamé Constants.

If the axes x_i are directed along the principal axes of strain, then by definition $e_{23} = e_{31} = e_{12} = 0$.

But from the above equation we see that in this case $\tau_{23} = \tau_{31} = \tau_{12} = 0$

Hence in an isotropic medium the principal axes of stress and strain are coincident.

The Lamé Constants may be expressed in the form

$$\lambda = \frac{\nu E}{(1+\nu)(1-2\nu)}, \qquad G = \frac{E}{2(1+\nu)}.$$

where E is the Modulus of Elasticity and ν is Poisson's ratio.

3.4 SOLUTIONS OF PROBLEMS IN ELASTICITY

The solution of the general problem is extremely difficult and complete analytical solutions are only available for a limited number of cases.
The following summarises the tasks involved on solving elastic problems.

The stress components τ_{ij} must satisfy the equilibrium equations, $\tau_{ij,j} + F_i = 0 \qquad (i,j = 1,2,3).$

throughout a region of the body, and the boundary condition

$$\bar{T}_i = \tau_{ij} n_j$$

Since there are six stress components and only three equilibrium equations the problem is statically indeterminate. In order to solve the problem, other equations are required and these equations come from the requirement of geometric fit of the body after distortion (Compatibility Equations) Thus to effect a solution there are three basic steps.

1. Equilibrium must be satisfied.
2. The strains implied by stress must be compatible.
3. The stress-strain relationships must be satisfied.

3.5. FUNDAMENTAL BOUNDARY PROBLEMS IN ELASTICITY

Elasticity problems can be classified into three types according to whether the loading is applied through prescribed forces or prescribed displacements, or both. The stresses and strains at any one point along any direction can be computed from six stress components τ_{ij} and six strain components e_{ij}.

The displacement at any one point along any direction can be computed from the three displacement components u_i at the point.

There are thus a total of fifteen unknowns and theoretically these will require fifteen equations for a complete solution.

3.6 PROBLEMS WHERE SURFACE DISPLACEMENTS ARE SPECIFIED

Express all equations in terms of displacements.
Using Hooke's Law,

$$\tau_{ij} = \lambda\theta\delta_{ij} + 2Ge_{ij} \qquad \text{where } \theta = e_{ii} = \text{Volumetric strain}$$

and from the strain analysis it can be shown that,

$$e_{ij} = \tfrac{1}{2}(u_{i,j} + u_{j,i})$$

so that

$$\tau_{ij} = \lambda\delta_{ij}u_{k,k} + G(u_{i,j} + u_{j,i})$$

Substituting the values of these stress components in the equilibrium equation,

$$\tau_{ij,j} + F_i = 0$$

Gives,

$$Gu_{i,jj} + (\lambda + G)u_{j,ji} + F_i = 0 \quad \text{(Navier's Equations)}$$

or

$$G\nabla^2 u_i + (\lambda + G)\theta_{,i} + F_i = 0$$

where $\theta = e_{ii} = u_{ii} = \mathrm{div}\,\bar{u}$.

Compatibility equations are not required because $e_{ij} = \frac{1}{2}(u_{i,j} + u_{j,i})$ implies compatibility.

Thus the problem is completely solved if a solution is obtained for Naviers Equations subject to the prescribed boundary displacements. From the derived internal displacements the strains can be determined and hence using the stress-strain relations the stresses are determined.

3.7 PROBLEMS WHERE THE BOUNDARY STRESSES ARE KNOWN

Not every solution of the system of three equilibruim equations $\tau_{ij,j} + F_i = 0$, corresponds to a possible state of strain in an elastic body, because the components of strain, defined by

$$e_{i,j} = \frac{1+\nu}{E}\tau_{ij} - \frac{\nu}{E}\tau_{kk}\delta_{ij}$$

must satisfy the equations of compatibility.

The equations of compatibility in terms of stresses,

$$\nabla^2 \tau_{ij} + \frac{1}{1+\nu} \tau_{kk,ij} = -\frac{\nu}{1-\nu} F_{kk} \delta_{ij} - (F_{i,j} + F_{j,i})$$

(Beltrami-Michell equations)

are obtained by inserting equations

$$e_{ij} = \frac{1+\nu}{E} \tau_{ij} - \frac{\nu}{E} \tau_{kk} \delta_{ij}$$

in the compatibility equations

$$e_{ij,kl} + e_{kl,ij} - e_{ik,jl} - e_{jk,ik} = 0$$

Thus in order to determine the state of stress in the interior of an elastic body the Beltrami-Michell equations and the equilibrium equations $\tau_{ij,j} + F_i = 0$ subject to the boundary conditions $T_i = \tau_{ij} n_j$ must be solved.

3.8 UNIQUENESS OF SOLUTION

The uniqueness theorem tells us that for the case where only boundary stresses are known there is a unique solution of stresses, strains and non rigid body displacements. In the case where the boundary displacements are known there is a unique solution of stresses, strains, and displacements.

3.9 SAINT-Venant's PRINCIPLE

Frequently problems can be solved if the system of forces acting on a portion of the boundary is replaced by a statically equivalent system of forces acting on the same portion of the body. In these cases the principle proposed by Saint-Venant is very useful. This principle can be stated as follows:- If some distribution of forces acting on a portion of the surface of a body is replaced by a different distribution of forces acting on the same portion of the body, then the effectd of the two different distributions on the parts of the body sufficiently far removed from the region of application of the forces are essentially the same, provided that the two distributions of forces are statically equivalent.

3.10 EXPERIMENTAL STRESS ANALYSIS

Over the past few years the subject of experimental stress analysis or strain measurement has served an increasingly important role in aiding designers to produce not only efficient but economic designs. The main experimental techniques in use today are Photoelasticity, Photoelastic reflective technique, Brittle lacquers and Strain gauges.

3.11 PHOTOELASTICITY

This is a model technique particularly useful at the design stage, especially for components having complicated shapes and loading conditions, in which a model of the component manufactured from a suitable transparent material is placed in the path of a beam of polarised light. When the model is stressed and the light is arranged to fall on a screen it is found to be in the form of an interference pattern. This pattern yields immediate qualitative results, i.e. indicates areas of high stress and, equally important, areas of particularly low stress where the material is not being used to its best advantage. It can also provide full quantative results of peak stresses at both the boundaries and interior of the model.
Although this is especially true of two-dimensional models the technique can be applied to three-dimensional problems.

3.12 PHOTOELASTIC REFLECTIVE TECHNIQUE

This technique is simply an extension of conventional model photoelasticity described above, but here the actual component under consideration is coated with a layer of a photoelastic material. Polarised light is then reflected off the surface of the compoment and the resulting interference is observed on the surface itself by viewing through an analyser instead of by projection on a screen. An indication of the stress variation across the whole of the coated area is thus readily

obtained and stress concentrations revealed immediately. The method is particularly useful for the investigation of stresses in the field,and in the investigation of residual stresses introduced into components during manufacturing processes.

3.13 BRITTLE LACQUERS

In this technique a specially prepared strain-sensitive coating is either sprayed or painted on the surface of the component under investigation.This coating will crack when the stress in the specimen reaches a certain critical value. It has been found that the cracks will always occur normal to the maximum tensile stress on the surface unless the maximum and minimum stresses have about the same value. By the use of a calibration bar(a simple cantilever which has been coated at the same time as the material under test) it is possible to determine the approximate value of the strain which produces the crack,Thus with complete coating of a component it is possible to obtain an overall picture of the strain distribution,and if necessary to plan for further strain measurements by fixing strain gauges at the peak positions.Brittle lacquers are very useful for the quick determination of stress concentrations and principal stress directions.Brittle lacquers are seldom used for accurate determination of stress values.

3.14 STRAIN GAUGES

This is the most widely used technique in industry today. It involves the fixing of one or more strain gauges (lengths of wire or foil of known resistance and suitable form cemented to a non-conductive backing) to the surface of the material whose strain is to be determined.It is essential that this bonding be done carefully so that intimate contact between the material and the gauge is assured.The gauge will then faithfully record the true surface strain.Surface preparation is probably the most vital factor affecting adhesion of the

gauge to the surface,and special cleaning techniques must be adopted.Assuming that the gauge is correctly bonded to the surface,any strain in the material is then transmitted directly to the gauge,which therefore increases or decreases in length and cross-sectional area.These changes in dimension are accompanied by a change of resistance which can be related directly to strain by multiplying by a constant known as the gauge factor.This is provided by the manufacturer and for the most conventional gauges is of the order of 2.In most strain measuring instruments or strain gauge bridges this step is done automatically and strain is read directly from a dial.Strain gauges thus represent a relatively simple method of obtaining actual surface strain values provided that points of maximum strain can be pre-determined.Here brittle lacquer plays a very important role.There are a number of specially developed gauges such as pneumatic and self adhesive gauges.High sensitivity semi-conductor gauges and fatigue gauges are also available.

3.15 OTHER EXPERIMENTAL TECHNIQUES

In addition to the above techniques there are a number of lesser used techniques,the most important of which are the grid methods.

The grid method consists of marking a grid,either rectangular or polar, on the surface of the material under investigation,and measuring the distortion of this grid under strain.There are various methods of obtaining the grid and measuring the distortion.They may be obtained by scratching ,machine scribing,ink drawing or by photographic process.

For strains that remain after the load is removed,measurement can be made by micrometer microscope, otherwise photographs of the grid can be taken before and during load,and measurements made from these. The so-called 'Replica' technique involves the firing of special pellets from a gun at the grid both before and during load.The surfaces of these pellets are coated with Woods metal which is heated in the gun prior to firing.On contact with the grid on the metal surface

replicas of the deformed and undeformed grids are obtained.These are then viewed in a vernier comparison microscope and measurements taken.
A special form of the grid method is the Moirē fringe technique, in which the undeformed grid is superimposed on the deformed grid.An interference pattern results known as Moirē fringes which can be analysed to yield strain values.This is a very sensitive method and promises to be an extremely valuable one.

A recent introduction has been the Holographic method,this method has considerable potential use in many fields,one of these fields being experimental stress analysis.

4. FINITE ELEMENT THEORY

4.I INTRODUCTION

The last few years have seen a revolution in the field of stress analysis. The wide use of finite element methods has made possible the analysis of shapes and loading conditions previously considered insoluble. The principles of stress analysis were well understood in the nineteenth century and the intricacies of stress analysis became a lifelong playground for many talented applied mathematicians. The purist would say that all problems were soluble. Only three equations governed the behaviour of a component: the equations of equilibrium and compatibility, and a stress-strain relationship. These equations could be stated in general form and would, in theory, solve any problem, the only difficulty was in applying them to the problem under consideration and if this could be done, in finding a solution.

Years of brilliant mathematical work followed these lines and many solutions were based on early work of Airy (1862), and his concept of 'stress functions'.

Much work was carried out, especially in Germany, on the analysis of thin shells but all progress hinged on manipulating complex differential equations into suitable form and conceiving an approximation which would simplify them and make a solution possible.

Each approximation limited the scope of the solution so in order to cover a range of problems a large number of solutions was required and all this work was limited to very simple geometries which did not often occur in practice.

The stress analysts job was to know as many classical solutions as possible (or where to find them) use skill and judgement to select the solution nearest to the problem he had to solve. The usual method of solution was to break an assembly down into components which were amenable to analysis and to find forces and moments necessary to match components together.

The first sign of a new approach to stress analysis came from Southwell(1946).He examined the possibilities of approximating to the differential equations with finite difference expressions.(First conceived by Runge(1908)-dormant for many years).This method transformed the problem from the solution of a differential equation to the solution of a series of linear simultaneous equations.When Southwell published his method,no digital computers as we know them today were available,so the solution of a large number of simultaneous equations still presented a considerable barrier.Southwell advocated an iterative method of solution called relaxation.This technique was extremely labourious and computation was done on desk calculators.The normal limit was 30 equations. An independently conceived but special case of this method is the Moment Distribution method(Hardy Cross).

High speed computers came into use in the 1950's and stress analysts saw it as a saviour from the labour of the relaxation method.

The simultaneous equations were produced and the computer used in the solution of the equations.

Stress analysis had thus gone through an evolution from basic laws,through various mathematical approximations,to differential equations;these equations were turned into finite difference form, a set of simultaneous algebraic equations derived,and solved by computer.

The tendency was for more and more of the analysis to be done by the machine.Describe the general shape to the computer,give it general equations in finite difference form and allow it to set up its own simultaneous equations and solve them.

There was still a tendency to use the computer to evaluate solutions based on approximations to basic equations.

At this stage,the finite element method was put forward,but this was not a new concept.

McHenry(1943) and Hrennikoff(1941) had tried to represent plane areas of difficult shape by a plane frame of equivalent stiffness.

It was seen by Clough (1960) and Argyris(1962)

that this was the basis of a method well suited to digital computation.They set about improving the representation of a structure by an assemblage of small simple components,i.e. finite elements. A net of small linear members was found to give insufficient stiffness,and this was followed by an assembly of small plane triangles joined at the corners for plane stress-strain problems.There has been continuous progress towards improvement of the elements and elements are now available for three dimensional solids.

Virtually any elastic problem is now soluble, the main restriction being on the size of the computor and its speed.The storage capacity of the computer governs the number of elements which can be used (hence complexity of geometry which can be described) and speed governs the economics of the solution.

4.2 THE FINITE ELEMENT METHOD

The finite element method is a powerful numerical technique,largely using matrix methods for the analysis of two and three-dimensional continuum.There are two fundamental matrix methods used in structural analysis,namely,Force Methods and Displacement Methods.The Force Method is concerned with the solution of the equation for unknown forces, the Displacement Method,which is the most widely used,has displacements as the unknowns.The computer programme used for the solution of the two dimensional analytical model of the lap welded connection was based on the Displacement Method.

The finite element method is basically one of breaking down a continuum into a finite number of finite elements.The continuum can then be synthesised in the form of an assembled stiffness matrix by the appropriate superposition of the stiffness matrices of the individual elements and hence if the external forces are known a solution can be obtained for the nodal displacements.

The main effect of dividing the continuum into

finite elements is to relax continuity requirements between elements except at the nodal points.Thus continuity is only specified between elements at the nodes,but continuity between the elements tends to the satisfied over the entire length of the sides due to the fact that forces required to produce unit displacements will not be concentrated forces at the nodes but distributed forces along the faces of the element.

One of the simplest forms of element is the plane triangle.

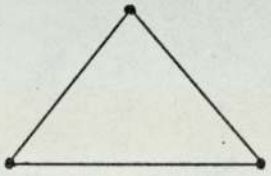

Plane Triangle
3 nodes.
Fig.4.I

Elements are described as having a certain number of degrees of freedom.This is merely the number of nodes multiplied by the various ways in which a node is allowed to move or rotate.The plane triangle for instance,can take up any position in the plane by movement of the three nodes in directions x and y.It therefore has six degrees of freedom.The triangle is a particularly useful shape as large numbers of such elements can describe curved boundaries very closely.

Over each element a simple strain distribution is assumed,in the simplest case of the triangle,the strain is constant.This ensures that lines which originally were straight remain straight so that the element sides remain in contact when the nodes move.The stress within a constant strain element will also be constant.Where a stress gradient is anticipated it is advisable to have a number of small elements so that a more correct distribution of stress will be obtained.The virtual work principle is used to determine the required nodal boundary forces.

4.3 PLANE STRESS/PLANE STRAIN PROBLEMS

The problem is formulated in terms of displacement and using the variational principle of

of total potential energy we obtain

$$V = U + \Omega = \text{Minimum}$$

where U = Strain Energy, Ω = Potential Energy due to external forces, V = total Potential Energy.
The first task is to divide the region into a finite number of sub regions(elements) of any shape (e.g. triangular, rectangular etc).

Using a simple triangle.

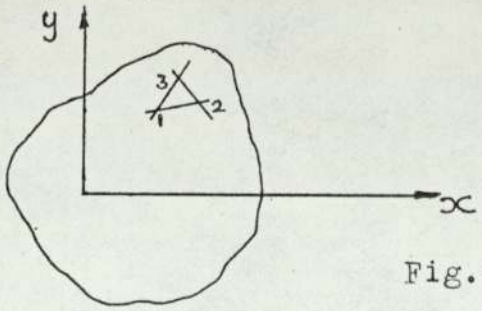

Fig.4.2

A function (shape function) is chosen to describe the displacement property of the element ensuring continuity of displacements between elements connected together.
For the triangular element we assume the displacements u and v are given by

$$u = \alpha_1 + \alpha_2 x + \alpha_3 y$$

$$v = \alpha_4 + \alpha_5 x + \alpha_6 y$$

or $$\begin{Bmatrix} u \\ v \end{Bmatrix} = \begin{bmatrix} 1 & x & y & 0 & 0 & 0 \\ 0 & 0 & 0 & 1 & x & y \end{bmatrix} \begin{Bmatrix} \alpha_1 \\ \alpha_2 \\ \alpha_3 \\ \alpha_4 \\ \alpha_5 \\ \alpha_6 \end{Bmatrix}$$

or $$\{f\} = [M]\{\alpha\}$$

Taking the nodal coordinates as the basic unknowns, the α's are expressed in terms of the element nodal displacements.
For a typical element 'e' we have, for each node taken in turn :-

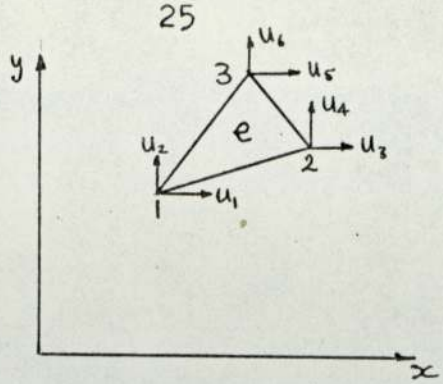

Fig 4.3

$$\begin{Bmatrix} u_1 \\ u_2 \\ u_3 \\ u_4 \\ u_5 \\ u_6 \end{Bmatrix} = \begin{bmatrix} 1 & x_1 & y_1 & 0 & 0 & 0 \\ 0 & 0 & 0 & 1 & x_1 & y_1 \\ 1 & x_2 & y_2 & 0 & 0 & 0 \\ 0 & 0 & 0 & 1 & x_2 & y_2 \\ 1 & x_3 & y_3 & 0 & 0 & 0 \\ 0 & 0 & 0 & 1 & x_3 & y_3 \end{bmatrix} \begin{Bmatrix} \alpha_1 \\ \alpha_2 \\ \alpha_3 \\ \alpha_4 \\ \alpha_5 \\ \alpha_6 \end{Bmatrix}$$

ie $$\{\delta\}_e = [A]\{\alpha\}$$

Then $$\{f\} = [M][A]^{-}\{\delta\}_e$$

or $$\{f\} = [N]\{\delta\}_e = \left[[N]_1 [N]_2 [N]_3\right] \begin{Bmatrix} \{\delta_1\}_e \\ \{\delta_2\}_e \\ \{\delta_3\}_e \end{Bmatrix}$$

ie $$\{f\} = \sum_{i=1}^{3} [N]_i \{\delta_i\}_e$$

Where $$[N]_i = \begin{bmatrix} 1 & 0 \\ 0 & 1 \end{bmatrix} \frac{(a_i + b_i x + c_i y)}{2\Delta} = [I]\left(\frac{a_i + b_i x + c_i y}{2\Delta}\right)$$

With $a_1 = x_2 y_3 - x_3 y_2$, $b_1 = y_2 - y_3$, $c_1 = x_3 - x_1$

and Δ = Element Area.

The other coefficients are obtained by cyclic change of the subscripts.

The $\{\delta\}_e$ listed refer to nodes I,2,3 for a typical element. For compatibility we must match the local co-ordinates to the global co-ordinates. Thus in assembling all elements together we have,

$$\frac{\partial U}{\partial (u_m)_{\text{global}}} = \sum_{\substack{\text{Elements} \\ \text{having } u_m \\ \text{in common.}}} \frac{\partial U_e}{\partial u_m}$$

now $$V = \sum_{\text{Elements.}} U_e + \Omega$$

then $$\frac{\partial V}{\partial u_m} = \sum_{\substack{\text{Elements} \\ \text{having } m \\ \text{in common.}}} \frac{\partial U_e}{\partial u_m} + \frac{\partial \Omega}{\partial u_m} = 0.$$

To obtain $\frac{\partial U_e}{\partial u_m}$

$$U_e = \frac{t}{2} \iint \{\sigma\}^t \{\varepsilon\} \, dx . dy.$$

Hooke's Law is

$$\{\sigma\} = \frac{E}{1-\nu^2} \begin{bmatrix} 1 & \nu & 0 \\ \nu & 1 & 0 \\ 0 & 0 & \frac{1-\nu}{2} \end{bmatrix} \{\varepsilon\} = [D]\{\varepsilon\}$$

$$U_e = \frac{t}{2} \iint \{\varepsilon\}^t [D] \{\varepsilon\} \, dx . dy.$$

Now $$\begin{Bmatrix} \varepsilon_x \\ \varepsilon_y \\ \gamma_{xy} \end{Bmatrix} = \begin{bmatrix} \frac{\partial}{\partial x} & 0 \\ 0 & \frac{\partial}{\partial y} \\ \frac{\partial}{\partial y} & \frac{\partial}{\partial x} \end{bmatrix} \{u\}$$

or $$\{\varepsilon\} = [\partial]\{f\} = [\partial][N]\{\delta\}_e$$

$$\{\varepsilon\} = [\partial]\left[[N]_1 [N]_2 [N]_3\right]\begin{Bmatrix}\{\delta_1\}\\ \{\delta_2\}\\ \{\delta_3\}\end{Bmatrix}_e = [\partial]\left(\sum_{i=1}^{3}[N]_i\{\delta\}_i\right)$$

Substituting for $[N]_i$ we obtain:-

$$\{\varepsilon\} = [B]\{\delta\}_e$$

where
$$[B] = \frac{1}{2\Delta}\begin{bmatrix} b_1 & 0 & b_2 & 0 & b_3 & 0 \\ 0 & c_1 & 0 & c_2 & 0 & c_3 \\ c_1 & b_1 & c_2 & b_2 & c_3 & b_3 \end{bmatrix}$$

then
$$U_e = \frac{t}{2}\iint \left[[B]\{\delta\}_e\right]^t [D][B]\{\delta\}_e \, dx.dy.$$

which reduces to
$$U_e = \frac{1}{2}\{\delta\}_e^t [k]_e \{\delta\}_e$$

$[k]_e$ = element stiffness matrix and since $[D]$ is symmetric $[B]^t[D][B] = [k]_e$ is symmetric.

and
$$\frac{\partial U_e}{\partial\{\delta\}_e} = [k]_e\{\delta\}_e$$

If at the nodes there happen to be concentrated forces, then
$$\Omega = -\{P\}^t\{u\}$$

and
$$\frac{\partial \Omega}{\partial u_i} = -P_i$$

For distributed loading the equivalent nodal applied forces are determined by application of the principle of virtual work.

Then for equilibrium,

$$\frac{\partial V}{\partial u_i} = \sum_{\text{Elements.}} \frac{\partial U_e}{\partial u_i} + \frac{\partial \Omega}{\partial u_i} = 0$$

then
$$\sum_{\substack{\text{Elements}\\ \text{having node } i\\ \text{in common.}}}\left(\sum_{j=1}^{6} k_{ij}\, u_j\right)_e - P_i = 0 \qquad i = 1, 2, \ldots\ldots N.$$

where N = number of degrees of freedom.

If these equations are listed(N of them) and displayed in matrix form,we have :-

$$[K]\{u\} = \{P\}$$

Element k_{ij} of $[K]$ is obtained by adding together the corresponding k_{ij}'s of all those elements which provide a connection between node i and node j.

$[K]$ is symmetric and bonded.Thus,

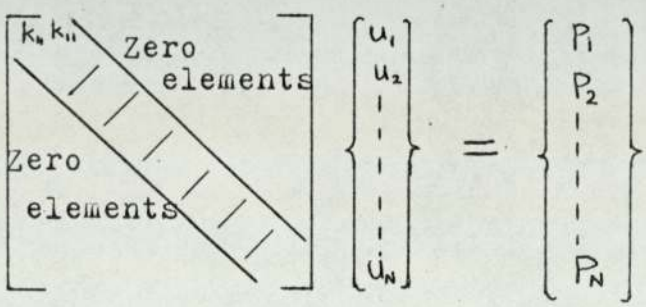

Equation 4.I

$\{u\}$ can be obtained by solving equation 4.I after inserting the boundary conditions. Then element deformations and hence stresses can be evaluated.

In order to obtain a good understanding of the Finite Element method of operation,plates subjected to uniform and parabolic tensile loading were solved manually using a very coarse mesh(Appendix II and III).Advantage was taken of symmetry and therefore only a quadrant of the plate needed to be considered.

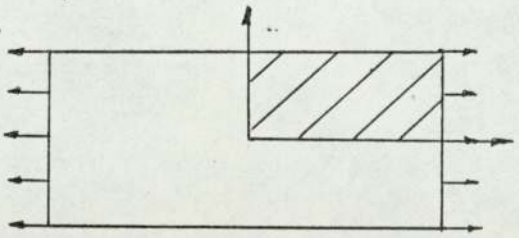

Fig 4.4

Each element stiffness matrix $[k]_e$ was written in extended form.this was necessary for assembling into the stiffness matrix of the whole structure.
The generalised co-ordinate stiffness matrix $[\tilde{k}]$ was determined for triangular element and from this each element stiffness matrix was calculated using the equation,

$$[k] = \left([A]^{-1}\right)^t [\tilde{k}] [A]^{-1}$$

Each part of the element stiffness matrices was assembled into the correct positions in the overall plate stiffness matrix $[K]$.

Known zero values of u and F were inserted in the equation,

$$\{F\} = [K]\{u\}$$

and the reduced equation obtained
The applied distributed loading was converted to the equivalent nodal forces using virtual work principle.These were then inserted into the reduced equation and the unknown displacements(u's) obtained.
Using the displacement values in the stress equation $\{\sigma\} = [S]\{\delta\}$, the stress values ($\sigma_{xx}$, σ_{yy}, σ_{xy}) for each element were determined.

The above processes were carried out completely manually.A smaller mesh was then used increasing the number of elements from four to thirty-six.Although this was repeating the processes it gave an idea of the size of the problems involved in producing the matrices and in solving the matrix equations.Considerable use was made of a computer 'Matrix Package' programme(Elliott) for the inversions,transposition and multiplication of the various matrices involved and a programme was written for use in determining the nodal displacements.

An initial investigation was carried out manually on the welded plate connection using a very coarse mesh in order to determine the best method of numbering the elements and nodes in the main and cover plates.

A start was made on the writing of a finite element computer programme for the solution of the welded connection problem but it was soon realised that the time involved would be considerable and Woo(Ref2I) had by now produced a programme that could be used in the solution of the welded connection problem.

4.4 COMPUTER PROGRAMME

This programme produced by Woo, is a general purpose two-dimensional finite element programme which is capable of analysing any plane stress problem in cartesian co-ordinates. The outline of the programme is shown in the following steps,

I. Input and output of structure load data

(I) The structure data contains: a suitable job title; the number of elements and the corresponding nodal connections, the modulus, Poisson's ratio, and the thickness of each element; the number of nodes and the corresponding nodal co-ordinates; the number of nodal constraints (zero displacements) and the corresponding location and direction of each constraint.

(II) The load date contains: the number of sets of nodal forces, the number of nodal forces in each set, and the location, direction and magnitude of each nodal force.

2 Formation of element stiffness matrices and assembly of overall stiffness matrix.

The overall stiffness matrix is both symmetrical and banded, and advantage is taken of this by storing only the lower band of the matrix in a rectangular array. The upper half of each element stiffness matrix is generated and in order to save computer storage, it is immediately transfered to the correct location in the overall stiffness matrix. Having dealt with all the elements the overall stiffness matrix will then be assembled, ready for the solution of the nodal displacements.

3. Computation of the unknown displacements.

The procedure SYMBANDSOLVE is used to calculate the unknown nodal displacements from the given nodal forces, the overall stiffness matrix having been previously decomposed into a lower triangular band matrix.

4.Evaluation of strains and stresses

Having computed the nodal displacements, the strains and stresses in each element are then calculated for each set of nodal forces.

5.Output of results

The nodal displacements of the complete structure,the strains and stresses in each element are printed out in the form shown in 4.6.

FLOW CHART FOR TWO-DIMENSIONAL PROGRAMME

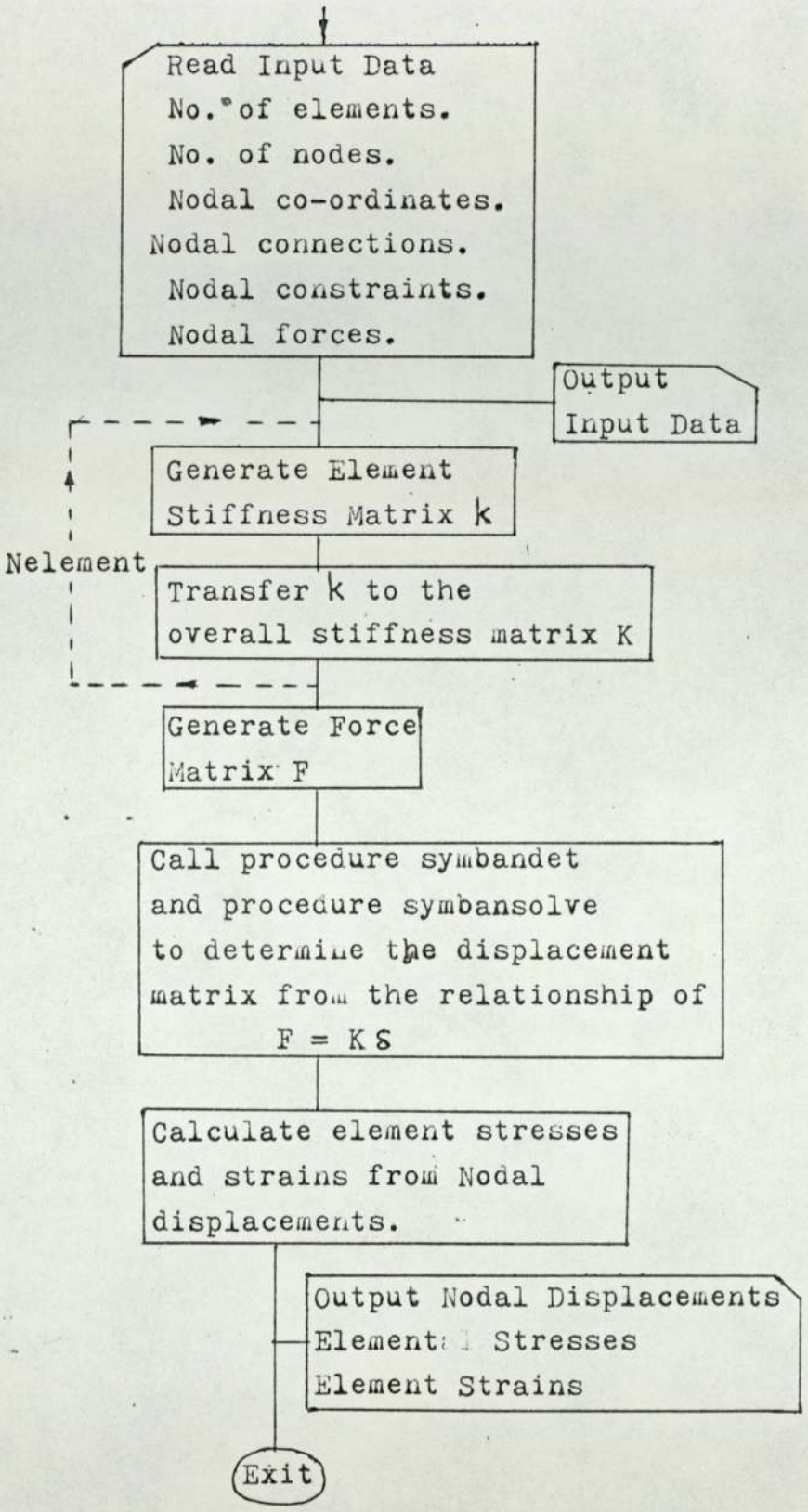

Fig 4.5

```
PROGRAM MK2/1/1
ANALYSIS OF TWO DIMENSIONAL PROBLEMS BY THE METHOD OF FINITE ELEMENT'

BEGIN INTEGER NPROBLEM,PPP'
READ NPROBLEM'
FOR PPP:=1 STEP 1 UNTIL NPROBLEM DO  %1
PROGRAM MK2/1
COMPUTATION OF DISPLACEMENTS,STRAINS AND STRESSES OF  A COMPLEX
STRUCTURE USING THE DISPLACEMENT METHOD'

BEGIN COMMENT THIS PROGRAM USES A SPECIAL TECHNIQUE TO CONSTRUCT THE
             OVERALL STIFFNESS MATRIX BY STORING ONLY THE NONZERO
             ELEMENTS OF THE CONNECTION MATRICES.THE FORCE DISPLACEM
             MATRIX EQUATION IS THEN SOLVED BY A EFFICIENT PROCEDURE
             WHICH OPERATES ONLY ON THE BAND PORTION OF THE OVERALL
             STIFFNESS MATRIX'
INTEGER NELEMT,NNODE,NNODE2,NZDISP,NCOND,JOBNO'
READ JOBNO,NELEMT,NNODE'
PRINT ££L14?TWO DIMENSIONAL ANALYSIS?,££L2?JOB NO.?,SAMELINE,JOBNO,
££L2?NO. OF ELEMENTS=?,SAMELINE,NELEMT,££L2?NO. OF NODES=?,SAMELINE,
NNODE2:=NNODE*2'
BEGIN REAL E,THICKNESS,PR,CONSTA,CONSTB,CONSTC,CONSTD'
      INTEGER I,J,V,W,BANDWIDTH'
      REAL ARRAY MU,CONST1,CONST2,CONST3(1:NELEMT),B,C(1:NELEMT,1:3),
                 DISP(1:NNODE2),XX,YY(1:NNODE)'
      INTEGER ARRAY NODE(1:NELEMT,1:3)'
FOR I:=1 STEP 1 UNTIL NNODE DO READ XX(I),YY(I)'
FOR V:=1 STEP 1 UNTIL NELEMT DO
BEGIN READ W'
IF W=0 THEN BEGIN READ E,THICKNESS,PR,W'
CONSTA:=E/(1-PR**2)'
CONSTB:=CONSTA*THICKNESS'
CONSTC:=0.5*(1-PR)  END'
MU(W):=PR'
CONST1(W):=CONSTA'
CONST2(W):=CONSTB'
CONST3(W):=CONSTC'
FOR I:=1 STEP 1 UNTIL 3 DO READ NODE(W,I)
END'

BEGIN INTEGER INTERCHANGE'
INTEGER ARRAY BAND(1:NELEMT),NOD(1:3)'
FOR W:=1 STEP 1 UNTIL NELEMT DO
BEGIN
FOR I:=1 STEP 1 UNTIL 3 DO NOD(I):=NODE(W,I)'
FOR I:=1, 2 DO
BEGIN IF NOD(I) GR NOD(I+1) THEN
BEGIN INTERCHANGE:=NOD(I)'
NOD(I):=NOD(I+1)'
NOD(I+1):=INTERCHANGE
END
END'
IF NOD(1) GR NOD(2) THEN NOD(1):=NOD(2)'
BAND(W):=NOD(3)-NOD(1)'
END'
FOR W:=1 STEP 1 UNTIL NELEMT-1 DO
BEGIN IF BAND(W) GR BAND(W+1) THEN
BEGIN INTERCHANGE:=BAND(W)'
BAND(W):=BAND(W+1)'
BAND(W+1):=INTERCHANGE
END
END'
```

```
BANDWIDTH:=(BAND(NELEMT)*4+3)'
CONSTD:=(BANDWIDTH+1) DIV 2'
PRINT ££L 2?BANDWIDTH=?,SAMELINE,BANDWIDTH'
END'

READ NZDISP'
NCOND:=NNODE2-NZDISP'
BEGIN INTEGER NNF,SUBSCP'
      INTEGER ARRAY P(1:NNODE,1:2)'
      REAL ARRAY Q(1:NCOND)'
FOR I:=1 STEP 1 UNTIL NNODE DO P(I,1):=P(I,2):=1'
FOR W:=1 STEP 1 UNTIL NZDISP DO BEGIN READ I,J'  P(I,J):=0  END'
V:=1'
FOR I:=1 STEP 1 UNTIL NNODE DO
FOR J:=1,2 DO IF P(I,J) NOTEQ 0 THEN BEGIN P(I,J):=V'  V:=V+1  END'
BEGIN REAL AREA,AREA2,C2AR,SUBP1,SUBP2,SUBP3'
      INTEGER ODDI,ODDJ,EVENI,EVENJ'
      REAL ARRAY X,Y(1:5),BB,CC,BC(1:3,1:3),KE(1:6,1:6),K(1:NCOND,
               1:BANDWIDTH)'
      INTEGER ARRAY CI,CJ(1:6)'
      PROCEDURE BANDSOLVE(C,N,M,V)' VALUE N,M' INTEGER N,M'
           REAL ARRAY C,V'
           BEGIN INTEGER JM,LR,I,PIV,R,J' REAL T' LR:=(M+1) DIV 2'
                 FOR R:=1 STEP 1 UNTIL LR-1 DO
                 FOR I:=1 STEP 1 UNTIL LR-R DO
                 BEGIN FOR J:=2 STEP 1 UNTIL M DO
                       C(R,J-1):=C(R,J)'
                       C(R,M+1-I):=C(N+1-R,M+1-I):=0
                 END'
                 FOR I:=1 STEP 1 UNTIL N-1 DO
                 BEGIN PIV:=I'
                       FOR R:=I+1 STEP 1 UNTIL LR DO
                       IF ABS(C(R,1)) GR ABS(C(PIV,1)) THEN
                       PIV:=R'
                       IF PIV NOTEQ I THEN
                       BEGIN T:=V(I)'
                             V(I):=V(PIV)'
                             V(PIV):=T'
                             FOR J:=1 STEP 1 UNTIL M DO
                             BEGIN T:=C(I,J)'
                                   C(I,J):=C(PIV,J)'
                                   C(PIV,J):=T
                             END
                       END'
                       V(I):=V(I)/C(I,1)'
                       FOR J:=2 STEP 1 UNTIL M DO
                       C(I,J):=C(I,J)/C(I,1)'
                       FOR R:=I+1 STEP 1 UNTIL LR DO
                       BEGIN T:=C(R,1)'
                             V(R):=V(R)-T*V(I)'
                             FOR J:=2 STEP 1 UNTIL M DO
                             C(R,J-1):=C(R,J)-T*C(I,J)'
                             C(R,M):=0
                       END'
                       IF LR NOTEQ N THEN LR:=LR+1
                 END'
                 V(N):=V(N)/C(N,1)'
                 JM:=2'
                 FOR R:=N-1 STEP -1 UNTIL 1 DO
                 BEGIN FOR J:=2 STEP 1 UNTIL JM DO
                       V(R):=V(R)-C(R,J)*V(R-1+J)'
                       IF JM NOTEQ M THEN JM:=JM+1'
                  END
           END'
```

```
      PROCEDURE PRINTMX(K,N,M)'
            VALUE N,M'
            INTEGER N,M'
            REAL ARRAY K'
            BEGIN INTEGER I,J,P,U,V,V12,W'
                  BOOLEAN COMPARE'
                  IF M LESSEQ 12 THEN BEGIN V:=1'  U:=M  END
                                 ELSE BEGIN V:=M DIV 12'  U:=12  END'
                  V12:=V*12'
                  COMPARE:=M GR V12'
                  FOR I:=1 STEP 1 UNTIL N DO
                   BEGIN FOR P:=1 STEP 1 UNTIL V DO
                         BEGIN PRINT ££L??'
                               W:=(P-1)*12'
                               FOR J:=W+1 STEP 1 UNTIL W+U DO
                                   PRINT SAMELINE,K(I,J)
                         END'
                        IF COMPARE THEN BEGIN PRINT ££L??'
                                        FOR J:=V12+1 STEP 1 UNTIL M DO
                                            PRINT SAMELINE,K(I,J)
                                               END
                   END
            END'
FOR I:=1 STEP 1 UNTIL NCOND DO
FOR J:=1 STEP 1 UNTIL BANDWIDTH DO K(I,J):=0'
FOR W:=1 STEP 1 UNTIL NELEMT DO
BEGIN
FOR I:=1 STEP 1 UNTIL 3 DO
BEGIN X(I):=XX(NODE(W,I))' Y(I):=YY(NODE(W,I))
END'
AREA2:=ABS(X(2)*Y(3)-X(3)*Y(2)-X(1)*Y(3)+X(3)*Y(1)+X(1)*Y(2)-X(2)*Y(1
X(4):=X(1)'
X(5):=X(2)'
Y(4):=Y(1)'
Y(5):=Y(2)'
AREA:=0.5*AREA2'
FOR I:=1 STEP 1 UNTIL 3 DO
BEGIN B(W,I):=(Y(I+1)-Y(I+2))/AREA2'  C(W,I):=(X(I+2)-X(I+1))/AREA2
END'
FOR I:=1 STEP 1 UNTIL 3 DO
FOR J:=1 STEP 1 UNTIL 3 DO
BEGIN BB(I,J):=B(W,I)*B(W,J)' CC(I,J):=C(W,I)*C(W,J)
END'
FOR I:=1 STEP 1 UNTIL 3 DO
FOR J:=1 STEP 1 UNTIL 3 DO BC(I,J):=B(W,I)*C(W,J)'
%1 FOR I:=1 STEP 1 UNTIL 6 DO
FOR J:=1 STEP 1 UNTIL 6 DO KE(I,J):=KE(J,I):=0'
C2AR:=CONST2(W)*AREA'
FOR I:=1 STEP 1 UNTIL 3 DO
BEGIN EVENI:=I*2' ODDI:=EVENI-1'
FOR J:=1 STEP 1 UNTIL 3 DO
BEGIN EVENJ:=J*2'   ODDJ:=EVENJ-1'
KE(ODDI,ODDJ):=(BB(I,J)+CC(I,J)*CONST3(W))*C2AR'
KE(EVENI,EVENJ):=(CC(I,J)+BB(I,J)*CONST3(W))*C2AR'
KE(ODDI,EVENJ):=(BC(I,J)*MU(W)+BC(J,I)*CONST3(W))*C2AR'
KE(EVENI,ODDJ):=(BC(J,I)*MU(W)+BC(I,J)*CONST3(W))*C2AR
END
END'
FOR I:=1 STEP 1 UNTIL 6 DO
FOR J:=1 STEP 1 UNTIL 6 DO KE(J,I):=KE(I,J)'
%1 PRINTMX(KE,6,6)'
```

```
V:=1'
FOR I:=1 STEP 1 UNTIL 3 DO
FOR J:=1,2 DO IF P(NODE(W,I),J) NOTEQ 0 THEN
BEGIN CI(V):=P(NODE(W,I),J)'  CJ(V):=I*2+J-2'   V:=V+1
END'
FOR I:=1 STEP 1 UNTIL V-1 DO
FOR J:=I STEP 1 UNTIL V-1 DO
BEGIN SUBP1:=CI(I)-CI(J)'  SUBP2:=CONSTD-SUBP1'  SUBP3:=CONSTD+SUBP1'
K(CI(I),SUBP2):=K(CI(J),SUBP3):=K(CI(I),SUBP2)+KE(CJ(I),CJ(J))
END
END'
%1 PRINTMX(K,NCOND,BANDWIDTH)'
PRINT ££L2?EXTERNAL NODAL FORCES£LS5?NODE£S2?DIRECTION£S5?MAGNITUDE?'
FOR I:=1 STEP 1 UNTIL NCOND DO Q(I):=0'
READ NNF'
FOR V:=1 STEP 1 UNTIL NNF DO BEGIN READ I,J' W:=P(I,J)'  READ Q(W)'
PRINT ££L??,I,SAMELINE,££S2??,J,££S4??,Q(W)   END'
%1 PRINT££L2?NODAL FORCES?'
%1 FOR I:=1 STEP 1 UNTIL NCOND DO PRINT ££L??,SCALED(4),Q(I)'
BANDSOLVE(K,NCOND,BANDWIDTH,Q)'
END'
%1 PRINT ££L2?NODAL DISPLACEMENTS?'
%1 FOR I:=1 STEP 1 UNTIL NCOND DO PRINT ££L??,SCALED(4),Q(I)'
V:=1'
FOR I:=1 STEP 1 UNTIL NNODE DO
FOR J:=1,2 DO
BEGIN
SUBSCP:=I*2+J-2'
IF P(I,J) NOTEQ 0 THEN
BEGIN DISP(SUBSCP):=Q(V)'
V:=V+1
END  ELSE DISP(SUBSCP):=0
END'%1
PRINT ££L2?NODAL DISPLACEMENTS?'%1
FOR I:=1 STEP 1 UNTIL NNODE2 DO PRINT ££L??,SCALED(4),DISP(I)'
PRINT ££L2?NODAL DISPLACEMENTS?,£££L?X DIRECTION£S3?Y DIRECTION?'
FOR I:=1 STEP 2 UNTIL NNODE2 DO
PRINT ££L??,SCALED(4),DISP(I),SAMELINE,££S4??,DISP(I+1)'
END'

BEGIN REAL SUMBODD,SUMBEVEN,SUMCODD,SUMCEVEN,EXX,EYY,EXY,SIGXX,SIGYY,
          SIGXY,SIGMA1,SIGMA2,SIGMA3,CONSTE,CONSTF'
      REAL ARRAY EVENN,ODDN(1:3)'
PRINT ££L3S2?ELEMENT£S16?STRAINS£S33?STRESSES?,£££L1S13?EXX£S9?EYY£S9?
      ££S9?SIGMAXX£S5?SIGMAYY£S5?SIGMAXY£S5?SIGMA1£S6?SIGMA2£S6?SIGMA
FOR W:=1 STEP 1 UNTIL NELEMT DO
BEGIN FOR I:=1 STEP 1 UNTIL 3 DO
BEGIN EVENN(I):=NODE(W,I)*2' ODDN(I):=EVENN(I)-1
END'
SUMBODD:=SUMBEVEN:=SUMCODD:=SUMCEVEN:=0'
FOR I:=1 STEP 1 UNTIL 3 DO
BEGIN SUMBODD:=SUMBODD+B(W,I)*DISP(ODDN(I))'
SUMBEVEN:=SUMBEVEN+B(W,I)*DISP(EVENN(I))'
SUMCODD:=SUMCODD+C(W,I)*DISP(ODDN(I))'
SUMCEVEN:=SUMCEVEN+C(W,I)*DISP(EVENN(I))
END'
```

```
EXX:=SUMBODD'
EYY:=SUMCEVEN'
EXY:=SUMBEVEN+SUMCODD'
SIGXX:=CONST1(W)*(EXX+MU(W)*EYY)'
SIGYY:=CONST1(W)*(MU(W)*EXX+EYY)'
SIGXY:=CONST1(W)*CONST3(W)*EXY'
CONSTE:=0.5*(SIGXX+SIGYY)'
CONSTF:=SQRT(0.25*(SIGXX-SIGYY)**2+SIGXY**2)'
SIGMA1:=CONSTE+CONSTF'
SIGMA2:=CONSTE-CONSTF'
SIGMA3:=CONSTF*2'
PRINT  ££L??,W,SAMELINE,££S3??,SCALED(4),EXX,££S2??,EYY,££S2??,EXY,££2
       SIGXX,££S2??,SIGYY,££S2??,SIGXY,££S2??,SIGMA1,££S2??,SIGMA2,
       ££S2??,SIGMA3
END
END
END'
END'


END'
```

4.5. SPECIFICATION OF DATA PRESENTATION TO THE COMPUTER PROGRAMME

The following gives the detailed order required for data presentation to the computer using the two-dimensional programme described in 4.4.

(A) Number of jobs to be analysed
Job Title.

Number of elements.
Number of nodes.
Nodal co-ordinates(in numerical order)
X co-ordinate Y co-ordinate
Young's Modulus
Thickness
Poisson's Ratio
} group I
Element number and nodal connections for group I
Element No. Nodal connections
Young's Modulus
Thickness
Poisson's Ratio
} group 2
Element number and nodal connections for group 2
Element No. Nodal connections.
(Repeat as many times as there are groups).

Number of zero displacements.
Node number and directions(x=I,y=2) of these:
Node No. Direction.
Number of nodal forces.
Node number,direction(x=I,y=2)and magnitude of force.
Node No. Direction Magnitude.

(B) Repeat above as many times as there are jobs to be analysed.

4.6 FORM OF PRINT OUT FROM COMPUTER.

The computer print out from the two-dimensional programme was in the form :-

No of elements.

No of nodes.

Band width.

External nodal forces.

Node Direction Magnitude.

Nodal displacements.

X direction Y Direction.

Element. Strains. Stresses.

e_{xx} e_{yy} e_{xy} σ_{xx} σ_{yy} σ_{xy} σ_1 σ_2 σ_{12}

CHAPTER 5

5.APPLICATION OF FINITE -ELEMENT METHOD TO LAP-WELDED CONNECTION.

5.I. WELDED CONNECTIONS.

Engineering structures and components can be manufactured by casting or forging,or they can be fabricated from a number of smaller components, by riveting,bolting,or welding parts together.Riveted or welded structures are permanent in so far as they cannot be taken to pieces without destruction of the joints.In a fabricated welded structure,the weld locates the component elements together and transmits the loads which occur under working conditions. Welding has been referred to as ' the art of joining parts of the same metal in such a way that the result is a continuity of homogenous material, of the composition and characteristics of the two parts which are being joined together'.

Welding processes are usually classified as fusion welding processes i.e. welding without pressure,or force welding processes.

Butt and Fillet welds are the basic types of weld generally applicable to all sections of material, i.e. plate,bars,structural sections and tubes. Typical Butt and Fillet welds are shown below.

Butt Welds

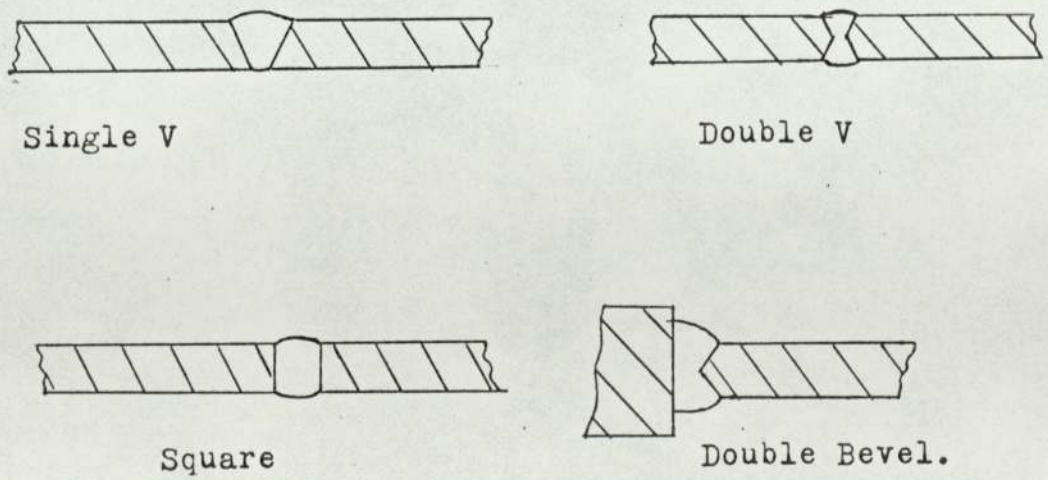

Fig. 5.I

Fillet Welds

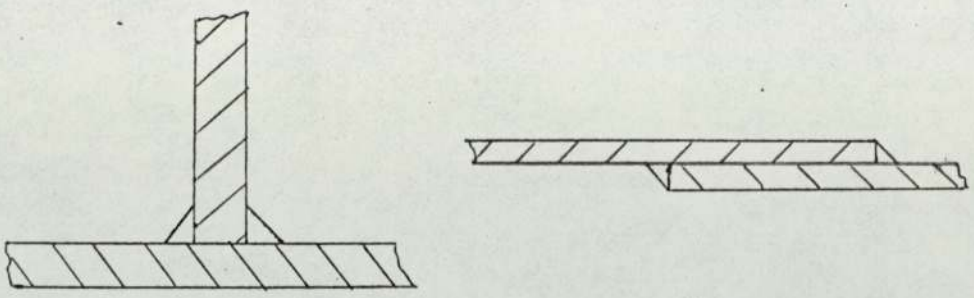

Tee Lap

Fig.5.2

One of the main features of properly made butt welds as compared with fillet welds is their continuity making them more suitable for dynamic loading.Fillet welds are the cheapest type of weld to make,for no edge preparation is required and setting up is simple.However,since fillet welds do not possess the continuity of butt welds,they are not capable of carrying high dynamic stresses.

Design of welded connections.

Besides considering the actual welds connecting two parts or components of a fabrication,consideration must be given to the adequacy of the joint connection as a whole,otherwise the connection between two parts that may be amply welded together could fail because of some inherent weakness.The arrangement and design of parts in the vicinity of the welds is of equal importance to that of the welds themselves.Stress or force flows from one component to the other by means of the welds,and the parts themselves must channel this flow to the welds so that the whole connection is direct and positive in action.

Stress Concentrations

Local discontinuities and abrupt changes in the section of a member cause a concentration of the stresses at these points and are usually called 'stress raisers'.The importance of stress raisers and the resulting stress concentrations are dependent on the ductility of the material and the type of loading, that is,whether it is,impact,static or

dynamic for many cycles.

Welded joints,because of their character and shape,are often stress raisers.Sharp corners and notches are well known stress raisers and are obtained with groove welds having incomplete penetration,at the heel and toe of fillet welds and at points of undercut or reinforcement.

In the fillet welded assembly shown in fig. 5.3 the load in the main plates well away from the cover plates is uniformly distributed.The load diffuses into the pair of cover plates and then back into the other main plate.The problem is to find the stress distribution in both the cover plates and the main plates.Since the conditions in the two cover plates are exactly the same,they can,for theoretical purposes,be regarded as a single plate of twice the actual thickness.The connection is also symmetrical about two axes and therefore only one quadrant needs to be considered.

It is assumed that the problem is two-dimensional so that there is no variation of stress across the thickness of the plate.

PICTORIAL VIEW OF WELDED CONNECTION.

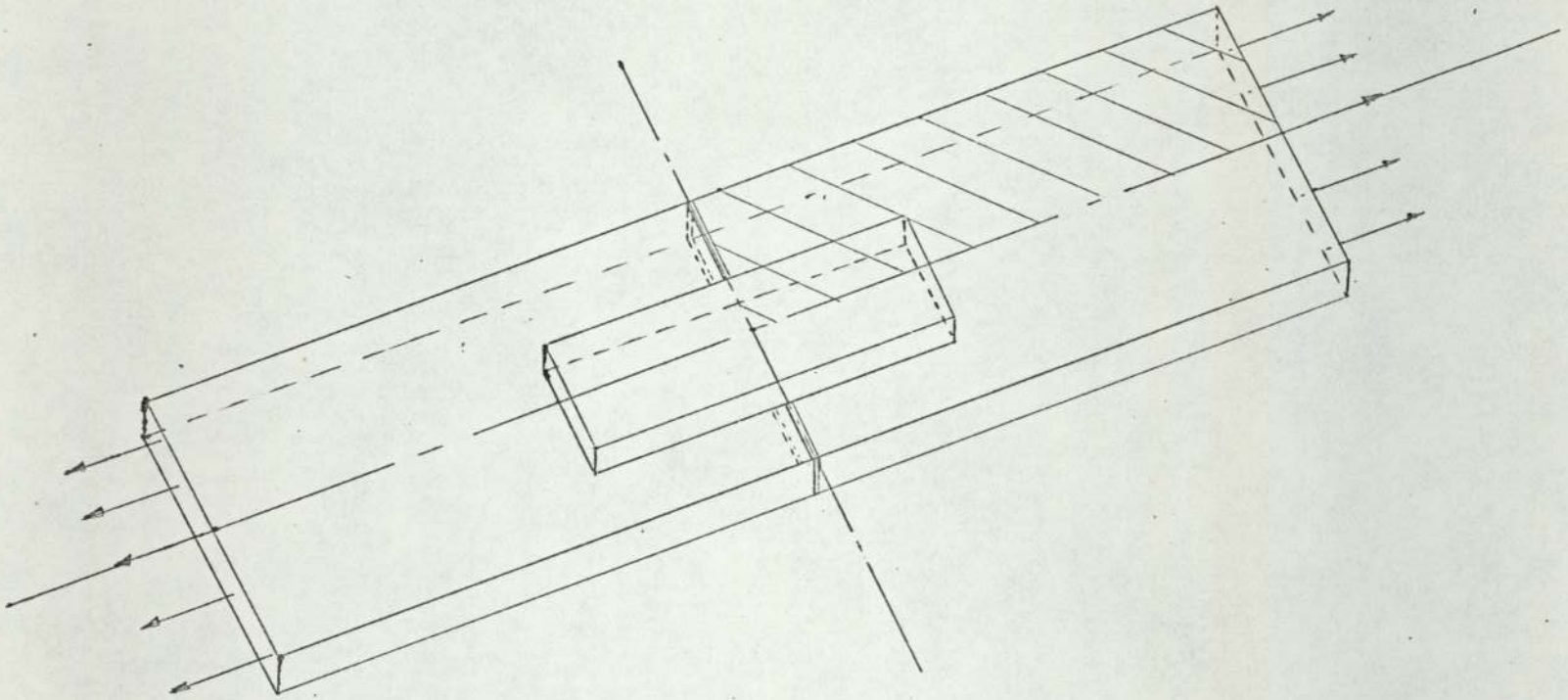

Fig 5.3

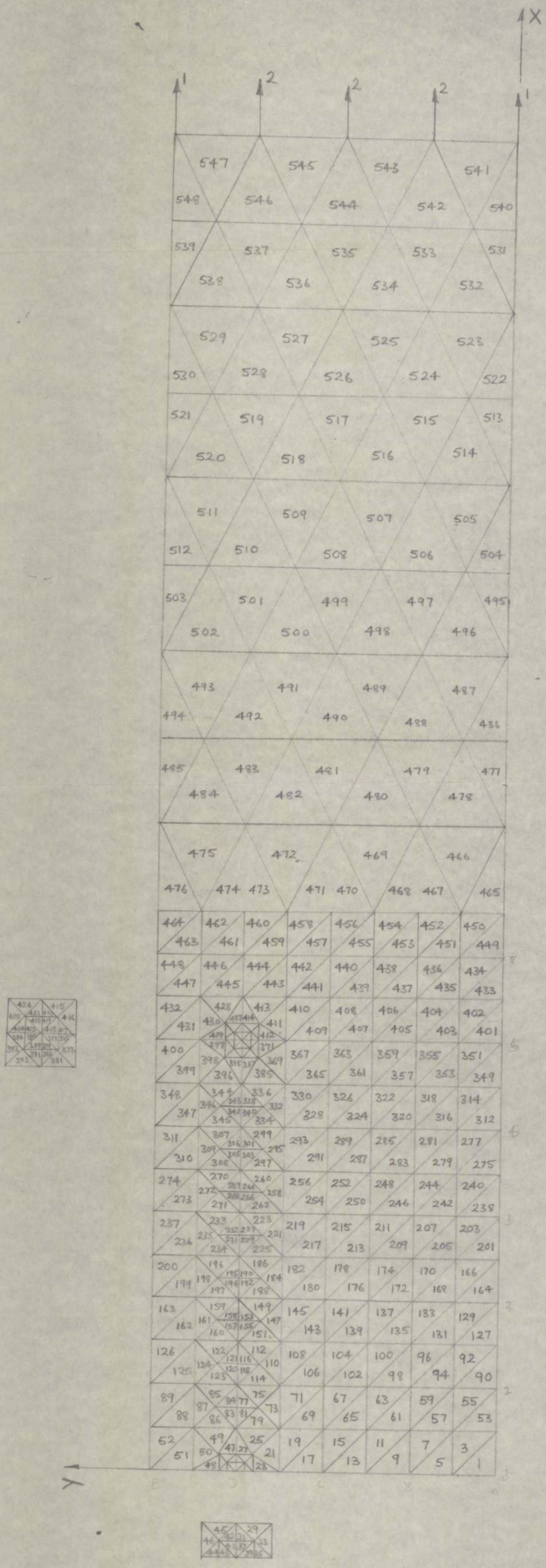
X
1
2
2
2
1
547 545 543 541
548 546 544 542 540
539 537 535 533 531
538 536 534 532
529 527 525 523
530 528 526 524 522
521 519 517 515 513
520 518 516 514
511 509 507 505
512 510 508 506 504
503 501 499 497 495
502 500 498 496
493 491 489 487
494 492 490 488 486
485 483 481 479 477
484 482 480 478
475 472 469 466
476 474 473 471 470 468 467 465
464 462 460 458 456 454 452 450
463 461 459 457 455 453 451 449
448 446 444 442 440 438 436 434
447 445 443 441 439 437 435 433
432 428 413 410 408 406 404 402
431 430 411 409 407 405 403 401
400 398 369 367 363 359 355 351
399 396 385 365 361 357 353 349
348 346 332 330 326 322 318 314
347 345 334 328 324 320 316 312
311 307 299 293 289 285 281 277
310 309 295 291 287 283 279 275
274 270 260 256 252 248 244 240
273 272 258 254 250 246 242 238
237 233 223 219 215 211 207 203
236 235 221 217 213 209 205 201
200 196 186 182 178 174 170 166
199 198 184 180 176 172 168 164
163 159 149 145 141 137 133 129
162 161 147 143 139 135 131 127
126 122 112 108 104 100 96 92
125 124 110 106 102 98 94 90
89 85 75 71 67 63 59 55
88 87 73 69 65 61 57 53
52 49 25 19 15 11 7 3
51 50 21 17 13 9 5 1
Y
E
D
C
B
A
6
5
4
3
2
1

5.2. FINITE ELEMENT MODEL.

In order to determine the best method of numbering the elements and nodes in the finite element model, several different models having very coarse meshes were partially analysed by hand. The final form of mesh used in dividing up the model lap-welded plates is shown in fig. 5.4 . A similar mesh was used for both main plate and cover plate, the method of element numbering being to start at the centre lines numbering first the main plate element, then the coincident cover plate element and moving progressively in horizontal lines throughout the model. The nodes were numbered in a similar manner except that along weld lines the nodes of both main plate and cover plate were given the same number. In the finite element method the external loads are applied at the nodes. The uniform load distribution was therefore replaced by a statically equivalent system of point loads applied at the nodes. Thus using Saint-Venant's Principle, the replacing of the uniform distribution of forces by the statically equivalent nodal forces will not affect the stress distribution around the weld area providing the surfacesare sufficiently removed from the weld area. It was noted from the photo-elastic model described later that the stress in the main plate was uniform at a distance of approximately one main width from the top of the coverplate.

In order to ensure that the finite element model had a similar distribution of stress at one main plat width from the top of the cover plate the external nodal forces were applied at $2\frac{5}{8}$ main plate widths from the top of the cover plate. The exact distance being determined by the convenient mesh sizes.

5.3. DETAILS OF WELDED CONNECTIONS.

Five plate connection problems were investigated, four dealing with side fillet welded cover plates and

in the fifth the weld was taken all around the cover plates.

Test	Main Plate Thickness. (inches)	Thickness of each Cover Plate (inches)	
I	o.I875	o.I875	side weld
2	0.I875	0.09375	side weld
3	0.09375	0.I875	side weld
4	0.I875	0.I875	side weld. Hole cut in centre of cover plate.
5	0.I875	0.I875	Weld taken all round cover plates.

No changes in the node or element numbering were required for the first four tests. The change in thickness of the plates only required substitution of one 'thickness' computer card for another. To simulate the cut out in the centre of the cover plates the elements representing the hole were given a very low modulus value.

In order to investigate taking the weld all round the cover plate some of the nodes required renumbering.

5.4. ANALYSIS OF COMPUTER RESULTS

From the computer results the stress values at the edges and at the weld had to be determined. The mean stress value between two elements was taken at the centroid point shown in the diagram below,

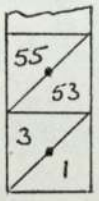

Fig 5.5

Having determined these values graphs of the mean values were drawn and the boundary values obtained by extrapolation. This process was very labourious and time consuming. The non-dimensional values of $(\sigma_1 - \sigma_2)$ divided by σ average stress in the main plate are given in the tables on pages 50 to 54.

Equilibrium checks were carried out on the side fillet welded model with equal thickness plates and the model welded all round the cover plate. For these two models diagrams showing the overall distribution of $\frac{\sigma_1 - \sigma_2}{\sigma_{AV(MP)}}$ in both the cover plate and main plate were drawn. (Fig. 5.7-5.10)

To compare the different types of weld connection and the effect of varying thicknesses of plate, graphs (I- 4) were plotted of $\frac{\sigma_1 - \sigma_2}{\sigma_{AV(MP)}}$ along the weld line and the plate centre line. A diagram (graph 5) was drawn to show how the load was transferred from the cover plates to the main plate for the two types of weld connection.

Reference Positions For Results.

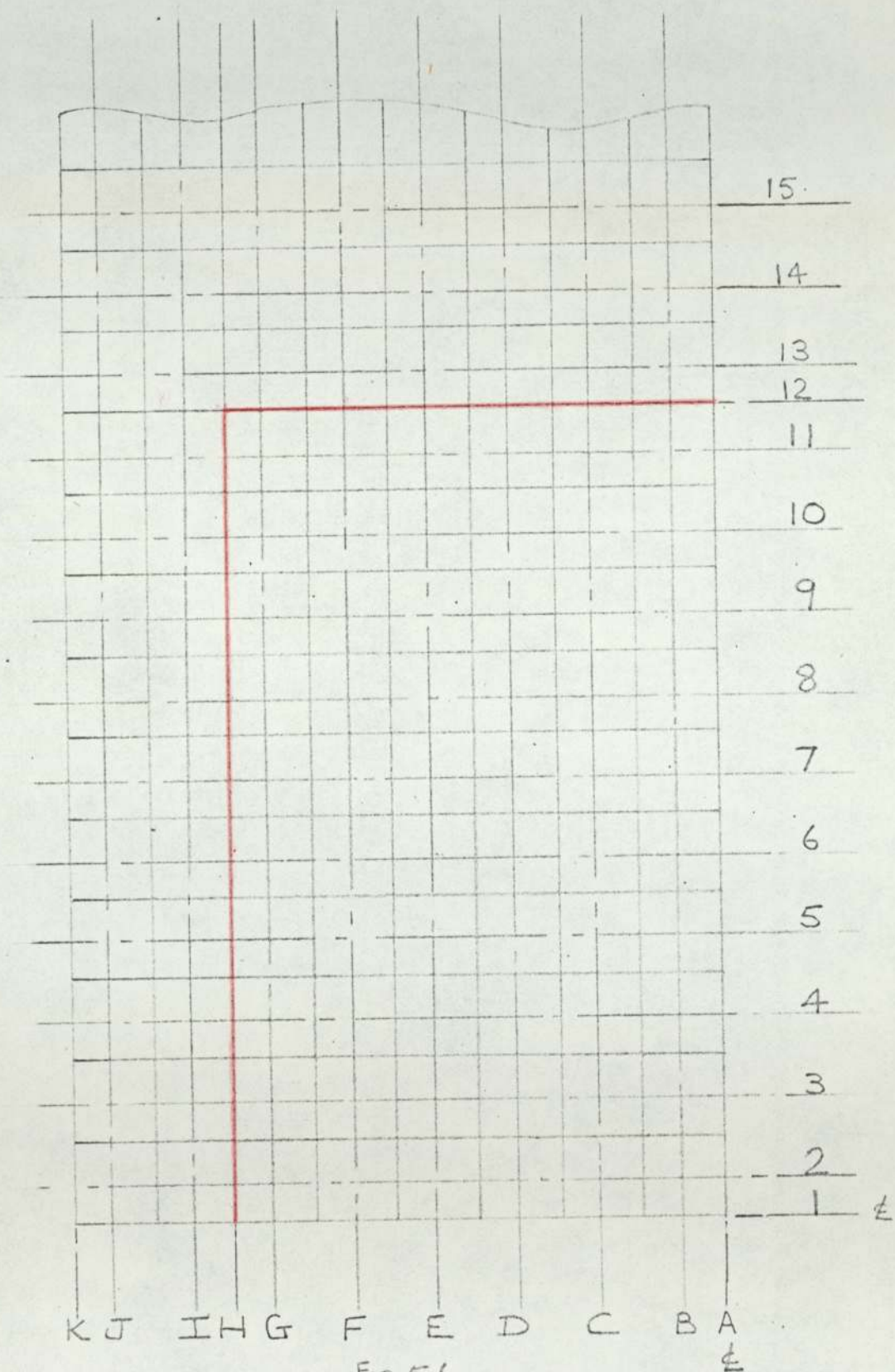

Fig 5.6.

The following tables indicate the values of $\frac{\sigma_1 - \sigma_2}{\sigma_{AV(MP)}}$ at the intersection of the various lines as shown in the reference diagram.

e.g.

	A	B	C	
1				
2			0·250	

This indicates the value at the intersection of line C and line 2.

SIDE WELD.

Thickness of each Cover Plate = 0·1875 inches

Thickness of Main Plate = 0·1875 inches.

Computer Results $\frac{\sigma_1 - \sigma_2}{\sigma_{av\ main\ plate}}$

Cover Plate.

	A	B	C	D	E	F	G	H
1	0·2	0·215	0·25	0·33	0·445	0·65	1·46	3·6
2	0·2	0·213	0·2502	0·3308	0·4597	0·6636	1·24	1·6
3	0·186	0·2035	0·2486	0·3381	0·4763	0·6767	0·93	1·06
4	0·177	0·1931	0·2471	0·3472	0·4885	0·6615	0·818	0·9
5	0·16	0·1777	0·2435	0·3546	0·4963	0·6498	0·773	0·83
6	0·135	0·159	0·2377	0·3596	0·5044	0·6532	0·756	0·795
7	0·11	0·1428	0·2312	0·3604	0·5111	0·6680	0·791	0·825
8	0·115	0·1398	0·2251	0·3516	0·5069	0·6844	0·839	0·89
9	0·14	0·1665	0·2268	0·3265	0·4737	0·680	0·91	1·015
10	0·24	0·2452	0·2711	0·3019	0·3899	0·5922	1·006	1·32
11	0·4	0·4018	0·4070	0·3813	0·3488	0·3590	1·242	1·88
12	0·55	0·51	0·47	0·44	0·345	0·25	1·4	2·4

Main Plate.

	A	B	C	D	E	F	G	H	I	J	K
1	0·575	0·53	0·46	0·29	0·12	0·22	1·35	1·97	1·0	0	0
2	0·455	0·4253	0·3677	0·3035	0·2631	0·4340	1·327	1·67	0·9393	0·0811	0
3	0·255	0·2558	0·2702	0·3562	0·5357	0·8536	1·186	1·27	0·8041	0·3551	0·2
4	0·17	0·2002	0·3001	0·4650	0·6809	0·9152	1·046	1·08	0·6947	0·4859	0·4
5	0·15	0·2120	0·3456	0·5273	0·7253	0·9031	0·9994	1·035	0·6450	0·5694	0·5
6	0·2	0·2594	0·3900	0·5634	0·7402	0·8905	0·9752	1·00	0·6363	0·6425	0·68
7	0·28	0·3291	0·4410	0·5972	0·7583	0·8986	0·9826	1·01	0·6582	0·7148	0·76
8	0·37	0·4112	0·5029	0·6416	0·7942	0·9367	1·029	1·05	0·7069	0·7921	0·83
9	0·47	0·4979	0·5736	0·6983	0·8496	1·012	1·130	1·155	0·7847	0·8735	0·94
10	0·56	0·5821	0·6458	0·7604	0·9163	1·116	1·323	1·36	0·8946	0·9278	0·9
11	0·63	0·6556	0·7093	0·8127	0·9653	1·192	1·824	2·21	1·027	0·9094	0·8
13	0·71	0·7136	0·7575	0·8455	0·9784	1·159	1·562	1·92	1·422	0·9916	0·91
14	0·74	0·759	0·7941	0·8656	0·9709	1·125	1·275	1·29	1·275	1·106	1·00
15	0·79	0·7969	0·828	0·8821	0·9709	1·073	1·172	1·23	1·171	1·119	1·11

Weld all round Cover Plate.

Thickness of each Cover Plate = 0·1875

Thickness of Main Plate = 0·1875

Computer Results. $\frac{\sigma_1 - \sigma_2}{\sigma_{AV\ main\ plate}}$

Cover Plate.

	A	B	C	D	E	F	G	H
1	0·4	0·415	0·425	0·44	0·47	0·546	1·01	2·1
2	0·42	0·4207	0·4287	0·4484	0·4856	0·5619	0·8736	1·24
3	0·42	0·4234	0·4333	0·4558	0·4975	0·5708	0·6550	0·7
4	0·43	0·4291	0·4396	0·4615	0·4969	0·5426	0·5565	0·54
5	0·43	0·4338	0·4426	0·4600	0·4842	0·5073	0·5012	0·476
6	0·43	0·4361	0·4418	0·4523	0·4670	0·4787	0·4704	0·45
7	0·43	0·4372	0·4395	0·444	0·4504	0·4571	0·4552	0·465
8	0·44	0·4403	0·4395	0·4380	0·4375	0·4413	0·4500	0·46
9	0·44	0·4486	0·4455	0·4388	0·4310	0·4301	0·4524	0·49
10	0·465	0·4637	0·4602	0·4498	0·4387	0·4299	0·4627	0·505
11	0·484	0·4834	0·4818	0·4763	0·4684	0·4637	0·4819	0·51
12	0·51	0·495	0·490	0·5	0·49	0·5	0·5	0·5

Main Plate.

	A	B	C	D	E	F	G	H	I	J	K
1	0·27	0·28	0·23	0·22	0·1	0	0·92	1·6	0·76	0	0
2	0·225	0·2245	0·2067	0·1866	0·1579	0·2172	0·8424	1·25	0·7031	0·0609	0
3	0·15	0·1407	0·1374	0·1604	0·2456	0·4502	0·7542	0·92	0·6124	0·2555	0·2
4	0·085	0·0998	0·1266	0·1923	0·3088	0·4749	0·6492	0·735	0·5357	0·3536	0·3
5	0·08	0·0901	0·1333	0·2096	0·3178	0·4504	0·5824	0·65	0·4985	0·4129	0·38
6	0·085	0·0972	0·1410	0·2126	0·3074	0·4201	0·5395	0·6	0·4856	0·4608	0·4
7	0·1	0·1139	0·151	0·2129	0·2949	0·3949	0·5119	0·59	0·4890	0·5052	0·56
8	0·135	0·1377	0·1668	0·2179	0·2878	0·4244	0·4954	0·51	0·5051	0·5534	0·6
9	0·165	0·169	0·1915	0·2321	0·2890	0·4138	0·4877	0·51	0·5358	0·6123	0·67
10	0·2	0·2107	0·2289	0·2598	0·3024	0·3626	0·4854	0·54	0·5927	0·6805	0·7
11	0·26	0·267	0·2822	0·3061	0·3377	0·3811	0·4680	0·6	0·7395	0·7286	0·69
12	0·295	0·31	0·33	0·34	0·36	0·425	0·45	0·645	0·79	0·79	0·70
13	0·965	0·9606	0·9644	0·9737	0·9869	1·008	1·047	1·1	0·8369	0·7483	0·7
14	1·0	1·002	1·008	1·016	1·028	1·033	1·004	0·95	0·9001	0·7946	0·7

SIDE WELD.

Thickness of each Cover Plate = 0.09375 inches

Thickness of Main Plate = 0.1875 inches.

Computer Results $\frac{\sigma_1 - \sigma_2}{\sigma_{AV\ main\ plate}}$

Cover Plate.

	A	B	C	D	E	F	G	H
1	0.31	0.35	0.4	0.53	0.73	1.095	3.6	6.0
2	0.31	0.3484	0.4074	0.5388	0.7576	1.132	2.38	3.6
3	0.31	0.3393	0.4102	0.5562	0.7936	1.163	1.666	1.8
4	0.3	0.3305	0.4156	0.5773	0.8156	1.122	1.405	1.55
5	0.28	0.3141	0.4145	0.5903	0.8205	1.073	1.276	1.335
6	0.25	0.287	0.4053	0.5948	0.8216	1.052	1.220	1.275
7	0.21	0.2567	0.3910	0.5913	0.8216	1.052	1.216	1.27
8	0.195	0.2381	0.3746	0.5744	0.8097	1.062	1.250	1.314
9	0.205	0.2549	0.3625	0.5306	0.7577	1.049	1.317	1.46
10	0.325	0.3432	0.3932	0.4616	0.6177	0.9021	1.414	1.665
11	0.535	0.5528	0.5539	0.5040	0.4470	0.4837	1.35	2.4
12	0.7	0.7	0.67	0.55	0.35	0.15	1.28	3.0

Main Plate.

	A	B	C	D	E	F	G	H	I	J	K
1	0.75	0.68	0.6	0.395	0.08	0.05	2.16	3.6	1.8	0	0
2	0.57	0.5347	0.4723	0.3998	0.3293	0.5169	1.94	2.6	1.564	0.1228	0.04
3	0.318	0.3189	0.3239	0.4119	0.6337	1.074	1.595	1.8	1.225	0.5281	0.3
4	0.2	0.2362	0.3424	0.5336	0.8042	1.122	1.338	1.4	1.006	0.6953	0.65
5	0.155	0.2388	0.4145	0.6014	0.8427	1.071	1.197	1.235	0.8961	0.7824	0.75
6	0.235	0.2854	0.4340	0.6333	0.8140	1.022	1.123	1.145	0.8492	0.8461	0.84
7	0.32	0.3583	0.4844	0.6600	0.8419	1.00	1.095	1.122	0.8428	0.8986	0.94
8	0.41	0.4452	0.5461	0.6972	0.8612	1.012	1.108	1.135	0.8667	0.9473	1.015
9	0.505	0.5361	0.6167	0.7473	0.9017	1.060	1.173	1.205	0.9189	0.9911	1.07
10	0.595	0.6229	0.6883	0.8035	0.9549	1.138	1.316	1.38	0.9918	1.004	1.03
11	0.67	0.6971	0.7504	0.8506	0.9939	1.196	1.68	2.34	1.02	0.9606	0.94
13	0.73	0.7539	0.7959	0.8782	0.9977	1.149	1.448	1.76	1.33	1.022	0.95
14	0.786	0.7959	0.8280	0.8916	0.9813	1.103	1.217	1.3	1.226	1.106	1.05
15	0.812	0.8288	0.8557	0.9015	0.9742	1.056	1.138	1.162	1.144	1.114	1.102

SIDE WELD.

Thickness of each Cover Plate = 0.1875

Thickness of Main Plate = 0.09375

Computer Results $\frac{\sigma_1 - \sigma_3}{\sigma_{nr\ main\ plate}}$

Cover Plate.

	A	B	C	D	E	F	G	H
1	0.11	0.122	0.143	0.19	0.258	0.365	0.7	1.0
2	0.11	0.1205	0.1427	0.19	0.262	0.367	0.613	0.8
3	0.11	0.1128	0.14	0.1925	0.269	0.371	0.491	0.58
4	0.09	0.1026	0.136	0.1954	0.275	0.368	0.45	0.505
5	0.075	0.0906	0.1321	0.199	0.282	0.37	0.443	0.472
6	0.055	0.0775	0.1287	0.203	0.2905	0.381	0.456	0.482
7	0.04	0.0693	0.1258	0.2042	0.298	0.398	0.485	0.53
8	0.04	0.0728	0.1236	0.199	0.296	0.413	0.528	0.575
9	0.085	0.0992	0.1304	0.1845	0.274	0.411	0.59	0.705
10	0.16	0.1614	0.174	0.185	0.2285	0.352	0.672	1.1
11	0.27	0.271	0.2775	0.268	0.255	0.2655	0.644	1.2
12	0.345	0.344	0.34	0.31	0.28	0.215	0.62	1.32

Main Plate.

	A	B	C	D	E	F	G	H	I	J	K
1	0.5	0.42	0.36	0.21	0.04	0.15	1.0	1.48	0.58	0	0
2	0.38	0.346	0.2925	0.236	0.219	0.367	0.932	1.4	0.537	0.052	0
3	0.2	0.210	0.231	0.312	0.457	0.685	0.888	1.17	0.495	0.228	0.1
4	0.14	0.174	0.266	0.408	0.58	0.752	0.851	0.86	0.45	0.322	0.3
5	0.14	0.1914	0.309	0.465	0.627	0.765	0.838	0.845	0.437	0.393	0.3
6	0.19	0.237	0.352	0.502	0.653	0.78	0.85	0.87	0.452	0.465	0.5
7	0.245	0.301	0.4	0.54	0.685	0.81	0.906	0.93	0.494	0.545	0.6
8	0.34	0.375	0.458	0.586	0.729	0.866	0.956	0.97	0.561	0.64	0.7
9	0.41	0.452	0.523	0.642	0.79	0.956	1.089	1.14	0.665	0.753	0.84
10	0.5	0.528	0.604	0.701	0.854	1.07	1.315	1.48	0.801	0.854	0.9
11	0.57	0.596	0.649	0.753	0.91	1.151	1.92	3.0	1.086	0.88	0.86
13	0.64	0.653	0.699	0.79	0.935	1.146	1.676	1.93	1.515	0.976	0.8
14	0.7	0.702	0.74	0.821	0.945	1.14	1.33	1.43	1.32	1.11	0.96
15	0.74	0.749	0.784	0.85	0.957	1.086	1.202	1.25	1.195	1.121	1.12

SIDE WELD. CENTRAL HOLE IN COVER PLATE.

Thickness of each Cover Plate = 0·1875 inches.
Thickness of Main Plate = 0·1875 inches.

Computer Results. $\frac{\sigma_1 - \sigma_3}{\sigma_{AT\ main\ plate}}$

Cover Plate.

	A	B	C	D	E	F	G	H
1	0	0	0	0	0	1·53	2·08	3·0
2	0	0	0	0	0	1·486	1·68	1·8
3	0	0	0	0	0	1·363	1·270	1·230
4	0	0	0	0	0·3853	0·8838	1·055	1·11
5	0	0	0	0·0682	0·4993	0·7515	0·9401	1·01
6	0·040	0·042	0·040	0·1592	0·3947	0·6424	0·6802	0·695
7	0·1	0·0644	0·0439	0·1119	0·3110	0·5668	0·8064	0·92
8	0·085	0·0514	0·0392	0·0892	0·2711	0·5250	0·7958	0·925
9	0·065	0·0418	0·0482	0·1041	0·2498	0·4983	0·8280	1·01
10	0·09	0·0953	0·1145	0·1414	0·2205	0·4315	0·9089	1·14
11	0·2	0·2139	0·2364	0·2547	0·2713	0·3160	1·12	1·38
12	0·28	0·28	0·31	0·35	0·31	0·23	1·43	1·74

Main Plate.

	A	B	C	D	E	F	G	H	I	J	K
1	0·72	0·7	0·63	0·52	0·26	0·22	2·1	2·88	1·15	0	0
2	0·6	0·593	0·5341	0·4666	0·3859	0·5052	1·72	2·38	1·14	0·1087	0
3	0·4	0·365	0·3582	0·4181	0·6019	1·00	1·270	1·37	1·122	0·4669	0·1
4	0·235	0·2553	0·3361	0·4993	0·7410	1·034	1·286	1·38	0·9806	0·6538	0·5
5	0·185	0·2287	0·3595	0·5486	0·7661	0·9761	1·120	1·16	0·8966	0·7592	0·7
6	0·2	0·2485	0·3874	0·5706	0·7602	0·9261	1·021	1·06	0·8365	0·8304	0·82
7	0·255	0·2968	0·4218	0·5896	0·7603	0·9065	0·9770	1·00	0·7975	0·8809	0·92
8	0·33	0·3640	0·4686	0·6191	0·7785	0·9202	0·9839	1·00	0·7881	0·9258	0·9
9	0·4	0·4419	0·5277	0·6622	0·8170	0·9705	1·053	1·08	0·8199	0·9767	1·0
10	0·5	0·5225	0·5932	0·7142	0·8693	1·053	1·215	1·26	0·9050	1·014	1·0
11	0·58	0·5981	0·6563	0·7636	0·9136	1·124	1·685	1·96	1·051	0·9869	0·9
13	0·65	0·6636	0·7110	0·8023	0·9344	1·113	1·5	1·83	1·365	1·026	0·9
14	0·7	0·7199	0·7579	0·8337	0·9420	1·096	1·246	1·3	1·249	1·107	1·0
15	0·765	0·7694	0·8029	0·8611	0·9526	1·057	1·153	1·175	1·156	1·109	1·0

PICTORIAL PLOT OF $\frac{\sigma_1 - \sigma_2}{\tau_{AY(MAIN\ PLATE)}}$ FOR COVER PLATE. (COMPUTER)

SIDE WELD COVER PLATE. (Fig 5.7)

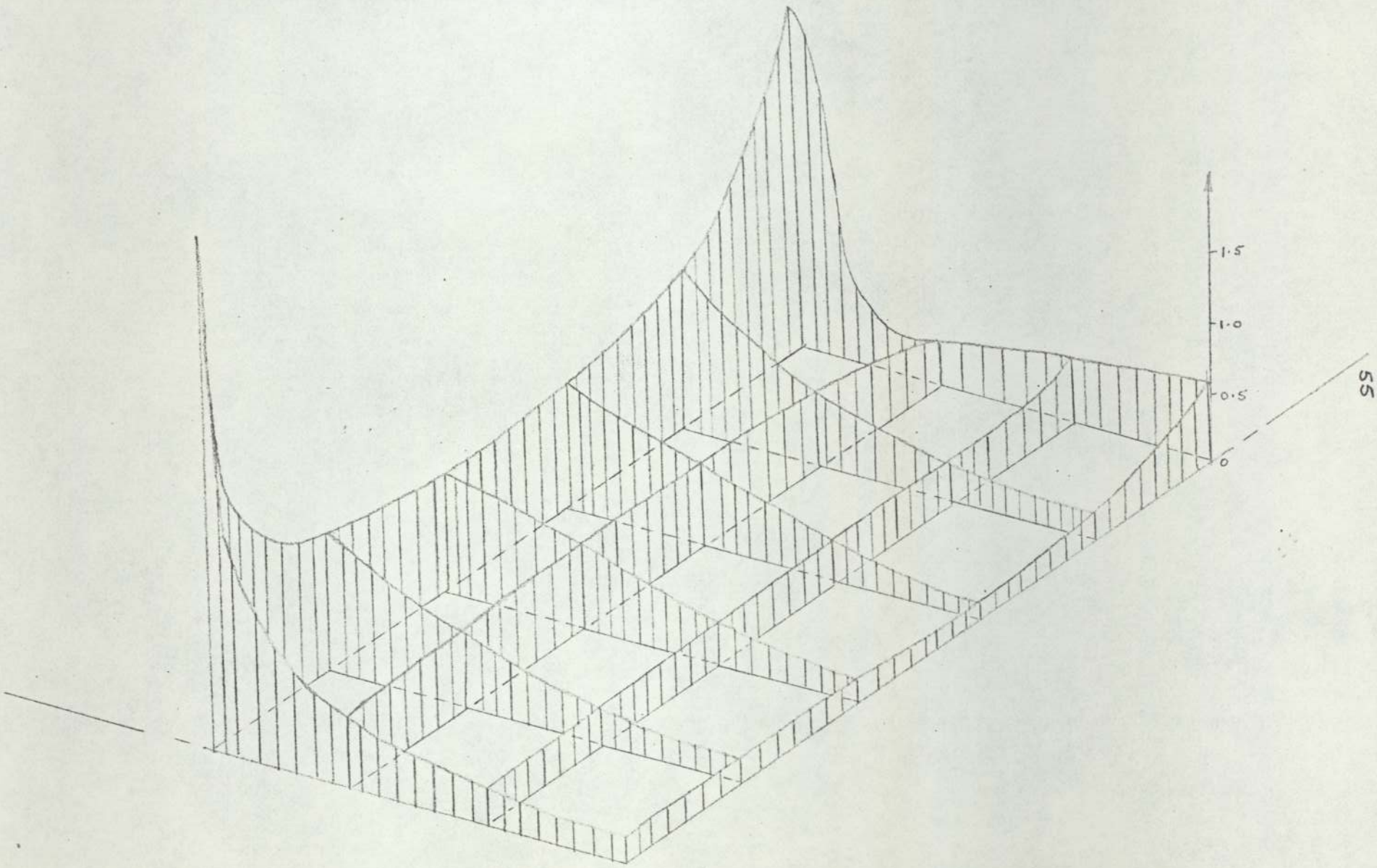

PICTORIAL PLOT OF $\frac{\sigma}{\sigma_{av(MAIN\ PLATE)}}$ FOR MAIN PLATE (COMPUTER.)

SIDE WELD COVER PLATE. (Fig 5.8.)

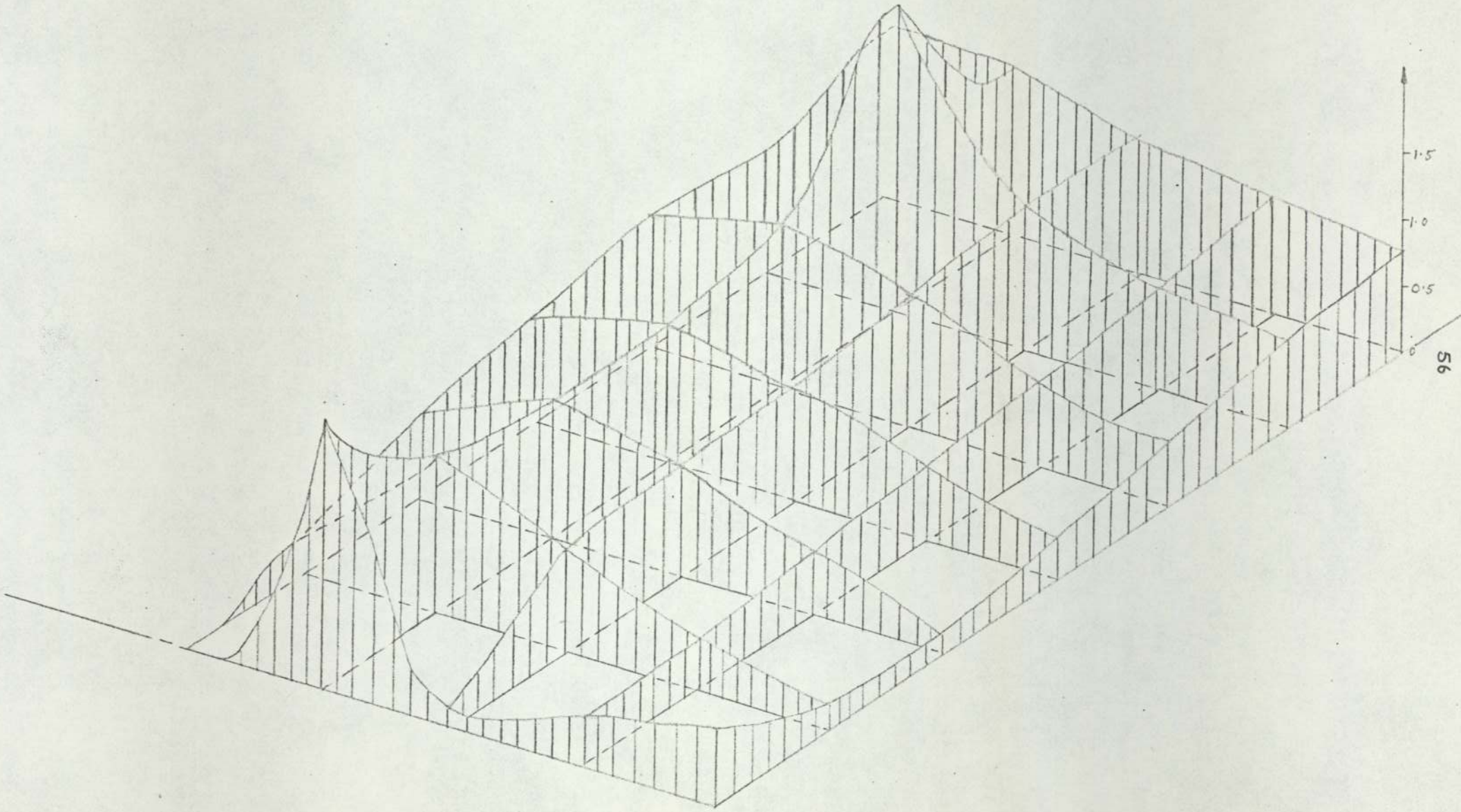

PICTORIAL PLOT OF $\frac{\sigma_1 - \sigma_2}{\sigma_{AV(MAIN\ PLATE)}}$ FOR COVER PLATE (COMPUTER)

WELD ALL ROUND COVER PLATE. (Fig 5.9)

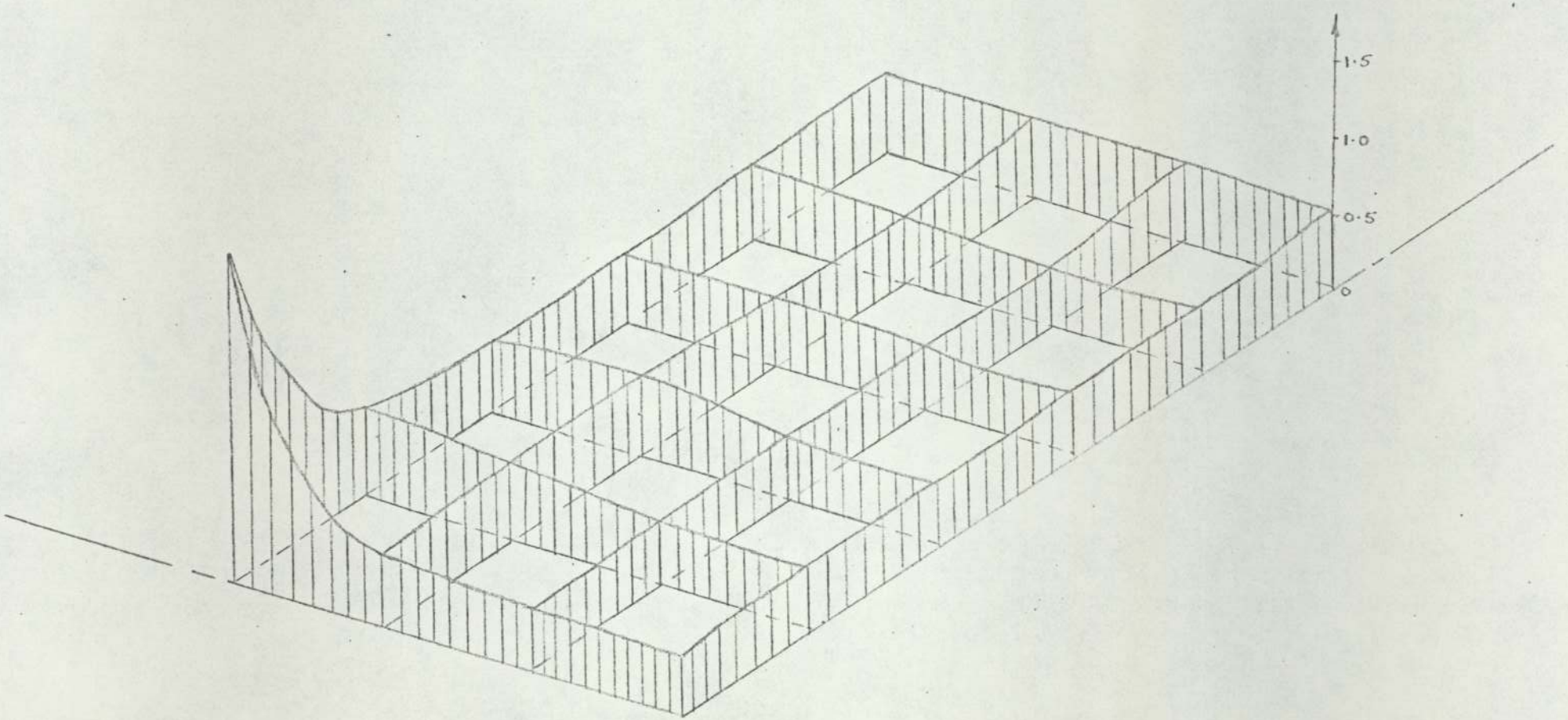

PICTORIAL PLOT OF $\frac{\sigma_1 - \sigma_2}{\sigma_{AV(MAIN\ PLATE)}}$ FOR MAIN PLATE (COMPUTER).

WELD ALL ROUND COVER PLATE. (Fig 5.10)

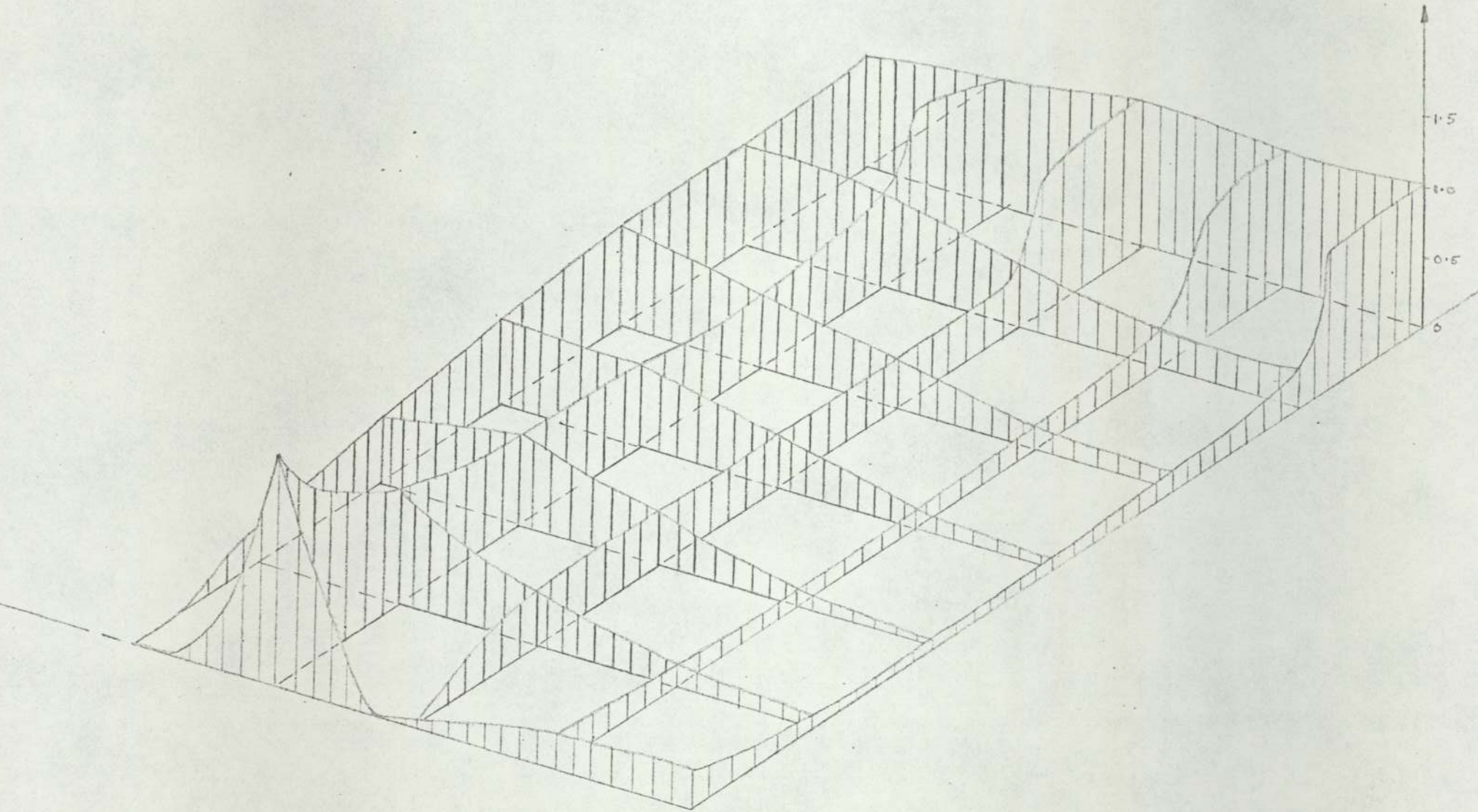

PLOT OF VALUES OF $\frac{\sigma_1 - \sigma_2}{\sigma_{AV(MP)}}$ FOR MAIN PLATE ALONG SIDE WELD LINE.

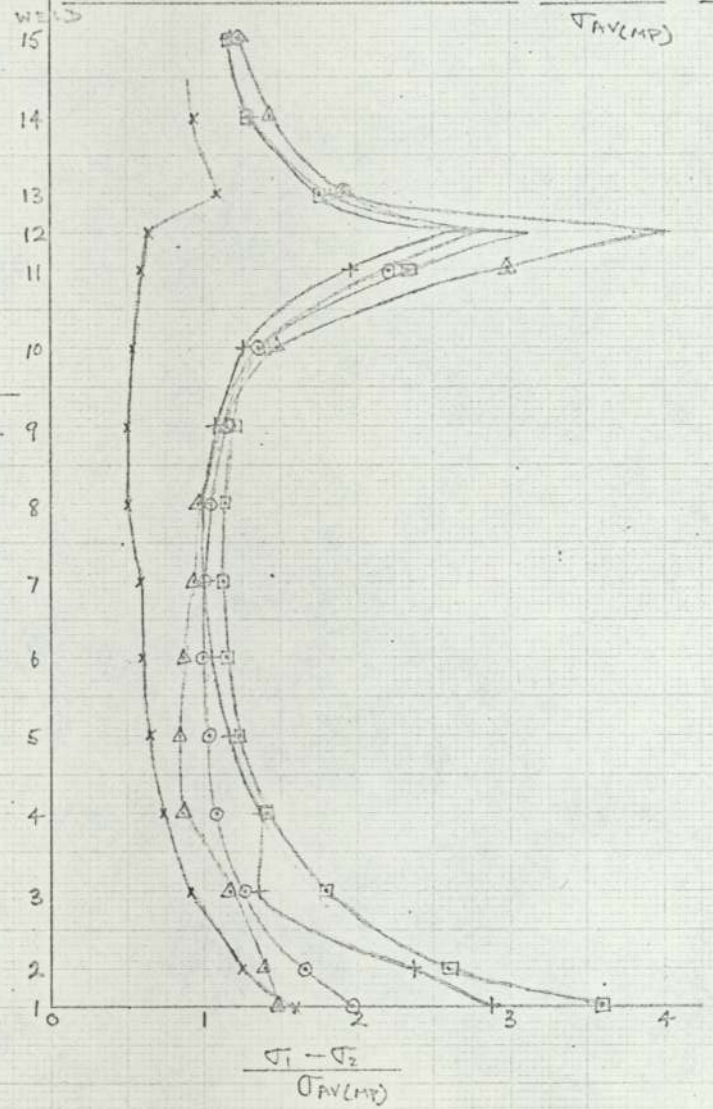

Graph 1.

× Weld all round cover plate. Each cover plate 3/16". Main plate 3/16".

⊙ Side weld cover plate. Each cover plate 3/16". Main plate 3/16".

△ Side weld cover plate. Each cover plate 3/16". Main plate 3/32".

⊡ Side weld cover plate. Each cover plate 3/32". Main plate 3/16".

\+ Side weld cover plate. Each cover plate 3/16". Main plate 3/16". (Hole cut in centre of cover plate).

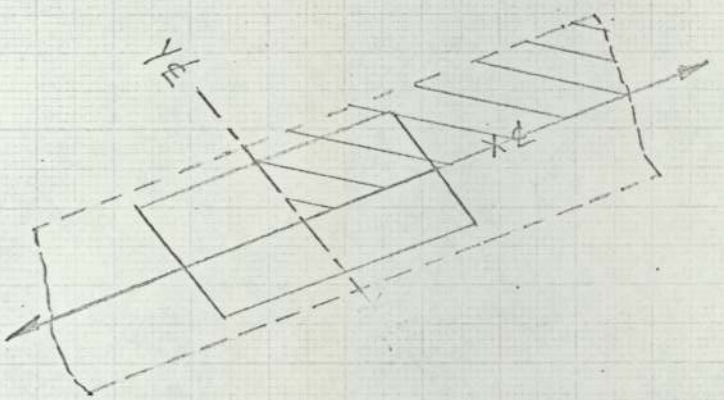

PLOT OF VALUES OF $\frac{\sigma_1 - \sigma_2}{\sigma_{AV(MP)}}$ FOR COVER PLATE ALONG SIDE WELD LINE.

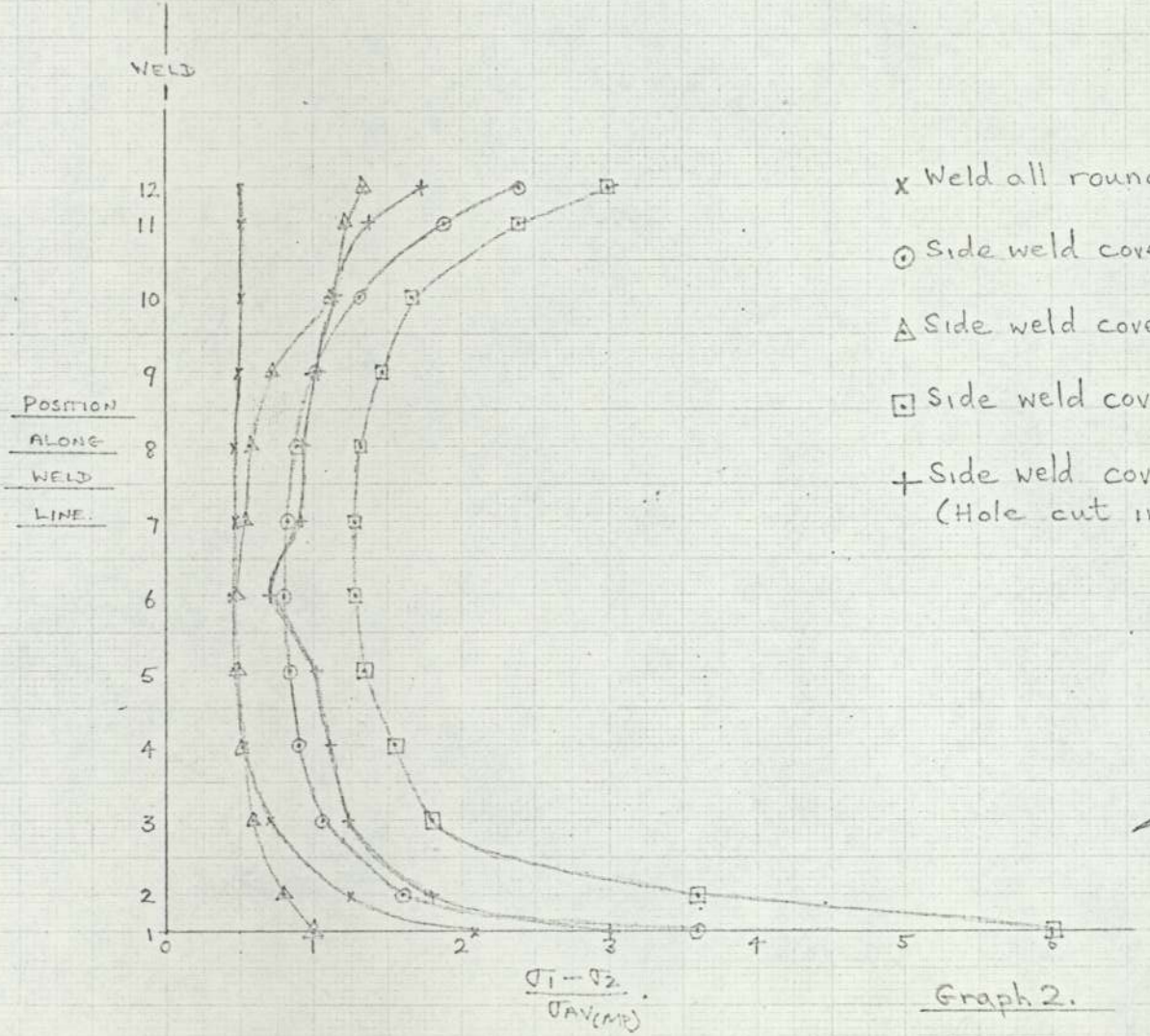

x Weld all round cover plate. Each cover plate 3/16". Main plate 3/16".

⊙ Side weld cover plate. Each cover plate 3/16". Main plate 3/16".

△ Side weld cover plate. Each cover plate 3/16". Main plate 3/32".

⊡ Side weld cover plate. Each cover plate 3/32" Main plate 3/16".

+ Side weld cover plate. Each cover plate 3/16". Main plate 3/16". (Hole cut in centre of cover plate).

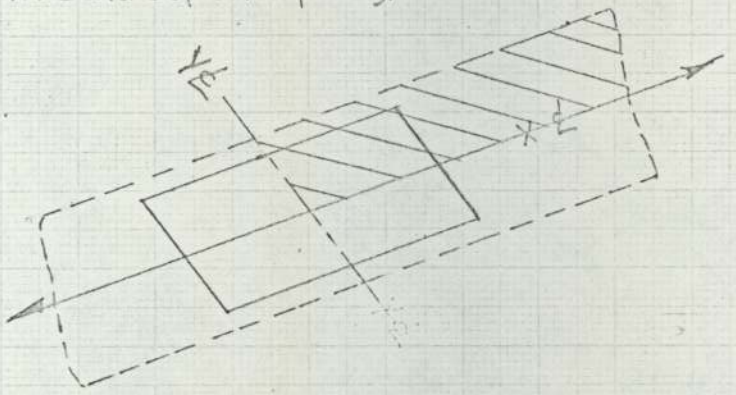

Graph 2.

PLOT OF $\frac{\sigma_1 - \sigma_2}{\sigma_{AV(MP)}}$ ALONG Y ℄ OF MAIN PLATE.

× Weld all round cover plate. Each cover plate $\frac{3}{16}$". Main plate $\frac{3}{16}$".

⊙ Side weld cover plate. Each cover plate $\frac{3}{16}$". Main plate $\frac{3}{16}$".

△ Side weld cover plate. Each cover plate $\frac{3}{16}$". Main plate $\frac{3}{32}$".

⊡ Side weld cover plate. Each cover plate $\frac{3}{32}$". Main plate $\frac{3}{16}$".

\+ Side weld cover plate. Each cover plate $\frac{3}{16}$" Main plate $\frac{3}{16}$". (Hole cut in centre of cover plate).

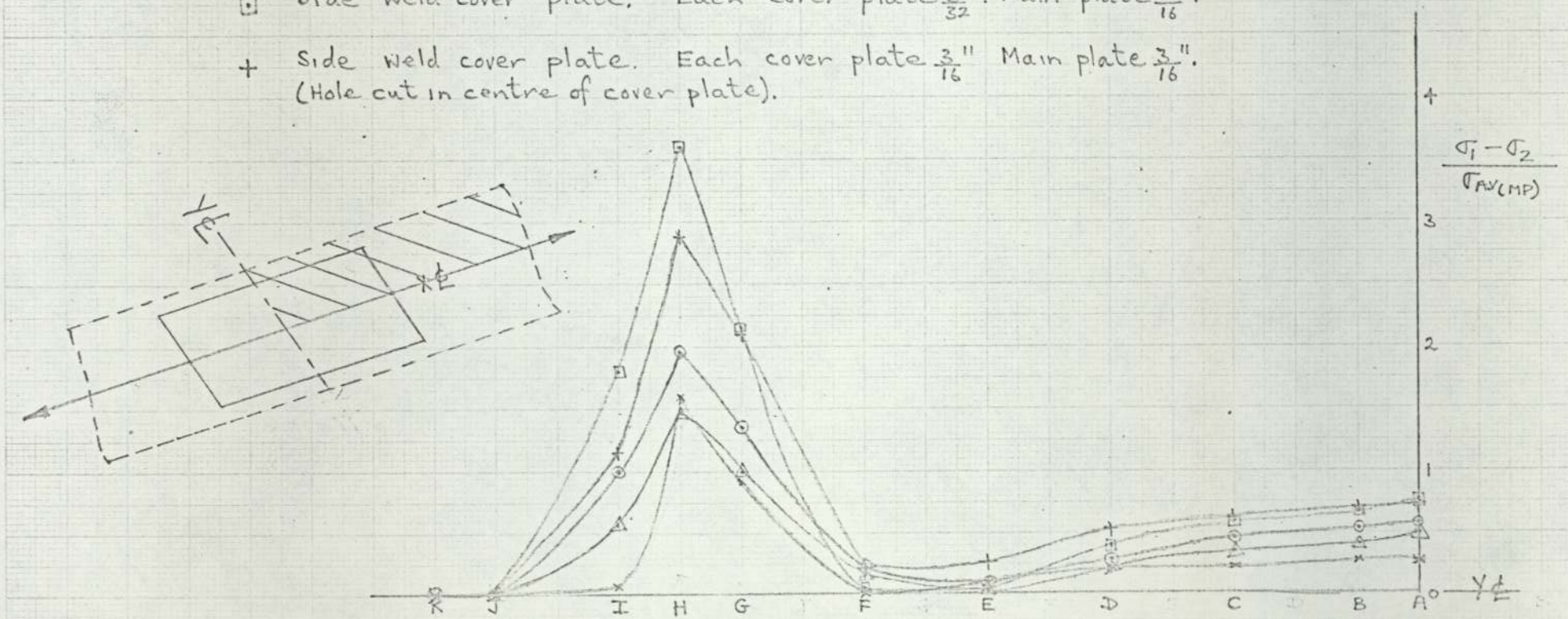

Graph 3

PLOT OF $\frac{\sigma_1 - \sigma_2}{\sigma_{AV(MP)}}$ ALONG Y/C OF COVER PLATE

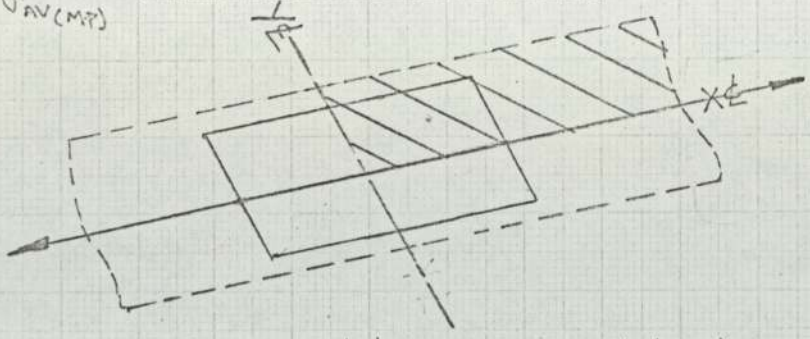

X Weld all round cover plate Each cover plate $\frac{3}{16}$" Main Plate $\frac{3}{16}$"

⊙ Side weld cover plate, Each cover plate $\frac{3}{16}$" Main Plate $\frac{3}{16}$"

△ Side weld cover plate. Each cover plate $\frac{3}{16}$" Main Plate $\frac{3}{32}$"

⊡ Side weld cover plate. Each cover plate $\frac{3}{32}$" Main Plate $\frac{3}{16}$"

+ Side weld cover plate Each cover plate $\frac{3}{16}$" Main Plate $\frac{3}{16}$". (Hole cut in centre of cover plate)

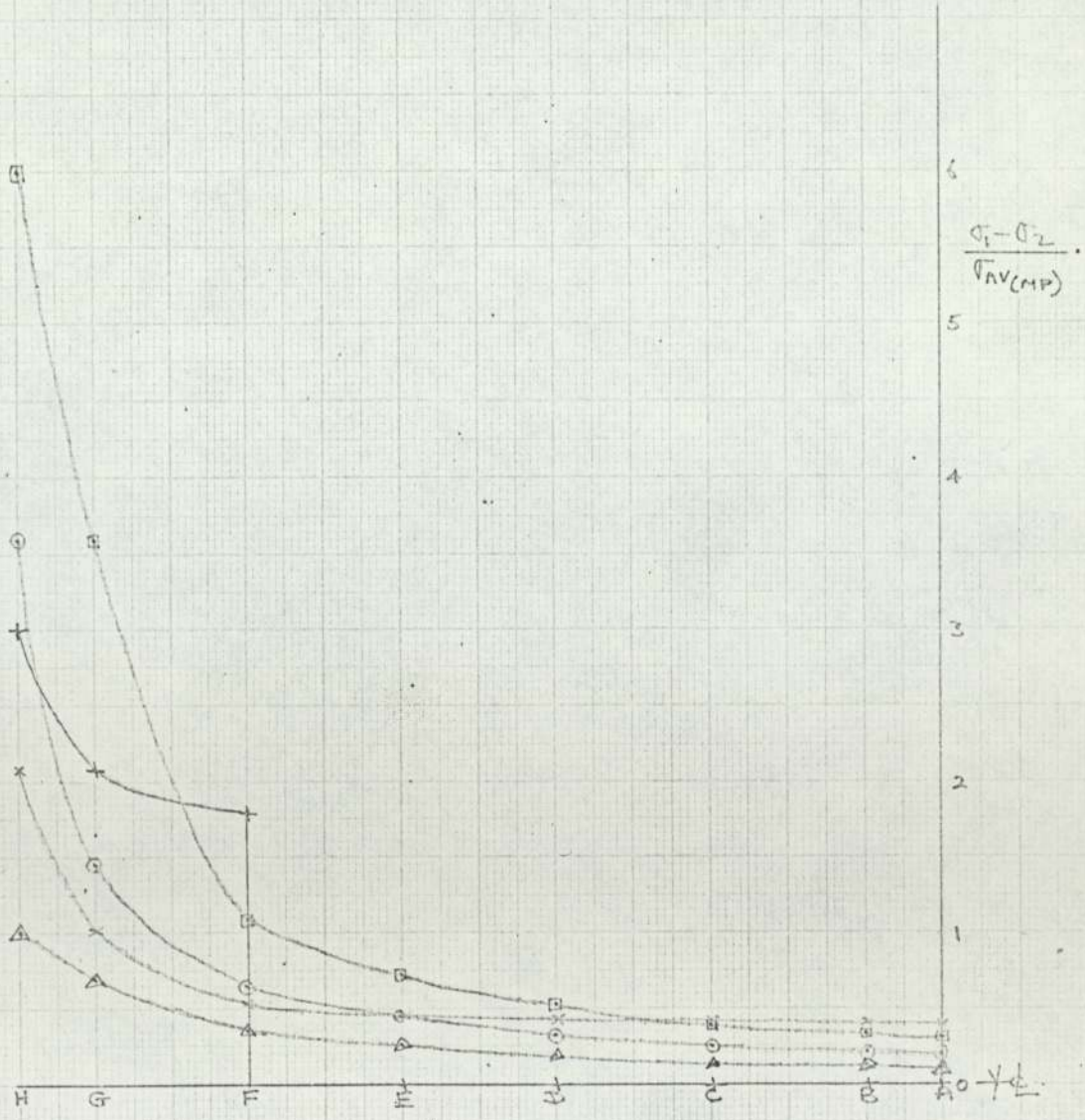

Graph 4

DIAGRAM SHOWING TRANSFER OF LOAD BETWEEN MAIN PLATE AND COVER PLATE.

—△— Load in Cover Plate (Weld all round).

—□— Load in Main Plate (Weld all round).

—⊙— Load in Cover Plate (Side Weld).

—×— Load in Main Plate (Side Weld).

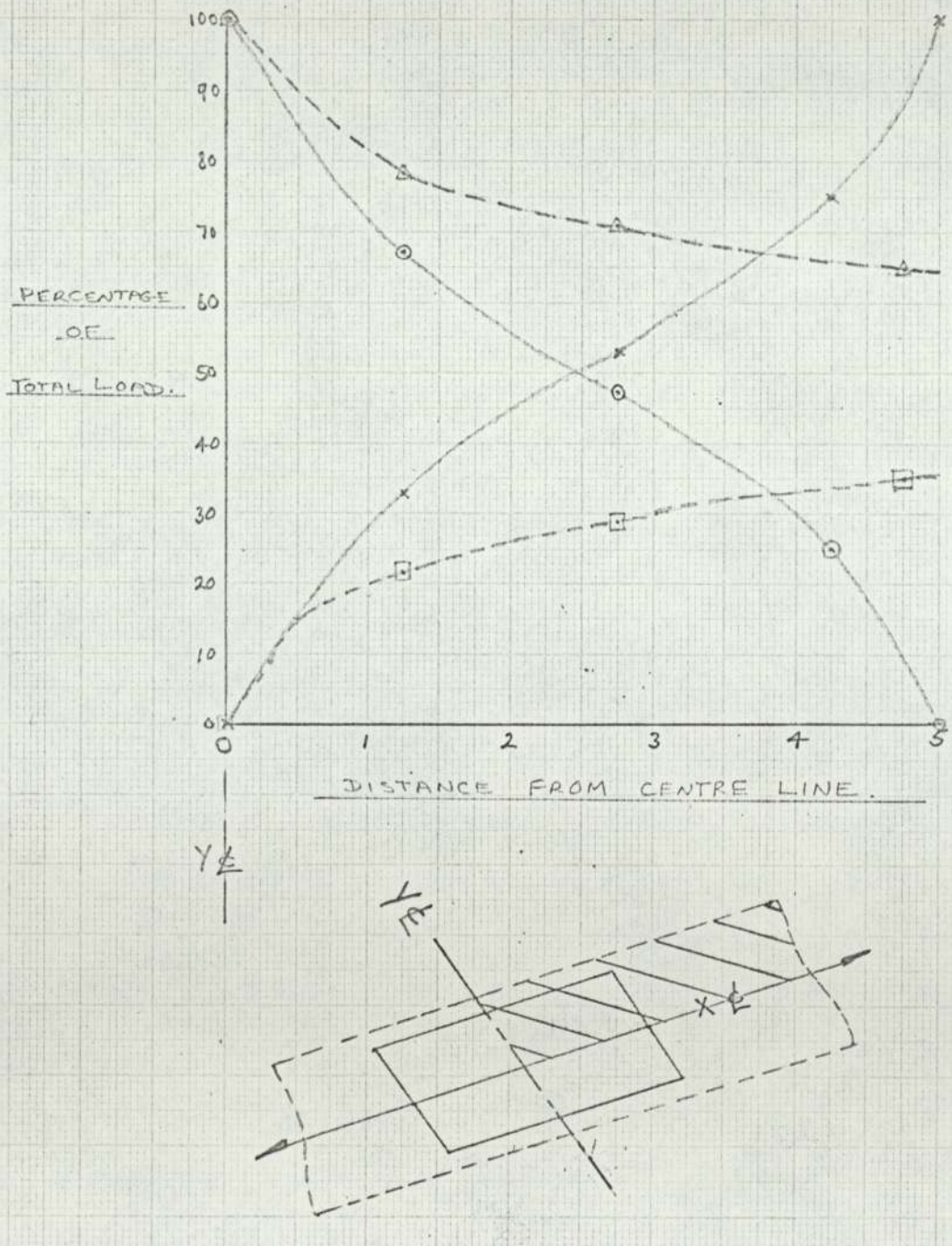

Graph 5.

5.5 EQUILIBRIUM CHECK FOR 3/16 INCH COMPUTER MODEL (SIDE WELD COVER PLATE)

As a verification of the computer results an equilibrium check was made at various sections of the welded connection.

ALONG Y ℄ (Graph 6)

Cover Plate $\sum \sigma_x = 41.38$ lbf/in² $\delta A = \frac{1}{2} \times \frac{3}{16} = \frac{3}{32}$ in²

Load carried by cover plate $= 41.38 \times \frac{3}{32} \times 4 = 15.52$ lbf

Applied Load = 16.0 lbf.

% Difference $= \frac{0.48 \times 100}{16} = 3\%$

Along line through elements 201/203 (Graph 7)

Cover Plate $\sum \sigma_x = 20.168$ lbf/in²

Load carried by Cover Plate $= 20.168 \times \frac{12}{32} = 7.563$ lbf.

Main Plate $\sum \sigma_x = 45.178$ lbf/in²

Load carried by Main Plate $= 45.178 \times \frac{3}{16} = 8.472$ lbf.

Total Load carried by plates = 16.035 lbf.

% Difference $= \frac{0.035 \times 100}{16} = 0.219\%$

Along line through top edge of cover plate. (Graph 8)

Main Plate $\sum \sigma_x = 80.76$ ibf/in²

Load carried by main Plate $= 80.76 \times \frac{3}{16} = 15.2$ lbf.

Applied Load = 16.0 lbf.

%Difference $= \frac{0.8 \times 100}{16} = 5\%$

Along line through elements 401/402 (Graph 9)

Main Plate $\sum \sigma_x = 85.93$ lbf/ in²

Load carried by main plate $= 85.93 \times \frac{3}{16} = 16.11$ lbf.

Applied Load = 16.0 lbf.

%Difference $= \frac{0.11 \times 100}{16} = 0.687\%$

COMPUTER RESULTS. SIDE WELD COVER PLATE.

EQUILBRIUM CHECK.

Cover Plate Values σ_x lbf/in². 16·0 7·42 5·7 4·6 4·0 3·6 Y ℄

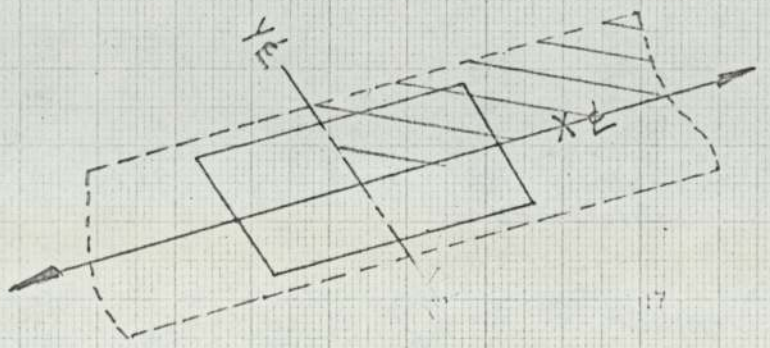

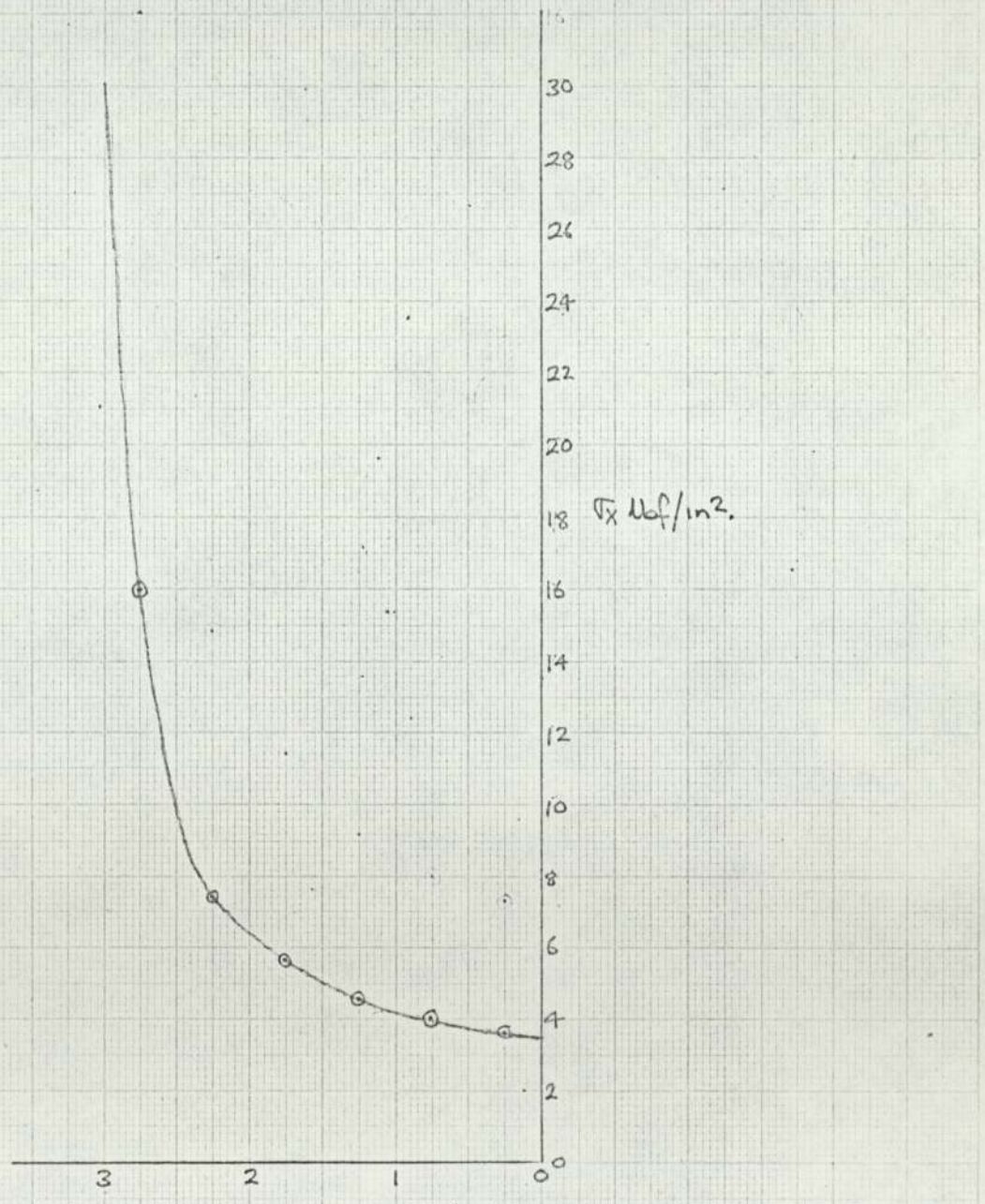

Graph 6

COMPUTER RESULTS. SIDE WELD COVER PLATE.

EQUILIBRIUM CHECK.

Cover Plate Values σ_x lbf/in^2. 5·768 4·505 3·418 2·598 2·014 1·815

2011
203

Main Plate Values σ_x lbf/in^2. 7·571 6·657 6·366 5·871 5·335 4·809 4·401 4·168

⊙ Cover Plate.
x Main Plate.

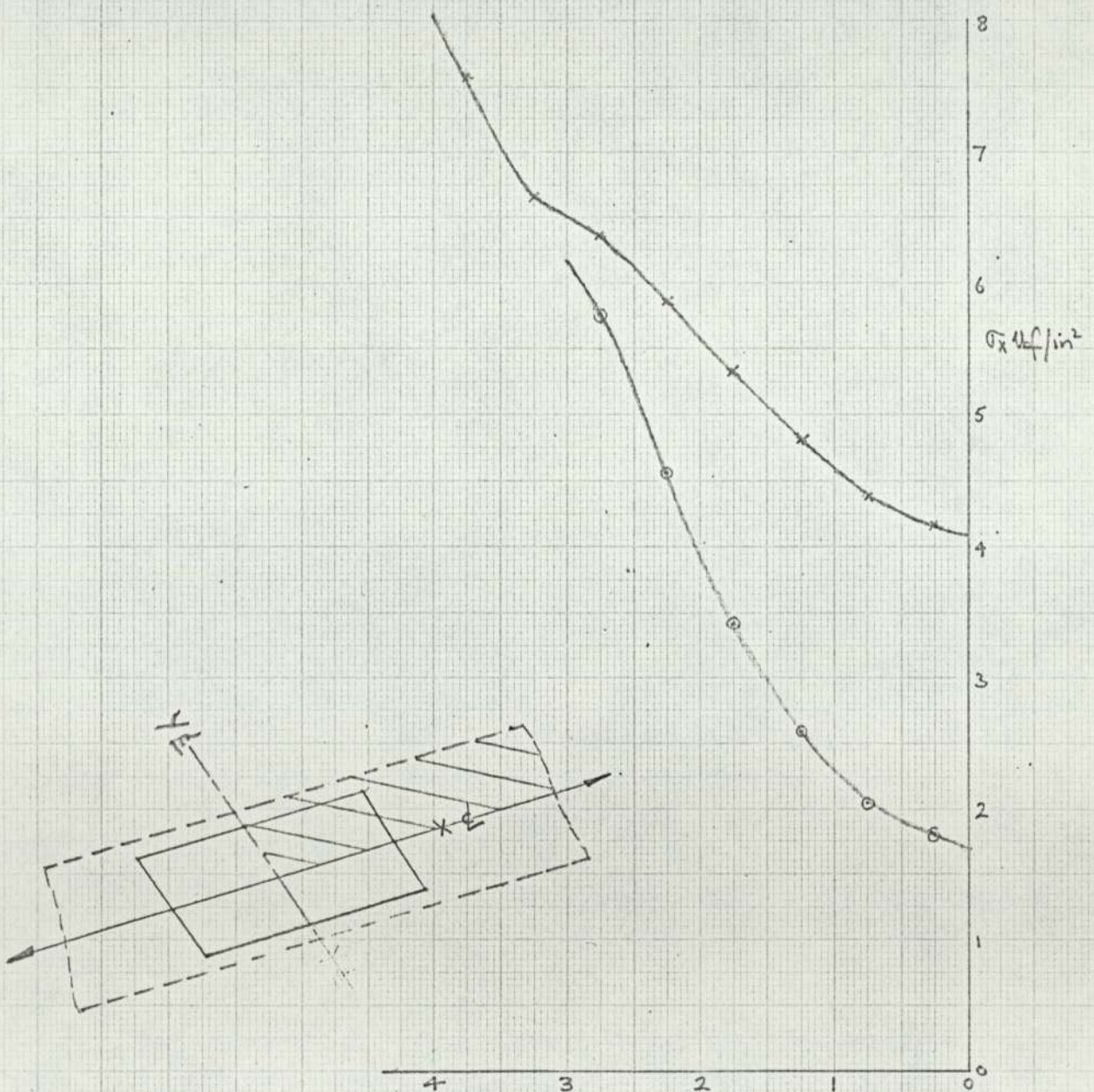

Graph 7

COMPUTER RESULTS. SIDE WELD COVER PLATE.

EQUILIBRIUM CHECK.

Main Plate values σ_x Ibf/in².	10·0	13·5	12·75	10·49	9·32	8·62	8·2	7·9

Top Edge of Cover Plate.

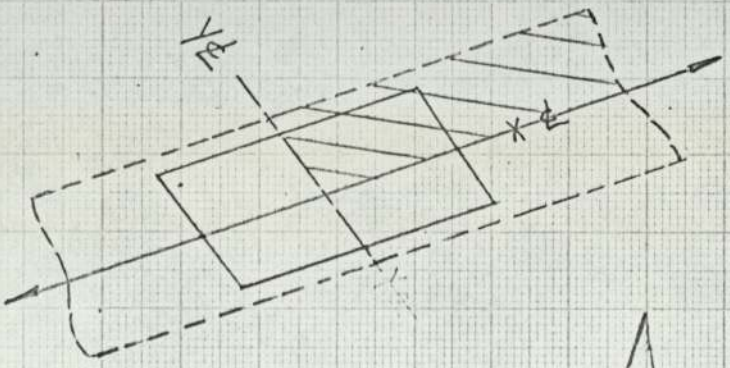

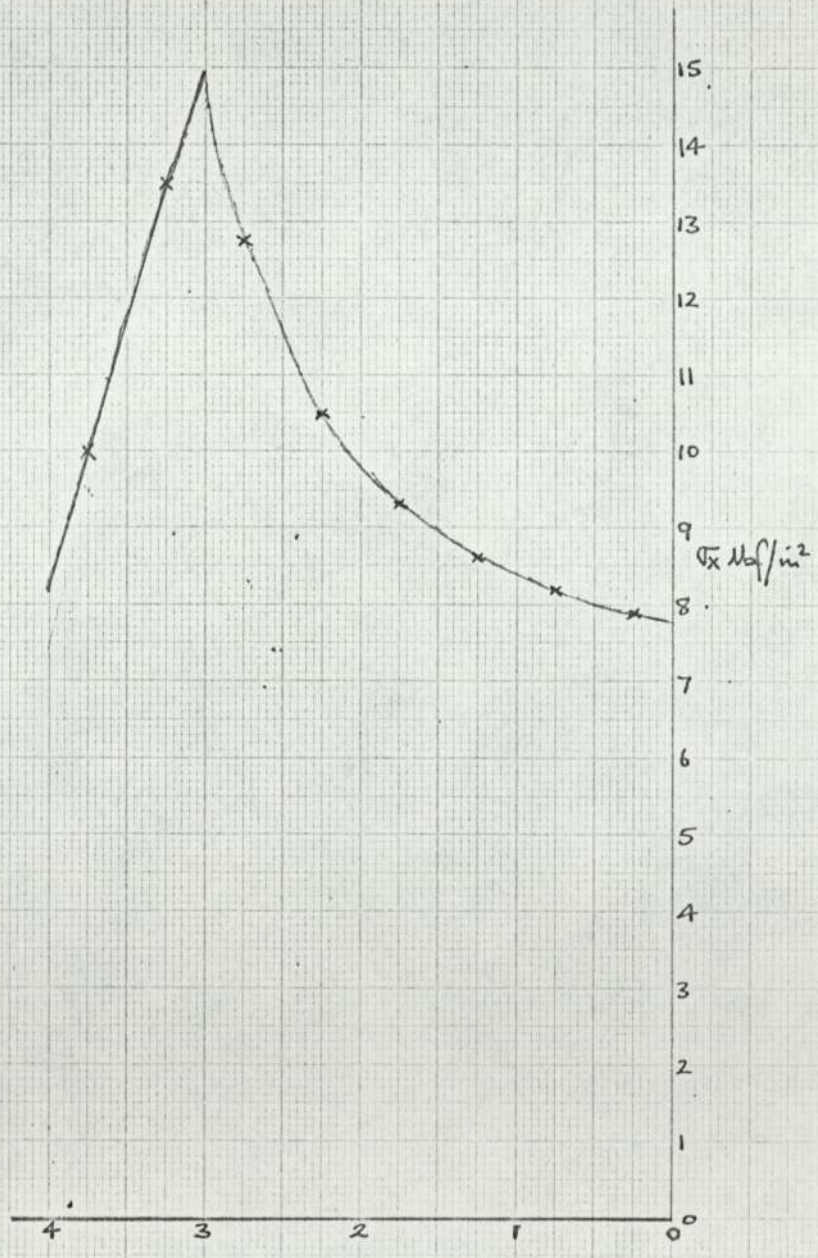

Graph 8

Computer Results. Side Weld Cover Plate.

Equilibrium Check

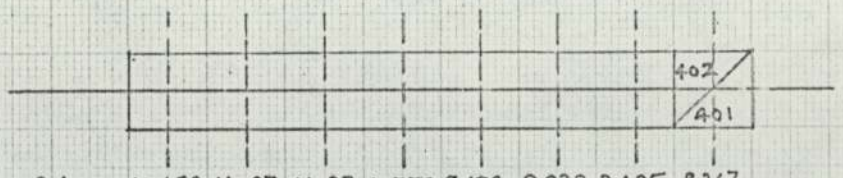

Main Plate Values σ_x Ibf/in^2. 10·652 14·87 14·27 10·758 9·692 8·938 8·485 8·267

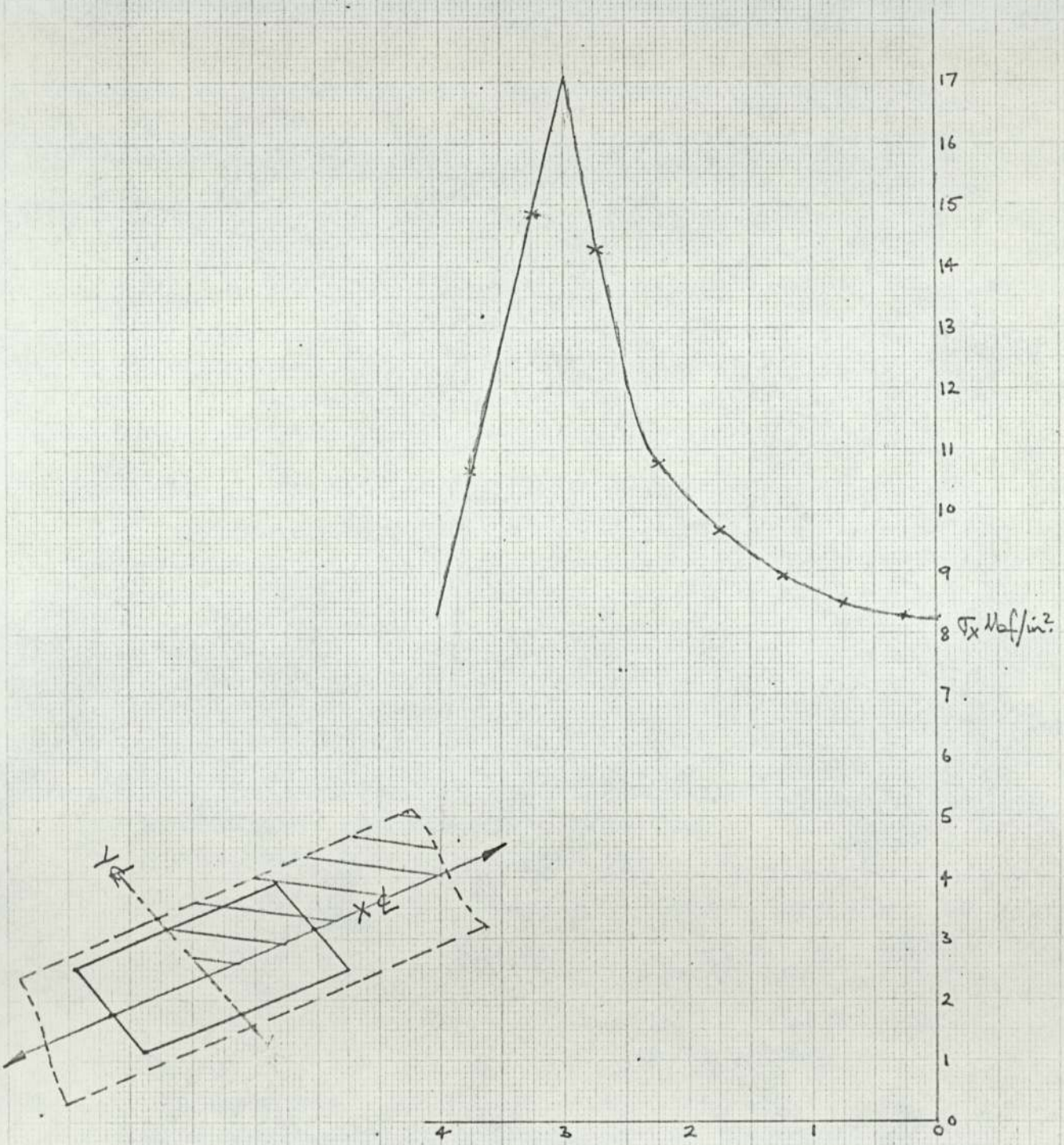

Graph 9

5.6 EQUILIBRIUM CHECK FOR COMPUTER MODEL (WELD ALL ROUND COVER PLATE)

As a verification of the computer results on equilibrium check was made at various sections of the welded connection.

ALONG Y ℄ (graph 10)

Cover Plate $\sum \sigma_x$ = 42.941 lbf/in^2 $\delta A = \frac{1}{2} \times \frac{3}{16} = \frac{3}{32}$ in^2

Load carried by Cover Plate = $42.94 \times \frac{3}{32} \times 4$ = 16.1 lbf.

Applied Load = 16.0 lbf.

%Difference = $\frac{0.1}{16} \times 100 = 0.625\%$

ALONG line through elements 201/203 (Graph 11)

Cover Plate $\sum \sigma_x$ = 30.307 lbf/in^2

Load carried by Cover Plate = $30.307 \times \frac{12}{32}$ = 11.365 lbf.

Main Plate $\sum \sigma_x$ = 24.864 lbf/in^2

Load carried by main plate = $24.864 \times \frac{3}{16}$ = 4.662 lbf.

Total load carried by plates = 16.027 lbf.

Applied load = 16.0 lbf.

%Difference = $\frac{0.027}{16} \times 100 = 0.169\%$

Along line through elements 349/351 (Graph 14)

Cover plate $\sum \sigma_x$ = 27.681 lbf/in^2

Load carried by cover plate = $27.681 \times \frac{12}{32}$ = 10.38 lbf.

Main Plate $\sum \sigma_x$ = 30.098 lbf/in^2

load carried by Main Plate = $30.098 \times \frac{3}{16}$ = 5.64 lbf.

Total load carried by plates = 16.02 lbf.

Applied load = 16 lbf.

%Difference = $\frac{0.02}{16} \times 100\% = 0.125\%$

ALONG Weld line (Graph 12)-

Cover Plate $\sum \sigma_x$ = 27.305 lbf/in^2

Load carried by cover plate = $27.305 \times \frac{12}{32}$ = 10.24 lbf.

Main Plate $\sum \sigma_x$ = 30.702 lbf/in^2

Load carried by main plate = $30.702 \times \frac{3}{16}$ = 5.76 lbf.

Load carried by plates = 16 lbf.

Applied Load = 16%

%Difference = 0%

ALONG Line through elements 401/402 (Graph 13)

Main Plate $\sum \sigma_x$ =85.423 lbf/in^2

Load carried by main plate=85.423 × $\frac{3}{16}$=16.02 lbf.

Applied Load-16lbf.

%Difference=$\frac{0.02}{16}$ × 100=0.125%

COMPUTER RESULTS, WELD ALL ROUND COVER PLATE.

EQUILIBRIUM CHECK.

Cover Plate Values σ_x lbf/in^2 13·75 6·820 5·995 5·615 5·42 5·34 Y ℄

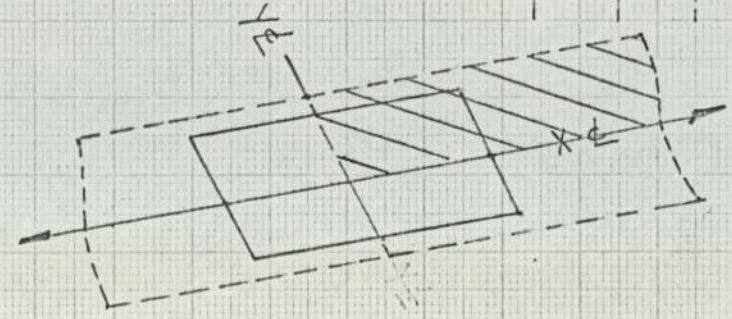

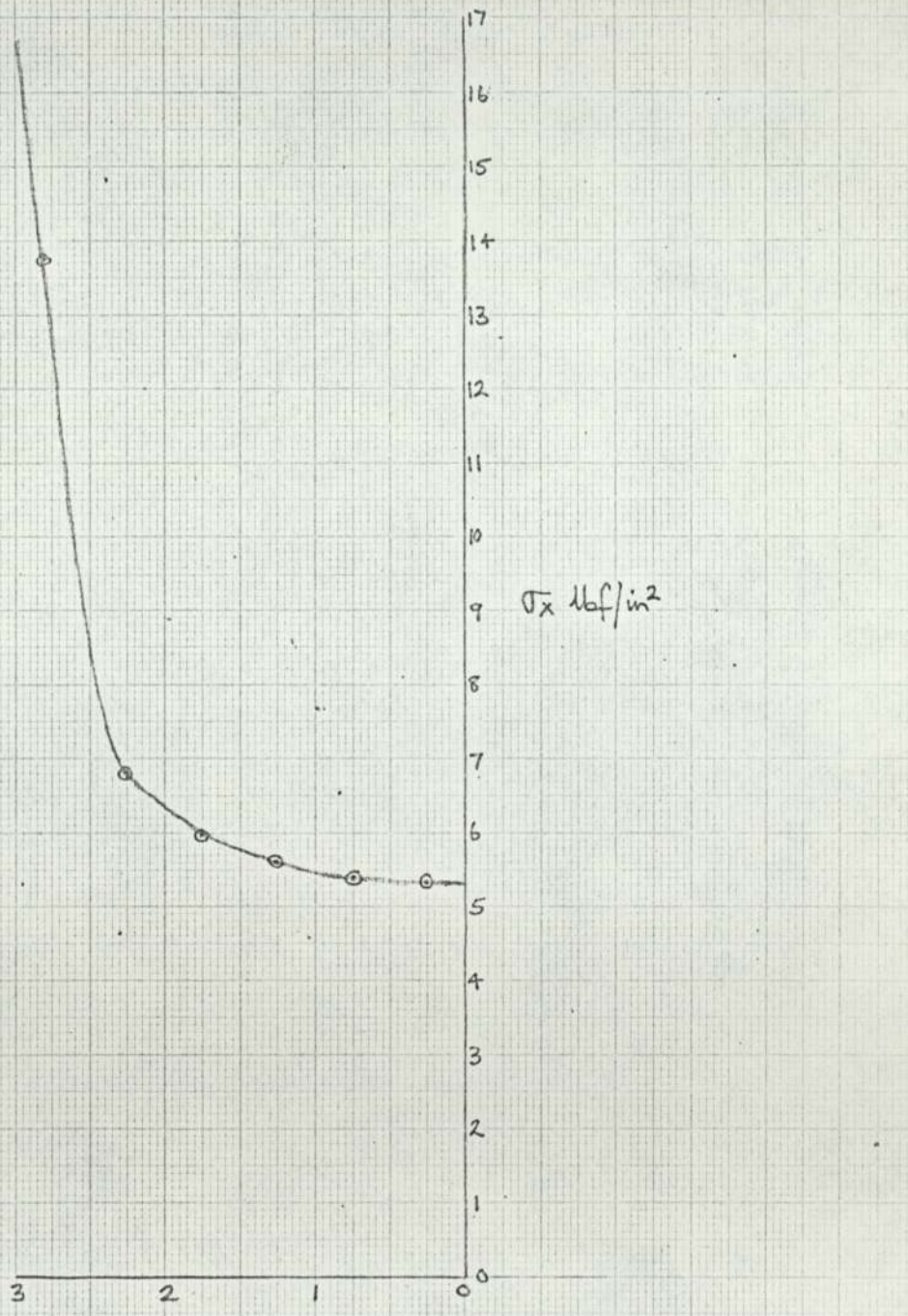

Graph 10

COMPUTER RESULTS. WELD ALL ROUND COVER PLATE.

EQUILIBRIUM CHECK.

Cover Plate Values σ_x lbf/in^2 5·070 5·096 5·068 5·038 5·014 5·001

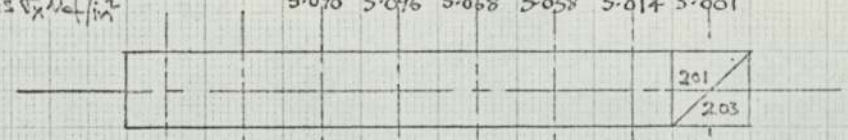

Main Plate Values σ_x lbf/in^2 5·383 5·053 4·330 3·266 2·450 1·813 1·383 1·66

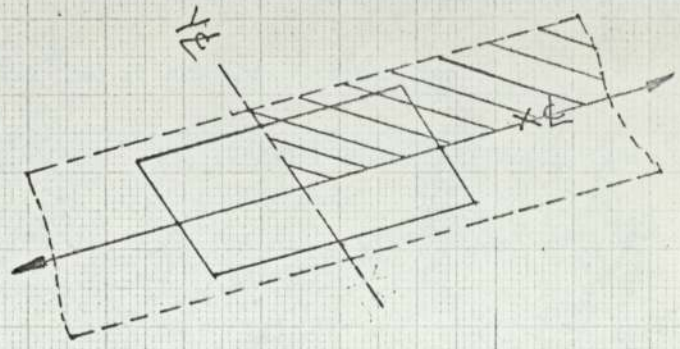

⊙ Cover Plate.

× Main Plate.

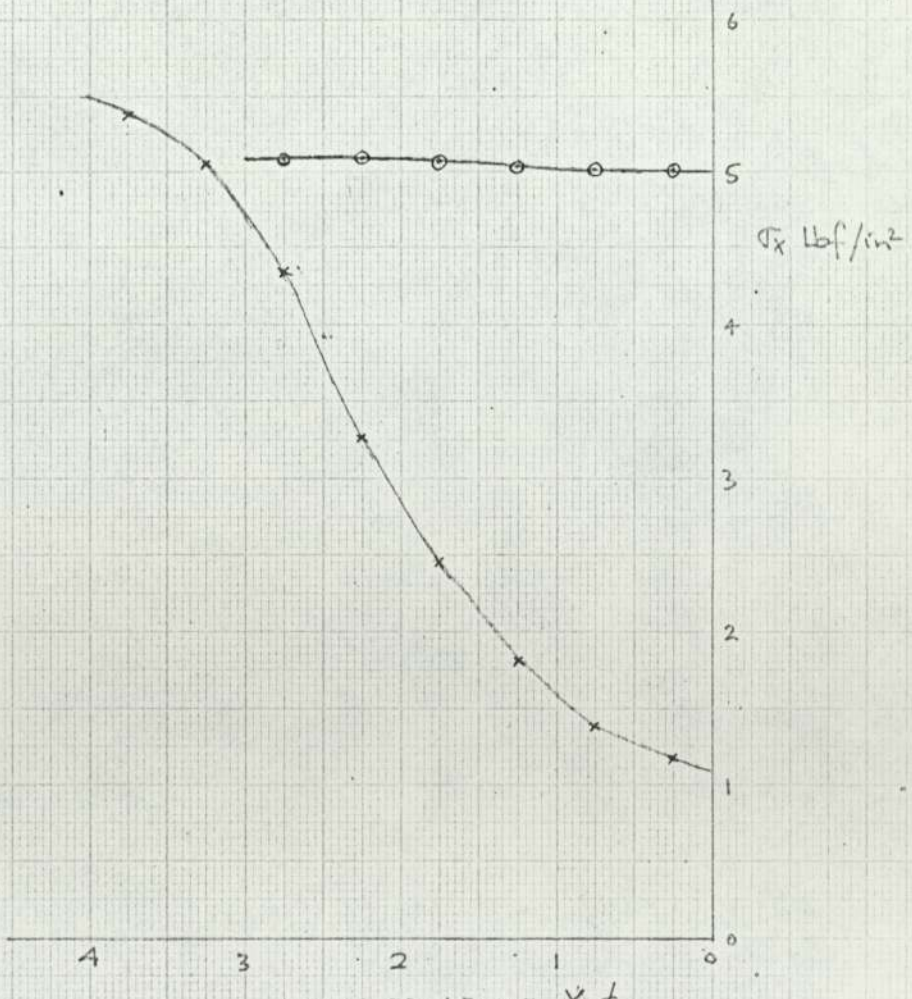

Graph II

COMPUTER RESULTS. WELD ALL ROUND COVER PLATE.

EQUILIBRIUM CHECK.

Cover Plate Values σ_x lbf/in^2			4·55	4·38	4·455	4·575	4·66	4·685
Main Plate Values σ_x lbf/in^2.	7·850	7·750	3·900	3·042	2·350	2·120	1·950	1·740

WELD LINE.

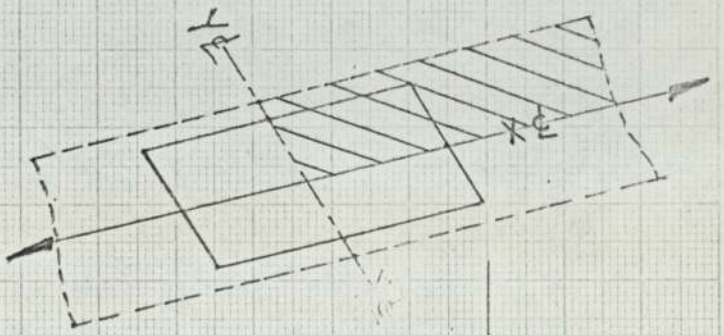

⊙ Cover Plate
× Main Plate

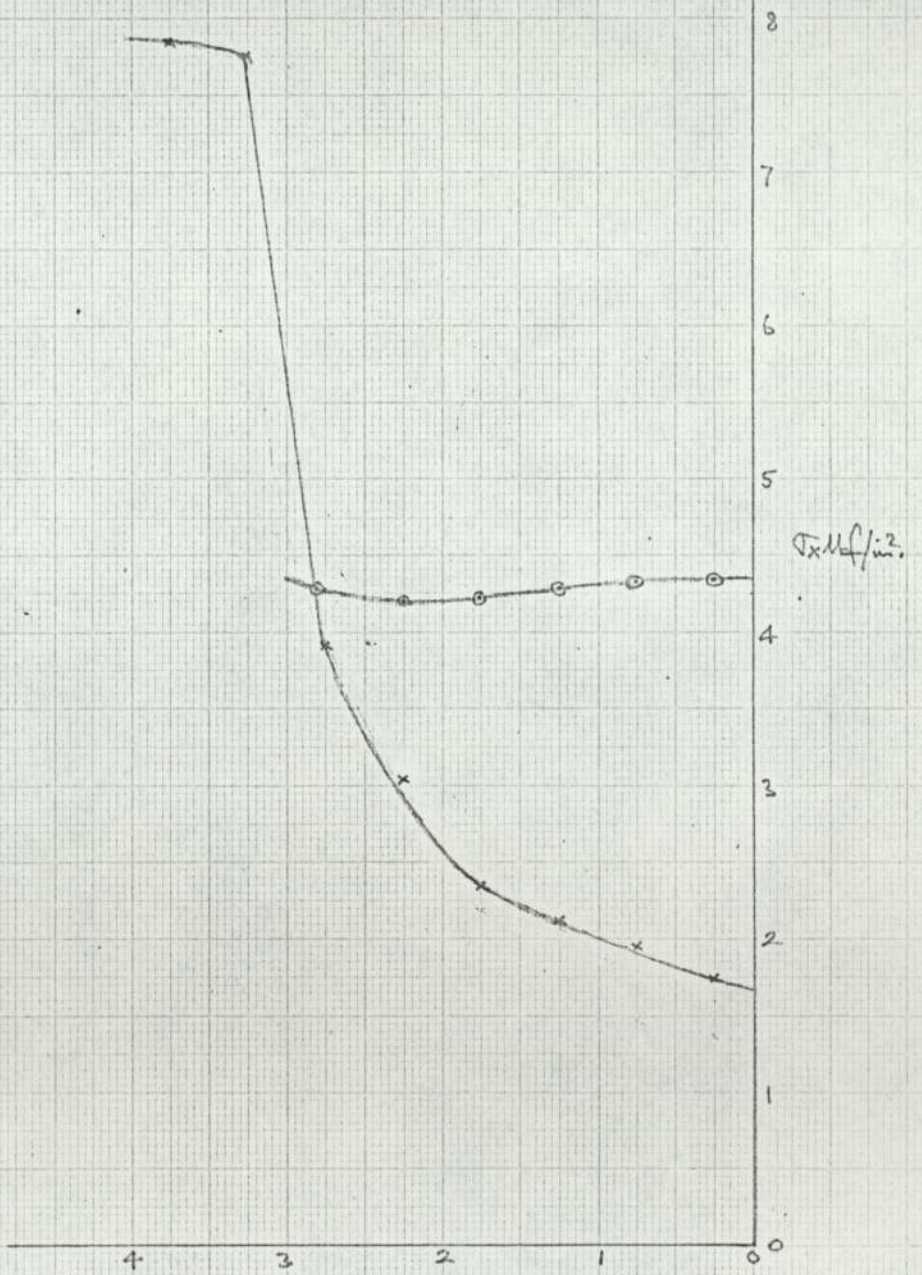

Graph 12

COMPUTER RESULTS. WELD ALL ROUND COVER PLATE.

EQUILIBRIUM CHECK.

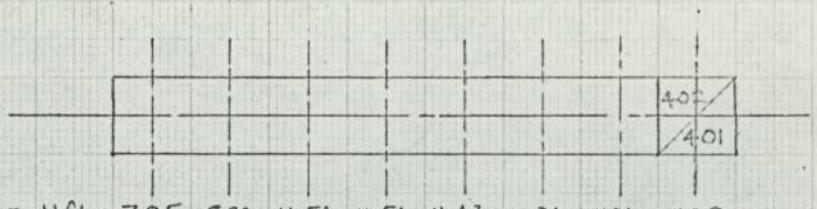

MAIN PLATE VALUES σ_x lbf/in^2 7·95 8·93 11·54 11·56 11·43 11·36 11·31 11·29

x MAIN PLATE.

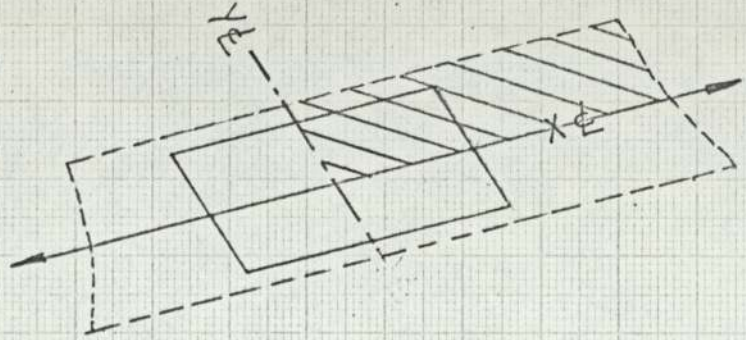

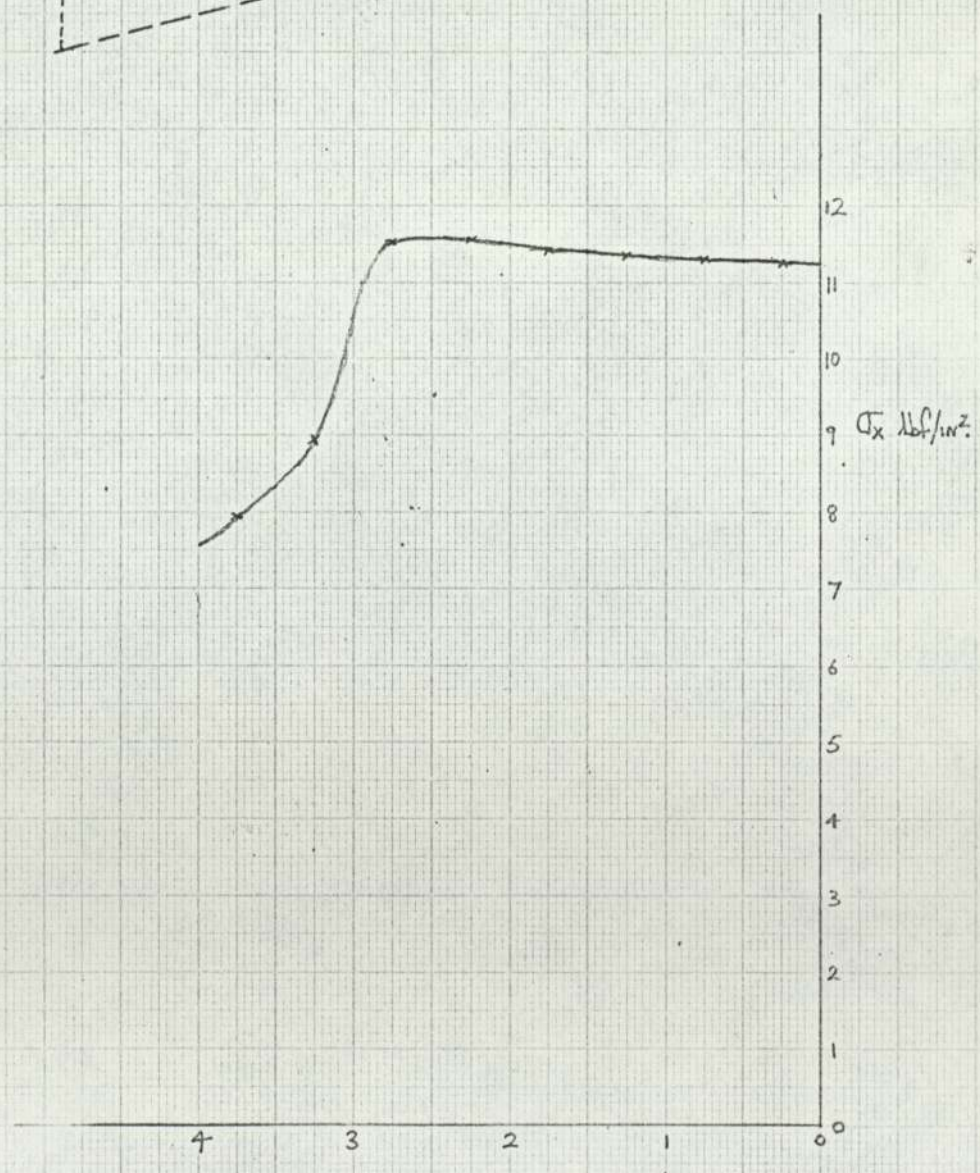

Graph 13

COMPUTER RESULTS. WELD ALL ROUND COVER PLATE.

EQUILIBRIUM CHECK.

Cover Plate Values σ_x lbf/in^2 4·767 4·464 4·497 4·591 4·668 4·694

35 / 349

Main Plate Values σ_x lbf/in^2 7·612 7·023 4·211 3·042 2·484 2·120 1·879 1·727

⊙ Cover Plate.

x Main Plate.

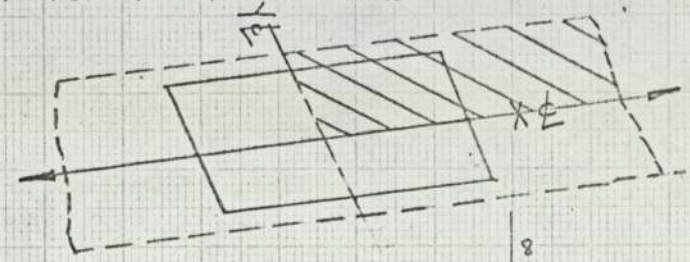

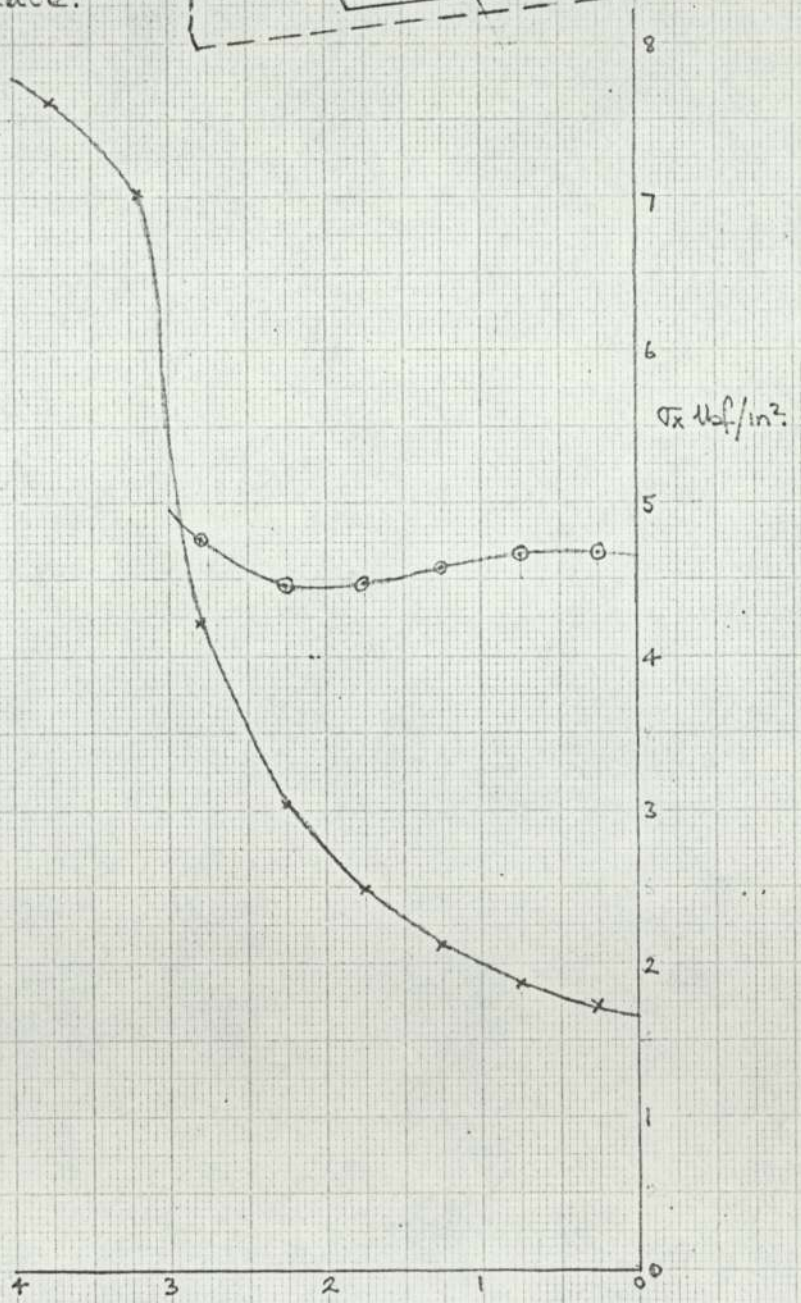

Graph 14

5.7 DISCUUSSION OF FINITE ELEMENT RESULTS

The overall plot of $\frac{\sigma_1 - \sigma_2}{\sigma_{AV(MP)}}$ shown on diagrams indicates that the stresses in the plates are far from uniform.

In the case of the side fillet welded plate peak values occur in both the cover plate and main plate at A and B.

When the weld is taken all round the cover plate, peak stresses occur only at A.

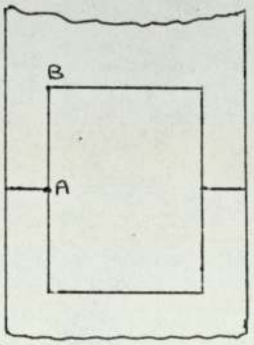

Fig 5.II

Taking the side fillet weld case, with plates of equal thickness as a reference, the table below shows the precentage change in the peak values of $\frac{\sigma_1 - \sigma_2}{\sigma_{AV(MP)}}$ for the variaus plate configurations considered.

PLATE

Change in peak values of $\frac{\sigma_1 - \sigma_2}{\sigma_{AV(MP)}}$ as a percentage of values in side fillet weld case, with each cover plate having the same thickness as the main plate.

	COVER PLATE		MAIN PLATE POSITION	
	A	B	A	B
Each cover plate one half of main plate thickness.	+67%	+25%	+84.5%	+II%
Each cover plate twice the thickness of the main plate.	−72.2%	−43.6%	−23%	+43%
Each cover plate having equal thickness to main plate (Hole cut in centre of cover plates).	−I6.7%	−27%	+48.5%	−5.4%
Each cover plate having equal thickness to main plate (Weld taken all round cover plate)	−4I.6%	−79.2%	−I8%	−76.8%
$\frac{\sigma_1 - \sigma_2}{\sigma_{AV(MP)}}$ Reference Values for equal thickness plates.	3.6	2.4	I.95	2.8

Fig 5.I2

The table shows that when each cover plate has a thickness one half of the main plate thickness, increases occur in all the peak values in both cover plate and main plate. When the main plate thickness is made equal to half the thickness of each cover plate a considerable decrease in peak values in the cover plate is produced while in the main plate one peak is reduced and the other increased.

Keeping the cover plates and main plate thicknesses equal, but cutting holes in the centre of the cover plates, has the effect of reducing the cover plate peaks while increasing considerably one main plate peak and only marginally affecting the other main plate peak.

The most dramatic effect is produced when the cover plates are welded all round, this reduces all the peak values in both cover plates and main plate.

Therefore the best result would be obtained by using a main plate thickness of half the thickness of each cover plate and then welding the cover plates all round. The advantage of this combination is that by using cover plates having twice the thickness of the main plate a considerable reduction is achieved in the peak values at A in the cover plate which is the highest peak obtained in the fully welded condition and also reduces the next highest peak which is in the main plate at A. The increase in the peak at B in the main plate will not effect the overall design as this value for the fully welded case is only approximately 60% of the main plate stress.

A very good connection can therefore be obtained by using cover plates welded all round and an appropriate ratio of plate thicknesses.

CHAPTER 6 PHOTO-ELASTICITY

6.I INTRODUCTION

To provide a check on the theoretical plane stress model used in the finite element analysis it was decided to make a photo-elastic model of the lap welded connections,freeze the stresses into the model and examine in a photo-elastic bench the resultant distribution in the plates.In order to carry out this work it was necessary to obtain a good understanding of the photoelastic experimental method of analysis.

Photoelasticity is an optical method of experimental stress analysis.Basically,it deals with the effect of polarised light in stressed transparent material,the characteristics being used to compute the nature and magnitude of the stresses therein.

The origin of the science of photoelasticity may be attributed to Sir David Brewster who,in 1816, observed the phenomenon of temporary double refraction produced by passing polarised light through a strained glass plate.Examination of the strained glass showed that the axes of polarisation in the glass contained the planes of principal stress.

Although this suggested a means of stress measurement by optical methods on transparent models,it was not until almost a century later that the science became fully developed.This was due to the fact that glass,which was the only available transparent material of necessary strength, was not very sensitive to the optical effect and in addition was difficult to machine.With the advent of celluloid as a photoelastic model material,however,these problems were overcome,with such success that rapid progress was made in establishing this method of stress measurement.

Considerable work was done by Coker and Filon early in the twentieth century in comparing experimental results with theoretical analyses for plane-stress problems.The publication of their findings resulted in the first comprehensive text on the subject.

The improvement in two-dimensional Photo-Elasticity since the 1930's has been confined mainly to improvements in apparatus, materials and techniques. Polaroid was introduced in the 1930's and this led to the manufacture of large field polariscopes without the expence of Nicol's prisms and elaborate analysing systems.

At the same time new Photo-Elastic materials began to appear, the earliest being Bakelite and in the 1950's Epoxys provided materials with much better Photo-Elastic properties. These improved materials led, in recent years, to the development of the 'frozen-stress' method whereby examination of stresses in three dimensions can be carried out. The introduction of low modulus materials has led to the extension of Photo-Elasticity into the fields of dynamic and impact loading.

Much of the present day research is directed towards the production of an automated Photo-Elastic bench.

6.2. NATURE OF LIGHT

Initial investigations as to the nature of light had, by the end of the seventeenth century, resulted in two distinct theories being put forward. That by Newton considered light to consist of a shower of particles, or corpuscles, emanating from a source, the characteristics of corpuscular motion varying with the type of light source. The other, propounded by Huygens, considered light to be propogated by waves in the ether, or medium through which it was travelling.

Additional weight was later given to the validity of the 'ether-wave' theory by Clerk-Maxwell whose investigations led him to believe that light was a disturbance produced by a train of electromagnetic waves, the disturbance being that produced on an ether particle in a direction normal to the direction of wave propogation.

However, in more recent years, the quantum theory has given rise to the possibility of light being of some form of corpuscular motion.

Whatever the true nature of light may be, the transverse wave theory gives a satisfactory explanation of the optical phenomena encountered in photo-elasticity and this theory is applied in the following analysis.

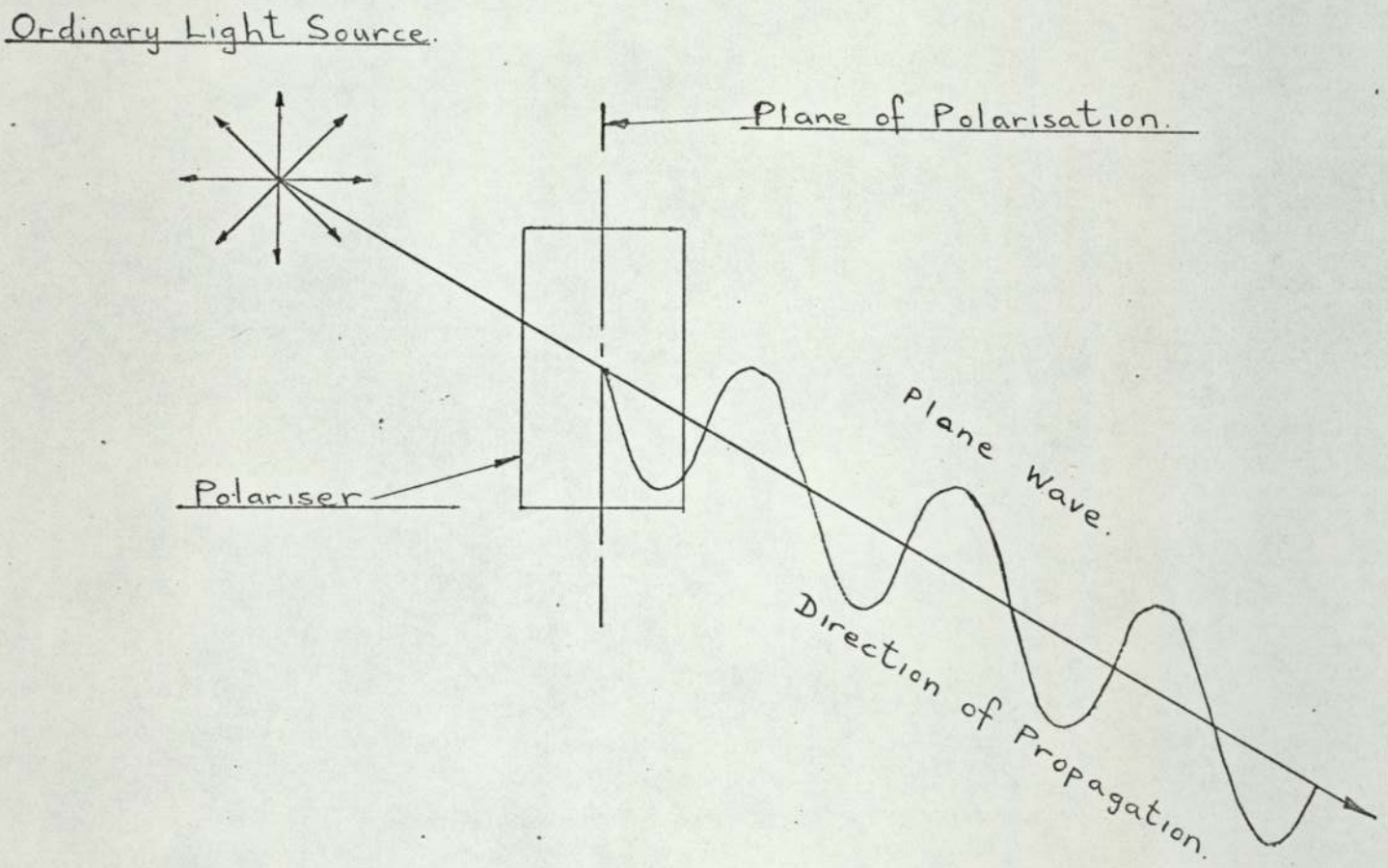

PLANE POLARISED LIGHT.

Fig 6.1.

ELLIPTICALLY POLARISED WAVE

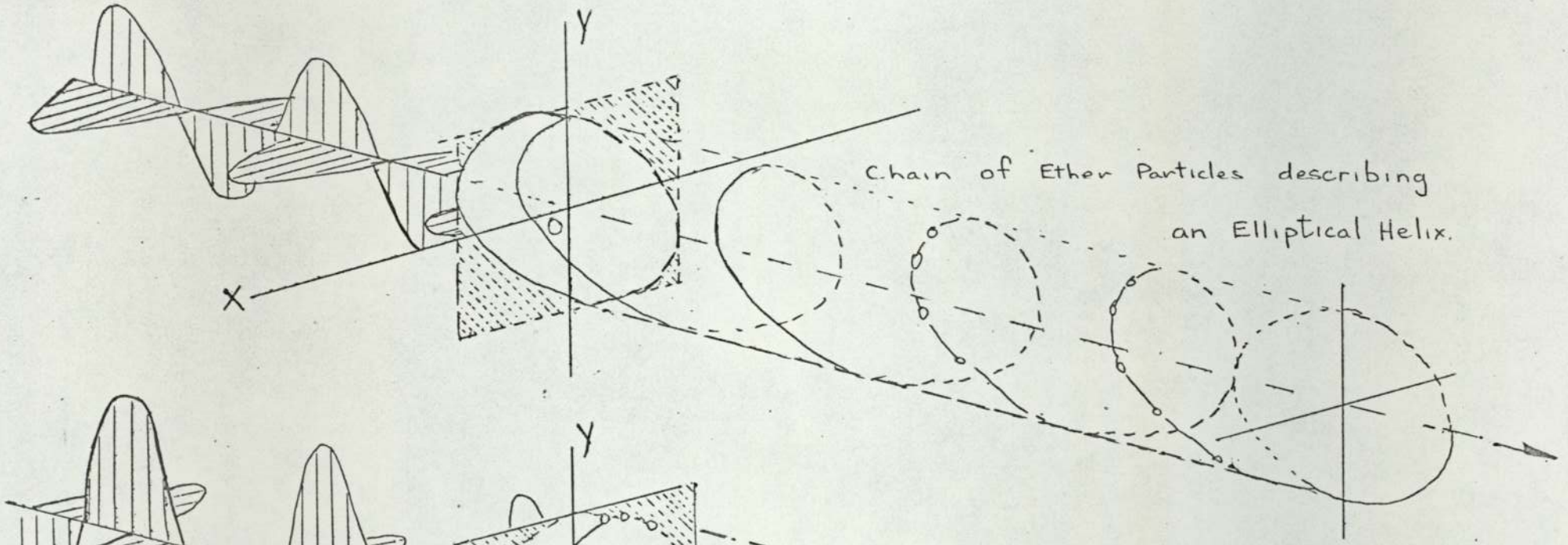

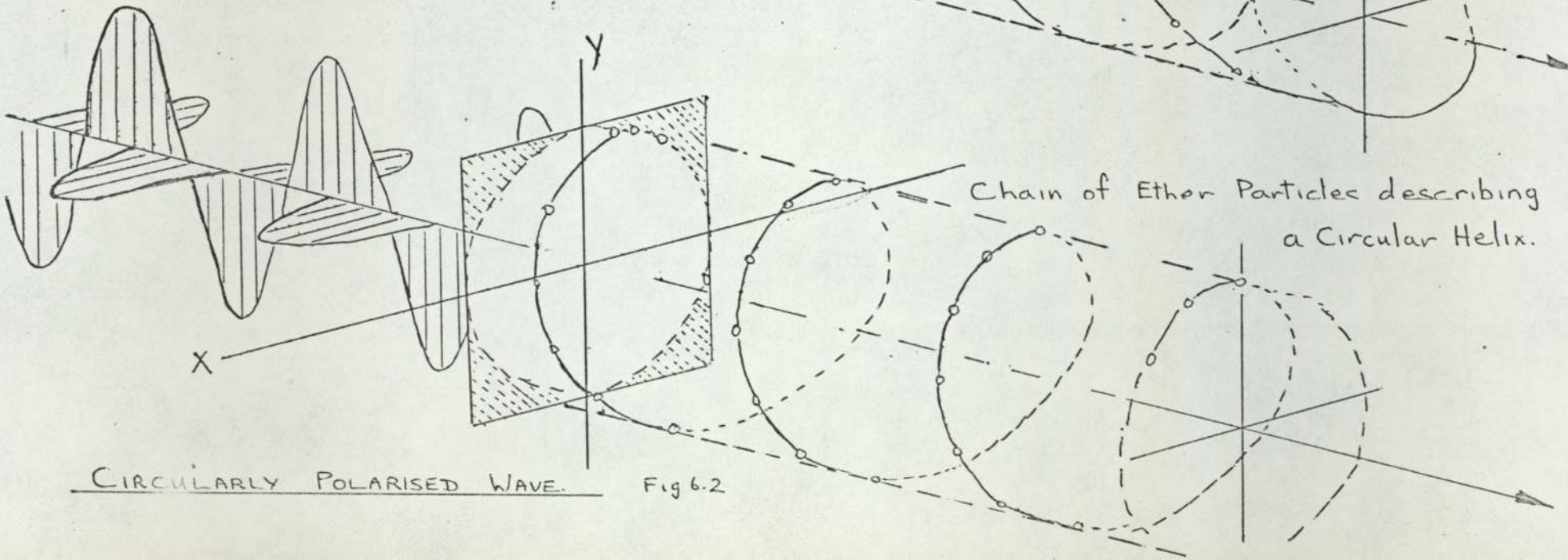

CIRCULARLY POLARISED WAVE.

Fig 6.2

6.3. TRANSVERSE WAVE THRORY OF LIGHT

As the motion of any particular ether particle in the path ofalight wave is periodic,the light wave may be represented by a sinusoidal wave train.

The magnitude and direction of the displacement of an ether particle from its original position can be represented at any instant by a vector,called the light vector.If the plane containing the light vector and the direction of propogation remains fixed from instant to instant, the light is said to 'plane polarised'.The inclination of the plane of polarisation relative to an arbitrary reference plane is termed the azmuth of polarisation.Plane polarised light may be obtained by passing white or monochromatic light through a type of transparent material,termed a polarizer,which determines the plane in which the vibrations of the ether particles take place.

If the light vector at any point remains of constant amplitude while continually altering its azimuth in such a way that its extremity traces out a circular path,the light wave is said to be circularly polarized.The light wave travels forward in a circular helical path,which may be either right or left handed,according to the propogation and direction of rotation of the light vector.If the extremity of the light vector traces out an elliptical path,the light is elliptically polarized.In general,the resultant motion of the ether particles when disturbed by two mutually perpendicular plane polarized light waves is elliptical. When the two component motions are equal in amplitude and out of phase by quarter of a wavelength the resultant motion is circular.Conversely any elliptical or circularly polarized wave may be regarded as the super position of two mutually perpendicular plane polarized waves.

6.4 POLARIZING MEDIUM

Crystals such as tourmaline and herapathite have only one optic axis,that is,light can only pass through in one direction;perpendicular to the optic axis,light is absorbed. Therefore,ordinary light falling on to one of these substances is resolved into components,that pass through along the optic axis and components that are stopped,thus

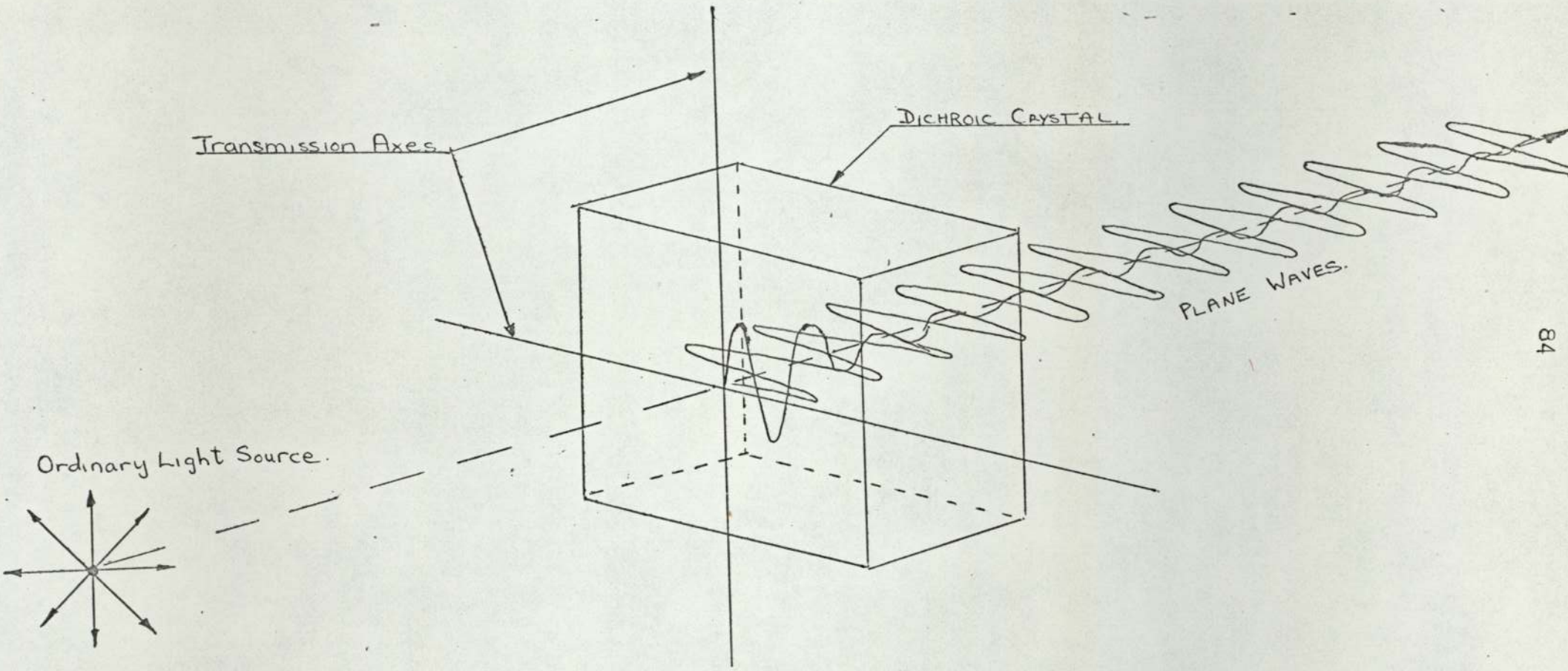

Dichroic Crystal with large absorption in vertical plane and slight absorption in horizontal plane.

Fig 6.3

resulting in plane-polarized light emerging. An artificial dichroic polarizing filter widely used in photo-elastic work is Polaroid. This gives extremely good polarizing properties as the absorbtion along the axis of polarization is very low whilst the absorbtion along the other axis is very high. In addition, it can be made available in large sheets, is relatively cheap, and gives good polarizing properties for all of the visible spectrum.

6.5 DOUBLE REFRACTION OR BIREFRINGENCE

Double refraction is a property of certain transparent substances such as calcite and mica, whereby light entering the material is split into two refracted components known as the ordinary and extra-ordinary rays. These rays are plane polarized in perpendicular planes and owing to a difference in refractive index in these two planes there is also a difference in the velocity of light passing through the substance. The extra-ordinary ray has a greater velocity than the ordinary ray and therefore on emerging from the material there is a phase difference or relative retardation, between the two rays, which is proportional to the length of the optical path or thickness of the material. This effect is temporarily produced in certain materials when they are subjected to stress.

6.6 WHITE LIGHT AND MONOCHROMATIC LIGHT

White light consists of vibrations of different frequencies, each frequency giving the sensation of a different colour.

Monochromatic light consisting of vibrations of one wavelength, may be effectively obtained from a sodium(yellow) or mercury vapour(green) source in conjunction with suitable filters to give consistancy of colour.

6.7 QUARTER-WAVE PLATES

A piece of material which is doubly

Arrangement For Circular Polarisation.

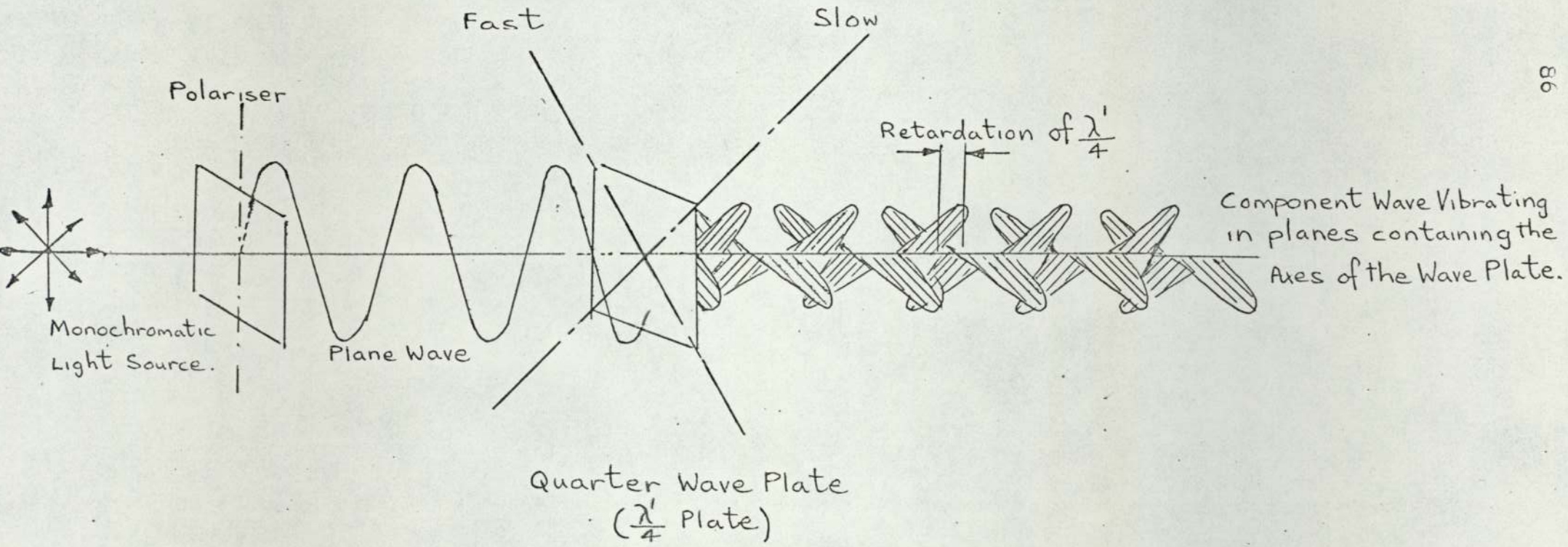

Fig 6.4

refracting and has a thickness related to the wavelength of the light used such as to produce a phase difference,or relative retardation of a quarter of a wavelength between the ordinary and extra-ordinary ray is known as a quarter-wave plate.

If the axes in the plate are arranged at 45° to an incoming plane-polarized ray,then the amplitude of the resolved components,which are the ordinary and extra-ordinary rays,will be equal,and circulary polarized light will result.For photoelasticity,mica is the material from which quarter-wave plates are generally made.

Circularly polarized light is used in the examination of the fringe patterns in photo-elastic models.

6.8 THE PLANE POLARISCOPE

This consists of two devices for producing plane polarized light,say two sheets of Polaroid,placed one behind the other,and a light source.The polarizing device nearest the light source is termed the Polarizer whilst the other is termed the analyser. Fig. 6.5 shows two possible arrangements for the plane polariscope:

(a) where the polarizing axes of polarizer and analyser are parallel in which case the plane polarized wave from the polarizer is completely transmitted by the analyser,and

(b) where the polarizing axes of polarizer and analyser are crossed resulting in complete extinction of the light behind the analyser.

6.9 THE CIRCULAR POLARISCOPE.

If two quarter wave plates,of the required thickness for a particular monochromatic light source, are inserted between polarizer and analyser of the plane polariscope and their axes suitably orientated relative to the axes of the polarizer,a circularly polarized light field will be obtained between the quarter wave plates.Such an arrangement is termed

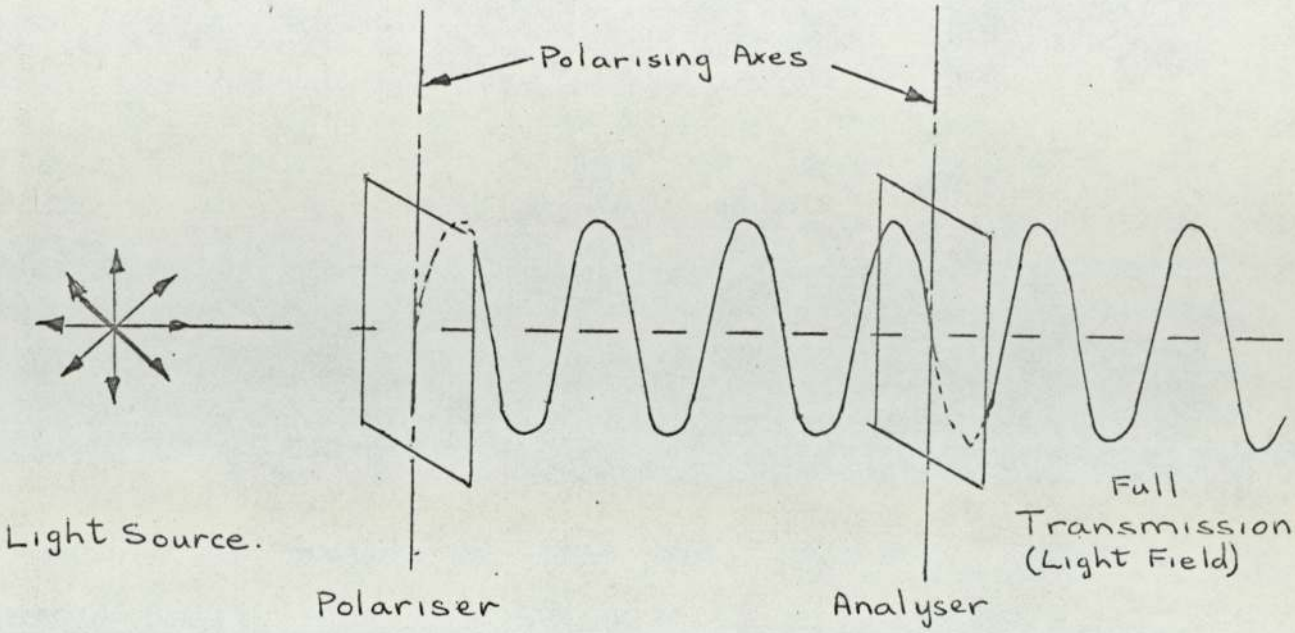

PARALLEL PLANE POLARISCOPE

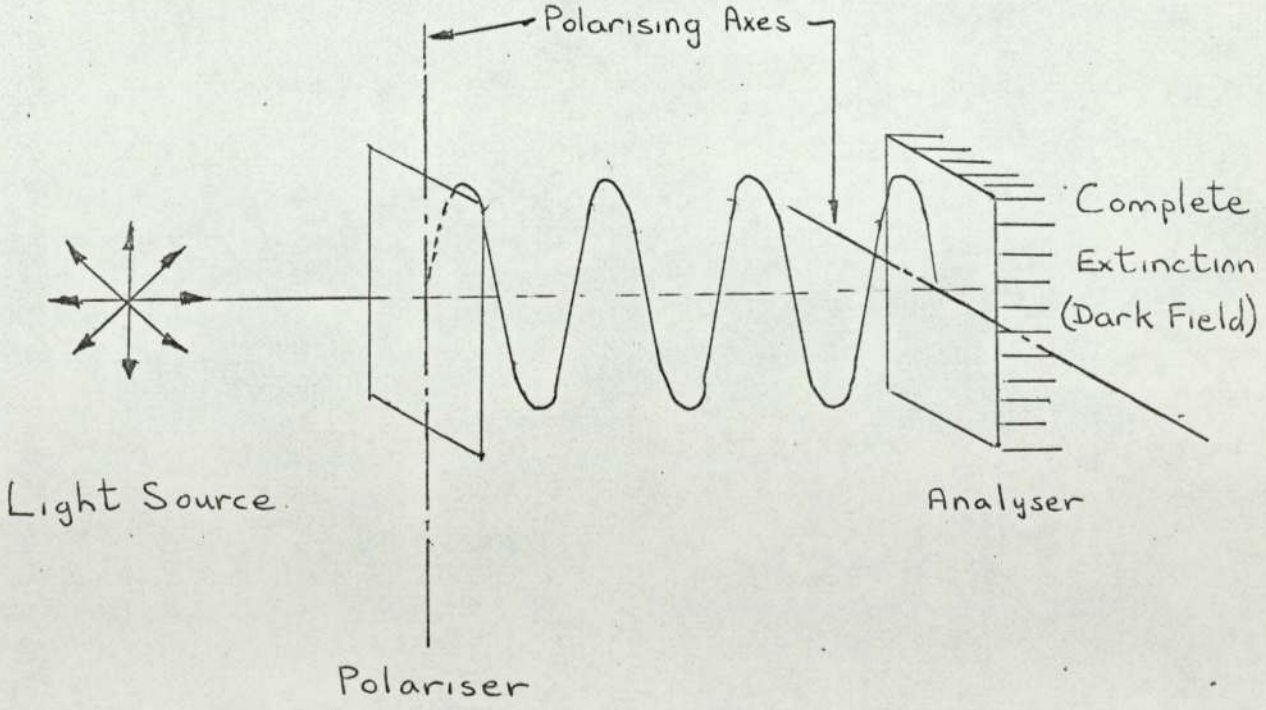

CROSSED PLANE POLARISCOPE.

Fig 6.5

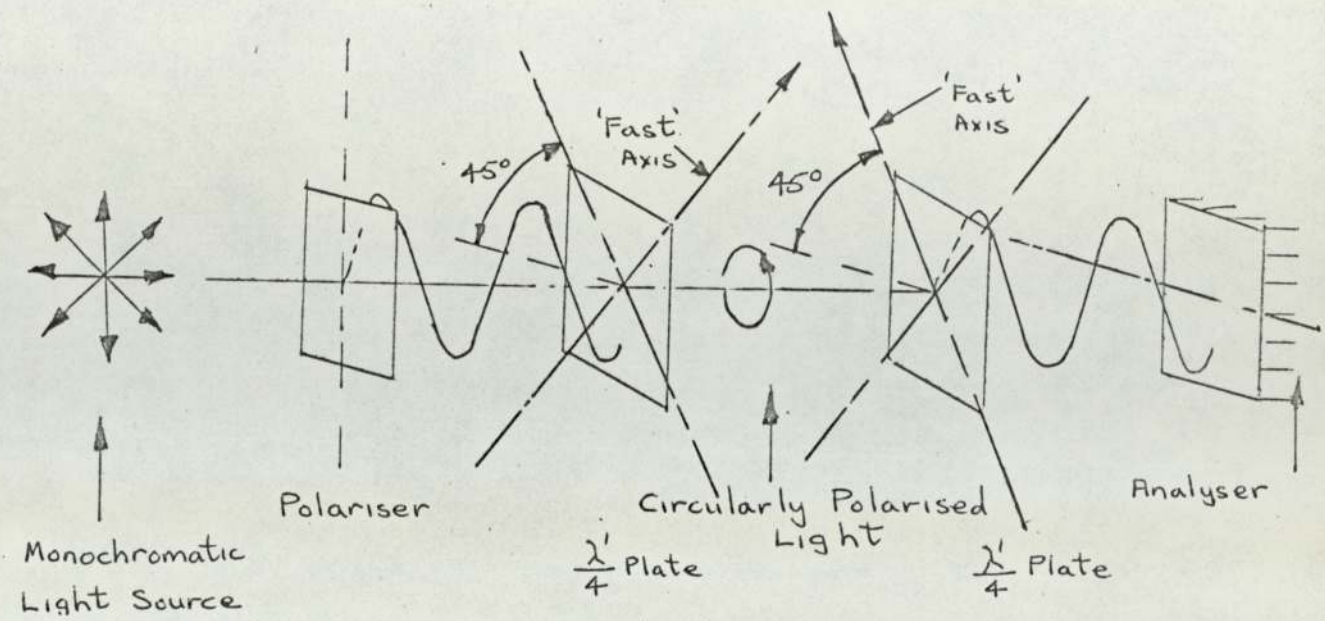

CROSSED CIRCULAR POLARISCOPE

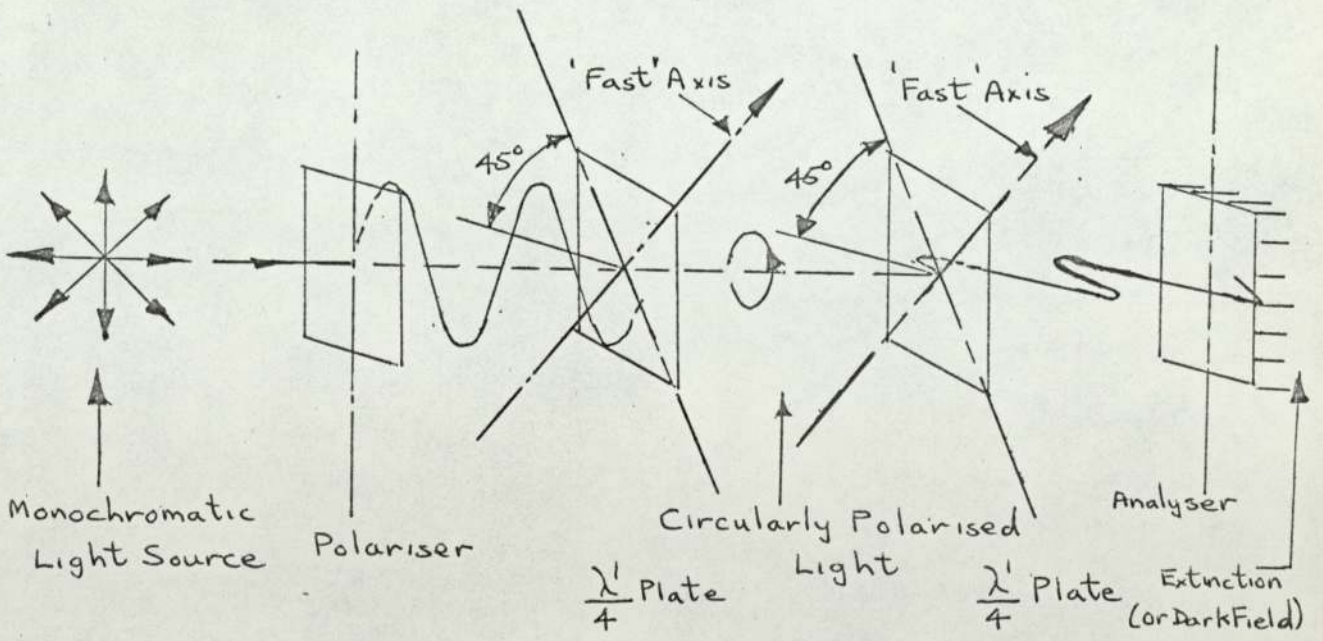

PARALLEL CIRCULAR POLARISCOPE

Fig 6.6

a'CIRCULAR POLARISCOPE'.

There are three possible arrangements of the plates and filters for photo-elastic measurements and these are shown in Fig. 6.6

(a) STANDARD OR CROSSED CIRCULAR POLARISCOPE

The axes of the first quarter wave plate are set at 45° to the axis of the polarizer, so producing circularly polarized light. With the fast axis of the second quarter wave plate parallel to the 'slow' axis of the first, the second quarter wave plate exactly undoes what the first quarter plate did, namely to transmit plane polarized light vibrating in the same plane as the plane wave from the polarizer. The axis of the analyser is crossed with the axis of the polarizer so producing complete extinction or a dark field behind the analyser.

(b) PARALLEL CIRCULAR POLARISCOPE

Circularly polarized light is obtained by placing the axis of the first quarter wave plate at 45° to the axis of the polarizer. The second quarter wave plate has its 'fast' axis parallel to the 'fast' axis of the first. Hence, the light transmitted by the second quarter wave plate will consist of two component waves, mutually perpendicular and having a relative retardation of half-a-wavelength resulting in a plane wave vibrating in the plane normal to that of the wave transmitted by the polarizer. Thus, with the axis of the analyser parallel to the axis of the polarizer, complete extinction or a dark field will result.

(c) CIRCULAR POLARISCOPE WITH LIGHT FIELD

This arrangement may be made when it is desired to transmit light through the analyser i.e. when a light background is desired. Either (I) place the polarizing axis of the analyser in Fig. 6.6 parallel to that of the polarizer, or (II) cross the polarizing axis of the analyser in Fig. 6.6 with that of the polarizer. Whether a light or dark background is desired will depend upon the particular examination that is being carried out in the polariscope. In general, if fringes near the boundary are being studied, a light background will be more satisfactory since the edge of the model will show as a dark line

against the light background. In addition, better alignment of the edge of the model can be obtained with a light background.

6.10 EFFECT OF LIGHT ON STRESSED TRANSPARENT MATERIAL -TEMPORARY DOUBLE REFRACTION

If a plate of normally isotropic transparent material such as araldite is stressed in its own plane and placed in the path of a light ray with normal incidence, the effect is analogous to that produced by a birefringent crystal in which the optic axis is perpendicular to the incident light. That is, the incident ray on the araldite is split into two plane polarized component waves travelling at different speeds through the plate and vibrating in mutually perpendicular planes. In addition, it has been found from experiment that the planes of polarization of the transmitted waves contain the principal planes of stress in the strained araldite.

Since the condition of plane stress on the araldite can be removed, or altered at will, the phenomenon of double refraction so exhibited is said to be temporary. Experimental evidence has also shown that the degree of retardation between the transmitted waves is dependent upon the difference in magnitude between the principal stresses in the strained material. Thus the relative retardation between emergent waves is dependent upon the material, the thickness of the material and the principal stress difference in the material and is given by the relationship

$$R = C.t(\sigma_1 - \sigma_2)$$

If the relative retardation can be measured, for a plate of given material and thickness, the difference between the principal stresses, $(\sigma_1 - \sigma_2)$, can be determined. It is possible to do this incrementally by having the analyser placed behind the plate and crossed with the polarizer such that only the components, in the plane of polarization of the analyser, of the waves emerging from the plate are transmitted. If the components are out of phase by 1, 2, 3 etc, wavelengths, no light will be transmitted by the analyser.

STRESSED TRANSPARENT MATERIAL IN PLANE POLARISCOPE

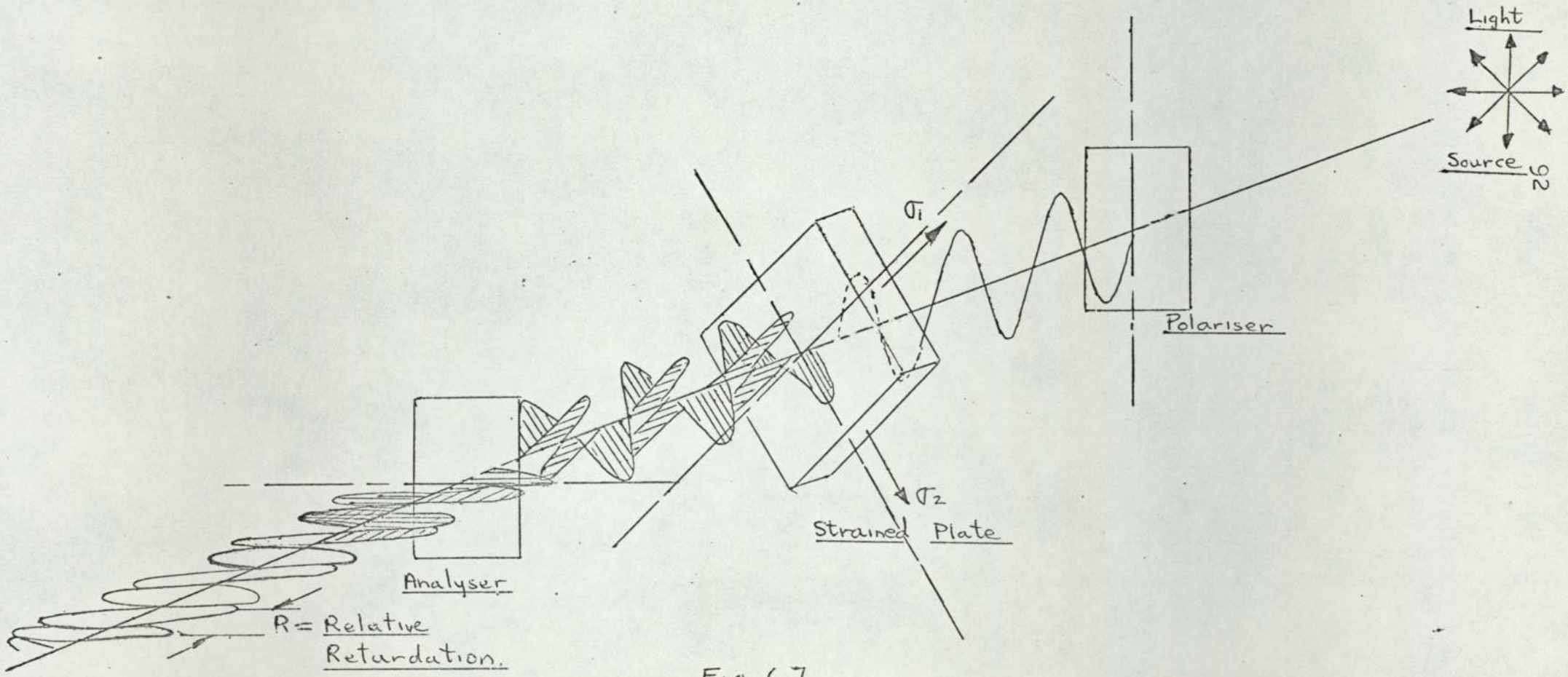

Fig 6.7

Thus when a stressed model is located in a plane polariscope with a monochromatic light source extinction of light takes place at the analyser when the principal stress directions coincide with the axes of the polarizer and analyser(Isoclinics) or when the relative retardation at a point is zero or an integral number of wavelengths.Since the changes in σ_1 and σ_2 will,in general,be gradual,the locus of all points at which the relative retardation is the same integral number of wavelengths will be as a series of dark lines,or 'FRINGES',interspaced with light bands having the same colour as the monochromatic light used.
If a white light source is used,the black Isoclinics appear against a coloured Isochromatic pattern i.e. all fringes except the zero order fringes will appear coloured.To distinguish between the Isoclinics and a zero order fringe,the polarizer and analyser are coupled together and rotated,the isoclinics move but the zero fringe does not.This is the normal polariscope arrangement for plotting Isoclinics.

6.II ELIMINATION OF ISOCLINICS

If the stressed model is placed in a circular polariscope the Isoclinics are eliminated as the light entering the model has no directional properties and only the fringes appear black.In the crossed circular polariscope an integral number of whole fringes are produced whereas in theparallel circular polariscope an integral number of half fringes are produced.

6.I2 PHOTO-ELASTIC MATERIALS

REQUIREMENTS FOR AN IDEAL PHOTO-ELASTIC MODEL MATERIAL

The following list gives some idea of the properties which an ideal photoelastic material should possess.

It must be transparent.
It must exhibit the property of bi-refringence under load.
It should be relatively colourless.
It must be free from initial stresses when unloaded

or be capable of some annealing process by which such stresses can be removed.
It should be optically sensitive i.e. the fringe orders obtained up to the elastic limit should be sufficient to produce reasonable accuracy without resort to special instrumentation.
It should be easy to machine.
The stress-strain and stress-fringe relationships should be linear.
It should be relatively free from creep.This aspect will be considered in detail later as will the next requirement.
Time-edge effects should be small.
It should produce reasonable fringe orders for relatively small deformations thus maintaining model shapes.
It must be sufficiently hard so that it can be clamped during machining and testing without becoming stressed or distorted in the process.It must,however,not be so brittle as to produce chipping difficulties during machining.
It must be of uniform properties throughout and maintain these properties under moderate changes in temperature and ambient conditions.
It should be capable of casting in block form for construction of three-dimensional models.
It must be reasonably inexpensive and readily available.

6.13 MODEL MATERIALS-ADVANTAGES DISADVANTAGES AND APPLICATIONS

The following are some commonly used Photo-Elastic materials

ARALDITE C T.-200

Advantages:Like Bakelite it approaches closely the ideal material.
Easily cast.
Suitable for 'stress-frezing' analysis
Easily machined
Sensitive
Not brittle
Readily available
Reasonable price
Can be joined using Araldite adhesive,the joins being practically invisible on the fringe pattern.

Disadvantages:Although small casting,maching or time-edge stresses can be easily annealed heavy stresses are almost impossible to remove.

Applications:Used extensively in the U.K. for all two and three-dimensional photoelastic studies. Especially useful in the casting or machining from large blocks of complicated models.

COLUMBIA RESIN CR-39

Advantages.Good transparency

Available in sheet form up to $\frac{1}{2}$ in thickness with exceptionally good quality surface finish.

Can be cemented to itself using the viscous liquid from which it is prepared the join being invisible.

Can be used for 'frozen-stress' studies

Disadvantages:Since it is formed under pressurs there is a marked residual stress distribution through its thickness.

This has no effect on the fringe pattern however, if models are carefully aligned to the light path. i.e.Normal incidence readings are possible, separation of the principal stress values using oblique incidence readings are not possible.

Quite brittle,requires care when machining.

Applications Frozen stress investigations where a relatively low optical sensitivity at the softening temperature is an advantage.

Occasionally used for general two-dimensional work.

BAKELITE BT-893

Advantages:Approaches closely the ideal properties listed previously.

Easily machined.

Not too brittle.

Sensitive.

Isotropic.

High Young's modulus.

Linear stress-strain and stress-fringe relationships up to quite high levels(6,000-7,000lbf/in^2)

Can be used for three-dimensional studies.

Disadvantages:Expensive

At medium temperature i.e. above 85°F the fringe value and Young's modulus change considerably. They are, however, constant to within about 2% at normal working temperatures.

Time-edge effects can be troublesome.

Applications : Can be used in practically all photoelastic applications. It is used extensively in the U.S.A.

POLYURETHANE. (PHOTOFLEX)

Advantages: Very sensitive.

Low Young's Modulus.

Useful for hand models.

Easily machined using standard procedures described later.

Excellent clarity.

Free from creep and time-edge effects.

Range of E values possible but Poisson's ratio constant.

Disadvantages .Easily deformed.

Normal testing almost impossible owing to high fringe orders produced at support points.

Applications: Demonstration hand models.

Soil Mechanics models.

Can be used as a medium to even-out loading across a large area i.e. to produce uniformly distributed load conditions accurately.

Dynamic or wave propogation studies where low modulus is an advantage.

Multi-layer problems requiring different E values.

Gravity dam investigations using mercury to simulate hydrostatic pressures.

Tunnel and mining cavity problems again rquiring different E values to simulate different rock strata.

Investigation of support and building foundation pressures.

Qualitative analysis of the deflected shape of structural members e.g. portal frames.

Since the material can be easily drawn or printed on, complete displacement fields can be easily obtained from Moire grids printed on the surface.

6.I4 CREEP AND TIME-EDGE EFFECTS

CREEP

The majority of photoelastic materials exhibit a certain amount of optical creep which is similar in nature to the mechanical creep in which extensions of metals increase with time under a constant load especially at high temperatures.

Optical creep is observed when the fringe pattern in a model under constant load changes with time. Generally this form of creep is very noticable in the first IO-I5 minutes after load application, the effect decreasing thereafter and becoming practically insignificant after half an hour or so. For consistent results therefore this latter period must be allowed to elapse before photographs are taken or investigations commenced

Creep effects increase with increasing stress levels When load is removed creep effects may be retained for some period depending on the magnitude of the stresses involved. Thus a material may not return immediately to its unstressed state when unloaded. This is a great disadvantage under conditions of repeated loading where a new zero load datum may exist for each application. This is also an argument against preliminary investigations followed too closely by accurate investigations after re-application of loads.

In addition to optical creep the majority of photoelastic materials also exhibit mechanical creep.

TIME-EDGE EFFECT

All photoelastic materials are to some extent moisture absorbent. If moisture is absorbed around the edge of a model this causes swelling of the model along the edge and induces local compressive stresses. Conversely in a different humidity condition moisture may be lost along the boundaries producing tensile stresses. Both types of edge effect are time-dependent and are therefore termed 'time-edge' effects'. In general the edge effects do not penetrate far into the model so that trimming of the edges will generally

produce a stress free boundary.
Time edge effects are seen in unloaded models as fringes which run parallel to the boundary. In frozen-stress models they are seen as sharp changes in contour or sudden zigzags of the fringes near the boundary.
On a compression edge fringes will cut back on themselves whilst on a tension edge they will tend to flatten out.
Time edge effects can be overcome using any of the following procedures.
a) Performing the test immediately after machining the model
b)Where the above is not practical rough shape the model some time before it is to be used and trim the edges to size immediately prior to testing.
c)Maintain the model at a fixed humidity both before and after machining so that the moisture content in the material remains in equilibrium with the atmosphere.
d)Smear the edges with a water-proofing agent to prevent moisture emmission or absorption.

In addition to the precautions taken above the consequences of the time-edge effect are as follows; Since the majority of photoelastic investigations involve the determination of boundary stresses, and since maximum stresses frequently occur at boundaries it is essential that time-edge effects are eliminated. Permanent records in the form of photographs or boundary stress values must therefore be taken as soon as possible after machining.

6.15 PHOTOELASTIC MODEL MAKING

It is essential that the photoelastic model is an accurately scaled reproduction of the prototype, the method of model manufacture depending on the shape of the model to be produced. Models may be made from precast sheets, cast to finished size, machined out of castings or manufactured from various materials in composite form.

6.16 REQUIREMENTS FOR A GOOD PHOTOELASTIC MODEL

In addition to the fact that models should be prepared from suitable materials(the ideal requirements for which have been stated previously) the following further conditions are essential:-

The dimensions of the component under test must be accurately reproduced,scaled up and down where necessary.

The edges of the model must be perpendicular to the faces of the material(two-dimensional models) and should be machined to a reasonably smooth finish.The use of emery cloth to polish the edges is not advised since this will inevitably'round-off' the corners.

The surface of the model should be free from machining scratches,chips,etc.

The edges should be free from machining stresses.

The model should be free from residual stresses.

In order to achieve these requirements the following general procedures should be followed:-

I.Accurate dimensions.

For two-dimensional models these are best achieved by the use of a metal template which has been accurately produced from steel gauge plate.The material is then fixed to the template using double-sidedadhesive tape and the edges machined using a side mill with the template guided against a pin which is approximately 0.005 in larger than the mill for the preliminary roughing operation and a second pin which is the same diameter as the mill for the final cut.

For three-dimensional models the same machining operation is normally used on the model as is used on the component under test.The use of Araldite C.T.200 makes this possible since this material can be shaped by any conventional machining process used on materials e.g. milling,grinding,turning in a lathe,etc.

The general machining rules are:-

Fast speed,low feed,negative rake,sharp tools, (Tungsten carbide or diamond tipped if possible) plenty of coolant and final cuts as small as possible.

In general, correct conditions are achieved when swarf comes off in ribbons, using these conditions the surface finish achieved will normally be completely acceptable and edge stresses produced in the machining operation will be very small and can be easily annealed out if necessary.

2. Perpendicular, smooth edges (Two-dimensional models)

These are automatically achieved using the system of a vertical milling cutter as stated previously. No polishing of the edges is required with this system, the final cut being sufficiently small to leave a good surface finish provided that the cutter is sharp.

3 Surface free from scratches

The sheet from which two-dimensional models are prepared should be inspected prior to machining and handled carefully to keep the surface in good condition Any scratches present will act as stress concentrations and should be avoided.

4.

Machining stresses

These are kept very low using the systems mentioned previously of small final cuts and are usually negligible. If not, they can be easily annealed out.

5.

Residual stresses.

If these are present in the model material they must be annealed out prior to testing using the following annealing cycle:-

Lay the models on a sheet of glass plate horizontally in the oven and temperature cycle as follows:

Raise temperature at 5 °C/hour to 140 °C
Maintain at 140 °C for approx. 8 hours.
Reduce to room temperature at 5 °C/hour.
(Complete cycle - 56 hours)

This cycle applies to two-dimensional models with thicknesses up to ½in

For thicker models or three-dimensional models special cycles should be used depending on their dimensions.

CASTING PROCEDURE FOR ARALDITE SHEETS AND THREE-DIMENSIONAL MODELS.

Casting Araldite C.T. 200 sheets using Duralumin Moulds

With new moulds.

Coat moulds with Releasil I4 and heat to I40 °C overnight.

Remove surplus releasil from the hot mould by polishing with a dry cloth. This prevents one type of surface defect.

THEREAFTER

Assemble Moulds using Releasil 7 grease to seal joints if metal strip spacers are used.
Pre-heat moulds to I40 °C.
Heat Araldite Resin to I40 °C.
Heat Hardener to I40 °C (in whistling kettle to prevent spitting)
Mix Resin and Hardener-stir thoroughly-filter.
After I0 minutes pour mix into the pre-heated moulds.
With thin plates, return the 'mould and mix' back into the oven for reheating at intervals when the mix shows a significant increase in viscosity.
When pouring is complete reduce oven temp. to II0 °C and allow the moulds to stand in the room until the temp. of the mix has also fallen to this value.
Return moulds to the oven and allow resin to gell for I6 hrs. at II0 °C before reducing the temp. at 5 °C per hour down to the room temp. (say 20 °C)
(Complete cycle =34 hrs.)

ANNEALING:

Remove partly cured sheets from moulds, lay them horizontically upon a sheet of paper placed upon a glass plate in the oven and temp. cycle as follows:-

Raise temp. at 5 °C/hour to I40 °C.
Maintain at I40 °C for 8 hours.
Reduce to room temp. at 5 °C/ hour.
(Complete cycle=56 hrs.)

TOTAL CYCLING TIME (PARTIAL CURING AND ANNEALING) = 90 hrs

6.17 CONVERSION OF STRESSES MODEL TO PROTOTYPE.

Stress distributions obtained photoelastically can be used directly for any material which follows Hooke's Law since the distribution is practically unaffected by the relative magnitudes of the elastic moduli.

Provided that the model is geometrically similar to the component and loads are similarly applied then any stress in the component σ_c is given by

$$\sigma_c = \frac{F_c}{F_m} \times \frac{L_m^2}{L_c^2} \times \sigma_m$$

where F_c = a force applied to the component.
F_m = a force applied to the model.
L_c = a linear dimension of the component.
L_m = a linear dimension of the model.

This equation will only apply when model and component thicknesses are equal. Where this is not true the equation becomes

$$\sigma_c = \frac{F_c}{F_m} \times \frac{L_m}{L_c} \times \frac{t_m}{t_c} \times \sigma_m$$

where t_c and t_m are the component and model thicknesses respectively.

Model and component strains are related by the formula.

$$e_c = \frac{F_c}{F_m} \times \frac{L_m^2}{L_c^2} \times \frac{E_m}{E_c} \times e_m$$

if the thicknesses are equal. If not, then

$$e_c = \frac{F_c}{F_m} \times \frac{L_m}{L_c} \times \frac{t_m}{t_c} \times \frac{E_m}{E_c} \times e_m.$$

Precise similarity between component and model distributions also requires that the value of Poisson's ratio for both materials are equal. It is thus fortunate that Poisson's ratio for most photoelastic materials lie in the range 0·3 to 0.36 and are therefore quite close to the values for structural materials. Those photoelastic materials used for three-dimensional studies, however, have a much higher Poisson's ratio approaching 0.5 and this has been shown to account

for small discrepancies in model and component stress values.

Scale Effects

Although nominally there should be no errors due to the scaling down of component size care must be taken to ensure that model similarity is maintained.e.g. ensure that radii much reduced do not introduce stress concentrations not really present.

Thick walls reduced to thin in the case of structural members may fail in a different mode i.e.buckling instead of crushing etc.

There are exceptions,however,as in the case of cylinders in contact,where stresses under the point of contact can vary widely from the theoretical if the thickness of the cylinder is less than 4 or 5 times the contact width.Thus in this case a thin model would not exhibit similar stress conditions to those existing in long cylinders in contact.

CALIBRATION OF FRINGE PATTERNS

In order to carry out a photo-elastic analysis it is necessary to establish the link between the relative retardation,or fringe order,and the principal stress difference.In a photo-elastic model the fringe pattern is known everywhere and if at a certain area in the model the stress can be calculated then the principal stress difference corresponding to the first order fringe,which is known as the model fringe value,can be determined.In other cases it may be possible to calculate the stress at any point in the model and in order to determine the fringe value a simple specimen is cut from the same sheet of material as the models and loaded for the same length of time.

If a test piece or rectangular cross-section,width b, thickness t is subjected to an axial tensile or compressive load P which produces a retardation of $n'\lambda'$ where, λ' is the wave length of the light then the stress in the specimen is $\frac{P}{bt}$ and the stress equivalent of the first order fringe is $\frac{P}{n'bt}$.

In comparing different materials it is often more convenient to state this value for a plate of standard thickness, so that this unit fringe value F' is

$$F' = \frac{P}{n'bt} \cdot \frac{t}{1} = \frac{P}{n'b}.$$

The material unit fringe value can therefore be determined without actually measuring the thickness of the test specimen. The wavelength of the light used in the calibration experiment must always be stated.

Although simple in principle, a tensile or compression test piece is rather inconvenient in practice because of the difficulties of ensuring precisely an axial load. The most satisfactory calibration test piece is a simple disc loaded in diametrical compression. The principal stress difference at the centre of the disc is given by :-

$$(\sigma_1 - \sigma_2) = \frac{8P}{\pi dt}$$

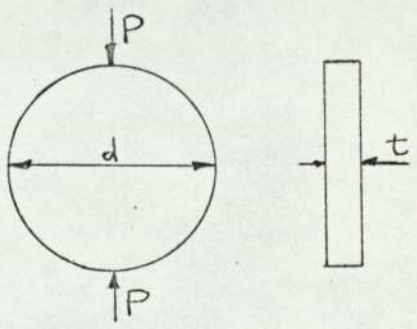

Fig 6.8

The loading equipment for this test is very simple, accuracy of loading is easily achieved, and a sufficiently large number of fringes can be developed for accurate determination of the fringe order at the centre of the disc.

6 18 ANALYSIS TECHNIQUE

Two dimensional models are surveyed in a circular polariscope and the fringe value computed at points of interest.

There are various methods of computing the fringe order at a point. Usually the whole fringe is obtained by counting from a known value (e.g. zero fringe) to the point under consideration. Frequently it is necessary to determine the fringe order at a point lying between whole fringes and therefore a means of determining fractional fringes is

required.The Tardy method,described below,is the most often used method for this purpose,another method was devised by Senarmont. Alternatively a digital compensator may be used,this giving the fringe order plus the fraction.

6.[19] TARDY METHOD OF COMPENSATION

Using a circular polariscope first determine the whole fringe values either side of the point under consideration (this can be achieved by using the simple compensator described in Ref II) The quarter wave plates are then removed,the polarizer and analyser being crossed an and coupled so that they rotate together.

Using a white light source the coupled polarizer and analyser are rotated until a black isoclinic appears over the point where the fringe value is required.The quarter wave plates are then inserted at 45° to polarizer and analyser to eliminate the isoclinic and give a dark field. Polarizer and analyser are uncoupled and the analyser is rotated until a fringe appears over the point where the fringe order is required.The angle turned through by the analyser is noted (θ') .The fringe order at the chosen point is then given by either $\left(n_1 + \frac{\theta'}{180^\circ}\right)$ if n_1, the nearest lower order fringe moved to the spot or $\left(n_2 - \frac{\theta'}{180^\circ}\right)$ if n_2, the nearest higher fringe moved to the spot.

The fringe pattern gives the principal stress difference in the plane of the model($\sigma_1 - \sigma_2$).On a free boundary either σ_1 or σ_2 is zero,and this allows the magnitude of the principal stress tangent to the boundary to be determined.There are various methods of determining the sign of the principal stress and a very good method is described in Ref II

In order to determine the magnitude of stresses within the model separation techniques are required.One such technique is the method of 'Oblique Incidence'.This involves viewing a model under normal incidence as shown in Fig. 6.9 and obtaining the fringe order n_o. at the point where the separate principal stresses are required.

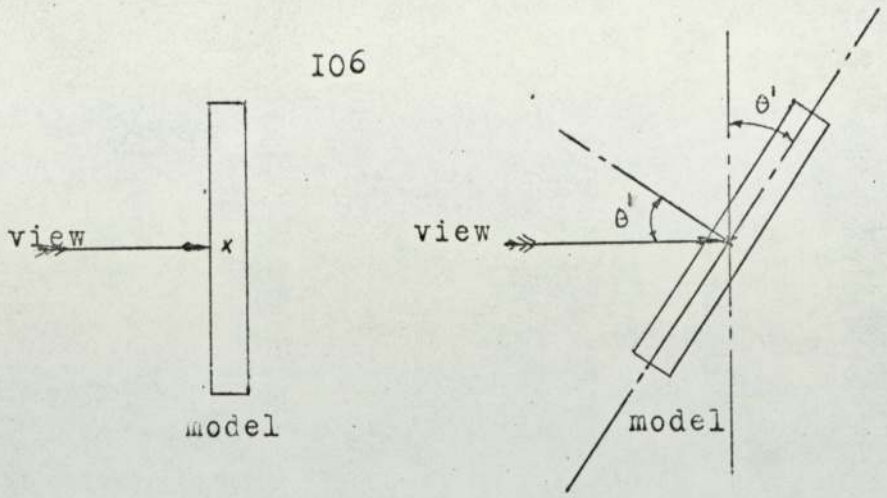

Fig 6.9

The model is then turned through some angle θ' about the axis of one of the principal stresses at the point and the fringe order $n_{\theta'}$ at the point again determined. The separate values of the principal stresses can then be determined using Drucker's equations:-
For rotation about the σ_1 axis:-

$$\sigma_1 = \frac{\cos\theta'}{\sin^2\theta'}\left[n_{\theta'} - n_0\cos\theta'\right]\frac{f}{t}$$

$$\sigma_2 = \frac{1}{\sin^2\theta'}\left[n_{\theta'}\cos\theta' - n_0\right]\frac{f}{t}$$

Similar equations, slightly modified, exist for rotation about the σ_2 axis.

To achieve no refraction at the surface of the model, the model is immersed in a tank of liquid whose refractive index matches that of the disc material.

It is always advisable when making oblique incidence measurements to scribe lines on both surfaces of the model at points where measurements are required. When viewing under normal incidence these lines will coincide but under oblique incidence they will appear separated and the fringe value required is that at the centre of the two lines i.e. at the middle surface of the specimen.

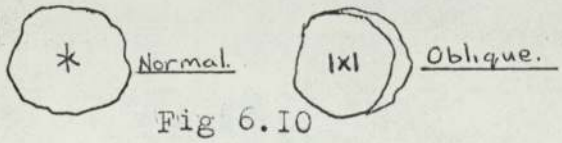

Fig 6.10

6.20 ISOCLINICS AND STRESS TRAJECTORIES

Isoclinics are sets of lines which appear black

against a coloured isochromatic background when viewed in a plane crossed polariscope using a white light source. At any point on one of these lines the directions of the principal stresses are co-incident with the directions of polarizer and analyser. Thus with a standard crossed polariscope a series of isoclinics can be obtained for various angular positions of the polarizer and analyser. Stress Trajectories are sets of orthogonal lines which can be constructed from the isoclinics to show the actual directions of the principal stresses at any point.

6.2I STRESS FREEZING

The discovery of the 'stress freezing phenomenon' led to a big surge forward in the use of photoelasticity. It made possible the examination of the stress distribution in a very complex three dimensional structures and allowed the stress patternto be frozen into fabricated models, such as the lap welded connection being analysed.

If a model constructed from certain photoelastic materials is loaded and heated to above its so-called "stress-freezing" temperture it will elastically deform at this temperature and the deformation will remain when the loaded model is slowly cooled. When load is removed a major part of the deformation remains and a photoelastic pattern corresponding to the elastic state of stress freezing temperature will be obtained in the model when it is viewed in a polariscope.

Very significantly no stress relaxation occurs when the model is cut. This allows a three-dimensional model to be cut into slices thin enough to be considered as effectively two-dimensional models. These slices are taken at particular points of interest and in such a manner that conventional two-dimensional techniques can be used for analysis in all but the most complicated cases.

The name of "Stress-Freezing" arises because of the analogy of a spring loaded in a beaker of water, see Fig. 6.I If the water is now frozen the load can be removed and the spring will be held in its stressed state by the

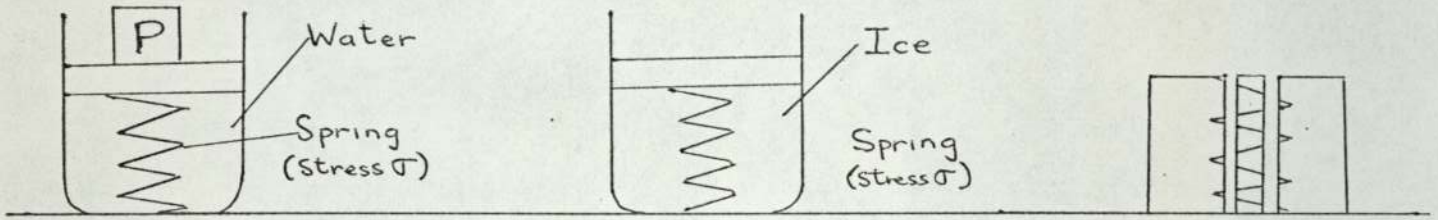

1 Spring loaded with weight P immersed in water

2 Water frozen, load removed, spring remains stressed

3 Spring and ice sliced for examination

THE 'FROZEN-STRESS' PRINCIPLE.

Fig 6.11

ice which surrounds it. Presuming that a cutting operation were possible without generating sufficient heat to melt the ice the spring and ice could be sliced for examination.

Two further analogies exist, however which explain the process more correctly.

SPRING IN WAX ANALOGY

Consider an unloaded spring enclosed in wax. When load is applied there will be a small strain produced as shown in Fig. 6.12. If heat is now applied to melt the wax the spring will extend and the strain therefore increase although the load remains unchanged. Cooling of the system will solidify the wax with the extension and hence the strain remaining unchanged. When load is removed a slight relaxation of strain occurs but the majority remains "frozen" in.

Thus when load is applied to a photoelastic model at room temperature a small elastic deformation takes place. When the temperature is raised above the critical or stress-freezing temperature there is a considerable lowering of the modulus of elasticity of the material and hence an associated large increase in extension δ_1. Cooling of the model to room temperature and removal of the load will produce a recovery of the small elastic extension δ but the large extension or deformation δ_1 will be retained.

It is evident that in addition to the change in length of the model there will also be an associated change in area. If we consider a test piece of original length L and area A the Young's Modulus at room temperature is defined as

$$E = \frac{\text{stress}}{\text{strain}} = \frac{P}{A} \times \frac{L}{\delta}$$

At the critical or stress freezing temperature however the modulus is defined in terms of the deformed geometry of the test piece and residual strain after the stress freezing cycle

$$\text{i.e. } E_{hot} = \frac{P}{A_1} \times \frac{L}{\delta_1} = \frac{\text{effective stress at the critical temperature}}{\text{residual strain}}$$

THE FROZEN STRESS PRINCIPLE.

SPRING IN WAX ANALOGY.

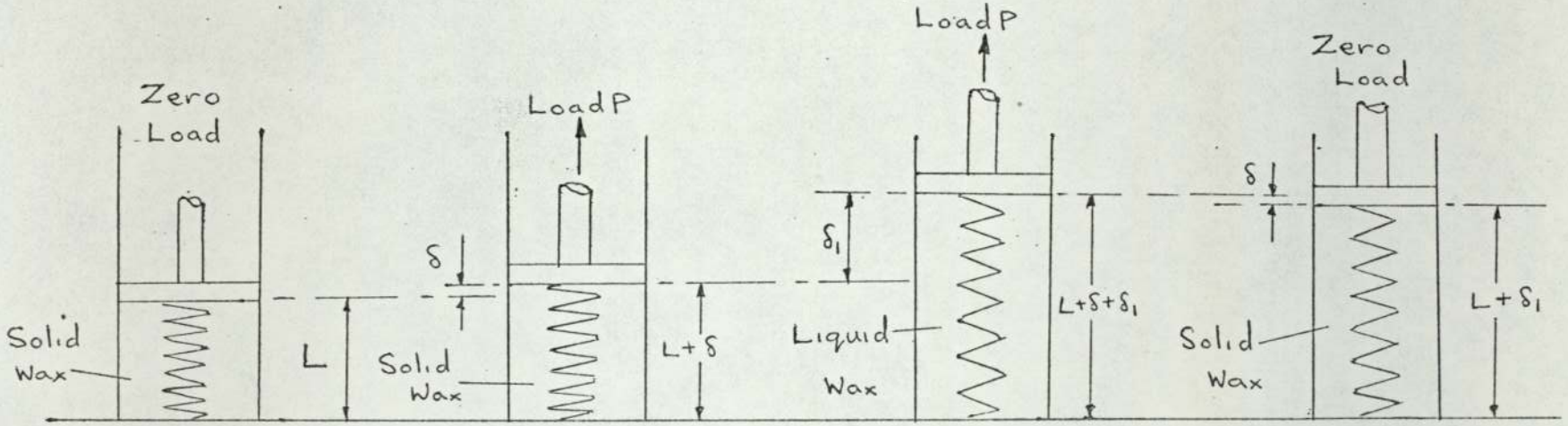

1 Unloaded Spring in solid wax. Room temp. Zero strain.

2 Loaded Spring in solid wax. Room temp. Small strain.

3 Loaded Spring in molten wax. Stress Freezing temp. Large strain.

4 Unloaded Spring solidified wax. Room temp. Large strain frozen in.

Fig 6.12

III

SPONGE AND TAR ANALOGY

It can be seen from the previous analogy that the materials which exhibit stress freezing properties must possess two types of molecular bond each affected in different ways by temperature changes.This diphase system can be represented again by two separate materials provided that they are "mixed homogenenously".Consider therefore a sponge which will act as the continuously elastic medium throughout the process completely filled with tar which will be solid at room temperature.At the elevated or"stress freezing" temperature,however,the tar will become liquid and will carry no load the whole of the load then being taken by the sponge which consequently deforms.This deformation will be retained during the cooling or "freezing" process and when load is removed a system of stresses is set up within the combination in which the forces set up by the sponge trying to relax are balanced by and opposite forces exerted by the tar. It has been proved that the magnitude of residual deformation achieved in this process is independent both of the time taken and of the maximum temperature reached in the thermal cycle.Further,it has been verified that the deformations correspond to the elastic strain distribution associated with the applied loading.If the stress frozen model is subjected to an annealing cycle in which it is once more heated above the stress-freezing temperature, whilst unloaded,both the deformation and the associated fringe pattern will be removed leaving the model completely unstrained and stress free.It therefore follows that the frozen stress phenomenon does represent linear ELASTIC behaviour rather than plastic as could be imagined at first sight.

CHEMICAL EXPLANATION OF THE FROZEN STRESS PHENOMENON

Not all photoelastic materials are subject to the stress freezing effect.One group of plastics which are sensitive to it,however,are the epoxy resins.These are composed of long chain molecules which are cross

linked during polymerisation when covalent bonds are formed between the ends of the short side arms attached to the main molecular chain. At room temperature the whole of the chain structure will be elastically deformed by the application of external loads. At the elevated or stress freezing temperature the primary C-C bonds become free to rotate. This results in a considerable reduction in the resistance to deformation and large strains result. The material behaviour however, continues to be linear and elastic.

When the temperature is reduced the C-C bonds are retained in their strained position and provide a mechanical restraint against recovery of deformation when load is removed.

FRINGE MULTIPLICATION

Three dimensional photoelasticity using the frozen stress method often leads to the taking of thin slices from the photoelastic model. These thin slices frequently exhibit broad low order fringes covering the whole field. Fringe multiplication can be used to increase the sensitivity of measurements, provide a graphic view of the stress field and the method is very quick and not as highly subject to human error in data taking as othe methods. The fringe multiplication instrument consists of two partial mirrors slightly inclined to each other, the frozen stress slice being placed in an immersion fluid (of the correct refractive index) between the mirrors. FigI3 shows an exploded view of the components in a fringe multiplication polariscope.

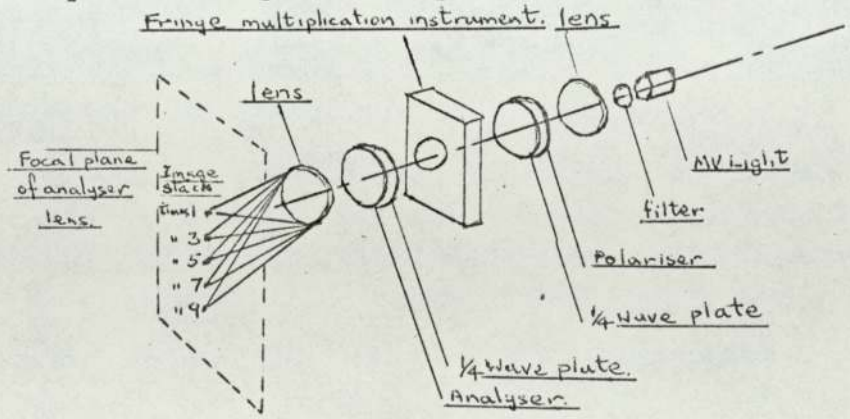

Fig. 6.13

After passing through the system the light converges to a series of foci all in one plane. If a card is placed in this plane a series of light spots of diminishing

intensity can be observed.These constitute an image stack of odd order.Light converging at one of these spots (e.g. that marked"times 3" in fig. 6,I3) has passed m times(3 times) through the specimen and observation of the corresponding image shows the corresponding multiplied fringe order.The pitch of the image stack should be as small as possible so as to minimise errors due to path spread,without causing image overlap.Photographs of the image can be taken with a camera positioned to collect the appropriate light rays and focused in the normal manner,the camera lens being screened off by a plate containing a single central hole.Satisfactory multiplications of I7 times for slices exhibiting low initial birefringence have been obtained but normally one works in the range up to 9 times.

CHAPTER 7

APPLICATION OF PHOTO-ELASTICITY TO LAP-WELDED CONNECTIONS

7.I INTRODUCTION

Having carried out model tests using Vybak and strain gauges (Appendix I) it was decided that the stress distribution in the plates for comparison with the computer results could be better obtained using a Photo-Elastic model.Some preliminary models were made and tested to determine the best method of producing the model,welding it and loading to obtain a good symmetrical pattern with a reasonable number of fringes.

7.2 MODEL MANUFACTURE

The Photo-Elastic model was made from 3/16 inch CT200 Araldite sheet having dimensions as shown in fig. 7.1 page II5

The method of manufacture finally adopted was to make two templates of $\frac{1}{8}$ inch gauge plate steel 3 inch × 5 inch and 4 inch × 9 inch .In order to cut the model plates the Araldite sheet was attached to the gauge plate templates with double sided tape and a Sharples model making kit(Photograph I) used to cut the models to size.The Sharples model maker consists of a special milling machine with a $\frac{1}{8}$ inch diameter high speed steel cutter,a 0.I35 inch diameter roughing plug and a 0.I25 inch diameter finishing plug.The roughing and finishing plugs can be fitted into the cast iron base plate,centrally under the milling head.This method of machining ensures that the model is free from edge stress and that the edges are perfectly square.
The roughing plug was first inserted in the base plate of the machine.The template was guided against the roughing plug,thus enabling the model to be cut within 0.005 inch of the finished size.The above procedure was repeated with the finishing plug replacing the roughing plug.
All sheets were examined in the polariscope to make sure they were free from stress. The cover plates were clamped in position on the main plates.Several methods of simulating the weld connections were tried.One of the

DETAILS OF PHOTO-ELASTIC MODEL

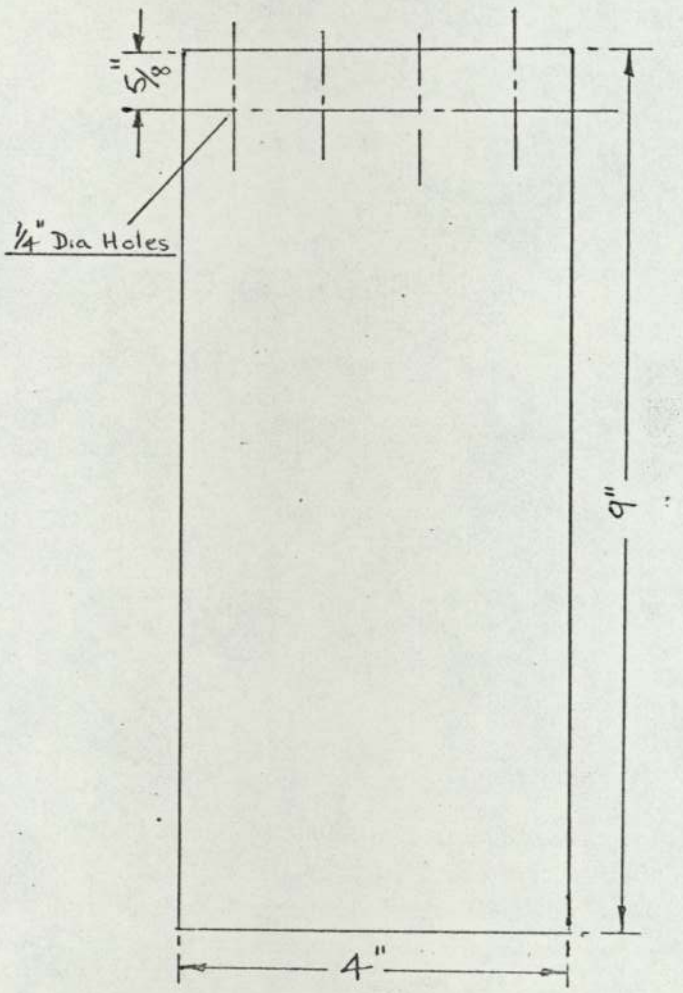

Main Plate (2 off)

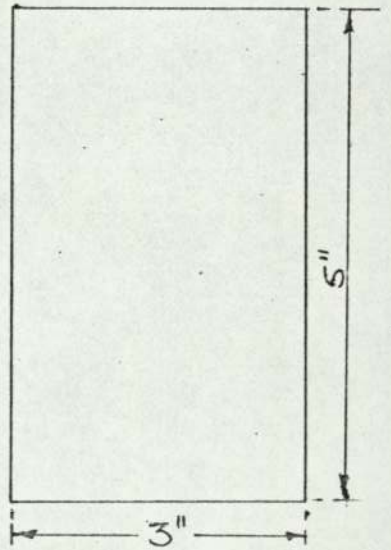

Cover Plate (2 off)

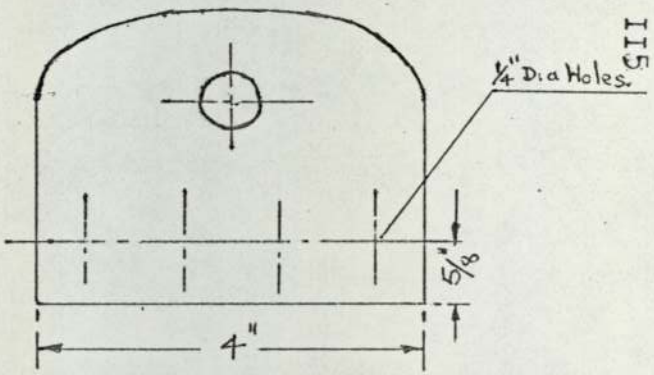

End Plates (4 off)

All Plates 3/16" Thick.

Fig 7.1

Sharples Model Maker
Photograph I

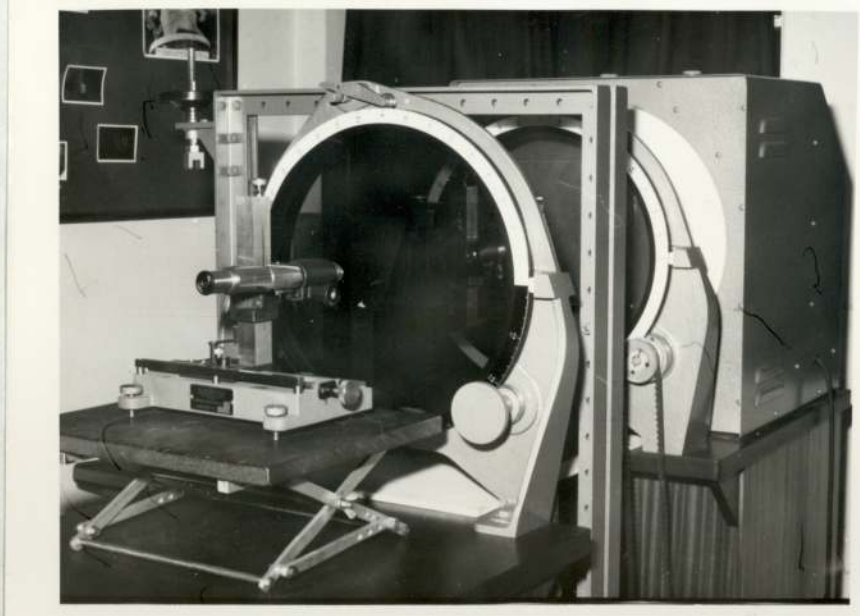

Sharples I5 inch Diameter Diffuse
Light Polariscope

Photograph 2

early problems was the seepage of adhesive between the cover and main plates.This was overcome by smearing areas where adhesion was not required with silicon grease.The best method of fixing the plates was found to be as follows.

Smear the non adhesive areas with silicon grease and insert a piece of 0.003 inch shim covered with silicon grease in the gap between the main plates.

Clamp the cover and main plates together and then clamp the whole assembly to a 45° angle plate using a dial gauge to ensure that the edge of the cover and main plates were level.Dams were formed at the ends of the cover plate using the silicon rubber.The final assembly is shown in photographs 3 & 4 on pages II8

An araldite mixture was poured into the dammed area and allowed to set for twenty four hours.The other three welds were prepared in a similar manner.The whole was then heat cured at I35°C in an oven for I4 hours.Eight quarter inch holes were drilled in the ends of the maim plates for loading.Four end plates were manufactured and then bolted to the main plates,the bolts being tightened to give a friction grip between the end and main plates. (Photographs page II9)

The whole assembly was inspected in the photo-elastic bench to ensure that it was free from initial stress and loaded to ensure symmetry.

7.3 STRESS FREEZING

The assembly was then suspended in a Sharples Photo-Elastic oven and a load of 7 lb hung from the weight hanger attached to a pin through the end plates (Photograph 7 page I20)

The oven was controlled by an Ether Controller (Photograph 8 page I2o) A stress freezing cam was fitted to the controller and this gave the following programme,

24 Hours to raise temperature to I40 °C

8 Hours to soak at I40 °C

24 Hours to bring oven temperature back to room temp.

After removing from the oven the model was viewed normally in the photo-elastic bench to make sure the

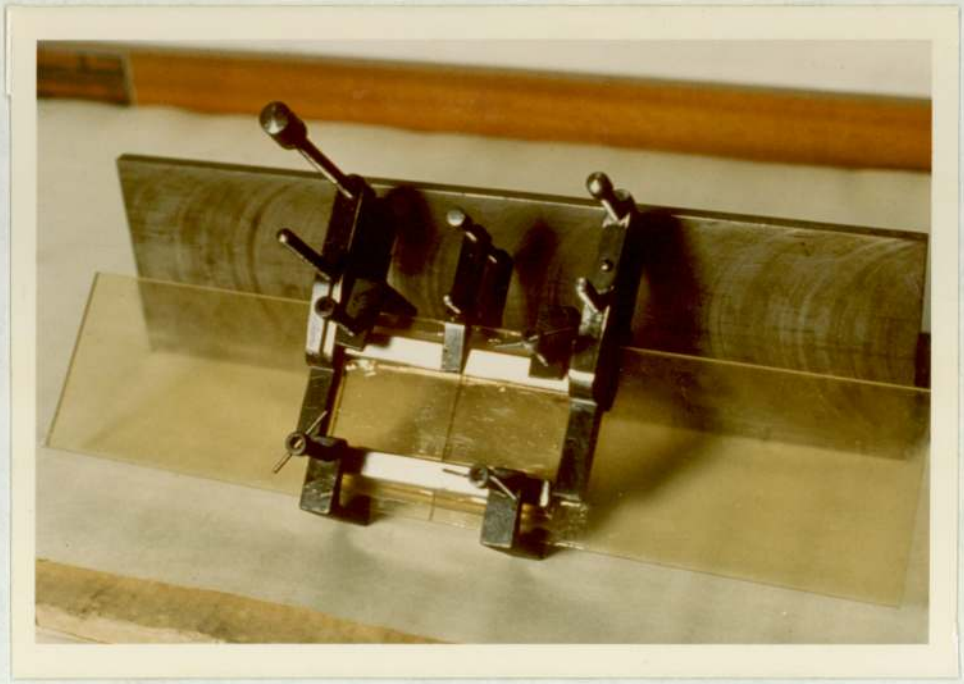

Plate connection set at 45° for formation of weld
Photograph 3

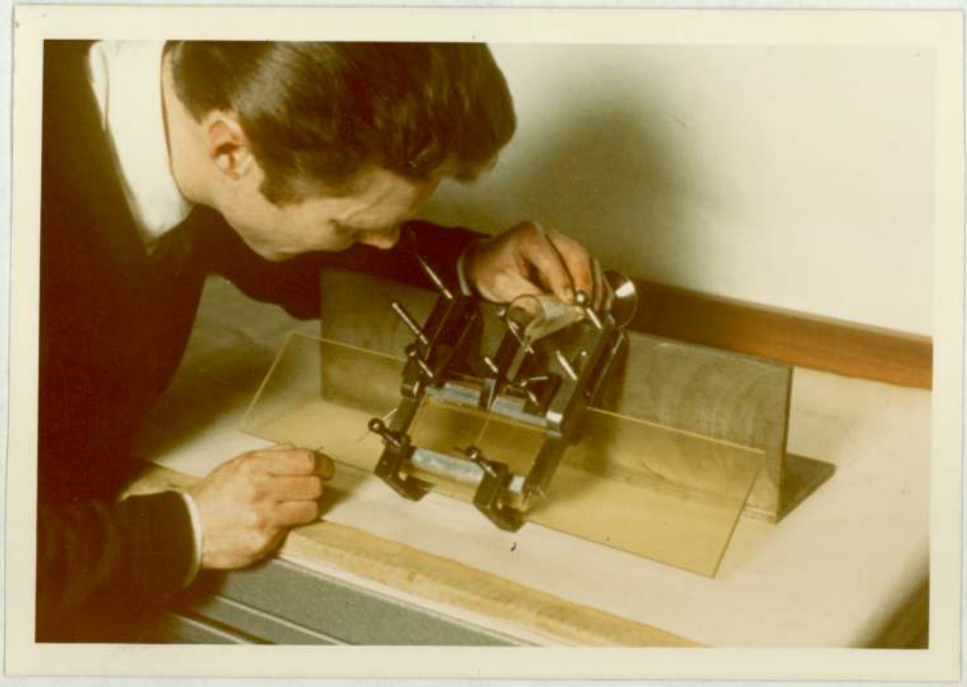

Pouring araldite mixture to form weld
Photograph 4

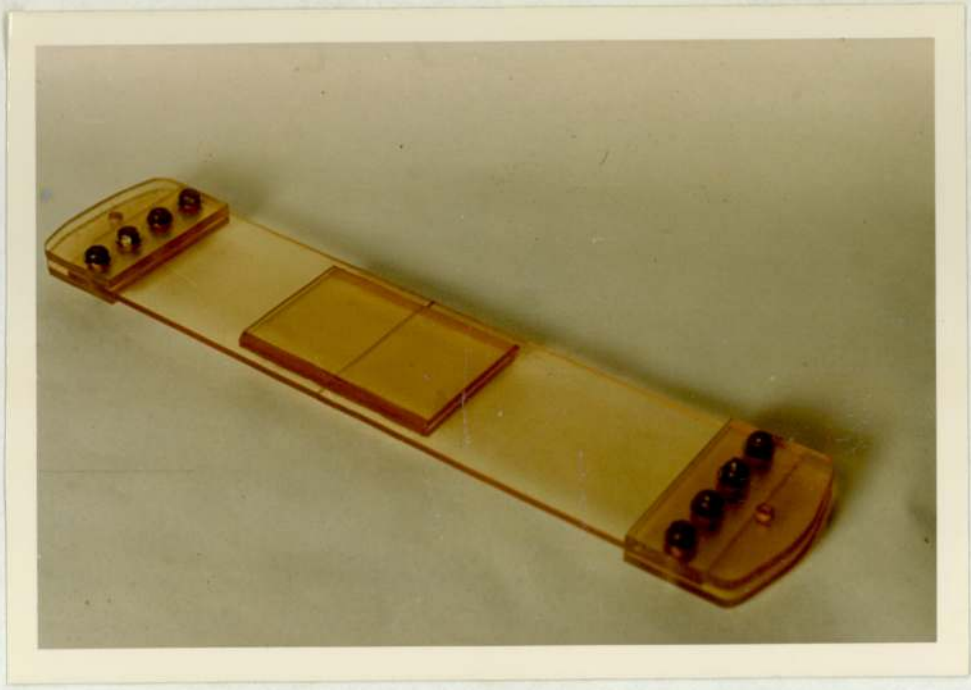

Assembled test specimen

Photo graph 5

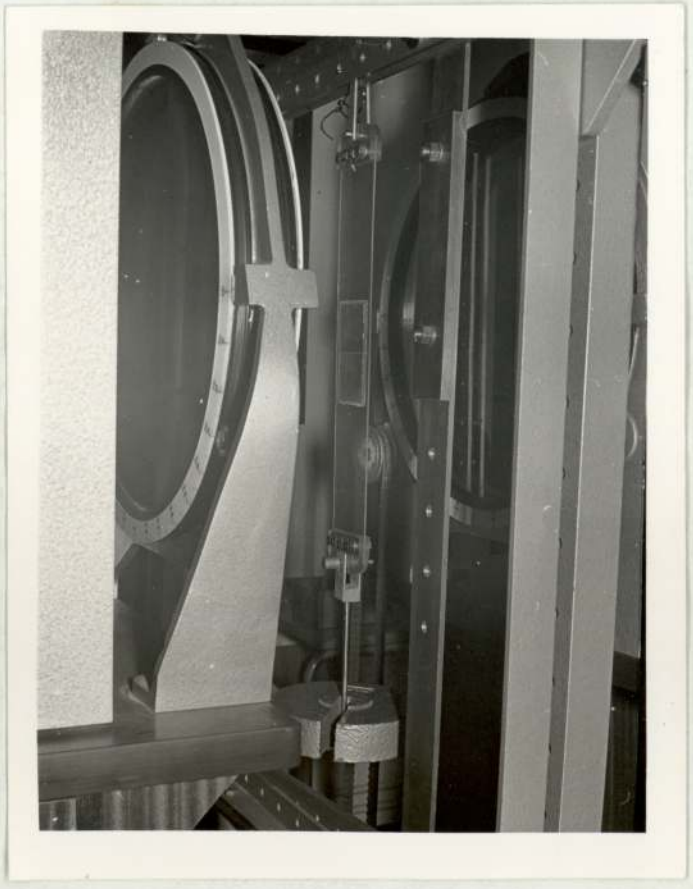

Preliminary viewing of assembled test specimen

Photograph 6

Model in stress freezing oven
Photograph 7

Oven Control unit.
Photograph 8

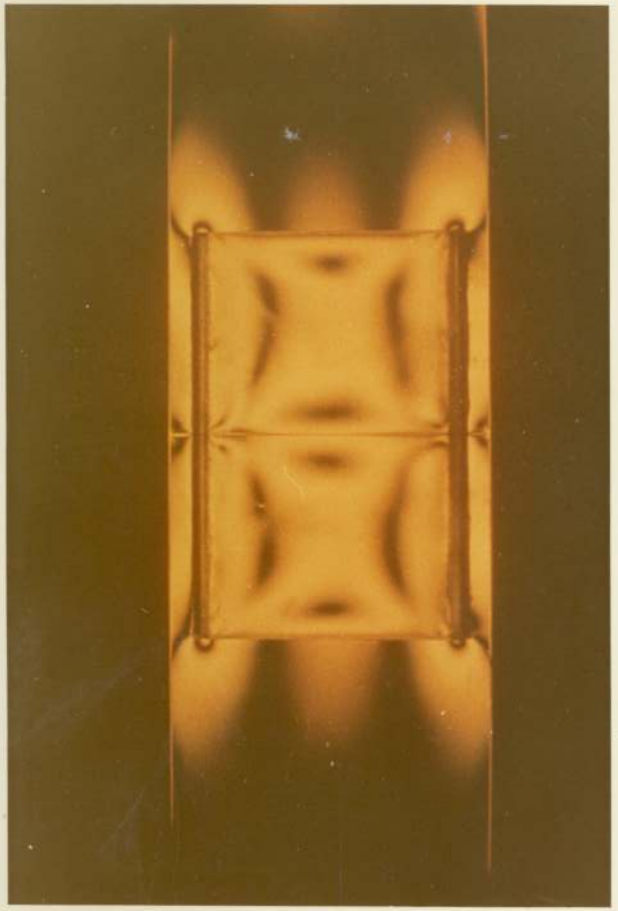

Frozen test specimen viewed in sodium light.
Photograph 9.

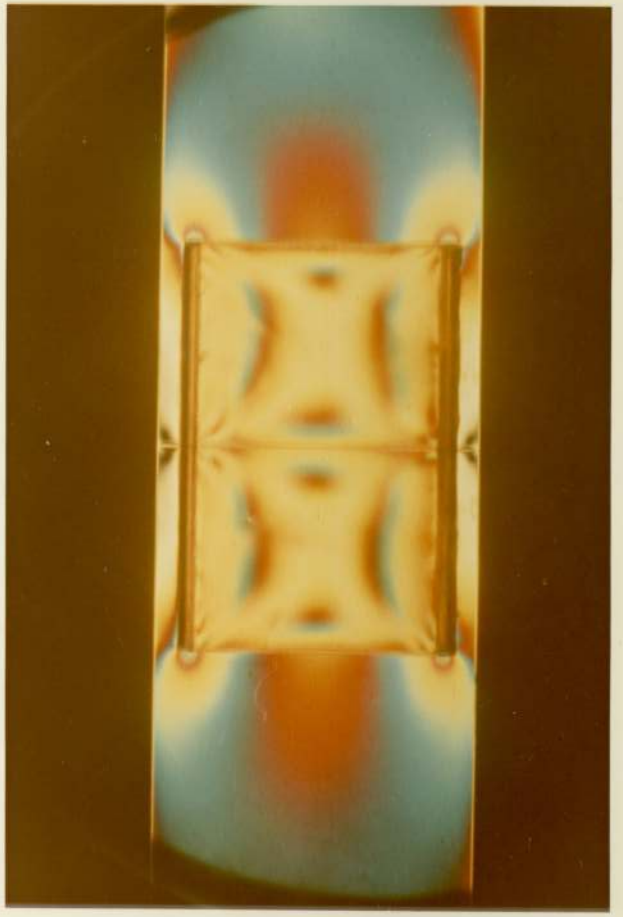

Frozen test specimen viewed in white light.
Photograph 10.

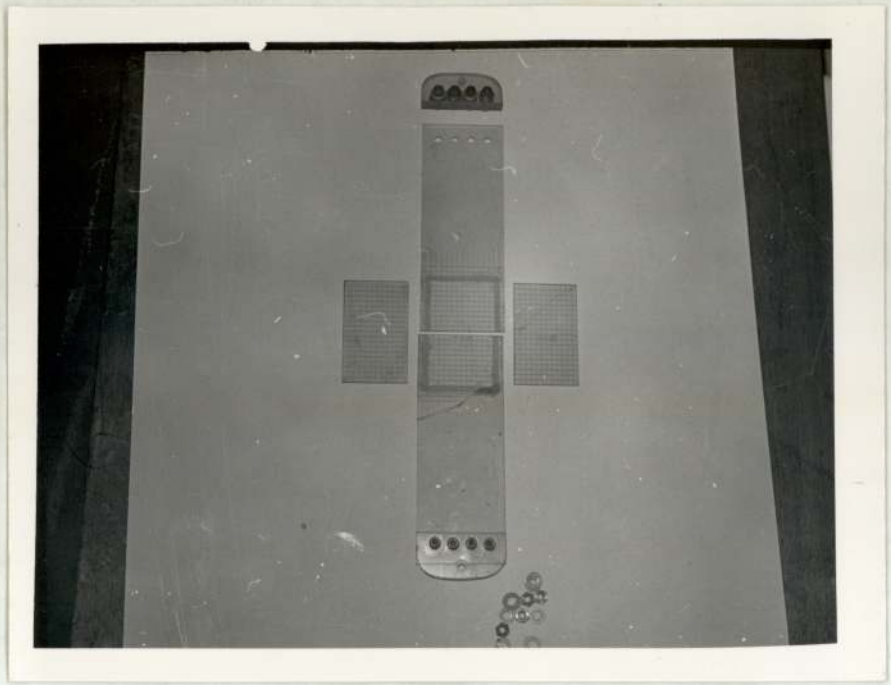

Separated test specimen.
Photograph II

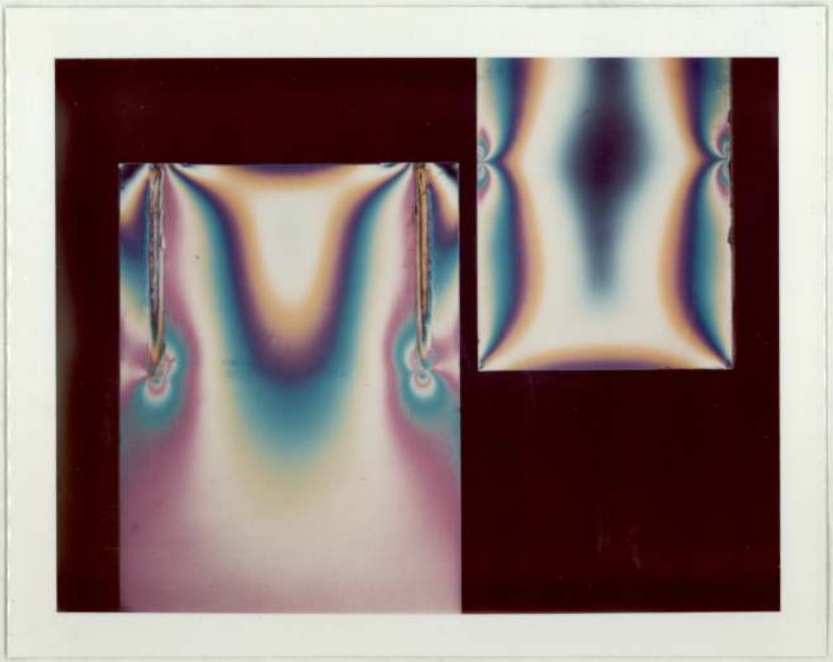

Isochromatic patterns in the
separated main and cover plates.
Photograph I2.

pattern was symmetrical,(Photographs 9&10 page I21)

The welds were then very carefully cut away using a very fine handsaw,cutting through the weld as shown in Fig. 7.2

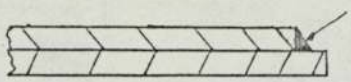

Fig 7.2

The separated pieces are shown in photograph II on page I22

Cover plates and end plates were examined in the photo-elastic bench to see that the patterns in corresponding plates were similar and symmetrical.

A typical set of isochromatic patterns for a cover plate and a main plate are shown in photograph I2 page I22

7.4 ANALYSIS OF FRINGE PATTERNS

A quarter inch square mesh was scribed on the surface of the main and cover plates.Each plate in turn was examined in the photo-elastic bench.A I5 inch diffuse light polariscope was used for the analysis.Photograph 2 page II6 .

The face and edges of the cover and main plates were smeared with an Araclor/ Liquid Parafin mixture,having the same refractive index as the model material, to give a smooth surface on the plates.This has the effect of producing clearer fringe patterns.Each plate was placed in the polariscope and the fringe value plotted at each mesh point with the aid of a microscope.The Tardy method of compensation was used in the analysis.

The results are listed in tables 7.2-7.5 on pages 127-130.

The $\frac{\sigma_1 - \sigma_2}{\sigma_{AV\,(MP)}}$ values were plotted pictorially to give an indication of the overall shear stress distribution in the plates.

The model of the joint having a weld all round the cover plate was tested by Mr Shipman under my supervision. The method of construction of the photo-elastic model was similar to that previously described.

The results are listed in tables 7.8-7.15 on page I37-I44.

The $\frac{\sigma_1 - \sigma_2}{\sigma_{AV\,(MP)}}$ pictorial plot is shown on page 148/9.

It was also decided to compare the separate σ_1 and σ_2 values in the model.The separation of the principal stress values was accomplished using the oblique incidence

Oblique incidence attachment
Photograph I3

Diamond wheel used for subslicing plate on grinder
Photograph I4

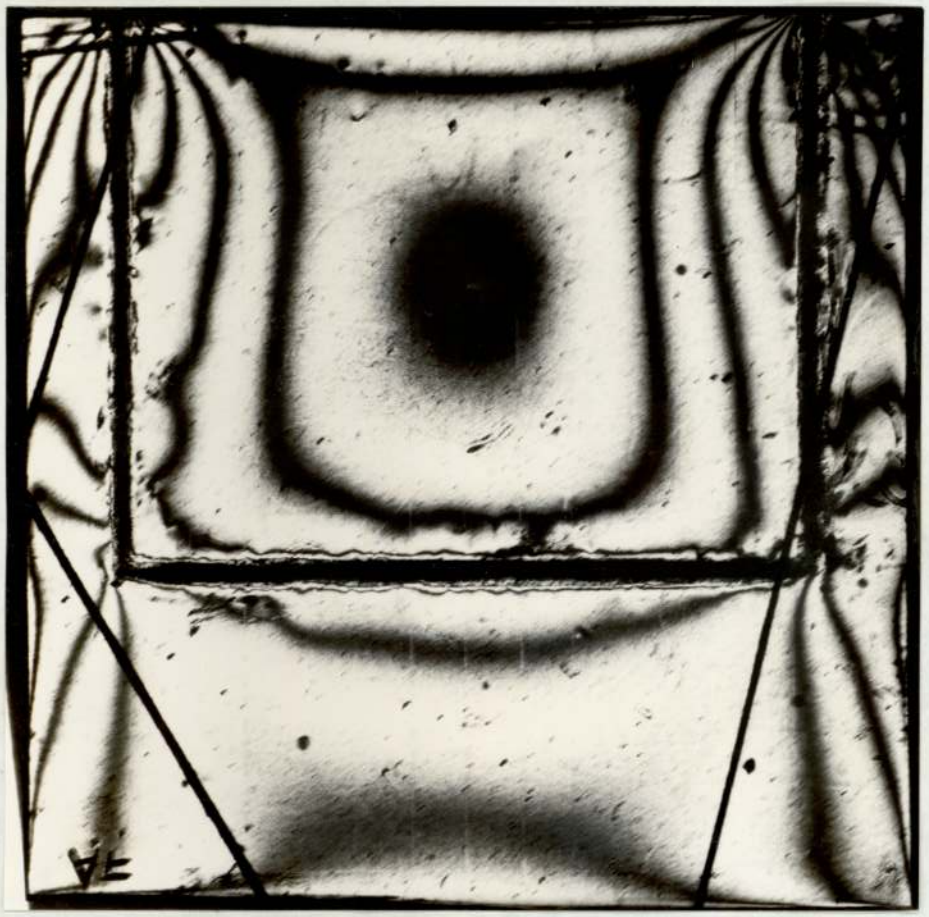

Main Plate
Fringe Multiplication x 9
Photograph 15

Cover Plate Fringe Multiplication x 9
Photograph 16

technique and by subslicing(Photographs I3 & I4 page I24) Fringe multiplication photographs were also taken of the cover and main plates (Photographs I5 & I6 page I25) and these results compared with those obtained by the Tardy method.

7.5 RESULTS Lap-welded connection(Side Fillet Weld)

The results given in the following tables are referenced as follows:-

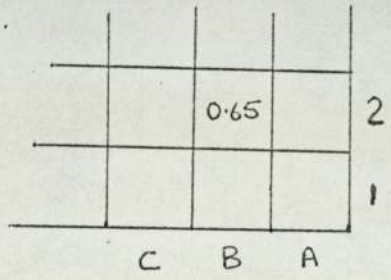

The value at the intersection of line B and line 2 in the reference diagram is 0.65

PHOTOELASTIC RESULTS. 3/16 MAIN PLATE (SIDE FILLET WELD).

FRINGE VALUES.

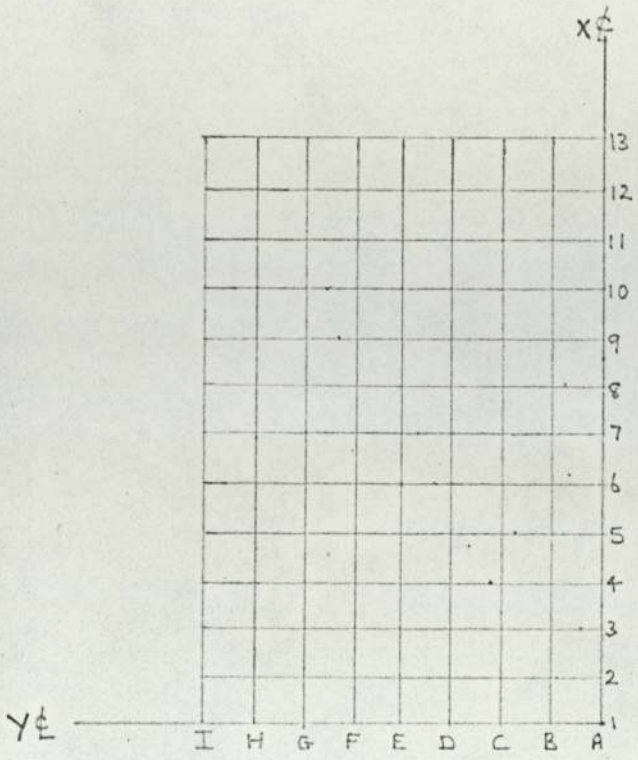

2·02	2·13	2·15	1·89	1·63	1·43	1·28	1·19	1·15	13
1·76	2·2	2·59	1·96	1·63	1·4	1·24	1·12	1·08	12
1·53	1·6	3·5	2·05	1·62	1·32	1·14	1·0	0·95	11
1·7	1·78	2·63	2·13	1·61	1·29	1·05	0·89	0·84	10
1·58	1·58	2·82	1·91	1·57	1·23	1·01	0·81	0·74	9
1·42	1·38	1·96	1·76	1·45	1·19	0·9	0·72	0·61	8
1·22	1·24	1·74	1·63	1·37	1·15	0·84	0·62	0·51	7
1·01	1·11	1·74	1·63	1·32	1·1	0·79	0·52	0·39	6
0·8	1·0	1·74	1·63	1·31	1·04	0·74	0·47	0·35	5
0·41	0·93	1·74	1·63	1·27	0·89	0·69	0·43	0·35	4
0·08	0·89	1·9	1·63	1·19	0·75	0·58	0·48	0·47	3
0	0·73	1·9	1·25	0·69	0·51	0·58	0·65	0·7	2
0	0	2·5	0	0·41	0·75	0·97	1·03	1·07	1
I	H	G	F	E	D	C	B	A	

Fig 7.2

PHOTOELASTIC RESULTS. 3/16 COVER PLATE (SIDE FILLET WELD)

FRINGE VALUES.

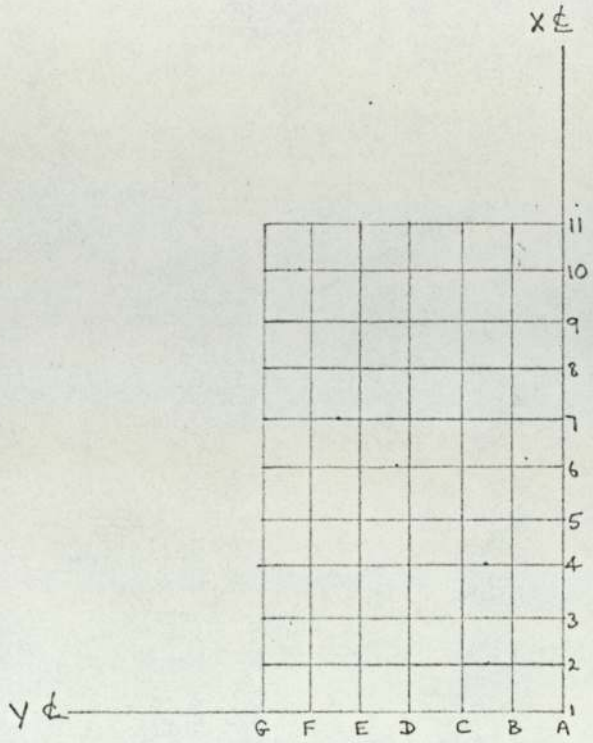

3·0	0·38	0·7	0·84	0·91	0·93	0·92	11
1·5	0·8	0·44	0·52	0·59	0·61	0·63	10
1·52	1·14	0·72	0·53	0·41	0·39	0·41	9
1·51	1·16	0·82	0·57	0·39	0·26	0·26	8
1·48	1·2	0·87	0·6	0·42	0·21	0·2	7
1·46	1·15	0·89	0·7	0·42	0·25	0·15	6
1·46	1·14	0·88	0·62	0·4	0·24	0·14	5
1·41	1·17	0·91	0·61	0·35	0·22	0·13	4
1·67	1·27	0·86	0·5	0·31	0·16	0·1	3
2·18	1·37	0·74	0·54	0·25	0·13	0·07	2
5·0	0·88	0·58	0·66	0·2	0·11	0·07	1
G	F	E	D	C	B	A	

Fig 7·3

PHOTOELASTIC RESULTS. 3/16 MAIN PLATE (SIDE FILLET WELD)

VALUES OF $\frac{\sigma_1 - \sigma_2}{\sigma_{AV(MAIN\ PLATE)}}$

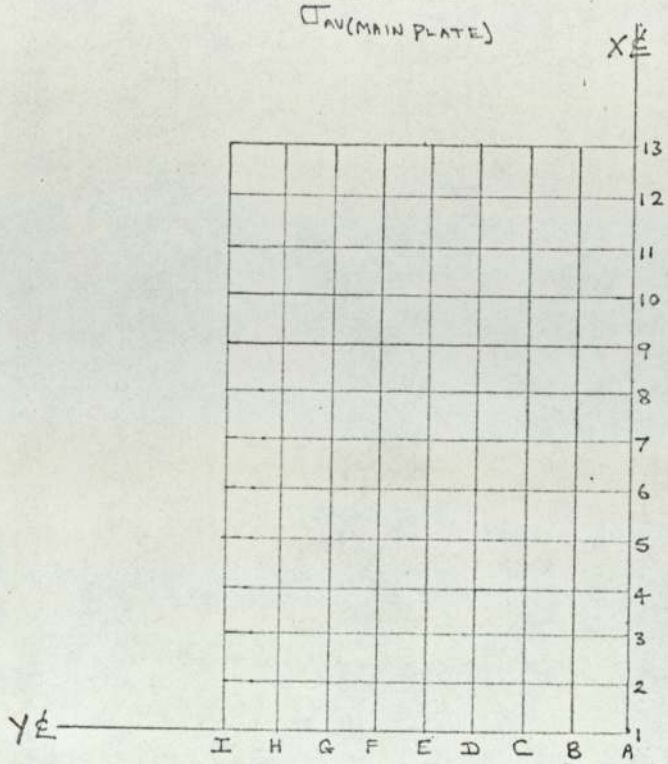

1·19	1·254	1·265	1·11	0·959	0·84	0·754	0·7	0·676	13
1·035	1·293	1·525	1·15	0·959	0·824	0·73	0·66	0·636	12
0·9	0·94	2·06	1·205	0·952	0·776	0·67	0·589	0·568	11
1·0	1·046	1·55	1·252	0·947	0·76	0·618	0·523	0·495	10
0·93	0·929	1·66	1·123	0·923	0·724	0·594	0·477	0·436	9
0·835	0·812	1·153	1·035	0·854	0·7	0·53	0·423	0·359	8
0·717	0·73	1·022	0·959	0·805	0·676	0·494	0·364	0·3	7
0·595	0·653	1·022	0·959	0·776	0·647	0·465	0·306	0·229	6
0·47	0·589	1·022	0·959	0·77	0·611	0·435	0·276	0·206	5
0·241	0·547	1·022	0·959	0·747	0·523	0·405	0·253	0·206	4
0·016	0·523	1·117	0·959	0·70	0·44	0·342	0·282	0·276	3
0	0·43	1·117	0·735	0·405	0·30	0·342	0·382	0·412	2
0	0	1·47	0	0·241	0·44	0·57	0·606	0·63	1
I	H	G	F	E	D	C	B	A	

Fig 7.4

PHOTOELASTIC RESULTS. 3/16 COVER PLATE (SIDE FILLET WELD).

VALUES OF $\sigma_1 - \sigma_2$

$\sigma_{N(MAIN\ PLATE)}$

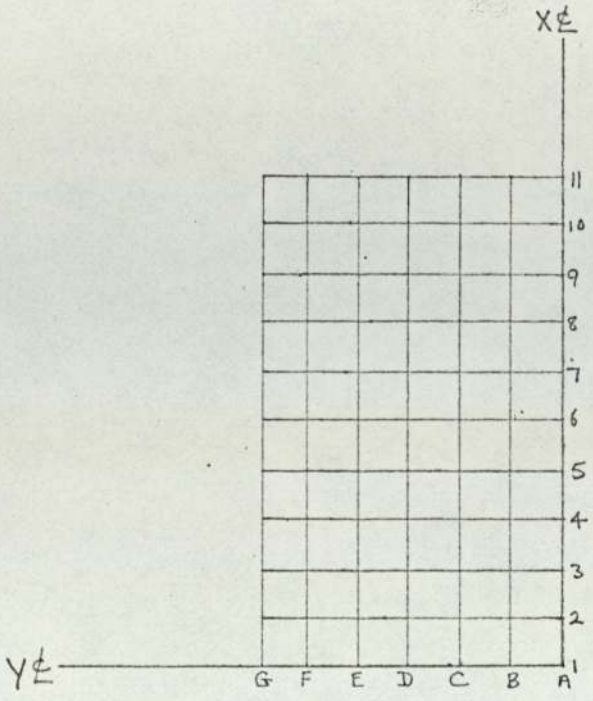

0·1765	0·1975	0·364	0·436	0·473	0·482	0·54	11
0·777	0·415	0·228	0·27	0·306	0·318	0·327	10
0·789	0·591	0·373	0·276	0·213	0·202	0·24	9
0·783	0·602	0·426	0·296	0·202	0·135	0·135	8
0·767	0·624	0·452	0·312	0·218	0·1095	0·0881	7
0·759	0·597	0·462	0·364	0·218	0·13	0·0784	6
0·759	0·591	0·457	0·322	0·208	0·125	0·0617	5
0·732	0·606	0·472	0·318	0·182	0·114	0·0576	4
0·865	0·659	0·446	0·259	0·161	0·083	0·0517	3
1·132	0·712	0·385	0·28	0·147	0·085	0·0365	2
2·94	0·456	0·3	0·206	0·103	0·057	0·0365	1
G	F	E	D	C	B	A	

Fig 7.5

PICTORIAL PLOT OF $\frac{\sigma_1 - \sigma_2}{\sigma_{AV(MAIN\ PLATE)}}$ FOR COVER PLATE. (PHOTOELASTIC)

SIDE WELD COVER PLATE. (Fig 7.6)

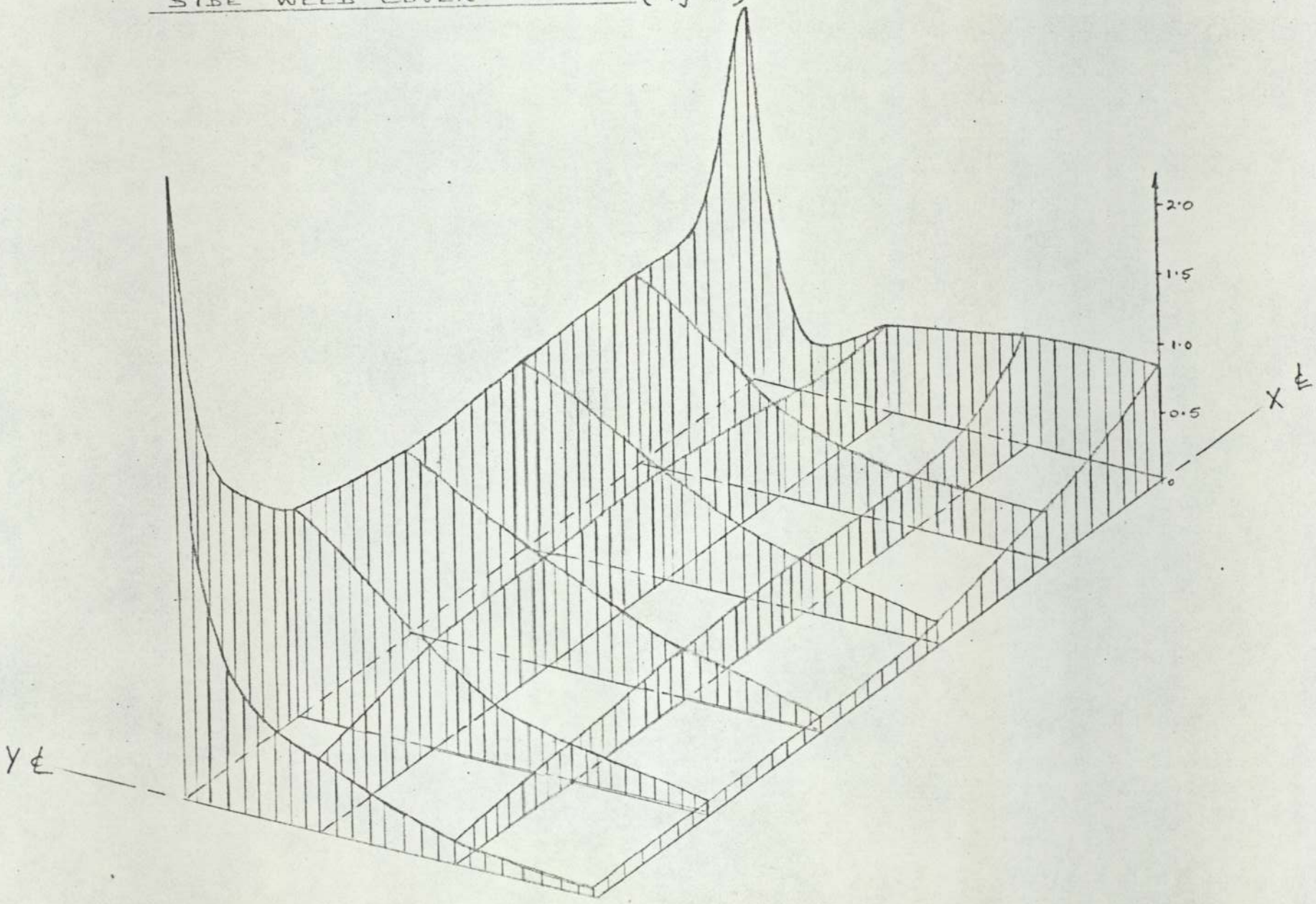

PICTORIAL PLOT OF $\frac{\sigma}{\sigma_{AV(MAIN\ PLATE)}}$ FOR MAIN PLATE. (PHOTOELASTIC)

SIDE WELD COVER PLATE. (Fig 7.7)

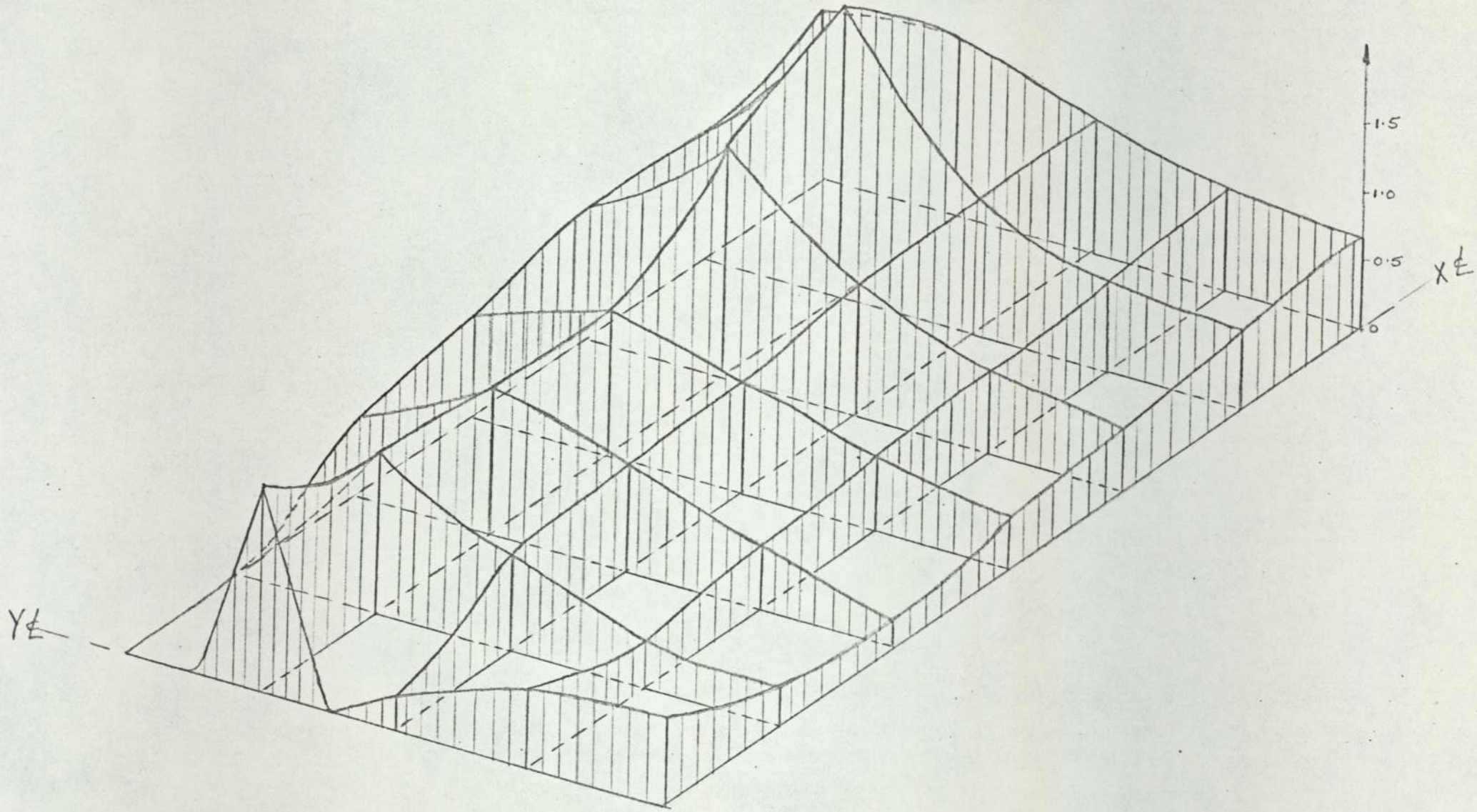

VARIATION OF $\sigma_1 - \sigma_2 / \sigma_{AV(MP)}$ ALONG THE CENTRE LINES OF THE 3/16" MODEL COVER PLATE (SIDE WELD).

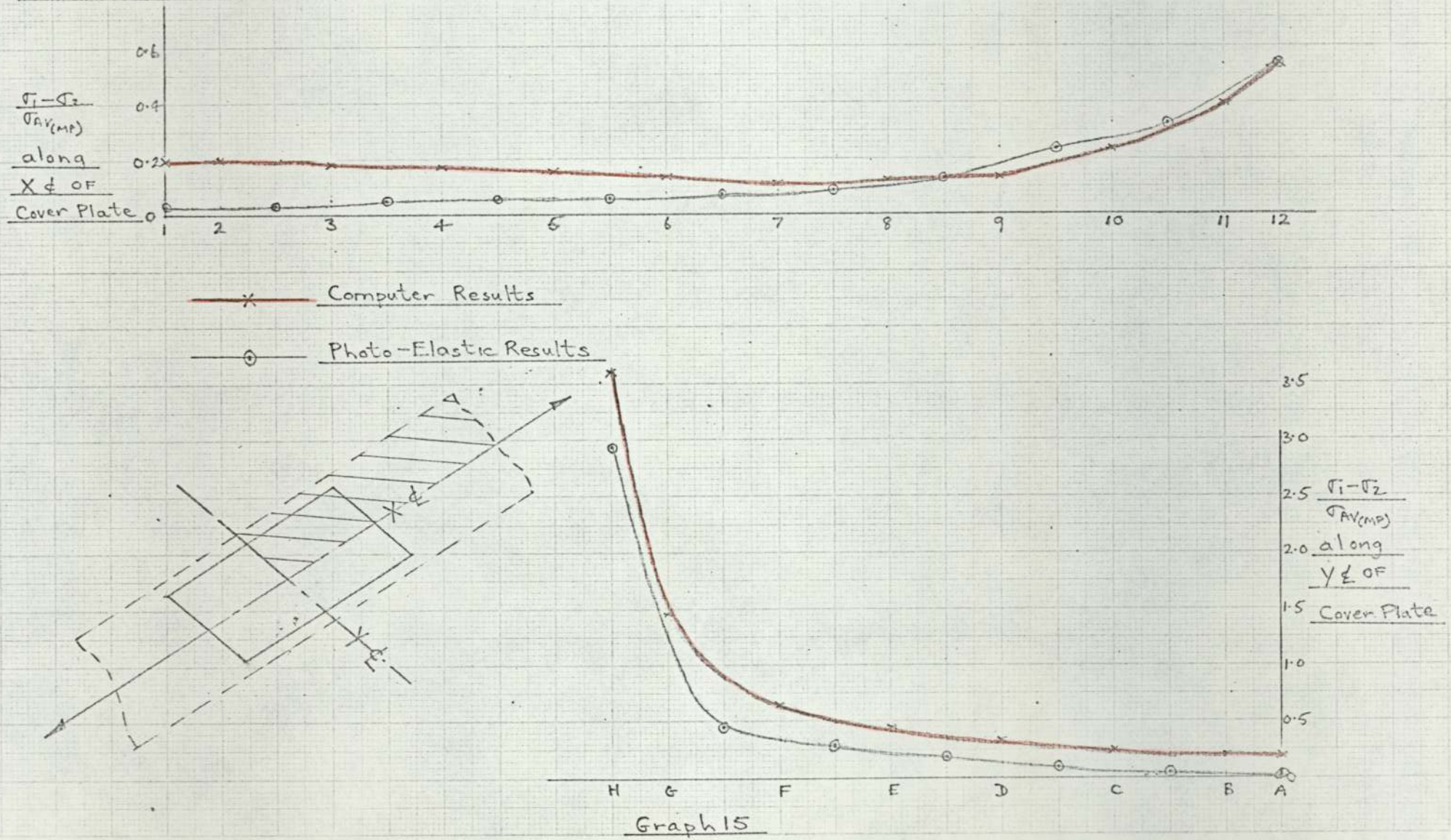

Graph 15

VARIATION OF $\sigma_1 - \sigma_2 / \sigma_{AV(MP)}$ ALONG THE X CENTRE LINE OF MAIN PLATE (SIDE WELD)

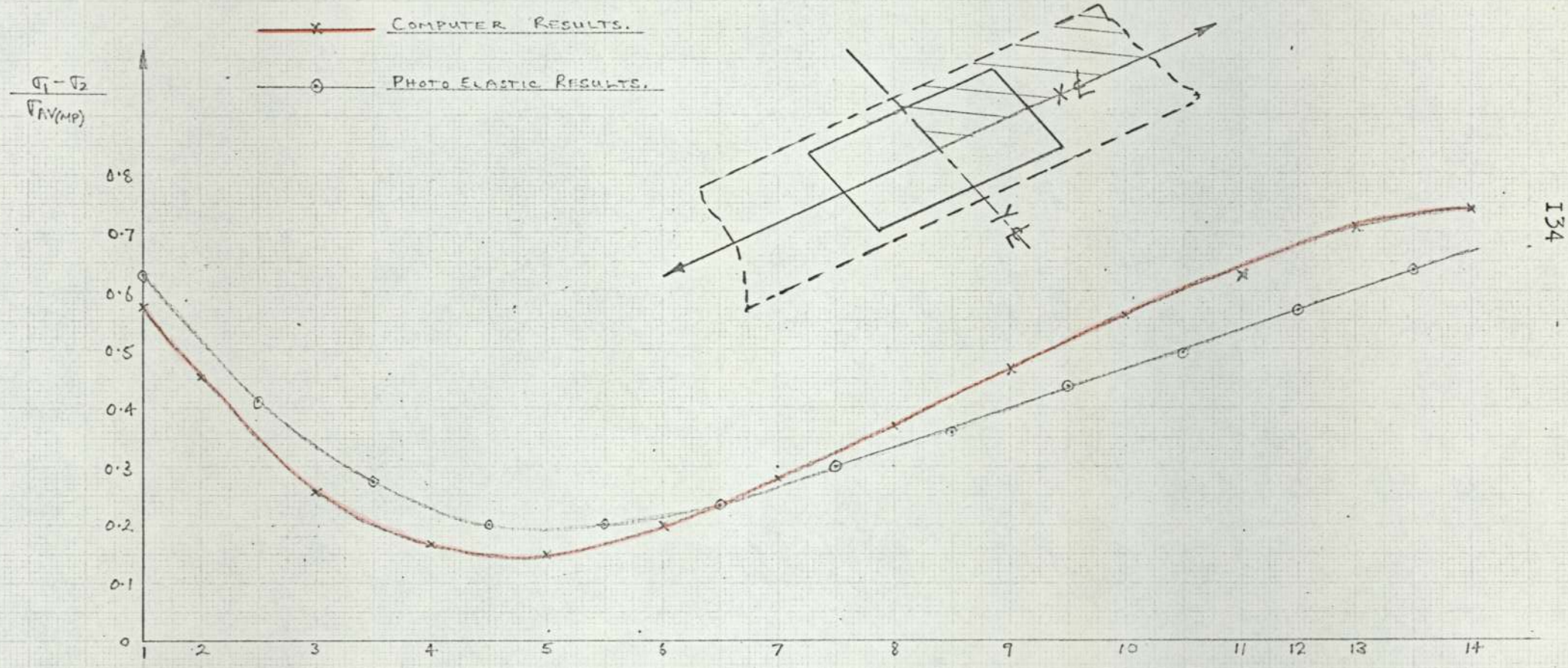

Graph 16

VARIATION OF $\sigma_1 - \sigma_2 / \sigma_{AVMP}$ ALONG THE Y CENTRE LINE OF MAIN PLATE (SIDE WELD).

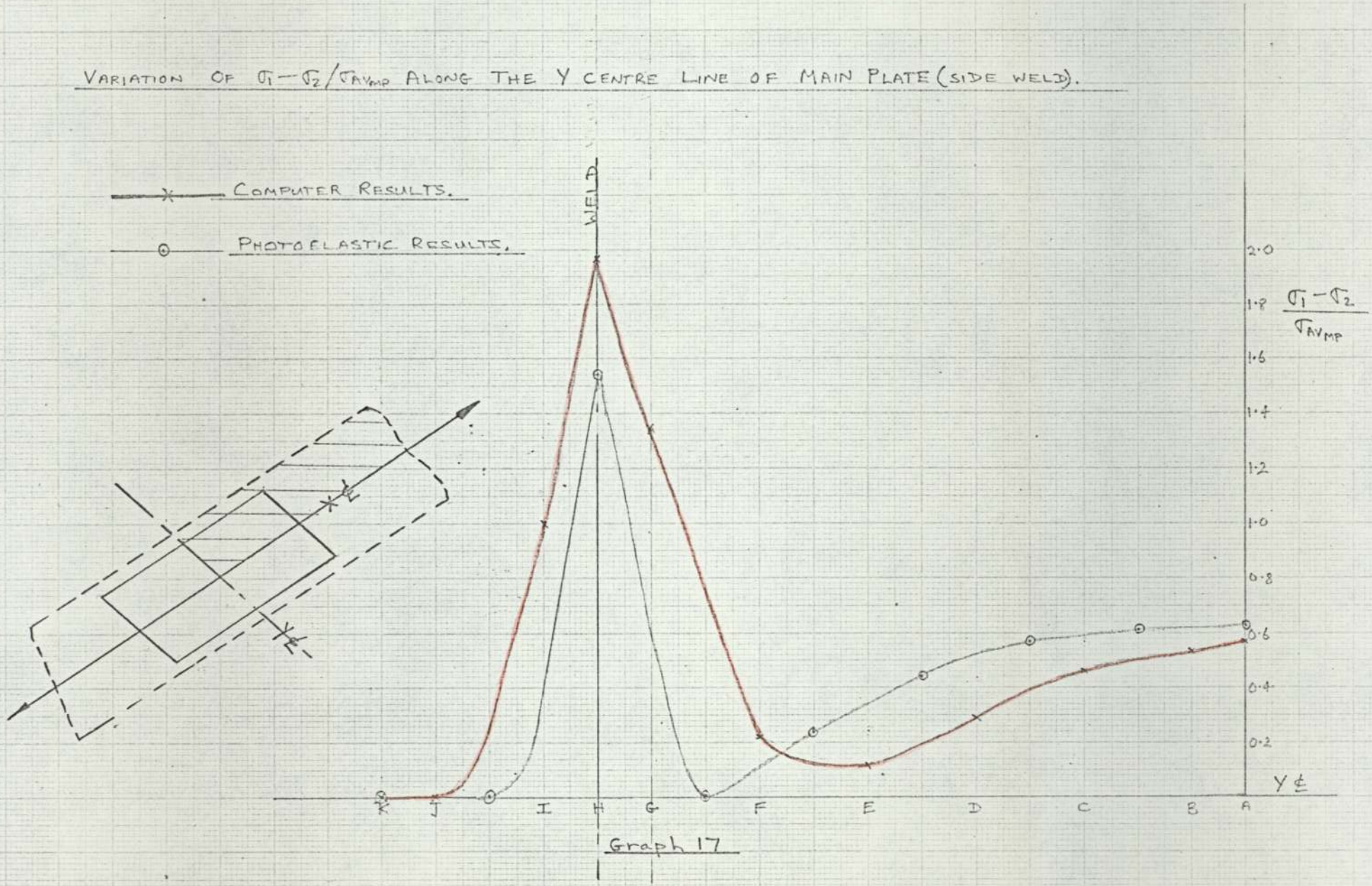

Graph 17

7.6 RESULTS Lap-welded connection(Weld all round cover plate)

The results given in the following tables are referenced as follows:-

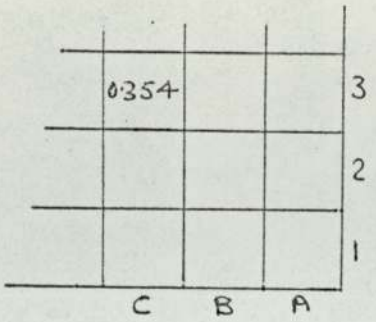

The value at the intersection of line C and line 3 in the reference diagram is 0.354

PHOTOELASTIC RESULTS — $\frac{1}{16}$" COVER PLATE.

VALUES OF $(\sigma_1 - \sigma_2)$ DIVIDED BY AVERAGE STESS MAIN PLATE

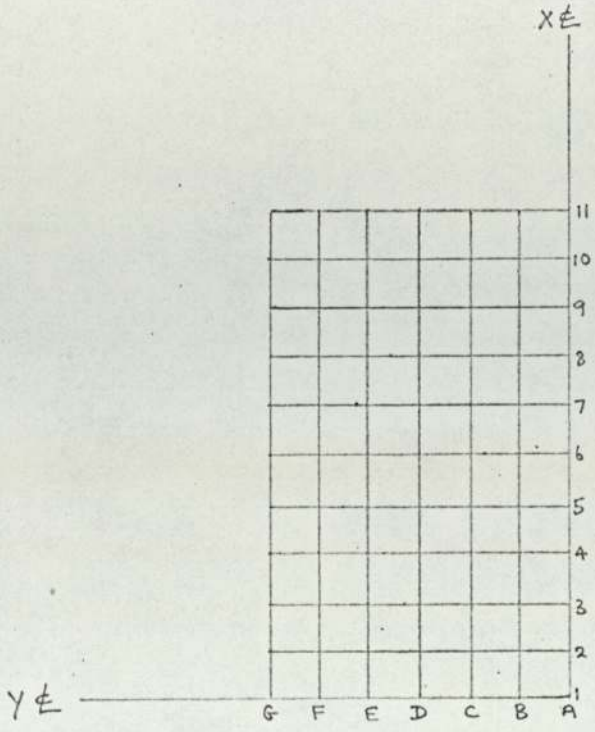

0·455	0·455	0·480	0·493	0·493	0·520	0·520	11
0·433	0·418	0·430	0·455	0·480	0·493	0·493	10
0·443	0·380	0·405	0·418	0·405	0·443	0·443	9
0·443	0·405	0·405	0·418	0·405	0·418	0·418	8
0·443	0·405	0·405	0·392	0·380	0·392	0·392	7
0·443	0·430	0·430	0·392	0·380	0·392	0·392	6
0·443	0·455	0·455	0·405	0·380	0·380	0·380	5
0·443	0·494	0·468	0·405	0·367	0·354	0·354	4
0·570	0·570	0·468	0·418	0·354	0·342	0·316	3
0·735	0·595	0·455	0·392	0·342	0·316	0·291	2
2·28	0·443	0·380	0·354	0·342	0·316	0·291	1
G	F	E	D	C	B	A	

Fig 7.8

PHOTOELASTIC RESULTS. 1/16 INCH MAIN PLATE.

VALUES OF $(\sigma_1 - \sigma_2)$ DIVIDED BY AVERAGE STRESS IN MAIN PLATE.

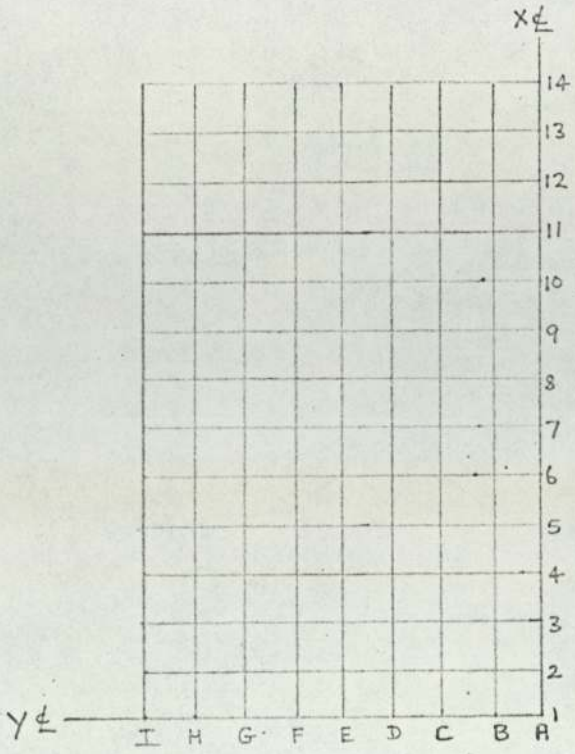

0·797	0·836	0·912	0·974	1·00	0·974	0·962	0·962	0·962	14
0·773	0·810	0·900	0·962	0·944	0·962	0·912	0·925	0·912	13
0·747	0·760	0·912	0·950	0·937	0·873	0·848	0·848	0·846	12
0·760	0·734	0·832	0·658	0·607	0·570	0·531	0·506	0·506	11
0·672	0·710	0·443	0·380	0·316	0·278	0·266	0·215	0·190	10
0·595	0·670	0·443	0·342	0·278	0·228	0·190	0·177	0·165	9
0·557	0·608	0·443	0·342	0·266	0·215	0·165	0·139	0·139	8
0·505	0·519	0·443	0·367	0·291	0·215	0·152	0·089	0·089	7
0·392	0·468	0·443	0·405	0·329	0·228	0·165	0·089	0·064	6
0·316	0·393	0·491	0·405	0·304	0·228	0·152	0·114	0·114	5
0·240	0·365	0·456	0·443	0·316	0·215	0·152	0·139	0·139	4
0·127	0·342	0·506	0·430	0·291	0·202	0·190	0·190	0·190	3
0	0·291	0·557	0·367	0·215	0·215	0·240	0·240	0·266	2
0	0	1·08	0·063	0·190	0·253	0·279	0·291	0·291	1
I	H	G	F	E	D	C	B	A	

Fig 7.9

PHOTOELASTIC RESULTS. 1/16" COVER PLATE

VALUES OF FRINGE ORDER — NORMAL (n_0) AND OBLIQUE INCIDENCE ($n_{\theta'}$)

$n_{\theta'}$ OBTAINED BY REVOLVING ABOUT σ_2 AXIS.

VALUES OF PRINCIPAL STRESSES σ_1 AND σ_2 IN lbf/in^2

n_0	$n_{\theta'}$	n_0	$n_{\theta'}$	n_0	$n_{\theta'}$	n_0	$n_{\theta'}$	n_0	$n_{\theta'}$	n_0	$n_{\theta'}$	n_0	$n_{\theta'}$	
σ_1	σ_2	σ_1	σ_2	σ_1	σ_2	σ_1	σ_2	σ_1	σ_2	σ_1	σ_2	σ_1	σ_2	
0·40	0·24	0·37	0·31	0·37	0·305	0·39	0·30	0·39	0·35	0·41	0·32	0·41	0·37	
10·9	-1·42	7·15	-1·42	7·35	-1·42	6·06	-1·56	6·73	-2·55	9·20	-0·52	7·10	-2·6	11
0·35	0·23	0·33	0·28	0·34	0·29	0·34	0·275	0·35	0·295	0·37	0·28	0·38	0·32	
8·2	0·38	6·25	-1·57	6·4	-1·66	6·95	-1·16	6·70	-1·59	8·10	-0·65	7·35	-1·66	10
0·35	0·22	0·32	0·23	0·31	0·23	0·33	0·25	0·33	0·27	0·35	0·27	0·35	0·28	
9·2	-0·90	7·45	-0·04	6·96	-0·38	7·25	-0·57	6·56	-1·23	7·54	-0·76	7·20	-1·09	9
0·35	0·23	0·32	0·22	0·31	0·215	0·31	0·22	0·32	0·25	0·35	0·24	0·33	0·25	
0·82	0·38	7·76	0·02	7·49	0·014	7·35	0	6·78	-0·805	8·53	0·24	7·25	-0·57	8
0·35	0·23	0·32	0·22	0·32	0·205	0·32	0·20	0·30	0·22	0·34	0·21	0·32	-0·22	
0·82	0·38	7·76	0·02	8·30	0·475	8·48	0·90	6·85	-0·294	9·10	1·04	7·80	0	7
0·35	0·23	0·34	0·22	0·33	0·21	0·32	0·195	0·29	0·195	0·32	0·185	0·30	0·19	
0·82	0·38	8·74	0·805	8·62	0·805	8·65	1·07	7·23	0·355	8·75	1·37	7·80	0·71	6
0·36	0·25	0·37	0·23	0·35	0·21	0·33	0·195	0·30	0·175	0·30	0·165	0·28	0·17	
8·67	0·014	9·80	1·042	9·86	1·32	8·90	1·30	8·36	1·26	8·70	1·59	7·58	0·95	5
0·37	0·25	0·39	0·24	0·37	0·215	0·34	0·18	0·29	0·16	0·28	0·15	0·27	0·14	
9·1	0·38	10·42	1·19	10·35	1·33	9·85	1·80	8·4	1·52	8·25	1·61	8·10	1·70	4
0·43	0·27	0·45	0·26	0·37	0·21	0·31	0·16	0·28	0·14	0·27	0·105	0·26	0·11	
11·3	1·13	12·6	1·71	10·5	1·75	9·35	1·99	8·58	1·94	9·26	2·87	8·68	2·51	3
0·60	0·36	0·46	0·25	0·33	0·175	0·29	0·12	0·27	0·105	0·25	0·09	0·25	0·09	
16·35	2·03	13·4	2·51	9·8	2·05	9·70	2·84	9·80	2·86	8·95	2·94	8·85	2·94	2
		0·85	0·11	0·29	0·10	0·27	0·09	0·26	0·09	0·25	0·08	0·24	0·07	
		12·9	4·60	10·40	3·50	9·84	3·41	9·35	3·17	9·15	3·22	9·0	3·32	1
G		F		E		D		C		B		A		

Fig 7.10

PHOTOELASTIC RESULTS. ½" MAIN PLATE.

VALUES OF FRINGE ORDER — NORMAL (n_0) AND OBLIQUE INCIDENCE (n_{θ}).

VALUES OF PRINCIPAL STRESSES σ_1 AND σ_2 IN lbf/in²

n_0	$n_{0'}$	n_0	$n_{0'}$	n_0	$n_{0'}$	n_0	$n_{0'}$	n_0	$n_{0'}$	
σ_1	σ_2	σ_1	σ_2	σ_1	σ_2	σ_1	σ_2	σ_1	σ_2	
0·69	0·96	0·71	1·0	0·75	1·06	0·78	1·10	0·78	1·10	
16·35	0	16·70	-0·119	17·75	0	18·40	-0·10	18·40	-0·10	10
0·70	0·93	0·071	0·99	0·75	1·06	0·77	1·10	0·77	1·08	
16·60	0	16·35	-0·494	17·45	0	18·6	0·37	17·90	-0·37	9
0·63	0·86	0·69	0·98	0·75	1·10	0·75	1·08	0·75	1·10	
14·90	0	16·45	0·119	19·05	1·305	18·4	0·64	19·05	1·305	8
0·62	0·87	0·68	0·99	0·71	0·98	0·67	1·04	0·67	1·03	
14·70	0	17·10	0·974	16·25	-0·570	19·00	3·12	18·60	2·75	7
0·545	0·76	0·30	0·39	0·22	0·285	0·20	0·22	0·20	0·20	
12·90	0	5·97	-1·14	4·36	-0·855	2·66	-2·09	1·98	-2·76	6
0·46	0·66	0·32	0·40	0·19	0·26	0·15	0·18	0·12	0·12	
10·90	0	5·83	-1·75	4·22	-0·284	2·46	-1·09	1·17	-1·67	5
0·36	0·50	0·32	0·405	0·20	0·245	0·12	0·15	0·07	0·09	
8·53	0	6·00	-3·96	3·49	-1·26	2·18	-0·664	1·34	-0·794	4
0·26	0·38	0·35	0·39	0·21	0·27	0·11	0·14	0·045	0·075	
6·55	0	4·75	-3·53	4·05	-0·925	2·08	-0·522	1·21	-0·570	3
0·01	0·07	0·40	0·945	0·19	0·23	0·11	0·13	0·11	0·09	
0·237	0	5·42	-4·05	3·22	-1·325	1·74	-0·865	0·403	-2·20	2
0	0	1·10	0·80	0·15	0·105	0·19	0·13	0·21	0·15	
0	0	0	23·4	0	-2·49	0	-4·50	0	-4·97	1
E		D		C		B		A		

Fig 7.11

PHOTOELASTIC RESULTS — 1/16 INCH COVER PLATE

VALUES OF σ_1 AND σ_2 DIVIDED BY AVERAGE STRESS IN MAIN PLATE.

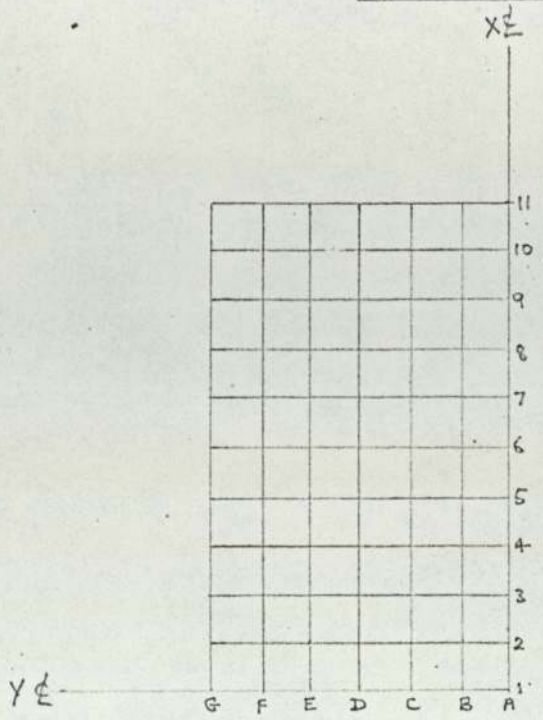

σ_1	σ_2	σ_1	σ_2	σ_1	σ_2	σ_1	σ_2	σ_1	σ_2	σ_1	σ_2	σ_1	σ_2	
0·591	-0·077	0·388	-0·077	0·398	-0·077	0·329	-0·045	0·375	-0·136	0·499	-0·028	0·385	-0·141	11
0·445	0·02	0·339	0·085	0·347	-0·09	0·377	-0·063	0·364	-0·086	0·449	-0·033	0·400	-0·09	10
0·500	-0·05	0·409	-0·0008	0·378	-0·02	0·394	-0·031	0·356	-0·067	0·409	-0·041	0·390	-0·06	9
0·445	0·02	0·421	0·001	0·406	0·0008	0·399	0	0·367	-0·04	0·443	0·013	0·393	-0·03	8
0·445	0·02	0·421	0·001	0·450	0·025	0·460	0·049	0·370	0·015	0·490	0·056	0·423	0	7
0·445	0·02	0·474	0·044	0·467	0·044	0·470	0·057	0·391	0·02	0·475	0·075	0·423	0·039	6
0·478	0·0008	0·531	0·056	0·519	0·072	0·482	0·07	0·454	0·068	0·472	0·086	0·410	0·052	5
0·494	0·02	0·565	0·064	0·560	0·072	0·534	0·098	0·455	0·082	0·446	0·087	0·440	0·093	4
0·614	0·061	0·673	0·093	0·570	0·098	0·507	0·108	0·465	0·105	0·502	0·155	0·470	0·136	3
0·886	0·111	0·726	0·136	0·530	0·111	0·526	0·154	0·505	0·156	0·480	0·159	0·460	0·159	2
		0·700	0·250	0·563	0·190	0·534	0·195	0·506	0·172	0·495	0·175	0·488	0·180	1
G		F		E		D		C		B		A		

Fig 7.12

PHOTOELASTIC RESULTS. K6 MAIN PLATE.

VALUES OF σ_1 AND σ_2 DIVIDED BY AVERAGE STRESS IN MAIN PLATE.

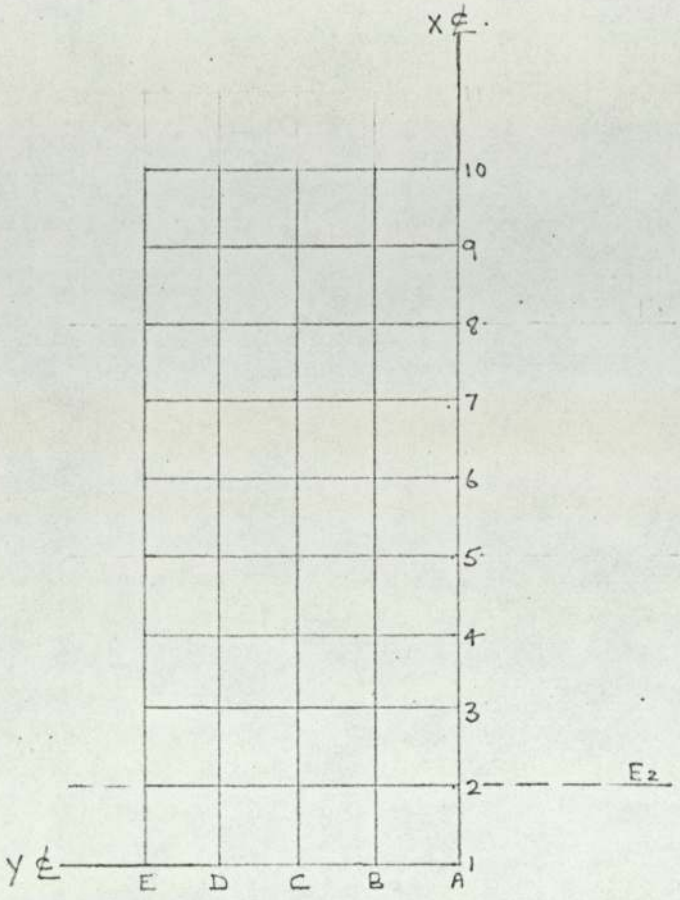

σ_1	σ_2	σ_1	σ_2	σ_1	σ_2	σ_1	σ_2	σ_1	σ_2	
0·885	0	0·896	-0·006	0·961	0	0·995	-0·005	0·995	-0·005	10
0·897	0	0·885	-0·026	0·961	0	1·01	0·019	0·980	-0·019	9
0·807	0	0·890	0·006	1·03	-0·071	0·997	0·035	1·03	-0·071	8
0·795	0	0·925	0·053	0·880	-0·031	1·02	0·169	0·996	0·149	7
0·692	0	0·323	-0·062	0·236	-0·046	0·141	-0·113	0·107	-0·117	6
0·590	0	0·315	-0·095	0·228	-0·015	0·133	-0·059	0·064	-0·090	5
0·461	0	0·324	-0·214	0·188	-0·068	0·118	-0·036	0·073	-0·043	4
0·333	0	0·258	-0·191	0·219	-0·050	0·113	-0·028	0·065	-0·031	3
0·013	0	0·294	-0·219	0·173	-0·069	0·094	-0·047	0·022	-0·119	2
0	0	0	0·990	0	-0·135	0	-0·244	0	-0·270	1
E		D		C		B		A		

Fig 7.13

PHOTOELASTIC RESULTS.

FRINGE MULTIPLICATION.

1/16 MAIN PLATE.

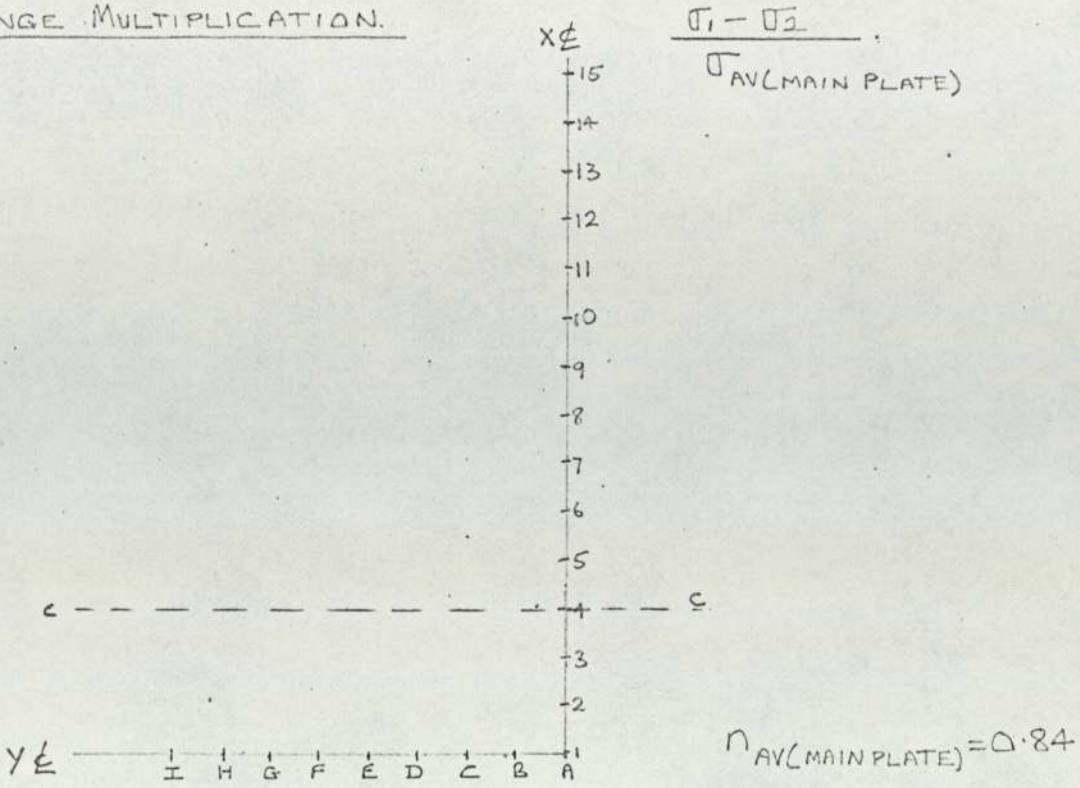

MULTIPLICATION FACTOR	POSITION ON CC AXIS	MULTIPLIED FRINGE ORDER	ACTUAL FRINGE ORDER	$\frac{n}{n_{AV}}$	POSITION ON X AXIS	MULTIPLIED FRINGE ORDER	ACTUAL FRINGE ORDER	$\frac{n}{n_{AV}}$
3	E+¼EF	1	0·333	0·396	1⅓	1	0·333	0·396
	H	1	0·333	0·396				
5	H+¾HI	1	0·200	0·238	2½	1	0·200	0·238
	G+½GH	2	0·400	0·476	9½	1	0·200	0·238
	E+¾EF	2	0·400	0·476	13	4	0·800	0·952
7	H+⅞HI	1	0·143	0·169	1½	2	0·286	0·340
	H	2	0·286	0·340	3½	1	0·143	0·170
	G	3½	0·500	0·575	8½	1	0·143	0·170
	F	3	0·429	0·510	10½	2	0·286	0·340
	F+½FG	3¼	0·465	0·554	11½	4	0·570	0·680
	E	2	0·286	0·340	14½	5	0·715	0·850
	D	1½	0·214	0·255				
9	H+⅞HI	1	0·111	0·132	1⅛	3	0·333	0·397
	H+½HI	2	0·222	0·264	2¼	2	0·222	0·264
	G+⅛GH	3	0·333	0·396	5, 6, 7	1	0·111	0·132
	F	4	0·445	0·550	9	1¼	0·167	0·197
	E+¼EF	3	0·333	0·396	10	2	0·222	0·264
	D	2	0·222	0·264	12¼	6	0·667	0·795
	C	1¾	0·194	0·236	14	6½	0·722	0·860
	A, B	1½	0·168	0·199	15½	7	0·788	0·926

Fig 7.14

PHOTOELASTIC RESULTS

FRINGE MULTIPLICATION

$\frac{1}{16}$ COVER PLATE

$\frac{\sigma_1 - \sigma_2}{\sigma_{AV}}$ (MAIN PLATE)

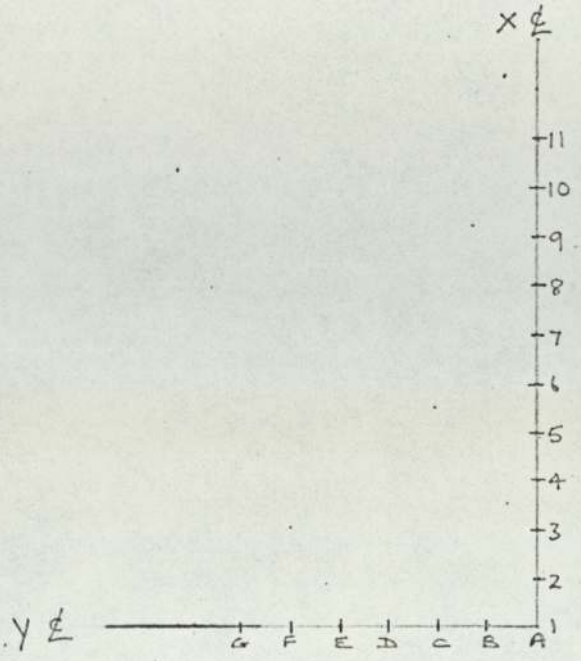

MULTIPLICATION FACTOR	POSITION ON Y-AXIS	MULTIPLIED FRINGE ORDER	ACTUAL FRINGE ORDER	$\frac{n}{n_{AV}}$	POSITION ON X AXIS	MULTIPLIED FRINGE ORDER	ACTUAL FRINGE ORDER	$\frac{n}{n_{AV}}$
3	E	1	0·333	0·393	4	1	0·333	0·393
5	A	1½	0·30	0·357	1	1½	0·30	0·357
	F+¼FG	2	0·40	0·476	8½	2	0·40	0·476
	F+¾FG	3	0·60	0·715				
7	A,B,C	2	0·287	0·340	7	2	0·287	0·340
	D+½DE	2¼	0·320	0·381	9½	3	0·428	0·510
9	F+½FG	4	0·445	0·530	4½	3	0·333	0·396
	E+½EF	3	0·333	0·396	10	4	0·445	0·530
					7½	3½	0·389	0·463
11	F	4	0·364	0·433	6½	4	0·364	0·433
					8½	4½	0·409	0·477
					10	5	0·455	0·541
13	F+¼FG	5	0·385	0·456	7½	5	0·385	0·458
	C+¾CD	4	0·308	0·366	2½	4	0·308	0·366
	F+⅞FG	11	0·845	1·0	5	4½	0·346	0·412
					11	6	0·461	0·550

Fig 7.15

VARIATION OF $\sigma_1 - \sigma_2 / \sigma_{AV(MP)}$ ALONG THE X CENTRE LINE OF MAIN PLATE (WELD ALL ROUND).

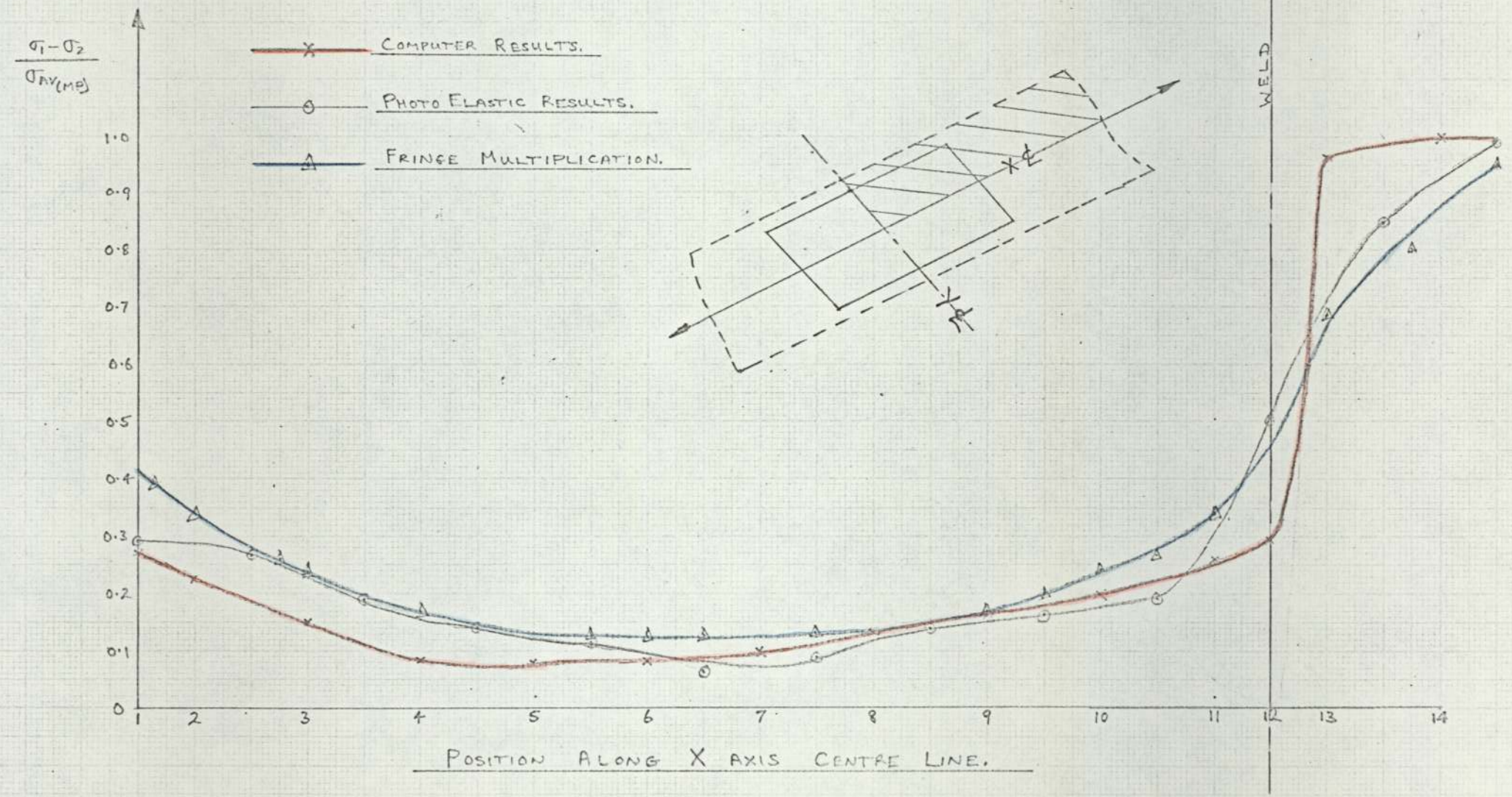

Graph 18

VARIATION OF $\sigma_1 - \sigma_2 / \sigma_{AV(MP)}$ ALONG THE CENTRE LINES OF THE COVER PLATE (WELD ALL ROUND)

$\frac{\sigma_1 - \sigma_2}{\sigma_{AV(MP)}}$ along X ℄ OF Cover Plate.

0·5
0·4
0·3
0·2
0·1
0
1 2 3 4 5 6 7 8 9 10 11 12

COMPUTER RESULTS.

PHOTO ELASTIC RESULTS.

FRINGE MULTIPLICATION.

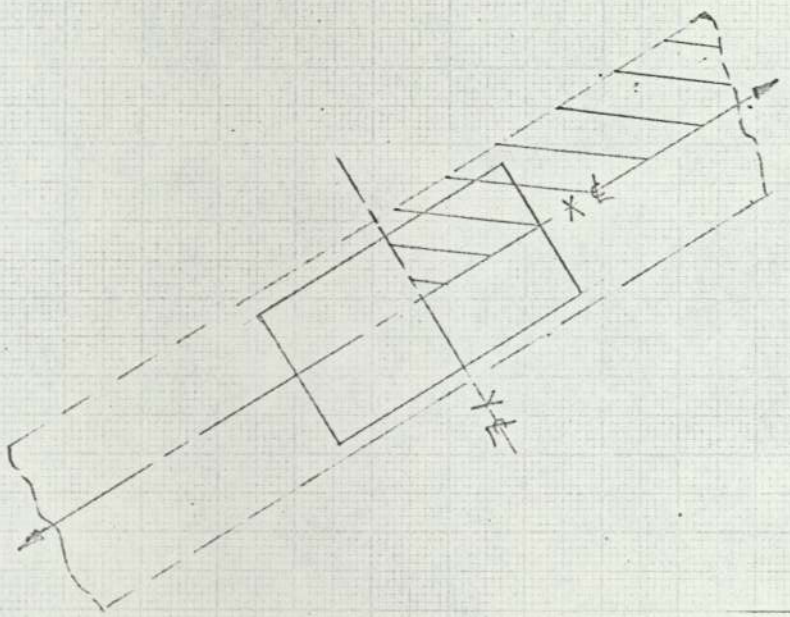

2·4
2·2
2·0
1·8
1·6
1·4
1·2
1·0
0·8
0·6
0·4
0·2
0

$\frac{\sigma_1 - \sigma_2}{\sigma_{AV(MP)}}$ along Y ℄ of Cover Plate.

H G F E D C B A Y ℄

Graph 19

VARIATION OF $\sigma_1 - \sigma_2 / \sigma_{AV(MP)}$ ALONG THE Y CENTRE LINE OF MAIN PLATE. (WELD ALL ROUND).

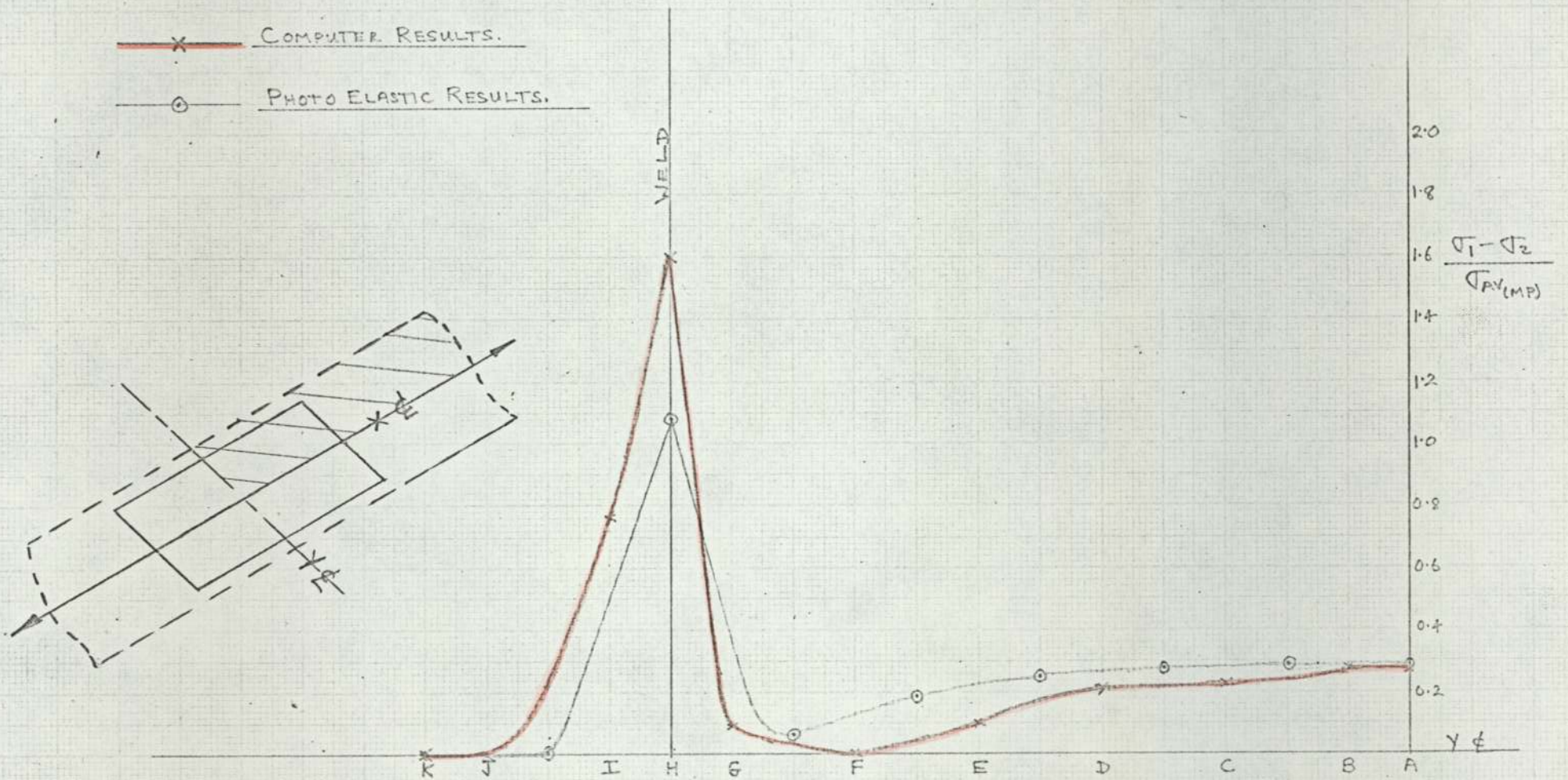

Graph 20

PICTORIAL PLOT OF $\frac{\sigma_1 - \sigma_2}{\sigma_{AV\,(MAIN\,PLATE)}}$ FOR COVER PLATE. (PHOTOELASTIC)

WELD ALL ROUND COVER PLATE. (7.16)

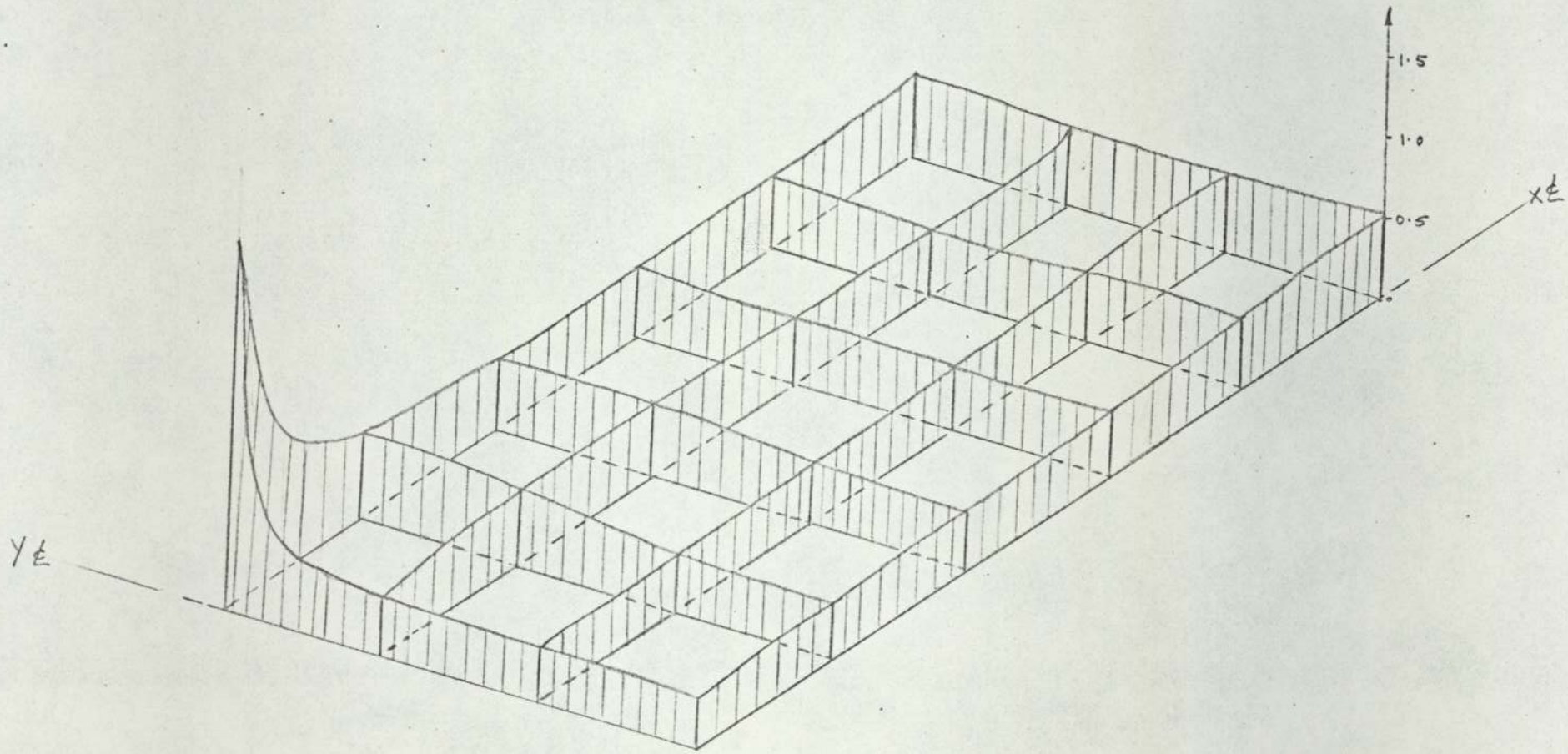

PICTORIAL PLOT OF $\frac{\sigma_1 - \sigma_2}{\sigma_{AV(Main\ Plate)}}$ FOR MAIN PLATE (PHOTOELASTIC)

WELD ALL ROUND COVER PLATE. (Fig 7.17)

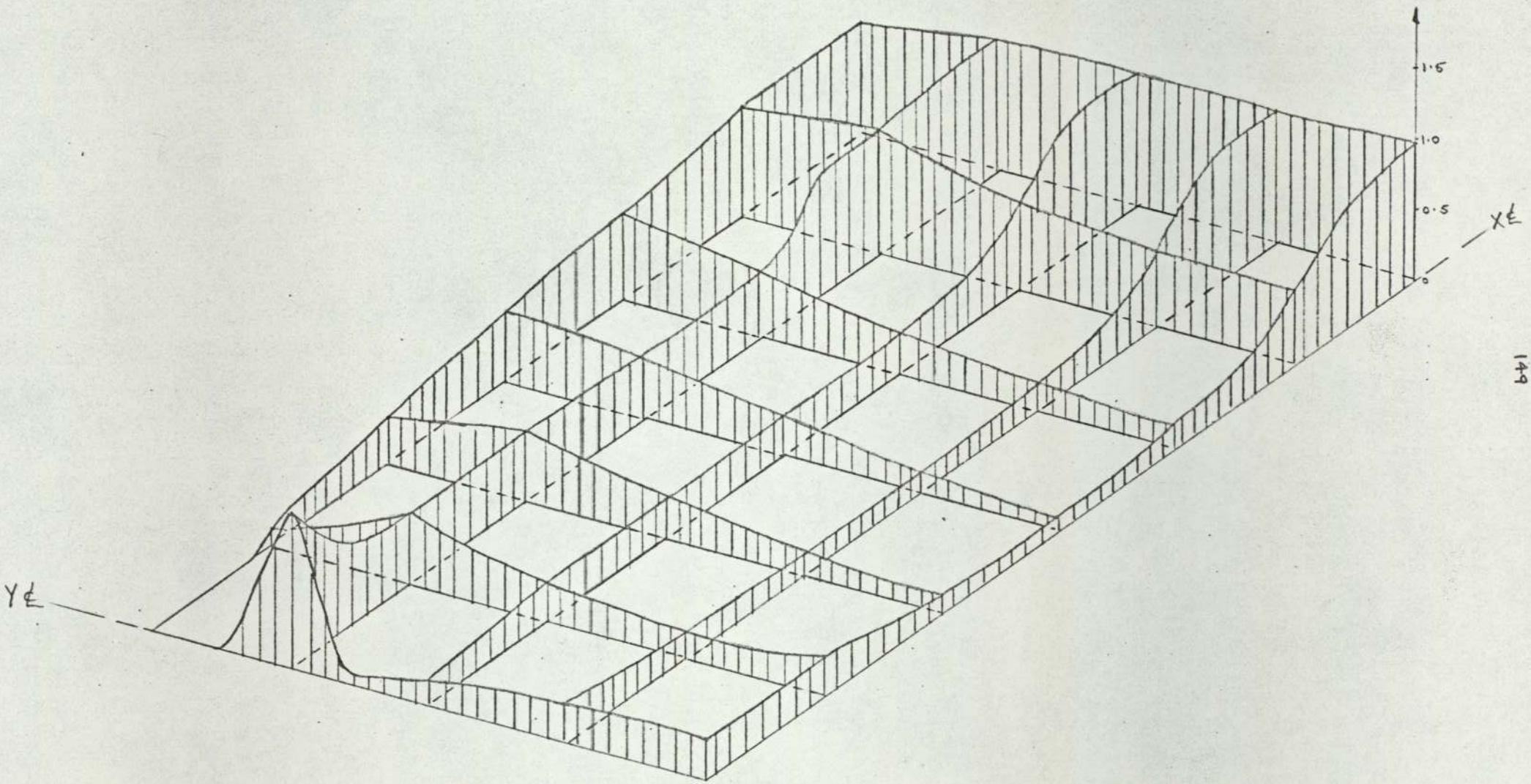

GRAPH OF σ_1 AND σ_2 DIVIDED BY $\sigma_{AV_{(MP)}}$ ALONG X ℄ OF COVERPLATE.

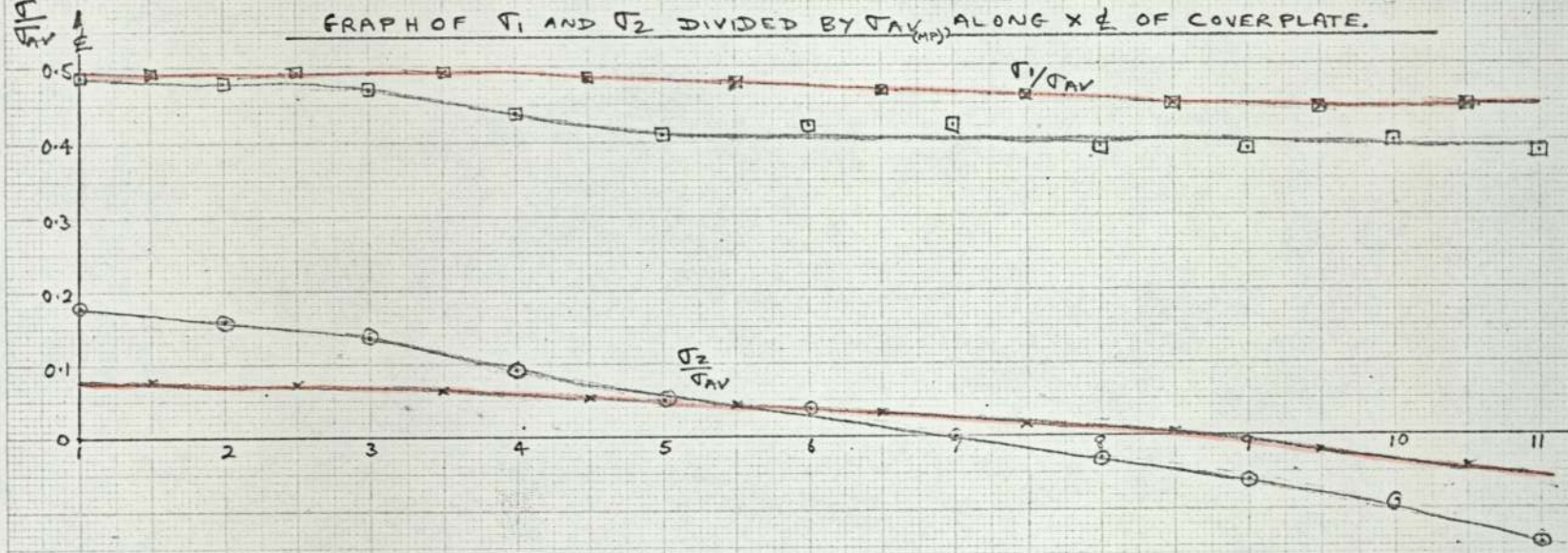

σ1/σAV σ2/σAV COMPUTER VALUES.

σ1/σAV σ2/σAV PHOTOELASTIC VALUES (BY OBLIQUE INCIDENCE)

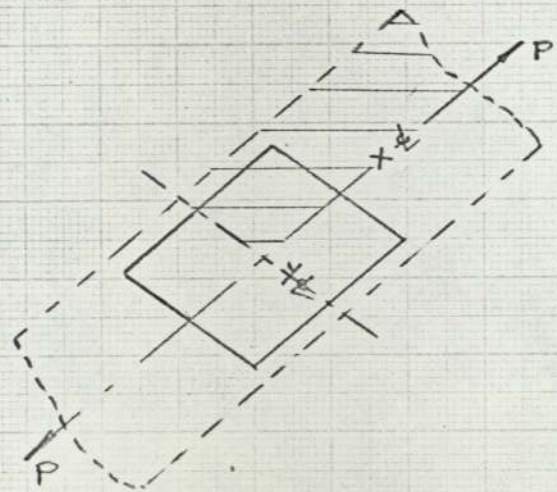

GRAPH OF σ_1 AND σ_2 DIVIDED BY $\sigma_{AV_{(MP)}}$ ALONG Y ℄ OF COVERPLATE

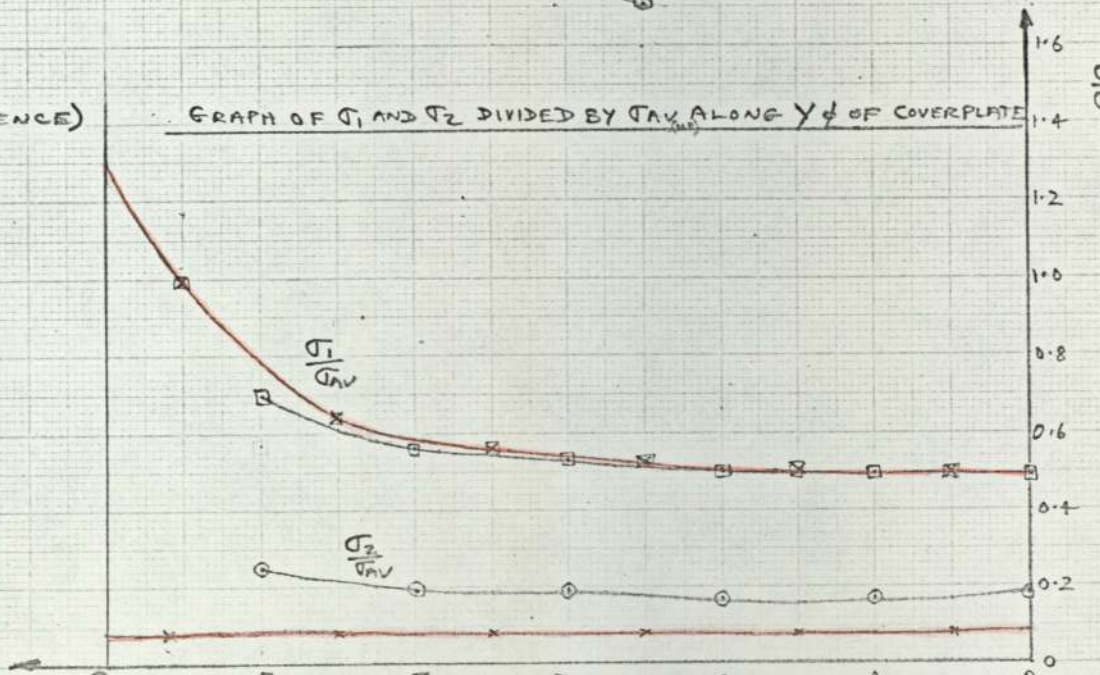

Graph 21.

GRAPH OF σ_1 and σ_2 DIVIDED BY $\sigma_{AV(AP)}$ ALONG X $\not{\text{C}}$ OF MAIN PLATE.

σ_1/σ_{AV} σ_2/σ_{AV} COMPUTER RESULTS.

σ_1/σ_{AV} σ_2/σ_{AV} PHOTOELASTIC RESULTS.

(BY OBLIQUE INCIDENCE).

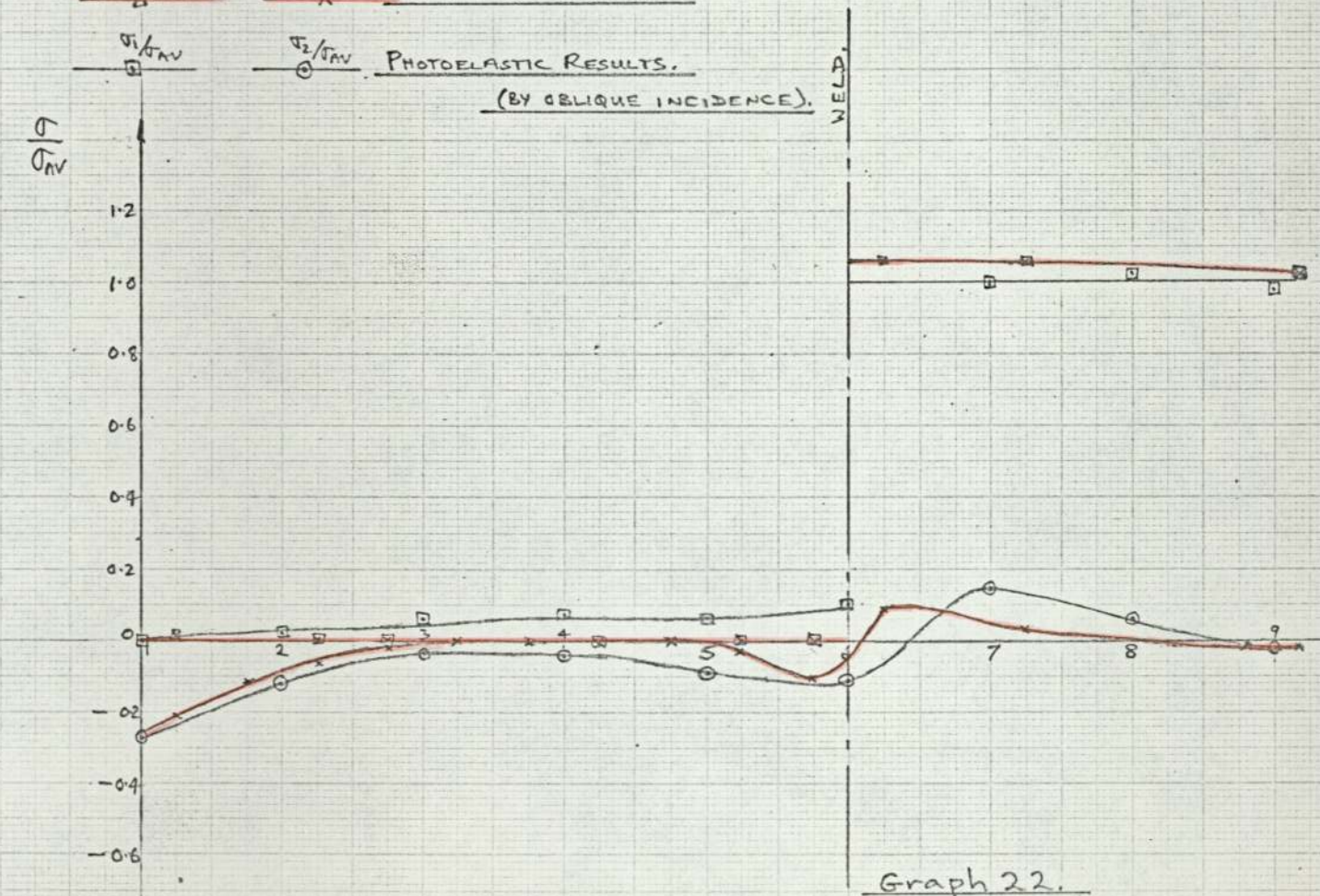

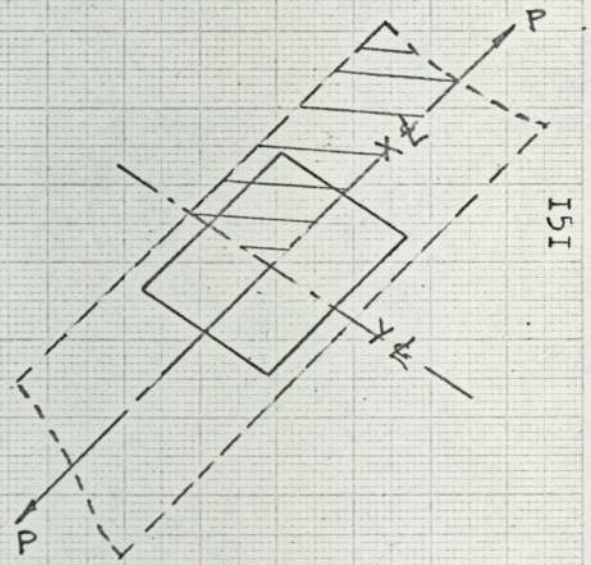

Graph 22.

GRAPH OF σ_1 AND σ_2 DIVIDED BY σ_{AV} (end) ALONG Y ℄ OF MAIN PLATE.

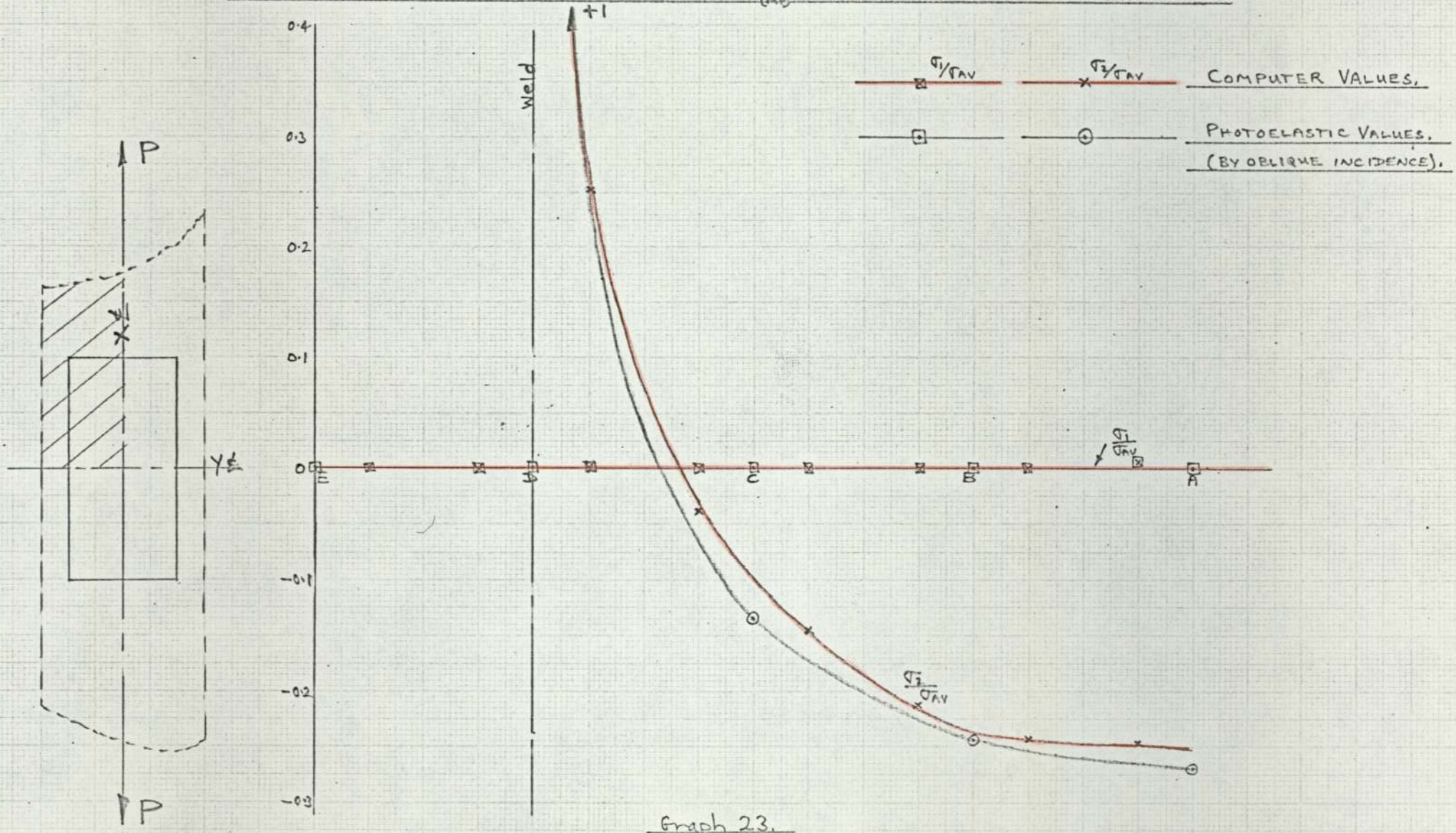

Graph 23.

7.7 Equilibrium Check for 1/16 inch Photo-Elastic Model

(Weld all round cover plate)

Along Y℄

Cover Plate

$$\sum \frac{\sigma_i}{\sigma_{AV(MP)}} = 6.888 .$$

Load carried by cover plate $= 6.88 \times \frac{3}{32} \times \frac{1}{16} \times 4$

$= 0.161\ \sigma_{AV(MP)}$

Load carried by weld(taking stress at cover plate edge).

Load $= \frac{1.0}{256} \times 2 = 0.008\ \sigma_{AV(MP)}$

Total Load Carried $= 0.169\ \sigma_{AV(MP)}$

Applied Load $= 0.188\ \sigma_{AV(MP)}$

%Difference $= \frac{0.019}{0.188} \times 100 = 10.1\%$

Along E_2 (Reference Diagram Page 142)

Cover Plate

$$\sum \frac{\sigma_i}{\sigma_{AV(MP)}} = 3.27$$

Load carried by cover plate $= 3.27 \times \frac{3}{16} \times \frac{1}{16} \times 4 = 0.1532\ \sigma_{AV(MP)}$

Main Plate

$$\sum \frac{\sigma_i}{\sigma_{AV(MP)}} = 1.082$$

Load carried by main plate $= 1.082 \times \frac{3}{16} \times \frac{1}{16} \times 2 = 0.0254\ \sigma_{AV(MP)}$

Load carried by weld(taking stress at cover plate edge).

Load $= \frac{0.615}{256} \times 2 = 0.0048\ \sigma_{AV(MP)}$

Total Load Carried $= 0.183\ \sigma_{AV(MP)}$

Applied Load $= 0.188\ \sigma_{AV(MP)}$

%Difference $= \frac{0.005}{0.188} \times 100 = 2.7\%$

Photoelastic Results (Weld all round cover plate).

Equilibrium Check. Along: Y ℄.

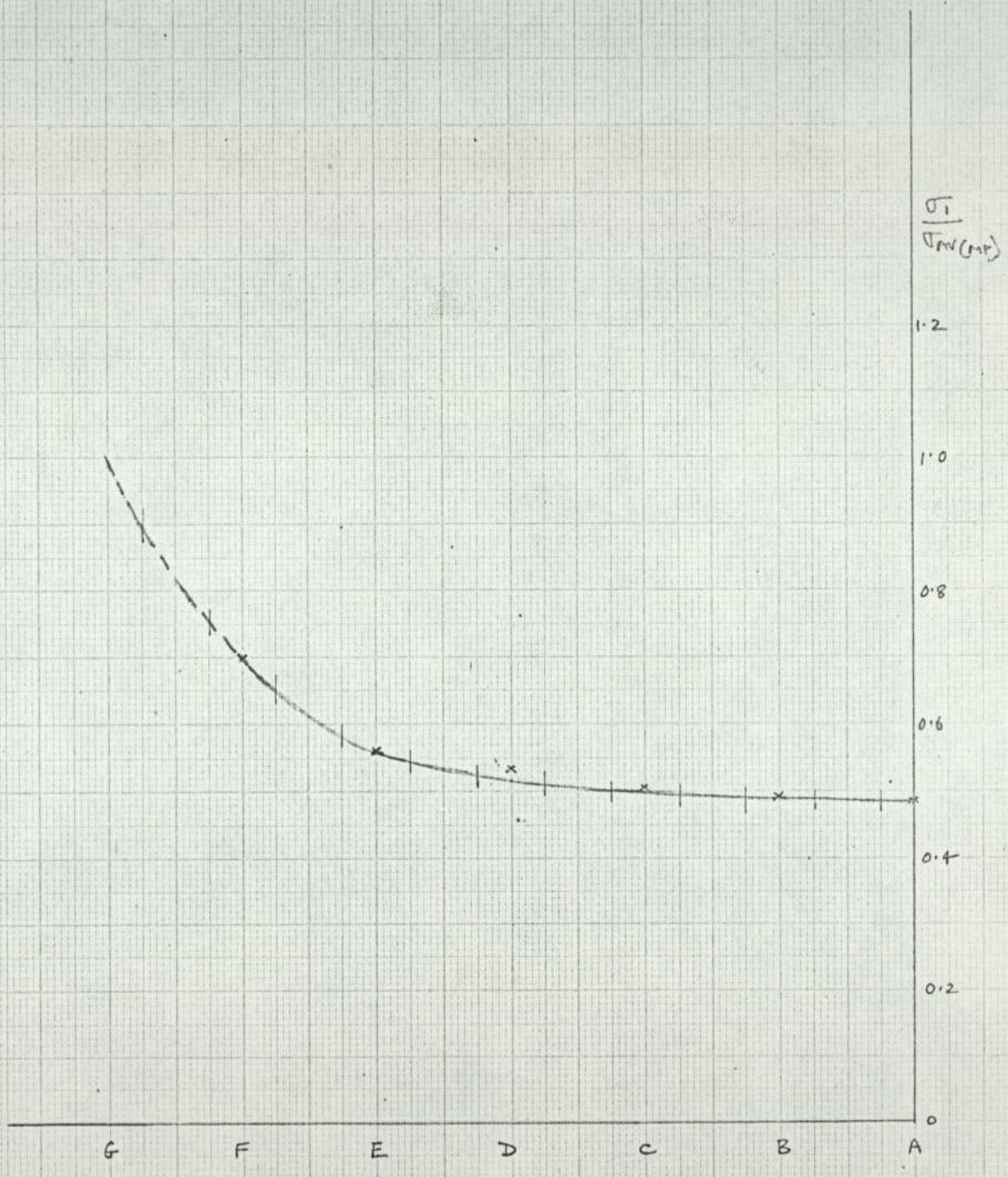

Graph 24.

Photoelastic Results (weld allround cover plate).

Equilibrium Check. Along E_2

× Cover Plate Values.

⊙ Main Plate Values.

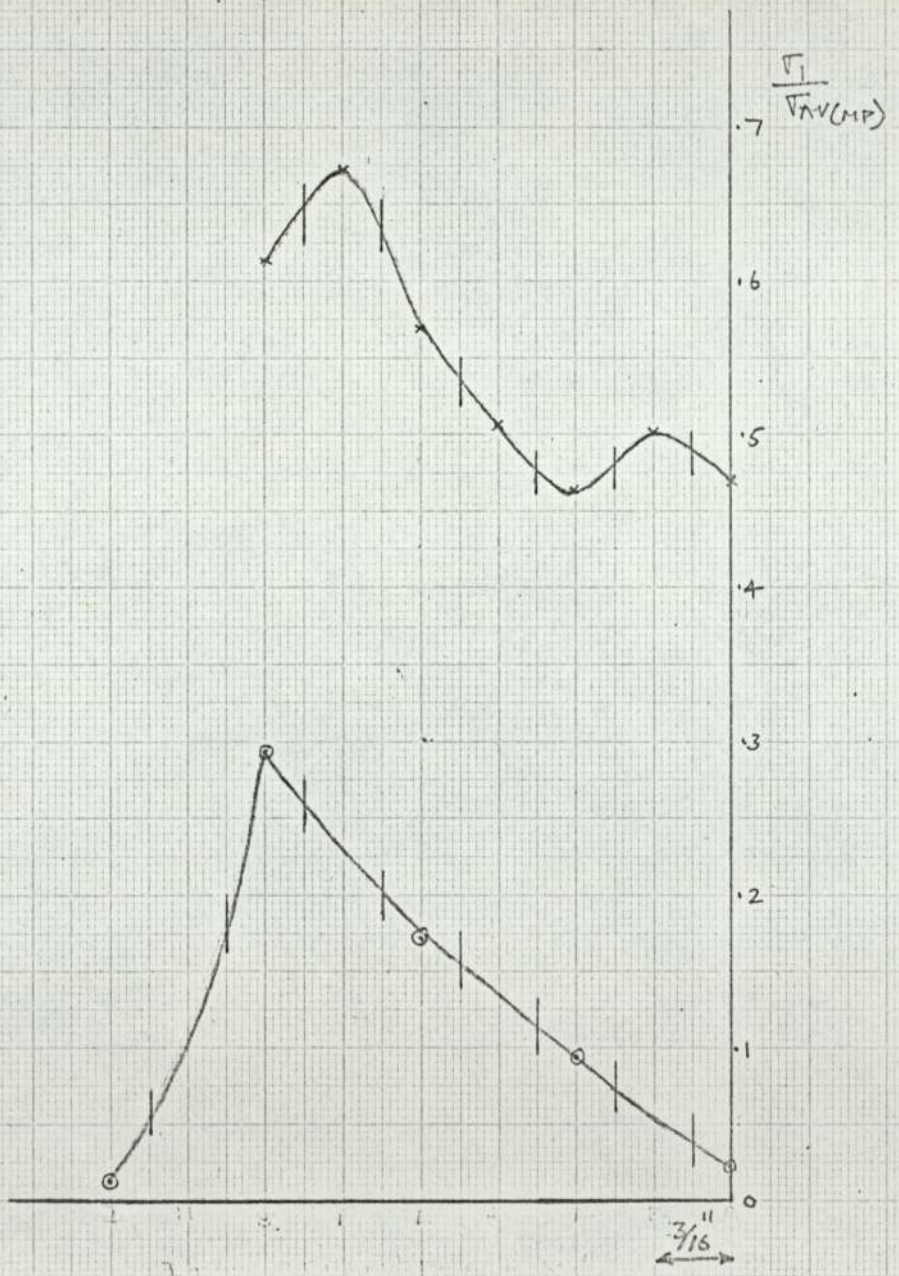

Graph 2.5.

7.8 DISCUSSION ON PHOTO-ELASTIC ANALYSIS

Results show clearly the peak stress points in the joints and comparison of the two joints tested indicate the advantage of taking the weld all round the cover plate. The peak value of $(\sigma_1 - \sigma_2)$ in both connections occurs at point A in the cover plate, The separated σ_1 and σ_2 values are shown in the graph 21 on page 1500 .These graphs indicate that the peak σ_1 value also occurs in the cover plate at A, but is considerably lower that the $(\sigma_1 - \sigma_2)$ value at this point.

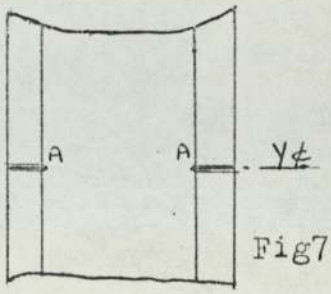

Fig7.18

The friction loading between the end plates and main plates gave a very uniform loading in the main plates. Symmetry of loading in the models was good, as was seen from the fringe and isoclinic patterns in the separated plates.

The simulated weld successfully transfered the load between the plates and the use of a thin saw blade to cut through the weld in order to separate the plates proved to be excellent, although rather tedious in operation. The most difficult area to analyse was along the weld line in the main plate, where the surface was rough and sometimes slightly pitted.

Except for the above point the analysis of the model plates in the large field polariscope was straightforward using the grid marked on the model as reference points for fringe measurement. The model was viewed through a microscope and the Tardy method used to determine the fractional fringes, the fringe brought to the intersection of the grid lines.

Good fringe multiplication photographs were obtained for the plates and the results from these compared favourably with those obtained by the Tardy method. The pictorial diagrams give a clear indication of the $(\sigma_1 - \sigma_2)$ stress distribution in the two connections, the distribution being much more uniform in the welded all round case.

The photo-elastic models proved very successful in verifying the analytical model.

8 DISCUSSION AND CONCLUSIONS

The Pictorial plots clearly indicate the non-uniformity of stress distribution in the plates. It is also seen from the finite element results that the relative thicknesses of the cover and main plates has a bearing on the stress distribution in the plates.

Tables 5.12 show the effect of variation in relative plate thicknesses on the peak stress values in the plates. The beneficial effect of welding the cover plates all round can be seen by comparing the pictorial plots for side fillet welded and welded all round cases(equal thickness cover and main plates).

The peak values of $\frac{\sigma_1 - \sigma_2}{\sigma_{AV(MP)}}$ in the two cases are:-

	Cover Plate		Main Plate	
	A	B	A	B
Side Fillet Weld	3.6	2.4	I.95	2.8
Weld All Round Cover plate	2.I	0.5	I.6	0.65

The pictorial plots of $\frac{\sigma_1 - \sigma_2}{\sigma_{AV(MP)}}$ obtained from the photo-elastic results and the finite element results show very good agreement. Experimental and analytical results are very similar and the peak values are shown to occur in the same positions in the connections.

The graphs comparing the photo-elastic and finite element results along the X and Y centre lines again show fair agreement. The difference between the results at point A in the main plate is probably due to errors in the photo-elastic value at this point. It was difficult to determine an accurate photo-elastic value in the main plate at this point due to the uneven surface left after plate separation.

The Photo-elastic results obtained by fringe multiplication are compared with the results obtained by Tardy compensation in the graphs on pages 145,146. The difference between these results is quite small but the fringe multiplication results give a smoother curve of stress distribution.

The separate principal stress values σ_1 and σ_2

for welded all round case are compared with the finite element results in graphs on pages 150-152 .The values compare favourably and it is noticable how close the agreement is in the sign change of the σ_2 stress.

The experimental results fully justify the analytical model used in the finite element analysis.

It is interesting to note from the graphs on page 63 how the load diffuses through the joint from the cover plates to the main plate.In the welded all round case the greater proportion of the load is always taken by the cover-plates,whereas with the side fillet welds the change over in the percentage load taken by cover plate and main plate occurs at about the mid position between the $\gamma \not\in$ and the extreme edge of the cover plate.

For the connections tested it is seen that the best connection can be obtained from using coverplates of twice the thickness of the main plate and welding the cover plates all round.

The length of weld will affect the peak stress values in the plates and this could form the basis for further work on the connection.It would also be interesting to carry out a three dimensional analysis of the connection to determine the effect of weld throat depth on peak stresses. The effect on the peak stresses of tapering and shaping of the cover plates could also be usefully investigated.

REFERENCES.

NO.	AUTHORS.	TITLE.
I	Zienkiewicz.O.C.	The Finite Element Method in Structural and Continuum Mechanics. McGraw-Hill.
2.	Sokolnikoff.I.S.	Mathematical Theory of Elasticity. McGraw-Hill.
3.	Clough.R.W.	"Use of Modern Computers in Structural Analysis". Proceedings,ASCE,Vol 84, No. ST-3,May I958.
4.	Koopman.K.H.	"Elements of Joint Design for Welding". The Welding Journal Vol 37 Pages 579-588,I958.
5.	Palmer.P.J.	"Stress Distribution in Side Fillet Welded Plates". British Welding Journal. Pages 55-60,February I955.
6.	Pian.T.H. &Tong.P.	Basis of Finite Element for Solid Continua. International Journal for Numerical Methods in Engineering. Vol. I,Pages 3-28 I969.
7.	Zienkiewicz.O.C. & Hollister.G.	Stress Analysis Wiley.
8.	Timoshenko.S. & Goodier.J.N.	Theory of Elasticity. McGraw-Hill.
9.	Dally.J.W.&Riley.F.R.	Experimental Stress Analysis. McGraw-Hill.
IO.	Heywood.R.B.	Photo-Elasticity for Designers. Pergammon Press.
II.	Hilborne.G.L. & Sharples.K.	A Cheap and Easily used Photoelastic Compensator. "Strain" Vol 6,No.4,I970
I2.	Norris.C.H.	"Photoelastic Investigation of Stress Distribution in Transverse Fillet Welds". Welding.Res.Suppl.Vol.24,No.IO Pages 5775-5605 I945.

I3. Solakian.A.G. "Sresses in Transverse Fillet Welds by Photoelastic Methods". Welding Journal.Vol.I3,No.2 Pages 22-29. I934.

I4. Solakian.A.G. "Effect of Weld Penetration on Stresses in Fillet Welded Joints". Welding Res.Suppl.,Vol.I5,No 9 Pages I3-I6,I936.

I5. Wallace.G. "Structural Model Analysis with Thermoplastics". Strain.Vol.3,No.3,Pages 4-I7,I967.

I6. Wooldridge.R. &Ratcliffe.J.E. "An INtroduction to Algol Programming". E.U.P. I963.

I7. Mocanu &Buga.M. "Distribution Des Contraintes Le Long Des Cordons Lateraux De Soudure et Dans Les Toles" Proceedings of the Fourth International Conference on Experimental Stress Analysis. I.Mech.E. London.I970.

I8. Swannell.P. "Deformation of Longitudinal Fillet Welds subjected to a Uniform Shearing Intensity". Ph.D.Thesis.Birmingham Univ.I967.

I9. Wade.D.H. "Welded Structural Connections in Aluminium Alloys".. M.Sc. Thesis. Birmingham Univ.I954

20. Anon. "Calculation Formula for Welded Connections subject to static Loads". Welding in the World.Vol.2, Part.4.I964.

2I. Woo.E. Application of the finite method to the design of solid wheels. Ph.D. Thesis. Univ. of Aston. I97I.

PRELIMINARY TESTS ON VYBAK 236/2 SHEET

In order to verify the analytical model used in the Finite Element analysis it was initially decided to examine the possibilities of using a strain gauged plastic model.The plastic chosen for preliminary tests was Vybak.Vybak rigid sheets(Bakelite Limited),are available in most 0.0I in increments of thickness from 0.0I in to 0.25 in and are made from vinyl chloride acetate and poly vinyl chloride resins.

A paper on 'Structural Model Analysis with Thermoplastics' by G.Wallace,published in the magazine 'Strain',advocated Vybak as a good material for model analysis.It was thought that this material might be usefully used for the analysis of a weld connection and a set of preliminary tests was initiated with this material.

Subsequent to these tests,it was decided that a photo-elastic model would give a better overall stress pattern for comparison with the computed results.For many weld connections there are very high stress concentrations and it was thought that without the use of very small,costly temperature compensated gauges,these peaks could not be measured.However preliminary work was carried out and it is briefly described here.

Details of The Tests Carried Out Were As Follows:

A template was already available for the manufacture of photo-elastic test specimen and this was used to make a Vybak specimen.Details of this specimen are shown in figureAI.I.Two 'Tinsley' electrical foil strain gauges having half an inch length were cemented to the centre of the test specimen using the following procedure.

Preparation of Plastic Surface

The plastic surface was lapped using a strip of Silicon Carbide Paper(400 grit)dipped in Metal Conditioner(Welwyn Electric).The residue was removed using a clean paper tissue.

VYBAK TEST SPECIMEN

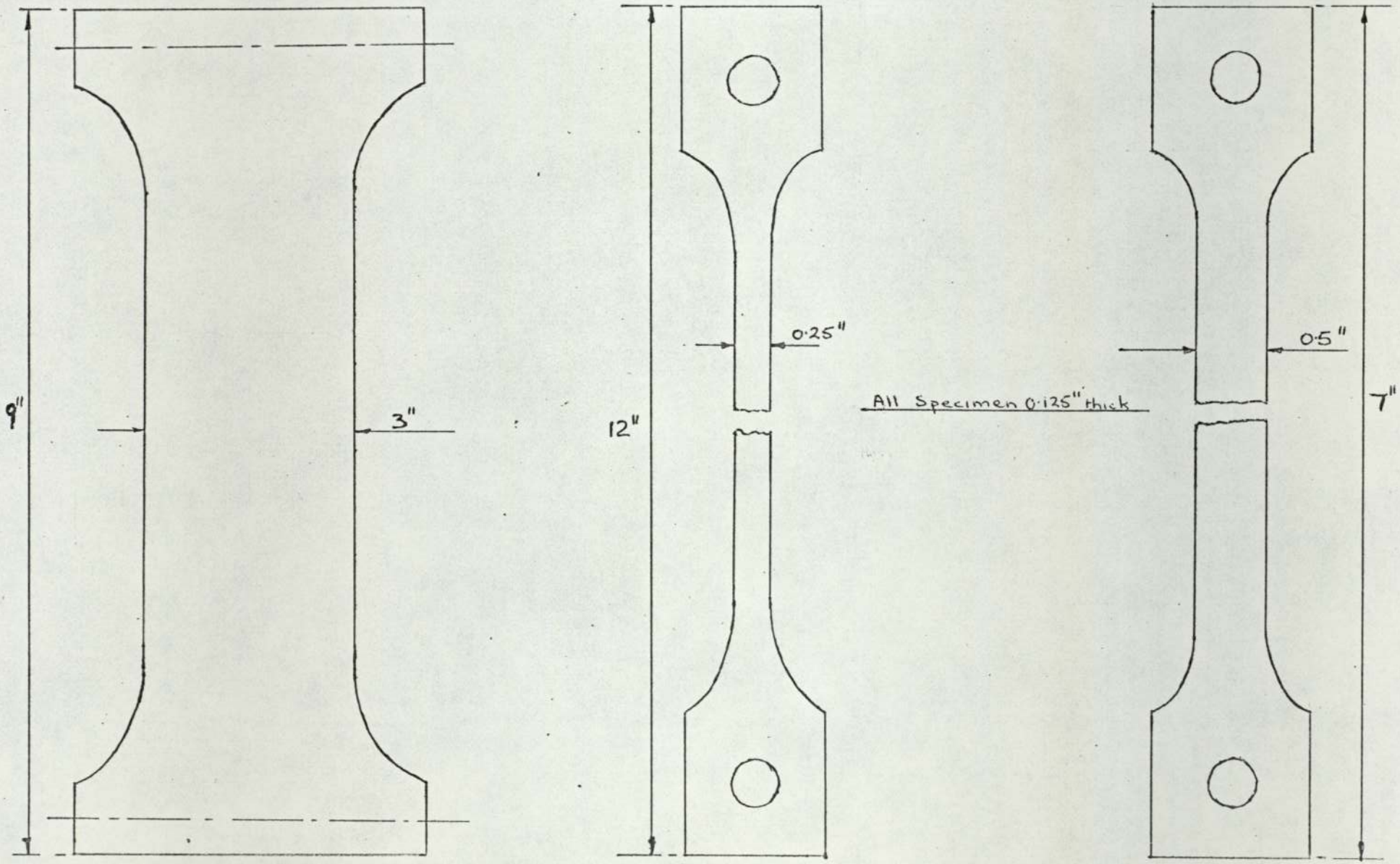

All Specimen 0·125" thick

Fig AI.1

The above procedure was repeated.

The strain gauge position was marked using a 5H pencil.

Metal Conditioner was applied to the gauge position using a cotton swab and then removed with one stroke of a clean tissue.

The gauge was then placed face up on a clean surface and a terminal strip positioned at the end of the gauge. Cellophane tape was applied over the top of the gauge and terminal strip. The gauge assembly was lifted from the working surface and the back of the gauge cleaned with a cotton bud moistened with neutralizer. Using the cellophane tape, the gauge assembly was positioned on the specimen. Starting at one end of the cellophane tape, the gauge assembly was lifted leaving the other end attached to the specimen. A thin film of blue 910 catalyst was applied to the back of the gauge and terminal strip and allowed to dry (approximately one minute).

Eastman 910 adhesive was applied to the gauge area of the specimen. The gauge and tape were fed onto the surface, holding the free end of the tape above the surface with one hand and using a ball of tissue in the other hand to quickly force the gauge assembly into place with one stroke. A thumb was used to apply pressure to the gauge, this pressure being maintained for approximately one minute. After five minutes, the cellophane tape was removed from the top of the gauge surface by peeling it back across the surface avoiding excessive lifting action.

All other gauges were applied using the above procedure.

Copper jumper wires were soldered between the gauge and terminal and lead wires soldered to the terminal strip.

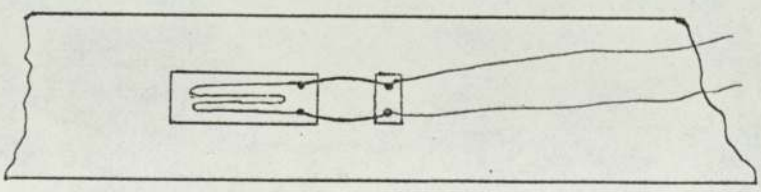

Fig AI.2

A protective coating of Gagekote (Welwyn) was applied to the gauge surface.

The test specimen was placed in the loading frame of a Photo-Elastic bench and the load applied through a lever arm.

The active strain gauges were wired with the appropriate dummy gauges in a Whetstone network such that the readings due to bending of the specimen were eliminated. A Tinsley strain gauge bridge type P3 was used to record the strain readings.

All work was carried out in the metrology laboratory which had the facilities for temperature and humidity control.

The load was applied in 10 lb increments up to 100 lb and the strain gauge readings noted. Graphs were plotted of load against strain gauge readings and the value of Young's Modulus for Vybak determined. Test 1, 2 and 3.

The values of Young's Modulus were up to 35% higher than the value of $0{\cdot}47 \times 10^6$ lbf/in^2 quoted by Wallace in his paper.

Mr. Wallace was contacted and he suggested that the type of specimen used was not the best and forwarded one of his specimen for testing together with some of his Vybak sheet.

The Wallace specimen was strain gauged using 0·5 inch Budd foil temperature compensated gauges. (Test 4.)

Specimen dimensions are shown in figure AI.1. The value obtained for Young's Modulus was 20% higher than the value quoted by Wallace. A similar specimen to that used in Test 1 was manufactured using Vybak sheet supplied by Wallace and from the tests carried out a value of Young's Modulus similar to the previous figure was obtained. (Test 5.)

The Wallace test specimen was strain gauged with ordinary 0·5 inch foil gauges (Tinsley) and tested using a Tinsley and a Peekel strain gauge bridge. (Test 6.) The value of Young's Modulus was again evaluated. In order to ensure that the strain gauges were recording the true strain, a grid in the form of two gauge lines was scribed on the surface of the plastic and microscopes used to measure the movement of each line. The experimental arrangement is shown in photograph 17 . (Test 7.)

The above arrangement was found to be very difficult to use and consistant results could not be obtained.

A more successful arrangement involved the use of a small loading frame from the photo-elastic overhead projector rig and the toolmakers microscope from the metrology laboratory.

The proving ring on the loading frame was first calibrated using dead loading.

A test specimen having dimensions shown in figure AI.1 was manufactured from Vybak sheet and two Tinsley 0·5 inch foil gauges cemented to opposite surfaces. Two gauge lines were also scribed on the surface. The test specimen was loaded in the frame which was placed on the table of the toolmakers microscope. The strain gauges were wired in a Whetstone network to eliminate bending and at each increment of load the strain gauge reading was noted together with the change in the distance between the gauge lines. (Test 8.)

In order to discover the effect on Young's Modulus of Vybak due to the surface being ground, a test specimen whose surfaces had been ground was strain gauged and tested. (Test 9.)

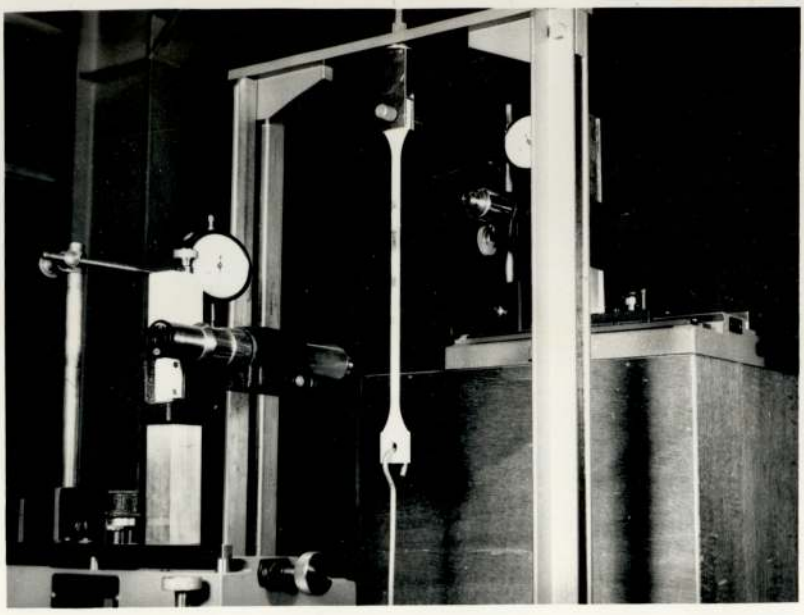

'Wallace' test specimen
Photograph I7

Test specimen on toolmakers microscope
Photograph I 8

From the results obtained, it appears that Vybak is a suitable model material having a linear stress-strain relationship within the range tested, (up to 1 800 lbf/in^2).

The very thin foil gauges used recorded the true strain value in the plastic there being no evidence of a reinforcing effect and the current through the gauges was kept low to avoid heating effects of the gauge. Similar results were obtained for the compensated and non-compensated gauges, but it is advisable to use compensated gauges in order to eliminate thermal effects.

The various tests gave an overall variation in the value of Young's Modulus of about 20% and the minimum difference with the value quoted by Wallace was about 14%.

From the results, it appears that the E value can vary quite considerably, even in the same sheet and this would be quite a disadvantage in using it for model analysis.

CALCULATIONS

Lever ratio (load arm) = 6 : 1.

Area of cross-section of specimen = $3 \cdot 113 \times 0 \cdot 128 = 0 \cdot 3985$ in^2.
for tests 1, 2 and 3.

Test 1

$$E = \frac{72 \times 6}{0 \cdot 3985} \cdot \frac{2}{3\,550 \times 10^{-6}} = 0 \cdot 6107 \times 10^6 \text{ lbf/in}^2.$$

Test 2

$$E = \frac{34 \times 6}{0 \cdot 3985} \cdot \frac{2}{1\,650 \times 10^{-6}} = 0 \cdot 6205 \times 10^6 \text{ lbf/in}^2.$$

Test 3

$$E = \frac{56 \times 6}{0 \cdot 3985} \cdot \frac{2}{2\,650 \times 10^{-6}} = 0 \cdot 6363 \times 10^6 \text{ lbf/in}^2.$$

Test 4

$$E = \frac{14 \cdot 8}{0 \cdot 0319} \cdot \frac{2}{1\,640 \times 10^{-6}} = 0 \cdot 566 \times 10^6 \text{ lbf/in}^2.$$

Test 5

$$E = \frac{76 \times 6}{0 \cdot 33} \cdot \frac{2}{4\,850 \times 10^{-6}} = 0 \cdot 57 \times 10^6 \text{ lbf/in}^2.$$

Test 6

$$E = \frac{11 \cdot 2}{0 \cdot 0319} \cdot \frac{2}{1\,260 \times 10^{-6}} = 0 \cdot 557 \times 10^6 \text{ lbf/in}^2.$$

Test 7

$$E = \frac{10{\cdot}6}{0{\cdot}0319} \cdot \frac{6}{3{\cdot}2 \times 10^{-3}} = 0{\cdot}623 \times 10^{6} \text{ lbf/in}^2.$$

Test 8

$$E = \frac{96 \times 2{\cdot}5}{3{\cdot}88 \times 0{\cdot}0645} \cdot \frac{1}{1\ 775 \times 10^{-6}} = 0{\cdot}54 \times 10^{6} \text{ lbf/in}^2.$$

Test 9

$$E = \frac{18{\cdot}8 \times 6}{0{\cdot}356} \cdot \frac{2}{1\ 180 \times 10^{-6}} = 0{\cdot}537 \times 10^{6} \text{ lbf/in}^2.$$

APPENDIX II

In order to fully understand the finite element method a single plate problem under uniform and parabolic tensile loading was analysed manually using a coarse mesh.

Due to the symmetry of the problem only a quadrant of the plate was used in the analysis. The plate quadrant was divided up as shown in fig.AII.1, this diagram also shows the element and node numbering.

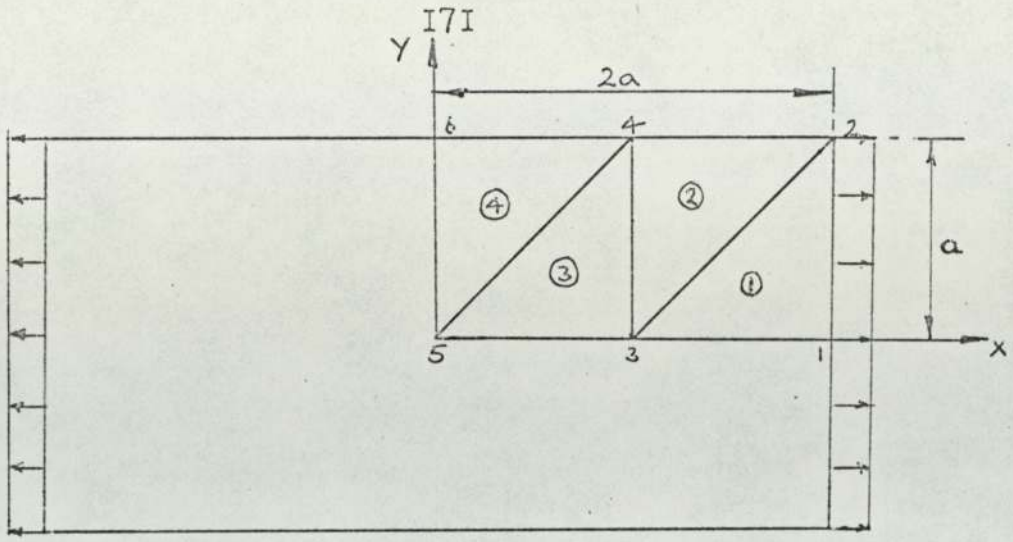

Fig AII.1

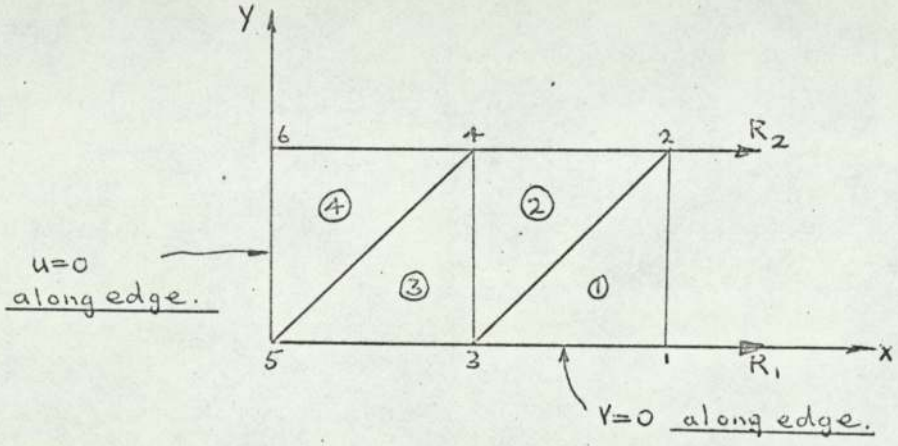

There is no self straining and no temperature effect hence for elements we have

$$\{F\}_e = \{k\}_e \{\delta\}_e \qquad (I)$$

where $\{k\}_e = \int_{Vol} [B]^t [D][B]\, dvol$

For $\triangle$ elements we can write (I) in a slightly extended form which is necessary when assembling the stiffness matrix for the whole structure.

Then

$$\begin{Bmatrix} F_i \\ F_j \\ F_m \end{Bmatrix}_e = \begin{bmatrix} k_{ii} & k_{ij} & k_{im} \\ k_{ji} & k_{jj} & k_{jm} \\ k_{mi} & k_{mj} & k_{mm} \end{bmatrix}_e \begin{Bmatrix} \delta_i \\ \delta_j \\ \delta_m \end{Bmatrix}_e$$

Element ①

$$\begin{Bmatrix} F_1 \\ F_2 \\ F_3 \end{Bmatrix}_1 = \begin{bmatrix} k_{11} & k_{12} & k_{13} \\ k_{21} & k_{22} & k_{23} \\ k_{31} & k_{32} & k_{33} \end{bmatrix}_1 \begin{Bmatrix} \delta_1 \\ \delta_2 \\ \delta_3 \end{Bmatrix}$$

Element ②

$$\begin{Bmatrix} F_3 \\ F_2 \\ F_4 \end{Bmatrix} = \begin{bmatrix} k_{33} & k_{32} & k_{34} \\ k_{23} & k_{22} & k_{24} \\ k_{43} & k_{42} & k_{44} \end{bmatrix}_2 \begin{Bmatrix} \delta_3 \\ \delta_2 \\ \delta_4 \end{Bmatrix}$$

Element ③

$$\begin{Bmatrix} F_3 \\ F_4 \\ F_5 \end{Bmatrix} = \begin{bmatrix} k_{33} & k_{34} & k_{35} \\ k_{43} & k_{44} & k_{45} \\ k_{63} & k_{54} & k_{55} \end{bmatrix}_3 \begin{Bmatrix} \delta_3 \\ \delta_4 \\ \delta_5 \end{Bmatrix}$$

Element ④

$$\begin{Bmatrix} F_5 \\ F_4 \\ F_6 \end{Bmatrix} = \begin{bmatrix} k_{55} & k_{54} & k_{56} \\ k_{45} & k_{44} & k_{46} \\ k_{65} & k_{64} & k_{66} \end{bmatrix}_4 \begin{Bmatrix} \delta_5 \\ \delta_4 \\ \delta_6 \end{Bmatrix}$$

Assembly of Stiffness Matrix for Whole Plate.

$$\{F\} = [K]\{\delta\}$$

$$\begin{Bmatrix} F_1 \\ F_2 \\ F_3 \\ F_4 \\ F_5 \\ F_6 \end{Bmatrix} = \begin{bmatrix} {}_1k_{11} & {}_1k_{12} & {}_1k_{13} & 0 & 0 & 0 \\ {}_1k_{21} & {}_1k_{22}+{}_2k_{22} & {}_1k_{23}+{}_2k_{23} & {}_2k_{24} & 0 & 0 \\ {}_1k_{31} & {}_1k_{32}+{}_2k_{32} & {}_1k_{33}+{}_2k_{33}+{}_3k_{33} & {}_2k_{34}+{}_3k_{34} & {}_3k_{35} & 0 \\ 0 & {}_2k_{42} & {}_2k_{43}+{}_3k_{43} & {}_2k_{44}+{}_3k_{44}+{}_4k_{44} & {}_3k_{45}+{}_4k_{45} & {}_4k_{46} \\ 0 & 0 & {}_3k_{53} & {}_3k_{54}+{}_4k_{54} & {}_3k_{55}+{}_4k_{55} & {}_4k_{56} \\ 0 & 0 & 0 & {}_4k_{64} & {}_4k_{65} & {}_4k_{66} \end{bmatrix} \begin{Bmatrix} \delta_1 \\ \delta_2 \\ \delta_3 \\ \delta_4 \\ \delta_5 \\ \delta_6 \end{Bmatrix}$$

Determining the ek_{ij}

Now $$[\tilde{k}] = \int [B]^t [D][B] \, dvol$$

Determining [B]

Now $$\begin{Bmatrix} u \\ v \end{Bmatrix} = \begin{bmatrix} 1 & x & y & 0 & 0 & 0 \\ 0 & 0 & 0 & 1 & x & y \end{bmatrix} \begin{Bmatrix} \alpha_1 \\ \alpha_2 \\ \alpha_3 \\ \alpha_4 \\ \alpha_5 \\ \alpha_6 \end{Bmatrix}$$

$$\text{i.e.} \quad \{f\} = [M]\{\alpha\} \qquad (2)$$

Let the generalised co-ordinates $\{\alpha\}$ be related to the nodal displacements $\{\delta\}$ by,

$$\{\delta\} = [A]\{\alpha\}$$

Then $[A]$ is obtained from (2) by writing $\{f\} = \{\delta\}$

$$\{\delta\} = \begin{Bmatrix} u_i \\ u_j \\ u_m \\ v_i \\ v_j \\ v_m \end{Bmatrix} \begin{bmatrix} 1 & x_i & y_i & 0 & 0 & 0 \\ 1 & x_j & y_j & 0 & 0 & 0 \\ 1 & x_m & y_m & 0 & 0 & 0 \\ 0 & 0 & 0 & 1 & x_i & y_i \\ 0 & 0 & 0 & 1 & x_j & y_i \\ 0 & 0 & 0 & 1 & x_m & y_m \end{bmatrix} \begin{Bmatrix} \alpha_1 \\ \alpha_2 \\ \alpha_3 \\ \alpha_4 \\ \alpha_5 \\ \alpha_6 \end{Bmatrix}$$

Then $$\{\alpha\} = [A]^{-1}\{\delta\}$$

and $$\{f\} = [M][A]^{-1}\{\delta\}$$

Denote $$\{\varepsilon\} = [B]\{\alpha\}$$

but $$\{\varepsilon\} = \begin{Bmatrix} \frac{\partial u}{\partial x} \\ \frac{\partial v}{\partial y} \\ \frac{\partial v}{\partial x} + \frac{\partial u}{\partial y} \end{Bmatrix} = \begin{bmatrix} \frac{\partial}{\partial x} & 0 \\ 0 & \frac{\partial}{\partial y} \\ \frac{\partial}{\partial y} & \frac{\partial}{\partial x} \end{bmatrix} \{f\} = [\partial]\{f\}$$

or $$\{\varepsilon\} = [\partial][M]\{\alpha\}$$

Now $$[\partial][M] = \begin{bmatrix} \frac{\partial}{\partial x} & 0 \\ 0 & \frac{\partial}{\partial y} \\ \frac{\partial}{\partial y} & \frac{\partial}{\partial x} \end{bmatrix} \begin{bmatrix} 1 & x & y & 0 & 0 & 0 \\ 0 & 0 & 0 & 1 & x & y \end{bmatrix}$$

$$= \begin{bmatrix} 0 & 1 & 0 & 0 & 0 & 0 \\ 0 & 0 & 0 & 0 & 0 & 1 \\ 0 & 0 & 1 & 0 & 1 & 0 \end{bmatrix}$$

Then

$$\{\varepsilon\} = \begin{bmatrix} 0 & 1 & 0 & 0 & 0 & 0 \\ 0 & 0 & 0 & 0 & 0 & 1 \\ 0 & 0 & 1 & 0 & 1 & 0 \end{bmatrix} \{\alpha\}$$

i.e. $$\{\varepsilon\} = [B]\{\alpha\} = [B][A]^{-1}\{\delta\}$$

Stress Matrix

$$\{\sigma\} = [D]\{\varepsilon\} = \frac{E}{1-\nu^2}\begin{bmatrix} 1 & \nu & 0 \\ \nu & 1 & 0 \\ 0 & 0 & \frac{1-\nu}{2} \end{bmatrix}\begin{Bmatrix} \varepsilon_x \\ \varepsilon_y \\ \gamma_{xy} \end{Bmatrix}$$

or $$\{\sigma\} = [D][B][A]^{-1}\{\delta\}$$

Element Stiffness Matrix

$$\{F\} = [k]\{\delta\}$$

Let nodes have virtual displacement $\{\bar{\delta}\}$, then from virtual work,

$$\{\bar{\delta}\}^t\{F\} = \int_{Vol}\{\bar{\varepsilon}\}^t\{\sigma\}\,dvol = \int_{Vol}\left([B][A]^{-1}\{\bar{\delta}\}\right)^t[D][B][A]^{-1}\{\delta\}\,dvol.$$

$$\therefore \{F\} = \left(([A]^{-1})^t\left(\int_{Vol}[B]^t[D][B]\,dvol\right)[A]^{-1}\right)\{\delta\}$$

i.e. $$\{F\} = [k]\{\delta\}$$

where $$[k] = ([A]^{-1})^t[\tilde{k}][A]^{-1}$$

Generalised co-ordinate stiffness matrix.

$$[\tilde{k}] = \int_{Vol} [B]^t [D][B]\, dvol$$

For Δ element

$$[\tilde{k}] = \text{Area} \cdot t \cdot [B]^t [D][B]$$

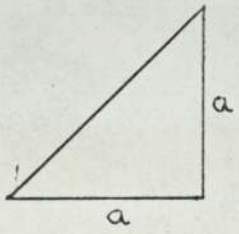

$$\text{Area} = \frac{a^2}{2}$$

$$[\tilde{k}] = \frac{E}{1-\nu^2} \cdot t \cdot \frac{a^2}{2} \begin{bmatrix} 0 & 0 & 0 \\ 1 & 0 & 0 \\ 0 & 0 & 1 \\ 0 & 0 & 0 \\ 0 & 0 & 1 \\ 0 & 1 & 0 \end{bmatrix} \begin{bmatrix} 1 & \nu & 0 \\ \nu & 1 & 0 \\ 0 & 0 & \frac{1-\nu}{2} \end{bmatrix} \begin{bmatrix} 0 & 1 & 0 & 0 & 0 & 0 \\ 0 & 0 & 0 & 0 & 0 & 1 \\ 0 & 0 & 1 & 0 & 1 & 0 \end{bmatrix}$$

$$[\tilde{k}] = \frac{E}{1-\nu^2} \cdot t \cdot \frac{a^2}{2} \begin{bmatrix} 0 & 0 & 0 & 0 & 0 & 0 \\ 0 & 1 & 0 & 0 & 0 & \nu \\ 0 & 0 & \frac{1-\nu}{2} & 0 & \frac{1-\nu}{2} & 0 \\ 0 & 0 & 0 & 0 & 0 & 0 \\ 0 & 0 & \frac{1-\nu}{2} & 0 & \frac{1-\nu}{2} & 0 \\ 0 & \nu & 0 & 0 & 0 & 1 \end{bmatrix}$$

Element (1)

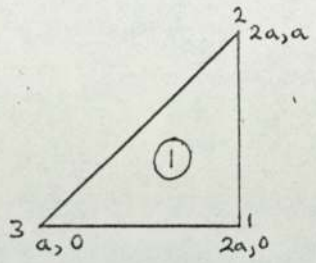

$$[A] = \begin{bmatrix} 1 & 2a & 0 & 0 & 0 & 0 \\ 1 & 2a & a & 0 & 0 & 0 \\ 1 & a & 0 & 0 & 0 & 0 \\ 0 & 0 & 0 & 1 & 2a & a \\ 0 & 0 & 0 & 1 & 2a & a \\ 0 & 0 & 0 & 1 & a & 0 \end{bmatrix}$$

Element (2)

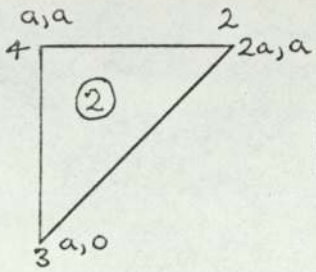

$$[A] = \begin{bmatrix} 1 & a & 0 & 0 & 0 & 0 \\ 1 & 2a & a & 0 & 0 & 0 \\ 1 & a & a & 0 & 0 & 0 \\ 0 & 0 & 0 & 1 & a & 0 \\ 0 & 0 & 0 & 1 & 2a & a \end{bmatrix}$$

Element (3)

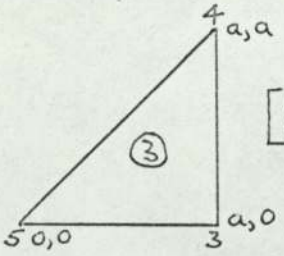

$$[A] = \begin{bmatrix} 1 & a & 0 & 0 & 0 & 0 \\ 1 & a & a & 0 & 0 & 0 \\ 1 & 0 & 0 & 0 & 0 & 0 \\ 0 & 0 & 0 & 1 & a & 0 \\ 0 & 0 & 0 & 1 & a & a \\ 0 & 0 & 0 & 1 & 0 & 0 \end{bmatrix}$$

Element (4)

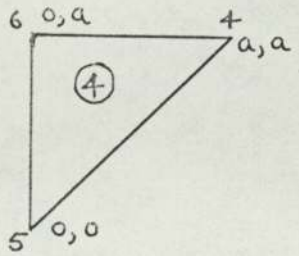

$$[A] = \begin{bmatrix} 1 & 0 & 0 & 0 & 0 & 0 \\ 1 & a & a & 0 & 0 & 0 \\ 1 & 0 & a & 0 & 0 & 0 \\ 0 & 0 & 0 & 1 & 0 & 0 \\ 0 & 0 & 0 & 1 & a & a \\ 0 & 0 & 0 & 1 & 0 & a \end{bmatrix}$$

The $[A]$ matrix was inverted and the element stiffness matrix determined from,

$$[k] = \left([A]^{-1}\right)^{t}[\tilde{k}][A]^{-1}$$

For elements (1) and (3).

$$[k] = \frac{E}{1-\nu^2}\cdot\frac{ta^2}{2}\begin{bmatrix} \frac{3-\nu}{2a^2} & -\frac{(1-\nu)}{2a^2} & -\frac{1}{a^2} & -\frac{(1+\nu)}{2a^2} & +\frac{\nu}{a^2} & +\frac{(1-\nu)}{2a^2} \\ -\frac{(1-\nu)}{2a^2} & +\frac{(1-\nu)}{2a^2} & 0 & +\frac{(1-\nu)}{2a^2} & 0 & -\frac{(1-\nu)}{2a^2} \\ -\frac{1}{a^2} & 0 & +\frac{1}{a^2} & +\frac{\nu}{a^2} & -\frac{\nu}{a^2} & 0 \\ -\frac{(1+\nu)}{2a^2} & +\frac{(1-\nu)}{2a^2} & +\frac{\nu}{a^2} & \frac{3-\nu}{2a^2} & -\frac{1}{a^2} & -\frac{(1-\nu)}{2a^2} \\ +\frac{\nu}{a^2} & 0 & -\frac{\nu}{a^2} & -\frac{1}{a^2} & +\frac{1}{a^2} & 0 \\ +\frac{(1-\nu)}{2a^2} & -\frac{(1-\nu)}{2a^2} & 0 & -\frac{(1-\nu)}{2a^2} & 0 & +\frac{(1-\nu)}{2a^2} \end{bmatrix}$$

For elements (2) and (4)

$$[k] = \frac{E}{1-\nu^2}\cdot\frac{ta^2}{2}\begin{bmatrix} +\frac{(1-\nu)}{2a^2} & 0 & -\frac{(1-\nu)}{2a^2} & 0 & -\frac{(1-\nu)}{2a^2} & +\frac{(1-\nu)}{2a^2} \\ 0 & +\frac{1}{a^2} & -\frac{1}{a^2} & -\frac{\nu}{a^2} & 0 & +\frac{\nu}{a^2} \\ -\frac{(1-\nu)}{2a^2} & -\frac{1}{a^2} & +\frac{(3-\nu)}{2a^2} & +\frac{\nu}{a^2} & +\frac{(1-\nu)}{2a^2} & -\frac{(1+\nu)}{2a^2} \\ 0 & -\frac{\nu}{a^2} & +\frac{\nu}{a^2} & +\frac{1}{a^2} & 0 & -\frac{1}{a^2} \\ -\frac{(1-\nu)}{2a^2} & 0 & +\frac{(1-\nu)}{2a^2} & 0 & +\frac{(1-\nu)}{2a^2} & -\frac{(1-\nu)}{2a^2} \\ +\frac{(1-\nu)}{2a^2} & +\frac{\nu}{a^2} & -\frac{(1+\nu)}{2a^2} & -\frac{1}{a^2} & -\frac{(1-\nu)}{2a^2} & \frac{3-\nu}{2a^2} \end{bmatrix}$$

$$\{F\} = [K]\{\delta\}$$

where K is the assembled stiffness matrix for the whole plate.

$$\begin{Bmatrix} F_{H_1} \\ F_{V_1} \\ F_{H_2} \\ F_{V_2} \\ F_{H_3} \\ F_{V_3} \\ F_{H_4} \\ F_{V_4} \\ F_{H5} \\ F_{V_5} \\ F_{H_6} \\ F_{V_6} \end{Bmatrix} = \frac{E}{1-\nu^2} \cdot \frac{t}{2} \begin{bmatrix} \frac{3-\nu}{2} & -\frac{(1+\nu)}{2} & -\frac{(1-\nu)}{2} & +\nu & -1 & +\frac{(1-\nu)}{2} & 0 & 0 & 0 & 0 & 0 & 0 \\ -\frac{(1+\nu)}{2} & \frac{(3-\nu)}{2} & +\frac{(1-\nu)}{2} & -1 & +\nu & -\frac{(1+\nu)}{2} & 0 & 0 & 0 & 0 & 0 & 0 \\ -\frac{(1-\nu)}{2} & +\frac{(1-\nu)}{2} & \frac{(3-\nu)}{2} & 0 & 0 & -\frac{1-\nu}{2} & -1 & +\nu & 0 & 0 & 0 & 0 \\ +\nu & -1 & 0 & \frac{3-\nu}{2} & -\frac{1-\nu}{2} & 0 & +\frac{1-\nu}{2} & -\frac{1+\nu}{2} & 0 & 0 & 0 & 0 \\ -1 & +\nu & 0 & -\frac{1-\nu}{2} & 3-\nu & -\frac{1-\nu}{2} & -1+\nu & +\frac{1+\nu}{2} & -1 & +\frac{1-\nu}{2} & 0 & 0 \\ +\frac{(1-\nu)}{2} & -\frac{(1-\nu)}{2} & -\frac{1-\nu}{2} & 0 & -\frac{1-\nu}{2} & 3-\nu & +\frac{1+\nu}{2} & -2 & +\nu & -\frac{1+\nu}{2} & 0 & 0 \\ 0 & 0 & -1 & +\frac{1-\nu}{2} & -1+\nu & +\frac{1+\nu}{2} & 3-\nu & -\frac{1-\nu}{2} & 0 & -\frac{1-\nu}{2} & -1 & +\nu \\ 0 & 0 & +\nu & -\frac{1+\nu}{2} & +\frac{1+\nu}{2} & -2 & -\frac{1-\nu}{2} & 3-\nu & -\frac{1-\nu}{2} & 0 & +\frac{1-\nu}{2} & -\frac{1+\nu}{2} \\ 0 & 0 & 0 & 0 & -1 & +\nu & 0 & -\frac{1-\nu}{2} & \frac{3-\nu}{2} & 0 & -\frac{1+\nu}{2} & +\frac{1-\nu}{2} \\ 0 & 0 & 0 & 0 & +\frac{1-\nu}{2} & -\frac{1+\nu}{2} & -\frac{1-\nu}{2} & 0 & 0 & \frac{3-\nu}{2} & +\nu & -1 \\ 0 & 0 & 0 & 0 & 0 & 0 & -1 & +\frac{1-\nu}{2} & -\frac{1+\nu}{2} & +\nu & +\frac{3-\nu}{2} & -\frac{1-\nu}{2} \\ 0 & 0 & 0 & 0 & 0 & 0 & +\nu & -\frac{1+\nu}{2} & +\frac{1-\nu}{2} & -1 & -\frac{1-\nu}{2} & +\frac{3-\nu}{2} \end{bmatrix} \begin{Bmatrix} u_1 \\ v_1 \\ u_2 \\ v_2 \\ u_3 \\ v_3 \\ u_4 \\ v_4 \\ u_5 \\ v_5 \\ u_6 \\ v_6 \end{Bmatrix}$$

The [K] matrix is singular and in order to solve, the zero boundary conditions are introduced.

Boundary Conditions $v_1 = v_3 = v_5 = u_5 = u_6 = 0$

Assuming $\nu = 0.3$ we obtain the reduced equations for the plate.

$$\begin{Bmatrix} F_{H_1} \\ F_{H_2} \\ 0 \\ 0 \\ 0 \\ 0 \\ 0 \end{Bmatrix} = \frac{Et}{2(1-0.09)} \begin{bmatrix} +1.35 & -0.35 & +0.3 & -1 & 0 & 0 & 0 \\ -0.35 & +1.35 & 0 & 0 & -1 & +0.3 & 0 \\ +0.3 & 0 & +1.35 & -0.65 & +0.35 & -0.35 & 0 \\ -1 & 0 & -0.65 & +2.7 & -0.7 & +0.65 & 0 \\ 0 & -1 & +0.35 & -0.7 & +2.7 & -0.65 & +0.3 \\ 0 & +0.3 & -0.35 & +0.65 & -0.65 & +2.7 & -0.35 \\ 0 & 0 & 0 & 0 & +0.3 & -0.35 & +1.35 \end{bmatrix} \begin{Bmatrix} u_1 \\ u_2 \\ v_2 \\ u_3 \\ u_4 \\ v_4 \\ v_6 \end{Bmatrix}$$

Once the u's and v's have been determined above, we may calculate the reaction force at the remaining nodes from:-

$$\begin{Bmatrix} F_{V_1} \\ F_{V_3} \\ F_{H_5} \\ F_{V_5} \\ F_{H_6} \end{Bmatrix} = \frac{Et}{2(1-0.09)} \begin{bmatrix} -0.65 & +0.35 & -1 & +0.3 & 0 & 0 & 0 \\ +0.35 & -0.65 & 0 & -0.65 & +0.65 & -2 & 0 \\ 0 & 0 & 0 & -1 & 0 & -0.65 & +0.35 \\ 0 & 0 & 0 & +0.35 & -0.65 & 0 & -1 \\ 0 & 0 & 0 & 0 & -1 & +0.35 & -0.65 \end{bmatrix} \begin{Bmatrix} u_1 \\ u_2 \\ v_2 \\ u_3 \\ u_4 \\ v_4 \\ v_6 \end{Bmatrix}$$

Since ultimately we wish to determine the stresses in the elements, we do not really need this calculation.

Determining the stress matrix for an element.

$$\{\sigma\} = [D][B][A^{-1}]\{\delta\}$$

or $\{\sigma\} = [S]\{\delta\}$ where $[S]$ = the stress matrix

It relates the stress components t within an element to its nodal displacements.

Finding the stress in the elements

$$\{\sigma\} = \frac{E}{1-\nu^2}\begin{bmatrix} 0 & 1 & 0 & 0 & 0 & \nu \\ 0 & \nu & 0 & 0 & 0 & 1 \\ 0 & 0 & \frac{1-\nu}{2} & 0 & \frac{1-\nu}{2} & 0 \end{bmatrix} [A^{-1}]\{\delta\}$$

Elements (I) and (3)

$$\{\sigma\}_{1,3} = \frac{E}{a(1-\nu^2)}\begin{bmatrix} +1 & 0 & -1 & -\nu & +\nu & 0 \\ +\nu & 0 & -\nu & -1 & +1 & 0 \\ -\frac{(1-\nu)}{2} & +\frac{(1-\nu)}{2} & 0 & +\frac{(1-\nu)}{2} & 0 & -\frac{(1-\nu)}{2} \end{bmatrix} \begin{Bmatrix} u_1 \\ u_2 \\ u_3 \\ v_1 \\ v_2 \\ v_3 \end{Bmatrix} \begin{Bmatrix} u_3 \\ u_4 \\ u_5 \\ v_3 \\ v_4 \\ v_5 \end{Bmatrix}$$

Elements (2) and (4)

$$\{\sigma\}_{2,4} = \frac{E}{a(1-\nu^2)}\begin{bmatrix} 0 & +1 & -1 & -\nu & 0 & +\nu \\ 0 & +\nu & -\nu & -1 & 0 & +1 \\ \frac{-1+\nu}{2} & 0 & +\frac{1-\nu}{2} & 0 & +\frac{1-\nu}{2} & \frac{-1+\nu}{2} \end{bmatrix} \begin{Bmatrix} u_3 \\ u_2 \\ u_4 \\ v_3 \\ v_2 \\ v_4 \end{Bmatrix} \begin{Bmatrix} u_5 \\ u_4 \\ u_6 \\ v_5 \\ v_4 \\ v_6 \end{Bmatrix}$$

To obtain the stress matrix for the whole plate

Now
$$\{\sigma_1\} = \begin{bmatrix} {}_1S_1 & {}_1S_2 & {}_1S_3 \end{bmatrix} \begin{Bmatrix} \delta_1 \\ \delta_2 \\ \delta_3 \end{Bmatrix}$$

$$\{\sigma_2\} = \begin{bmatrix} {}_2S_2 & {}_2S_3 & {}_2S_4 \end{bmatrix} \begin{Bmatrix} \delta_2 \\ \delta_3 \\ \delta_4 \end{Bmatrix}$$

$$\{\sigma_3\} = \begin{bmatrix} {}_3S_3 & {}_3S_4 & {}_3S_5 \end{bmatrix} \begin{Bmatrix} \delta_3 \\ \delta_4 \\ \delta_5 \end{Bmatrix}$$

$$\{\sigma_4\} = \begin{bmatrix} {}_4S_4 & {}_4S_5 & {}_4S_6 \end{bmatrix} \begin{Bmatrix} \delta_4 \\ \delta_5 \\ \delta_6 \end{Bmatrix}$$

Then,

$$\begin{Bmatrix} \sigma_1 \\ \sigma_2 \\ \sigma_3 \\ \sigma_4 \end{Bmatrix} = \begin{bmatrix} {}_1S_1 & {}_1S_2 & {}_1S_3 & 0 & 0 & 0 \\ 0 & {}_2S_2 & {}_2S_3 & {}_2S_4 & 0 & 0 \\ 0 & 0 & {}_3S_3 & {}_3S_4 & {}_3S_5 & 0 \\ 0 & 0 & 0 & {}_4S_4 & {}_4S_5 & {}_4S_6 \end{bmatrix} \begin{Bmatrix} \delta_1 \\ \delta_2 \\ \delta_3 \\ \delta_4 \\ \delta_5 \\ \delta_6 \end{Bmatrix}$$

Stress Matrix Equation for Whole Plate.

$$\{\sigma\} = \frac{E}{a(1-0.09)} \begin{bmatrix} +1 & -0.3 & 0 & +0.3 & -1 & 0 & 0 & 0 & 0 & 0 & 0 & 0 \\ +0.3 & -1 & 0 & +1 & -0.3 & 0 & 0 & 0 & 0 & 0 & 0 & 0 \\ -0.35 & +0.35 & +0.35 & 0 & 0 & -0.35 & 0 & 0 & 0 & 0 & 0 & 0 \\ 0 & 0 & +1 & 0 & 0 & -0.3 & -1 & +0.3 & 0 & 0 & 0 & 0 \\ 0 & 0 & +0.3 & 0 & 0 & -1 & -0.3 & +1 & 0 & 0 & 0 & 0 \\ 0 & 0 & 0 & +0.35 & -0.35 & 0 & +0.35 & -0.35 & 0 & 0 & 0 & 0 \\ 0 & 0 & 0 & 0 & +1 & -0.3 & 0 & +0.3 & -1 & 0 & 0 & 0 \\ 0 & 0 & 0 & 0 & +0.3 & -1 & 0 & +1 & -0.3 & 0 & 0 & 0 \\ 0 & 0 & 0 & 0 & -0.35 & +0.35 & +0.35 & 0 & 0 & -0.35 & 0 & 0 \\ 0 & 0 & 0 & 0 & 0 & 0 & +1 & 0 & 0 & -0.3 & -1 & +0.3 \\ 0 & 0 & 0 & 0 & 0 & 0 & +0.3 & 0 & 0 & -1 & -0.3 & +1 \\ 0 & 0 & 0 & 0 & 0 & 0 & 0 & +0.35 & -0.35 & 0 & +0.35 & -0.35 \end{bmatrix} \begin{Bmatrix} u_1 \\ v_1 \\ u_2 \\ v_2 \\ u_3 \\ v_3 \\ u_4 \\ v_4 \\ u_5 \\ v_5 \\ u_6 \\ v_6 \end{Bmatrix}$$

Now $V_1 = V_3 = V_5 = U_5 = U_6 = 0$

Reduced Stress Matrix Equation for Whole Plate. (AII.1)

$$\begin{Bmatrix} {}_1\sigma_x \\ {}_1\sigma_y \\ {}_1\tau_{xy} \\ {}_2\sigma_x \\ {}_2\sigma_y \\ {}_2\tau_{xy} \\ {}_3\sigma_x \\ {}_3\sigma_y \\ {}_3\tau_{xy} \\ {}_4\sigma_x \\ {}_4\sigma_y \\ {}_4\tau_{xy} \end{Bmatrix} = \frac{E}{a(1-\nu^2)} \begin{bmatrix} +1 & 0 & +0.3 & -1 & 0 & 0 & 0 \\ +0.3 & 0 & +1 & -0.3 & 0 & 0 & 0 \\ -0.35 & +0.35 & 0 & 0 & 0 & 0 & 0 \\ 0 & +1 & 0 & 0 & -1 & +0.3 & 0 \\ 0 & +0.3 & 0 & 0 & -0.3 & +1 & 0 \\ 0 & 0 & +0.35 & -0.35 & +0.35 & -0.35 & 0 \\ 0 & 0 & 0 & +1 & 0 & +0.3 & 0 \\ 0 & 0 & 0 & +0.3 & 0 & +1 & 0 \\ 0 & 0 & 0 & -0.35 & +0.35 & 0 & 0 \\ 0 & 0 & 0 & 0 & +1 & 0 & +0.3 \\ 0 & 0 & 0 & 0 & +0.3 & 0 & +1 \\ 0 & 0 & 0 & 0 & 0 & +0.35 & -0.35 \end{bmatrix} \begin{Bmatrix} U_1 \\ U_2 \\ V_2 \\ U_3 \\ U_4 \\ V_4 \\ V_6 \end{Bmatrix}$$

Vector of applied nodal forces.

Let the applied boundary tractions be the

vector $$\{g\} = \begin{Bmatrix} \bar{X} \\ \bar{Y} \end{Bmatrix}$$

To find equivalent nodal applied forces.

Let boundary nodes receive virtual displacements $\{\bar{\delta}\}$, then $\{\bar{f}\}$ is a virtual displacement field within the element (and along its boundaries), so that

$$\int_S \{\bar{f}\}^t \{g\}\, t\, ds = \{\bar{\delta}\}^t \{F_{appl.}\} \qquad \text{(AII.2)}$$

but $$\{\bar{f}\} = [M]\{\bar{\alpha}\} = [M][A]^{-1}\{\bar{\delta}\}$$

then $$\{\bar{\delta}\}^t \int_S \left([A]^{-1}\right)^t [M]^t \{g\}\, t\, ds = \{\bar{\delta}\}^t \{F_{appl.}\}$$

then $$\{F_{appl.}\} = \int_S \left([A]^{-1}\right)^t [M]^t \{g\}\, t.ds.$$

Simple Tension

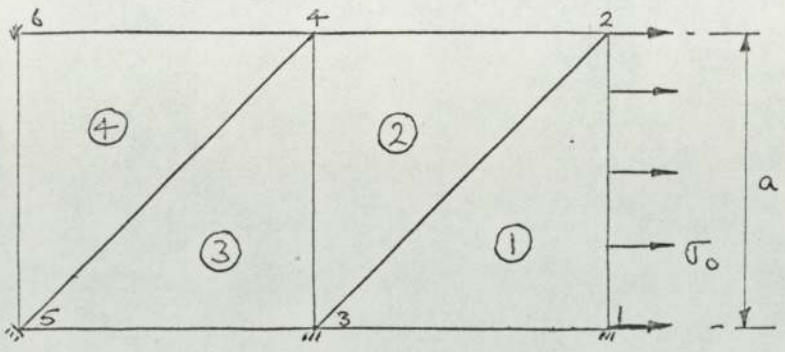

$$\{F\} = -\int [N]^t \{g\}\, d(\text{area})$$

where $[N] = [M][A^{-1}]$

and $$[M] = \begin{bmatrix} 1 & x & y & 0 & 0 & 0 \\ 0 & 0 & 0 & 1 & x & y \end{bmatrix}$$

and $$[A^{-1}] = \begin{bmatrix} 0 & 0 & 0 & 0 & +1 & 0 \\ +\frac{1}{a} & 0 & 0 & 0 & -1/a & 0 \\ -\frac{1}{a} & 0 & +\frac{1}{a} & 0 & 0 & 0 \\ 0 & 0 & 0 & 0 & 0 & +1 \\ 0 & +1/a & 0 & 0 & 0 & -1/a \\ 0 & -1/a & 0 & +1/a & 0 & 0 \end{bmatrix}$$

$$\therefore [N] = \begin{bmatrix} +\frac{x}{a} - \frac{y}{a} & 0 & +\frac{y}{a} & 0 & +1 - \frac{x}{a} & 0 \\ 0 & +\frac{x}{a} - \frac{y}{a} & 0 & +\frac{y}{a} & 0 & +1 - \frac{x}{a} \end{bmatrix}$$

Then

$$[N]^t = \begin{bmatrix} +\frac{x}{a}-\frac{y}{a} & 0 \\ 0 & +\frac{x}{a}-\frac{y}{a} \\ +\frac{y}{a} & 0 \\ 0 & +\frac{y}{a} \\ +1-\frac{x}{a} & 0 \\ 0 & +1-\frac{x}{a} \end{bmatrix} = \begin{bmatrix} +1-\frac{y}{a} & 0 \\ 0 & +1-\frac{y}{a} \\ +\frac{y}{a} & 0 \\ 0 & +\frac{y}{a} \\ 0 & 0 \\ 0 & 0 \end{bmatrix}$$

In this case $\bar{X} = \sigma_0$, $\bar{Y} = 0$ and substituting in (AII.2) we obtain,

$$\{F\} = -\int \begin{bmatrix} 1-\frac{y}{a} & 0 \\ 0 & 1-\frac{y}{a} \\ +\frac{y}{a} & 0 \\ 0 & +\frac{y}{a} \\ 0 & 0 \\ 0 & 0 \end{bmatrix} \begin{Bmatrix} \sigma_0 \\ 0 \end{Bmatrix} d(\text{area})$$

$$\{F\} = -\sigma_0 t \int_0^a \begin{bmatrix} 1-\frac{y}{a} & 0 \\ 0 & 0 \\ +\frac{y}{a} & 0 \\ 0 & 0 \\ 0 & 0 \\ 0 & 0 \end{bmatrix} dy = -\sigma_0 t \begin{bmatrix} +\frac{a}{2} \\ 0 \\ +\frac{a}{2} \\ 0 \\ 0 \\ 0 \end{bmatrix}$$

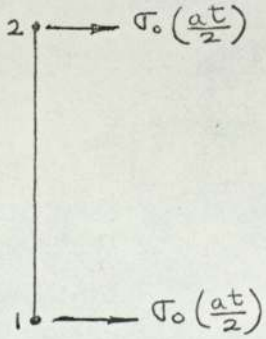

Parabolic Loading

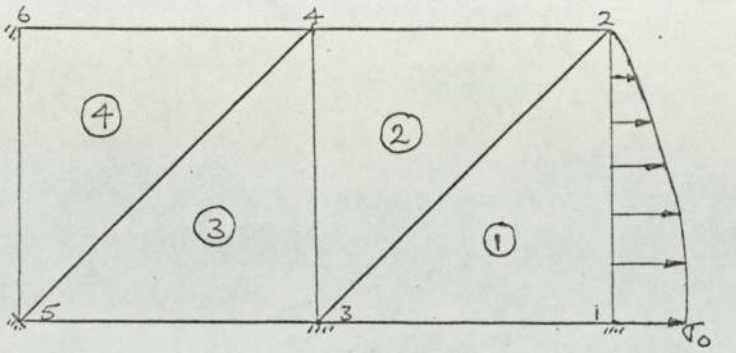

In this case $\bar{y} = 0$, $\bar{x} = \sigma_0\left[1-\left(\frac{y}{a}\right)^2\right]$ and substituting in (AII.2), we obtain,

$$\{F\} = -\int \begin{bmatrix} +1-\frac{y}{a} & 0 \\ 0 & +1-\frac{y}{a} \\ +\frac{y}{a} & 0 \\ 0 & +\frac{y}{a} \\ 0 & 0 \\ 0 & 0 \end{bmatrix} \begin{Bmatrix} \sigma_0\left(1-\left[\frac{y}{a}\right]^2\right) \\ 0 \end{Bmatrix} d(\text{area}).$$

$$\therefore \{F\} = -\sigma_0 t \int_0^a \begin{bmatrix} 1+\frac{y^3}{a^3}-\frac{y}{a}-\frac{y^2}{a^2} & 0 \\ 0 & 0 \\ +\frac{y}{a}-\frac{y^3}{a^3} & 0 \\ 0 & 0 \\ 0 & 0 \\ 0 & 0 \end{bmatrix} dy = -\sigma_0 t \begin{bmatrix} +\frac{5}{12}a \\ 0 \\ +\frac{a}{4} \\ 0 \\ 0 \\ 0 \end{bmatrix}.$$

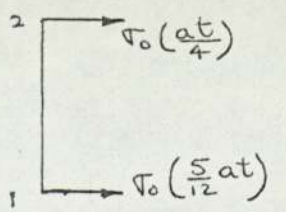

Uniform Tension

Substituting the following values

$F_{H_1} = \sigma_0 \cdot \frac{at}{2}$. $F_{H_2} = \sigma_0 \cdot \frac{at}{2}$ in the reduced equation(AII.1)

for whole plate we obtain the following displacements,

$$u_1 = a\frac{(1-\nu^2)}{E}\sigma_0(+2.1983) \qquad u_2 = a\frac{(1-\nu^2)}{E}\sigma_0(+2.1983)$$

$$v_2 = \frac{a(1-\nu^2)}{E}\sigma_0(-0.32970) \qquad u_3 = \frac{a(1-\nu^2)}{E}\sigma_0(+1.0989)$$

$$u_4 = \frac{a(1-\nu^2)}{E}\sigma_0(+1.0989) \qquad v_4 = \frac{a(1-\nu^2)}{E}\sigma_0(-0.3297)$$

$$v_6 = \frac{a(1-\nu^2)}{E}\sigma_0(-0.3297)$$

Using the above displacements in the reduced stress matrix for the whole plate we obtain,

$\sigma_x = \sigma_0(u_1 + 0.3v_2 - u_3) = +\sigma_0$

$\sigma_y = \sigma_0(0.3u_1 + v_2 - 0.3u_3) = 0$ Element (I)

$\tau_{xy} = \sigma_0(-0.35u_1 + 0.35u_2) = 0$

$\sigma_x = \sigma_0(u_2 - u_4 + 0.3v_4) = +\sigma_0$

$\sigma_y = \sigma_0(0.3u_2 - 0.3u_4 + v_4) = 0$ Element (2)

$\tau_{xy} = \sigma_0(+0.35v_2 - 0.35u_3 + 0.35u_4 - 0.35v_4) = 0$

$\sigma_x = \sigma_0(u_3 + 0.3v_4) = +\sigma_0$

$\sigma_y = \sigma_0(0.3u_3 + v_4) = 0$ Element (3)

$\tau_{xy} = \sigma_0(-0.35u_3 + 0.35u_4) = 0$

$\sigma_x = \sigma_0(u_4 + 0.3v_6) = \sigma_0$

$\sigma_y = \sigma_0(0.3u_4 + v_6) = 0$ Element (4)

$\tau_{xy} = \sigma_0(+0.35v_4 - 0.35v_6) = 0$

Parabolic Loading

$F_{H_1} = \sigma_0 . at . \frac{5}{12}$ and $F_{H_2} = \sigma_0 . at . \frac{1}{4}$ substituting these values in the reduced equation for the whole plate(AII.1) we obtain the following displacements,

$$u_1 = a\frac{(1-\nu^2)}{E}\sigma_0 (+1.5832) \qquad u_2 = a\frac{(1-\nu^2)}{E}\sigma_0 (+1.3470)$$

$$V_2 = a\frac{(1-\nu^2)}{E}\sigma_0 (-0.2206) \qquad u_3 = a\frac{(1-\nu^2)}{E}\sigma_0 (+0.7670)$$

$$u_4 = a\frac{(1-\nu^2)}{E}\sigma_0 (+0.7964) \qquad V_4 = a\frac{(1-\nu^2)}{E}\sigma_0 (-0.2228)$$

$$V_6 = a\frac{(1-\nu^2)}{E}\sigma_0 (-0.2126)$$

Using the above displacements in the reduced stress matrix for whole plate we obtain,

$\sigma_x = +0.7500\,\sigma_0$

$\sigma_y = +0.0121\,\sigma_0$ Element(I)

$\tau_{xy} = -0.0827\,\sigma_0$

$\sigma_x = +0.5838\,\sigma_0$

$\sigma_y = -0.0138\,\sigma_0$ Element (2)

$\tau_{xy} = -0.0342\,\sigma_0$

$\sigma_x = +0.7500\,\sigma_0$

$\sigma_y = +0.0037\,\sigma_0$ Element (3)

$\tau_{xy} = -0.0249\,\sigma_0$

$\sigma_x = +0.6326\,\sigma_0$

$\sigma_y = -0.0037\,\sigma_0$ Element (4)

$\tau_{xy} = -0.0036\,\sigma_0$

Rectangular Plate (Fine mesh)

Considering again one quarter of plate.

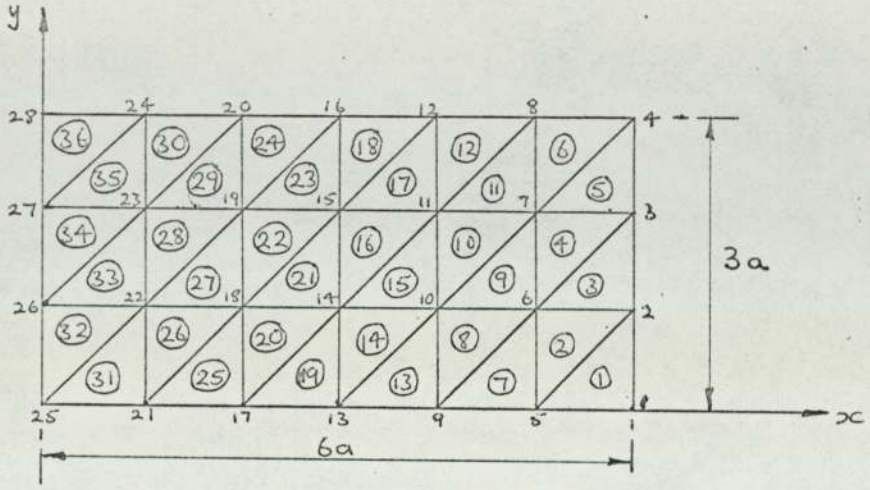

This was a repeat of the previous problem using a fine mesh. The element stiffness matrices were similar to those in the previous problem. The main work involved was in assembling the plate stiffness and stress matrices. A computer programme was used to invert the large matrices and solve the matrix equations.

Diagram showing part of assembly of stiffness matrix for whole plate.

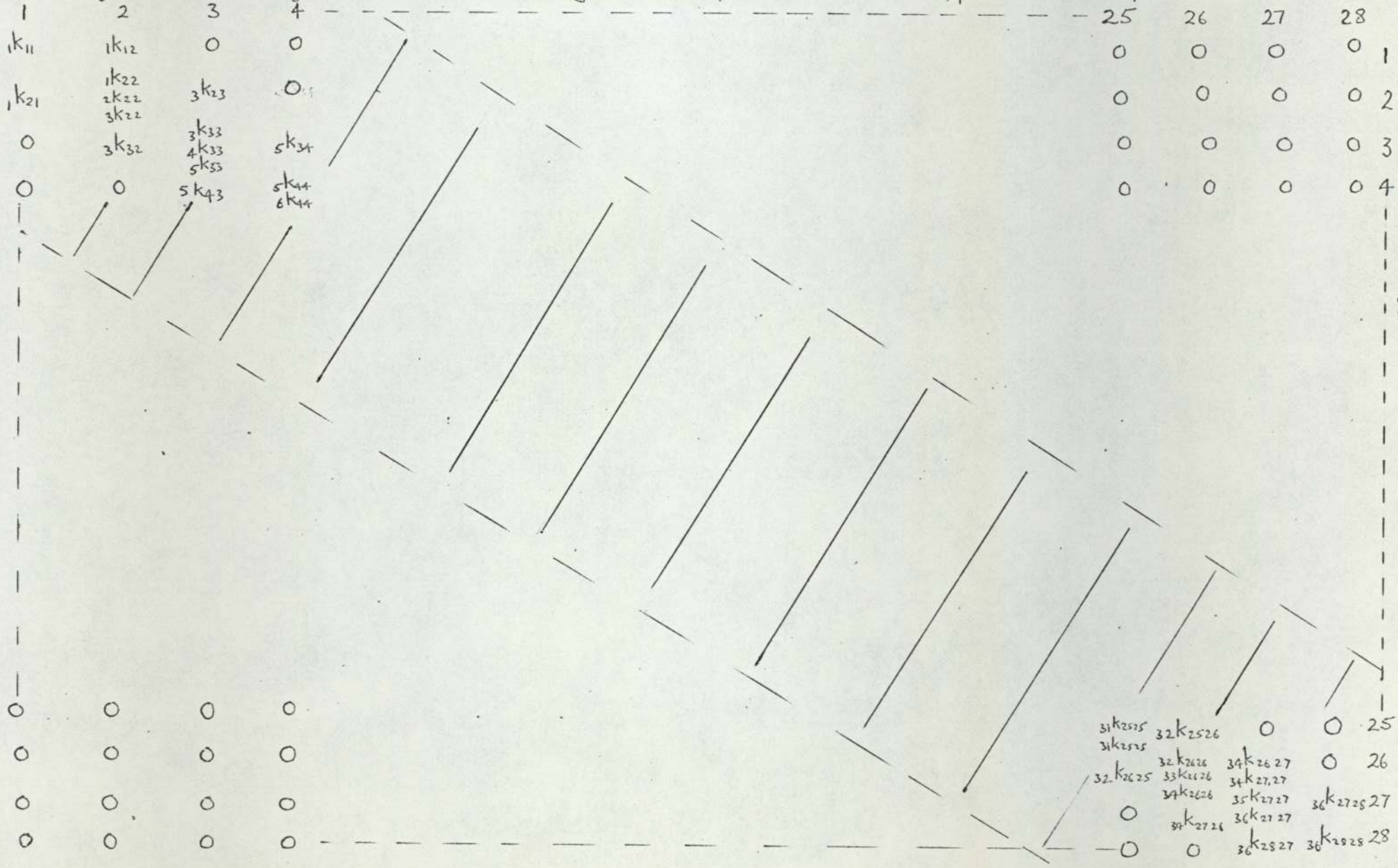

$\{F\}=[K]\{\delta\}$ Diagram showing part of assembled Matrix equation for whole plate.

$$
\begin{Bmatrix} F_{H_1} \\ F_{V_1} \\ F_{H_2} \\ F_{V_2} \\ \vdots \\ F_{H_{28}} \\ F_{V_{28}} \end{Bmatrix}
=
\begin{bmatrix}
+1.35 & -0.65 & \cdots & 0 & 0 \\
-0.65 & +1.35 & \cdots & 0 & 0 \\
-0.35 & +0.35 & \cdots & 0 & 0 \\
+0.2 & -1 & \cdots & 0 & 0 \\
\vdots & \vdots & & \vdots & \vdots \\
0 & 0 & \cdots & +1.35 & -0.65 \\
0 & 0 & \cdots & -0.65 & +1.35
\end{bmatrix}
\begin{Bmatrix} u_1 \\ v_1 \\ u_2 \\ v_2 \\ \vdots \\ u_{28} \\ v_{28} \end{Bmatrix}
$$

The reduced matrix equation for the whole plate was obtained from the matrix equation for the whole plate by inserting the known boundary conditions $v_1 = v_5 = v_9 = v_{13} = v_{17} = v_{21} = v_{25} = 0$ and $u_{25} = u_{26} = u_{27} = u_{28} = 0$ into the equation.

The element stress matrices were similar to the previous example and these were assembled into the stress matrix equation for the whole plate in the same manner as in the previous example.

PLACE HOLDER

PORTION OF PLATE STRESS MATRIX.

$$
\begin{Bmatrix} \sigma_{x_1} \\ \sigma_{y_1} \\ \tau_{xy_1} \\ \sigma_{x_2} \\ \sigma_{y_2} \\ \tau_{xy_2} \\ \sigma_{x_3} \\ \vdots \end{Bmatrix}
= \frac{E}{a(1-\nu^2)}
\begin{bmatrix}
+1 & -0.3 & 0 & +0.3 & 0 & 0 & 0 & 0 & -1 & 0 & & & \cdots \\
+0.3 & -1 & 0 & +1 & 0 & 0 & 0 & 0 & -0.3 & 0 & & & \\
-0.35 & +0.35 & +0.35 & 0 & 0 & 0 & 0 & 0 & 0 & -0.35 & & & \\
0 & 0 & +1 & 0 & 0 & 0 & 0 & 0 & 0 & -0.3 & -1 & +0.3 & \\
0 & 0 & +0.3 & 0 & 0 & 0 & 0 & 0 & 0 & -1 & -0.3 & +1 & \\
0 & 0 & 0 & +0.35 & 0 & 0 & 0 & 0 & -0.35 & 0 & +0.35 & -0.35 & \\
0 & 0 & +1 & -0.3 & 0 & +0.3 & 0 & 0 & 0 & 0 & -1 & 0 & \\
\vdots & & & & & & & & & & & &
\end{bmatrix}
\begin{Bmatrix} u_1 \\ v_1 \\ u_2 \\ v_2 \\ \vdots \end{Bmatrix}
$$

Uniform Tension

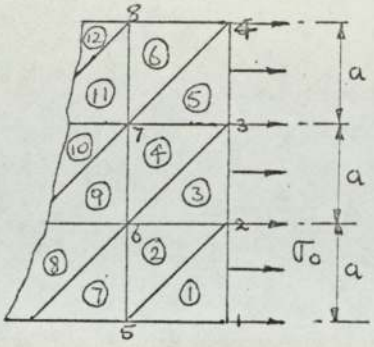

By applying the virtual work principle we obtain the following equivalent nodal forces.

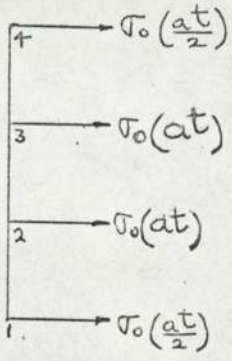

Parabolic Loading

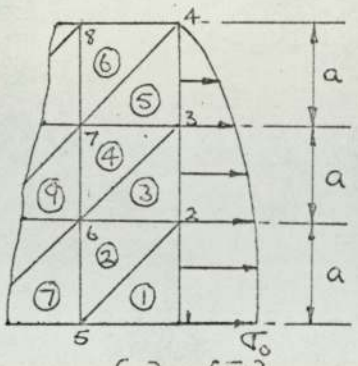

As in the previous example $\{g\} = \begin{Bmatrix} \bar{X} \\ \bar{Y} \end{Bmatrix}$

In this example $\bar{X} = \sigma_0\left(1 - \left[\frac{y}{3a}\right]^2\right)$ and $\bar{Y} = 0$

$$\{F\} = -\int \begin{bmatrix} +1 - \frac{y}{a} & 0 \\ 0 & +1 - \frac{y}{a} \\ +\frac{y}{a} & 0 \\ 0 & +\frac{y}{a} \\ 0 & 0 \\ 0 & 0 \end{bmatrix} \begin{Bmatrix} \sigma_0\left(1 - \left[\frac{y}{3a}\right]^2\right) \\ 0 \end{Bmatrix} d(\text{area})$$

Applying the above equation successively between I and 2, 2 and 3, 3 and 4, we obtain the equivalent nodal forces.

Section I-2

$$\{F\} = -\sigma_0 . t \int_0^a \begin{bmatrix} 1 - \frac{y}{a} - \frac{y^2}{9a^2} + \frac{y^3}{9a^3} \\ 0 \\ +\frac{y}{a} - \frac{y^3}{9a^3} \\ 0 \\ 0 \\ 0 \end{bmatrix} dy = -\sigma_0 at \begin{bmatrix} +\frac{53}{108} \\ 0 \\ \frac{+51}{108} \\ 0 \\ 0 \\ 0 \end{bmatrix}$$

Section 2-3

$$\{F\} = -\sigma_0 t \int_{+a}^{+2a} \begin{bmatrix} 2 - \frac{y}{a} \\ 0 \\ -1 + \frac{y}{a} \\ 0 \\ 0 \\ 0 \end{bmatrix} \left\{ \left(1 - \left[\frac{y}{3a}\right]^2\right) \right\} dy = -\sigma_0 a t \begin{bmatrix} +\frac{43}{108} \\ 0 \\ \frac{+37}{108} \\ 0 \\ 0 \\ 0 \end{bmatrix}$$

Section 3-4

$$\{F\} = -\sigma_0 t \int_{+2a}^{+3a} \begin{bmatrix} 3 - \frac{y}{a} \\ 0 \\ -2 + \frac{y}{a} \\ 0 \\ 0 \\ 0 \end{bmatrix} \left\{ \left(1 - \left[\frac{y}{3a}\right]^2\right) \right\} dy = -\sigma_0 . a t \begin{bmatrix} \frac{+21}{108} \\ 0 \\ \frac{+11}{108} \\ 0 \\ 0 \\ 0 \end{bmatrix}$$

Equivalent nodal forces

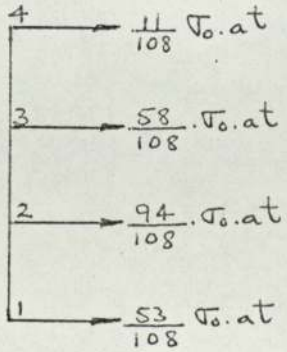

Portion of Inverted Reduced Matrix $[K]^{-1}$

ROW/COL	1	2	3	4	5
1	2.1066555	1.1581619	.04293873	.78407875	.05235367
2	1.1581619	1.4931517	.10945305	.88714025	.05458899
3	.04293873	.10945305	.69010849	-.13285497	.54582981
4	.78407875	.88714025	-.13285497	1.4579146	-.10014611
5	.05235367	.05458898	.54582980	-.10014612	1.2123726
6	.60227046	.67466139	-.32580526	1.1192187	-.62058015
7	.03759732	.03110234	.52010682	-.19015783	1.1185499
8	1.4515099	1.0737514	.22669126	.70815072	.21532026
9	1.0230897	1.1072910	.07365650	.82794888	.16819050
10	-.08753317	-.07123707	.16175484	-.01691561	.25129381
11	.74054903	.81120076	-.10047696	1.0646755	-.11393507
12	-.10605794	-.11169706	.22214035	-.11897897	.41416189
13	.59079788	.65338484	-.27269654	.98639434	-.50676453
14	-.11700366	-.12872728	.24664036	-.18855323	.46947450
15	1.0114516	.84841449	.17413825	.62372457	.21982926
16	.82076866	.83290717	.06929025	.68114079	.13773540
17	-.10941226	-.09762126	.03107761	-.02581022	.05864494
18	.64108624	.68207152	-.06295581	.79706635	-.07928686
19	-.16084531	-.15928765	.05912628	-.10099659	.10219557
20	.54314707	.58966705	-.18751609	.79295329	-.33488224
21	-.18725223	-.19154173	.08315053	-.16711895	.14645056
22	.69065004	.61678301	.11003866	.49332558	.15658221
23	.60599144	.60069527	.05073070	.51973435	.09209217
24	-.10298379	-.09239339	-.00976285	-.03459519	-.01407780
25	.50390957	.52569137	-.03618615	.57779565	-.04872802
26	-.16696713	-.15975897	-.00604296	-.09377208	-.01359255
27	.44985342	.48004431	-.11196020	.58790557	-.19342397
28	-.20609089	-.20325244	.00977109	-.15555079	.01369078
29	.43328799	.39981105	.06090834	.33873022	.09120841
30	.39717812	.39070163	.03055123	.35056145	.05291209
31	-.09084651	-.08177848	-.02015106	-.04041408	-.03332745
32	.34510930	.35583802	-.01902798	.37860938	-.02662523
33	-.15692714	-.14774560	-.02579482	-.09377630	-.04606304
34	.31939329	.33641892	-.05889831	.38683268	-.09914266
35	-.20407322	-.19771833	-.01680778	-.15240416	-.03118093
36	.20909208	.19611540	.02627565	.17207071	.04012975
37	.19636694	.19280952	.01390517	.17641864	.02353637
38	-.08131383	-.07367671	-.02061613	-.04405663	-.03435277
39	.17482688	.17923157	-.00822025	.18788399	-.01173242
40	-.14632183	-.13731073	-.02851700	-.09588584	-.04931183
41	.16530899	.17267836	-.02462482	.19163001	-.04079207
42	-.19748434	-.19039232	-.02331180	-.15292399	-.04113207
43	-.07820489	-.07143335	-.02043083	-.04492730	-.03427405
44	-.14023247	-.13247067	-.02635043	-.09791654	-.04556828
45	-.19181088	-.18586036	-.02009045	-.15476218	-.03535325

In order to solve the reduced equation $\{F\} = [K]\{\delta\}$ the $[K]$ matrix was inverted using an Eliott 803 Matrix Package.

For inversion by the Matrix Package the stiffness matrix data was fed into the computer row by rwo.

The inverted $[K]$ matrix was printed out in the form shown on page 201.

$$\{\delta\} = [K]^{-1}\{F\}$$

The only non zero forces are F_{H_1}, F_{H_2}, F_{H_3} and F_{H_4} and we therefore only require columns I,2,4 and 6 from the inverted matrix to solve for the displacements.

The following Eliott Algol programme was used to determine the nodal displacements.

```
PLATE DISPLACEMENTS HILBORNE MECH ENG'.
BEGIN REAL A,B,C,D,DISP1,DISP2'
      INTEGER N,COUNT'
       SWITCH SS:=BACK'
      READ N' COUNT:=0'
  BACK:READ A,B,C,D'
     DISP1:=.91*(A+2*B+2*C+D)'
     DISP2:=(.91/54)*(53*A+94*B+58*C+11*D)'
      PRINT ££L??,DISP1,££S8??,SAMELINE,DISP2'
      COUNT:=COUNT+1'
      IF COUNT LESS N THEN GOTO BACK'
END'
```

The displacement values obtained were then used in the stress matrix equation to solve for the element stresses. For the uniform tension case all elements had stress values of $\sigma_x = \sigma_o$, $\sigma_y = 0$ and $\tau_{xy} = 0$

The stress values for the parabolic loading case are shown in the diagrams on page 203 and the σ_x values were compared with the values quoted in Timoshenko and Goodier page 170.

Parabolic Loading

STRESS VALUES. (All values to be multiplied by σ_0).

σ_x

0.64549 / 0.65932	0.62741 / 0.65606	0.58801 / 0.64759	0.52024 / 0.63279	0.4238 / 0.60836	0.30627 / 0.57013
0.65442 / 0.68012	0.64779 / 0.68736	0.6340 / 0.70517	0.61136 / 0.73625	0.57993 / 0.78386	0.56005 / 0.86365
0.67530 / 0.68527	0.68258 / 0.69878	0.69689 / 0.72832	0.72006 / 0.77923	0.75504 / 0.85039	0.810399 / 0.88949

σ_y

-0.00324 / 0.00147	-0.00809 / 0.00614	-0.01427 / 0.01521	-0.02297 / 0.03079	-0.03232 / 0.05078	-0.03985 / 0.01638
-0.01487 / -0.01173	-0.02142 / -0.01408	-0.03008 / -0.01248	-0.04062 / 0.00293	-0.04396 / 0.04993	-0.0172 / -0.0588
-0.02779 / -0.02919	-0.03001 / -0.03951	-0.04007 / -0.04859	-0.05106 / -0.03886	0.04613 / 0.03536	0.02336 / 0024537

τ_{xy}

-0.00323 / -0.00821	-0.00986 / -0.0214	-0.01801 / -0.0420	-0.02576 / -0.07054	-0.0273 / -0.09975	-0.0468 / -0.10256
-0.00345 / -0.0112	-0.01679 / -0.02779	-0.18056 / -0.0514	-0.04904 / 0.09439	-0.05932 / -0.13951	0.03473 / -0.17519
-0.00169 / -0.00398	-0.00951 / -0.01131	-0.01821 / -0.02439	-0.02652 / -0.04574	-0.0254 / -0.07302	0.00324 / -0.07782

Graph of σ_x stress distribution across centre line of plate ($x=0$).

× Values quoted in Timoshenko and Goodier (page 170) and obtained by the application of the Principle of Least Work.

⊙ Finite element values.

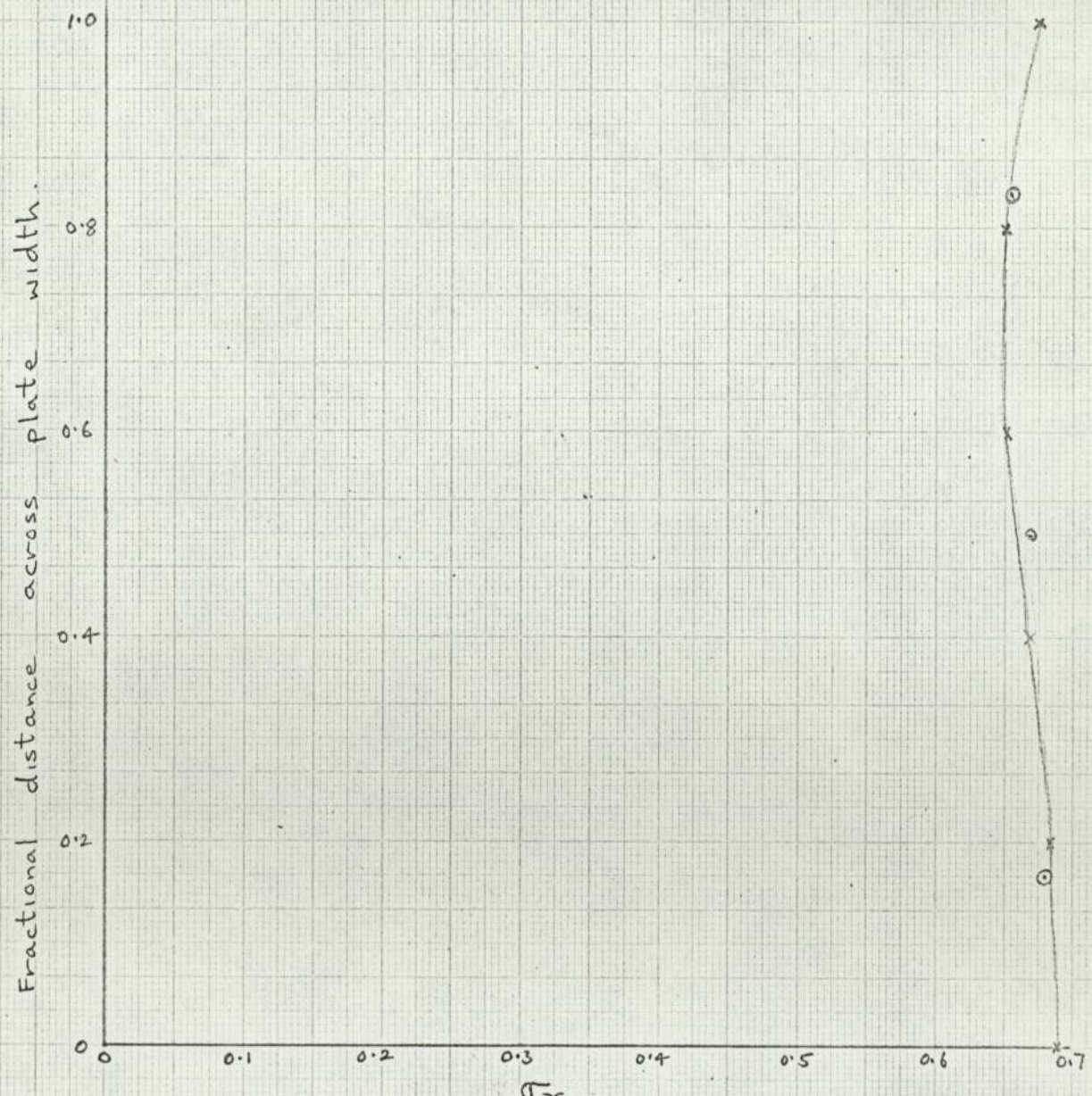

Graph 2.6.